THESE DE DOCTORAT

L'UNIVERSITE DE NANTES
COMUE UNIVERSITE BRETAGNE LOIRE

ECOLE DOCTORALE N°598
Sciences de la Mer et du littoral
Spécialité : « *Biotechnologie* »

Par
Eva COINTET

« Diatomées marines benthiques : une ressource originale de souches "oléagineuses" pour une application en santé et nutrition »

Thèse présentée et soutenue à Nantes, le 15/07/2019

Unité de recherche : EA 2160 MMS

Thèse N° :

Rapporteurs avant soutenance :

Arlette Baillet-Guffroy, Professeur, université Paris-sud 11
Cédric Hubas, Maître de conférences, MNHN

Composition du Jury :

Président : Claire Hellio, Professeur, Université de Bretagne occidentale
Examinateur : Pascal Claquin, Professeur, Université de Caen Normandie
Directeur de thèse : Gaëtane Wielgosz-Collin, Maître de conférences, HDR, Université de Nantes
Co-directeur de thèse : Olivier Gonçalves, Maître de conférences, HDR, Université de Nantes
Vona Méléder, Maître de conférences, Université de Nantes

The difficult i'll do right now

The impossible will take a little while

- Billie Holiday -

Remerciements

Je remercie tous les membres du jury pour m'avoir fait l'honneur d'accepter d'évaluer ce travail, la Pr. Arlette BAILLET-GUFFROY et le Dr. Cédric HUBAS en tant que rapporteurs ainsi que la Pr. Claire HELLIO et le Pr. Pascal CLAQUIN en tant qu'examinateurs.

Je souhaite remercier toutes les personnes qui m'ont aidée à mener à bien ces travaux, en particulier mes encadrants de thèse Gaëtane WIELGOSZ-COLLIN, Vona MELEDER et Olivier GONÇALVES. Un grand merci pour vos qualités scientifiques et surtout humaines. Merci de m'avoir offert l'opportunité de réaliser cette thèse et merci pour votre accompagnement pendant ces trois années ou j'ai énormément appris auprès de vous.

Je remercie tous les membres du laboratoire avec qui j'ai échangé de près ou de loin durant ces trois années. Merci à toute l'équipe de doctorant Lucie, Marta, Antoine et bien évidemment Daphné mon binôme de toujours.

Je remercie également Alexandra PETIT, merci d'avoir su garder ta patience et ton calme quand je mettais le laboratoire sens dessus dessous avec mes expérimentations interminables. Merci à Véronique MARTIN-JEZEQUEL pour avoir pris le temps de répondre à mes questions traitant du métabolisme de mes petites diatomées. Un très grand merci à Vony RABESAOTRA pour ta patience et ton soutien technique dans mon apprentissage des extractions lipidiques.

Je voudrais également remercier l'équipe du GEPEA qui m'a accueillie pendant quatre mois. Merci à Raphaëlle TOUCHARD pour m'avoir aidée à prendre en main les photobioréacteurs et de m'avoir épaulée dans mes moments de panique. Merci à Alexandra BUSNELL et Rémi NGHIEM XUAN Pour m'avoir aidée à prendre mes marques durant mon séjour et m'aider à souffler. Merci à Rémi COAT et à Delphine KUCMA pour votre soutien technique lors de mon séjour.

Je remercie également Elise SEVERIN, merci d'avoir fait équipe avec moi durant 6 mois pour explorer le potentiel lipidique de mes microalgues, sans toi une grande partie de ce travail n'aurait pas pu être réalisée.

J'ai également énormément de gens à remercier qui n'ouvriront probablement jamais ce manuscrit, il y a tout d'abord Adrien, merci de partager ta vie avec moi depuis presque 10 ans et de m'avoir toujours tirée vers le haut, tu sais bien plus que moi de quoi je suis capable. Merci à ma famille, mes grands-parents, mes parents et mes deux formidables petites sœurs sans votre amour et votre soutien ce travail n'aurait pas été possible. Merci à mes amis et tout particulièrement Emilie, Killian, Axel, Laurent, Keven et Hubert si je me suis lancée dans la réalisation de cette thèse vous n'y êtes pas pour rien.

Ce travail a été financé par la région Pays de la Loire dans le cadre du projet AtlanticMicroAlgae (AMI).

Sommaire

Liste des travaux et publications

Publications

2017 – Publication : Abstract – Exploration of the bioactive lipids diversity of the marine benthic diatoms of the Nantes Culture Collection (NCC*). Eva Cointet, Vona Méléder, Olivier Gonçalves, Gaetane Wielgosz-Collin*. *Phycologia*, 2017, vol. 56, no sp4, p. 1-226.

2019 – Publication : Lipids in benthic diatoms : a new suitable screening procedure. *Cointet, E., Wielgosz-Collin, G., Méléder, V., & Gonçalves, O.* ***Algal Research****, 39,* 101425. https://doi.org/10.1016/j.algal.2019.101425

2019 – Publication : Lipid production and fatty acid quality impacted by photosynthetic efficiency of three original benthic diatom strains selected for biotechnology applications. *Cointet, E., Wielgosz-Collin, G.,Bougaran, G.,Rabesaotra, V., Gonçalves, O & Méléder, V.* ***PLOS One****,(submitted).*

2019 – Publication : Assessment of lipid production potential of six original benthic diatoms grown in airlift PBR. *Cointet, E., Séverin, E., Couzinet A., Méléder, V., Gonçalves, O., Wielgosz-Collin, G.* ***Algal Research****, (submitted).*

2019 – Publication : Antibacterial and antiproliferative activity against breast cancer and lung cancer cell lines of extracted lipid fraction from three benthic diatom species. *Cointet, E., Gonçalves, O., Séverin, E., Couzinet-Mossion, A., Lakdhar, F., Etahiri, S., Ory, L., Nazih, E-H., Roussakis, C., Méléder, V., Wielgosz-Collin, G.* ***Marine Drugs****, (in writting).*

Communication scientifiques

2017 – Poster : Exploration of the bioactive lipids diversity of the marine benthic diatoms of the Nantes Culture Collection (NCC). *Cointet, E., Wielgosz-Collin, G., Méléder, V., & Gonçalves, O.* 6th International congress and Annual meeting of the society for applied phycology – 18 au 23 juin 2017 – Nantes, France.

2017 - Poster : Nantes Cultures Collection: the microphytobenthos biodiversity, a new and original resource for biotechnology applications. *Méléder V., Mouget J.-M., Cointet E., Petit A. & Denise J.* 6th Congress of the International Society for Applied Phycology – ISAP, 18-23 juin, Nantes, France.

2017 – Communication orale : Exploration of the bioactive lipids diversity of the marine benthic diatoms of the Nantes Culture Collection (NCC). *E., Wielgosz-Collin, G., Méléder, V., & Gonçalves, O.* 11th international congress of the international phycological society – 13 au 19 aout – Szczecin, Poland.

2017 – Poster : Nantes Cultures Collection: the microphytobenthos biodiversity, a new and original resource for biotechnology applications. *Méléder V., Mouget J.-M., Cointet E., Petit A. & Denise J.* Phycological Congress, IPC 2017, 13-19 Aug 2017, University of Szczecin, Szczecin, Poland.

2017- Communication orale : Nantes Culture Collection: a local heritage registered in the World Data Center for Microorganisms**.** *Méléder V., Mouget J.L., Cointet E., Petit A. & Jahan D.* BioSciences 2017, International Conference of the High School in Biological Sciences, 28-29 Novembre, Oran, Algeria.

2018 – Communication orale : Exploration of the bioactive lipids diversity of the marine benthic diatoms of the Nantes Culture Collection (NCC). *Cointet, E., Wielgosz-Collin, G., Méléder, V., & Gonçalves, O.* Atlantic microalgae symposium – 1er juin – Nantes, France.

2018- Poster : Lipid analysis of six diatoms species from the Nantes Culture Collection. *Séverin E., Cointet E., Rabesaotra V., Méléder V., Couzinet-Mossion A., Gonçalves O., & Wielgosz-Collin G.* 3ieme congrès international de l'AFERP, 18-20 juillet, Rennes, France**.**

2019 – Poster : Nantes Cultures Collection: the microphytobenthos biodiversity, the "secret garden" for new biotechnology resources. *Méléder V., Cointet E., Wielgosz-Collin G., Petit A., Goncalvez O. and Mouget JL.* 7th European Phycological Congress, 25-30 August 2019 Zagreb, Croatia.

Liste des abréviations

AG :	Acide gras
AGL :	Acide gras libre
AGPI-LC :	Acides gras polyinsaturés à chaîne longue
AGS :	Acide gras saturés
ARA :	Acide arachidonique
CCM :	Chromatographie sur couche mince
Chl *a* :	Chlorophylle *a*
CI_{50} :	Concentration inhibitrice mediane
CPG-SM :	Chromatographie en phase gazeuse couplée à la spectrométrie de masse
DAG :	Diacylglycérol
DGDG :	Digalactosyldiacylglycérol
DHA :	Acide docosahexaénoïque
DMSO :	Diméthyl sulfoxyde
EBL :	Extrait brut lipidique
EMAG :	Ester methylique d'acide gras
EPA :	Acide eicosapentaénoïque
F0 :	Fluorescence minimale
Fm :	Fluorescence maximale
FTIR-HTSXT :	Fourrier transform infrared spectroscopie
GL :	Glycolipides
HBI :	Hydrocarbures isoprénoïdes hautement ramifié
LN :	Lipide neutre
MGDG :	Monogalactosyldiacylglycérol
MMS :	Mer Molécules Santé
m/z :	Rapport masse sur charge

NAP :	*N*-Acyl pyrrolidide
NCC :	Nantes Culture Collection
PAM :	Pulse amplitude modulated
PBR :	Photobioréacteur
PL :	Phospholipides
PSI :	Photosystème I
PSII :	Photosystème II
Px :	Productivité
SQDG :	Sulfoquinovosyldiacylglycérol
TG :	Triacylglycérol
v/v :	Volume sur volume

Liste des figures

Liste des tableaux

Introduction et objectifs de l'étude

Les océans et les mers, de par leur immensité, sont traditionnellement considérés comme une richesse inépuisable, jouant un rôle majeur dans notre vie sociale et culturelle. Différents types de ressources (biologique, minérale, énergétique) sont puisées quotidiennement pour répondre au besoin de l'Homme. En 2016, la production mondiale de poisson a culminé à environ 171 millions de tonnes, la pêche de capture représentant 53 % du total (FAO, 2018) et 10 % de cette production mondiale est utilisée pour la production d'huiles (FAO, 2018). Ces huiles sont source d'oméga 3 et d'oméga 6, acides gras essentiels à notre santé, puisqu'ils jouent un rôle important dans le fonctionnement des systèmes nerveux, cardiovasculaire et immunitaire (SanGiovanni and Chew, 2005; Simopoulos, 2008; Yashodhara *et al*., 2009). Mais depuis une cinquantaine d'années les ressources halieutiques sont en baisse sur l'ensemble du globe terrestre alors que la demande pour ces lipides est en constante augmentation. Une augmentation de 23% de la proportion des stocks exploités à un niveau biologiquement non-durable a été observée entre 1974 et 2015 (FAO, 2018). De nombreuses recherches concernant la valorisation de nouvelles sources de lipides ont permis de mettre en avant le potentiel des microalgues en tant que source pour ces acides gras.

Les premières études sur l'utilisation des microalgues comme source lipidique datent de 1950 (Oswald and Golueke, 1960) et depuis les années 1970 plusieurs programmes ont financé des études sur le potentiel lipidique des microalgues (Pohl and zurheide 1979). Contrairement aux huiles de poisson, les lipides de microalgues ne contiennent pas ou peu de cholestérol (Ryckebosch *et al*., 2014), d'où une meilleure adaptation pour des applications thérapeutiques visant à réduire le taux de lipides sériques. Constitués non seulement de triglycérides, mais également de phospholipides et de glycolipides, les lipides de microalgues offrent un large éventail d'application (Bellou *et al*., 2014; de Jesus Raposo *et al*., 2013; Mata *et al*., 2010; Pulz and Gross, 2004; Spolaore *et al*., 2006). La pertinence de l'utilisation des microalgues comme source de lipides d'intérêt réside également dans la possibilité d'exploiter de manière

concomitante d'autres produits à haute valeur ajoutée comme l'astaxanthine, le beta-carotène et la phycoérythrine, utilisés comme colorants alimentaires (Mata *et al*., 2010; Pulz and Gross, 2004; Spolaore *et al*., 2006).

Malgré un intérêt croissant pour l'utilisation des microalgues comme source de lipide, des difficultés techniques et économiques restent encore à ce jour des verrous à leur utilisation. Les défis techniques les plus cruciaux à résoudre sont d'augmenter le taux de croissance des microalgues et la synthèse de produits valorisables (Khan *et al*., 2018). C'est pourquoi il est nécessaire de sélectionner des souches performantes et d'optimiser leurs conditions de culture pour que leur production soit compétitive avec la production des huiles de poisson. C'est dans cette démarche que s'inscrit ce travail.

Le travail présenté dans ce manuscrit s'intéresse plus particulièrement à un groupe de microalgues que sont les diatomées, appartenant à la classe des bacillariophycées. Bien que différentes espèces de diatomées ont déjà été utilisées pour leur potentiel lipidique dans les années 1980 : *Amphiprora hyalina*, *Cyclotella cryptica*, *Navicula acceptata* et *Nitzschia palea* (Shifrin and Chisholm, 1981; Tadros and Johansen, 1988) ce groupe, et en particulier les diatomées benthiques, sont sous-représentées dans la recherche et la littérature relatives au développement de produits valorisable à base de microalgues (Hildebrand *et al*., 2012). Pourtant les diatomées sont très diverses, et présentent d'importantes différences dans l'organisation cellulaire et les procéssus métaboliques comparés aux chlorophytes qui sont quant à elles largement eploitées en biotechnologie.

L'objectif de ce travail de thèse a donc été d'identifier de nouvelles souches de microalgues productrices de lipides d'intérêt à partir d'un gisement de biodiversité sous exploitées que sont les diatomées marines benthiques. Pour atteindre cet objectif, le présent manuscrit s'articule autour de cinq chapitres qui aborderont successivement la recherche et la caractérisation de nouvelles souches.

Le premier chapitre établi les connaissances actuelles existantes sur les lipides des microalgues marines et plus particulièrement des diatomées marines benthiques. Le deuxième chapitre porte sur le criblage des souches de diatomées marines benthiques, qui a permis de sélectionner six espèces : *Amphora* sp., *Entomoneis paludosa*, *Navicula* sp., *Nitzschia alexandrina*, *Opephora* sp. et *Staurosira* sp. Ces espèces sélectionnées ont ensuite été produites en photobioréacteur Airlift en condition non-limitante. Ces six espèces ont fait l'objet d'une étude lipidique approfondie à la fois sur les lipides neutres (acide gras, stérols) et les lipides polaires (glycolipides, phospholipides) cette étude fait l'objet du chapitre 3. Par la suite, les trois espèces possédant des profils lipidiques intéressants pour des applications technologiques ont été cultivées en ballon de 25 L et la bioactivité des fractions lipidiques obtenues ont été testées pour leur potentiel antibactérien et antiprolifératif sur des cellules cancéreuses humaines (cancer du sein, cancer du poumon) tout en s'assurant que la production des composés chimiques majoritaires soit restée la même entre les cultures en ballon et en airlift. Cette étude fait l'objet du chapitre 4. L'impact des conditions de cultures sur la physiologie et la production lipidique a été finalement étudié sur ces trois espèces et fait l'objet du dernier chapitre.

I- Etat de l'art

1 Pourquoi les lipides des diatomées ?

Le monde vivant marin peut être considéré comme un gisement naturel riche en composés très variés, en molécules biologiquement actives, souvent sans équivalent terrestre. Les organismes marins peuvent vivre dans des conditions extrêmes et produisent une large variété de substances à activité spécifique, en particulier des lipides, source majeure d'énergie métabolique et matériaux essentiels pour la formation des membranes cellulaires et tissulaires (Bergé and Barnathan, 2005). Dans le domaine marin, les substances nouvelles ayant une activité biologique potentiellement intéressante seraient au moins 100 fois plus nombreuses que celle des organismes terrestres. Ainsi, plus de 28 000 nouveaux métabolites marins ont été identifiés à ce jour (Blunt *et al*., 2015). L'étude systématique des extraits algaux, pour la recherche d'une activité biologique, a commencé dans les années cinquante avec la détection de produits antibiotiques (Chesters and Stott, 1956). À l'occasion des premiers criblages à grande échelle menés sur les algues, de nombreuses activités biologiques intéressantes ont été découvertes et surtout de nouvelles méthodes de criblage avec des biosuivis d'activités ont permis l'orientation des extractions et purifications. Certaines microalgues présentent un avantage par rapport aux macroalgues car elles peuvent être aisément cultivées en masse et peuvent donc devenir des sources potentielles de molécules difficilement accessibles par synthèse chimique. De nos jours, se sont surtout les algues vertes et bleu-vert comme *Chlorella* sp., *Dunaliella salina*, *Arthrospira* sp. qui sont cultivées à grande échelle (Spolaore *et al*., 2006) alors que les espèces de diatomées sont sous exploitées (Levitan *et al*., 2014). L'un des exemples d'espèces de diatomées commercialisées avec succès est *Odontella aurita* qui est cultivée à l'échelle industrielle et présentée sur le marché comme un complément alimentaire riche en oméga 3 (Mimouni *et al*., 2012). Dans cette étude, nous nous intéresserons à une classe particulière de microalgues : les diatomées et plus particulièrement les diatomées benthiques.

2 Généralités sur les diatomées

2.1 Histoire des diatomées

Les premières études sur les diatomées remontent au 18^{éme} siècle ; en 1703 le chercheur néeerlandais Antoni van Leeuwenhoek (1632-1723), découvre une structure que l'on a identifiée à posteriori comme étant une diatomée, mais qu'il prit pour un cristal. Différentes espèces de diatomées ont été décrites dans la moitié du 18^{éme} siècle, le travail de O. F. Muller est d'un intérêt tout particulier, car c'est une de ses espèces *Vibrio paxillifer*, qui a servi comme type pour la description du genre Bacillaria (Gmelin, 1791). Ce n'est qu'au début du 20ème siècle que la classification des diatomées prend forme. Cette classification s'étoffera ensuite durant la seconde moitié du 20^{éme} siècle grâce à divers auteurs qui proposeront des classifications plus ou moins différentes les unes des autres. Ainsi au début du 20^{éme} siècle, plus de 1000 espèces sont déjà connues et classifiées pour les seuls environnements aquatiques de France. Des applications pratiques à leur étude commencent alors à voir le jour au milieu des années 1920, les diatomées vont être utilisées comme outils stratigraphiques. Dans les années 1960 commencent l'étude de l'écologie de ces cellules et l'étude des molécules qu'elles produisent.

2.2 Définition des diatomées

Les diatomées (Bacillariophyta) sont des microorganismes, unicellulaires et eucaryotes appartenant au clade des hétérocontes (ou straménopiles) (Figure I-1), dont la taille peut varier de 2 µm pour les plus petites, à plus de 2 mm pour l'espèce *Ethmodiscus rex* (Sarthou *et al*., 2005). Les diatomées sont présentes dans tous les milieux aquatiques. Elles peuvent vivre isolées ou en colonie, être libres ou fixées. Les formes pélagiques appartiennent au phytoplancton, les formes benthiques appartiennent au microphytobenthos. Les diatomées sont un constituant majeur du phytoplancton participant à 50 % de la production primaire océanique globale (Nelson *et al*., 1995). Ces micro-algues jouent un rôle primordial dans la vie des

écosystèmes marins, puisqu'elles sont à la base des réseaux trophiques. Il existerait plus de 20 000 espèces de diatomées (Guiry, 2012), dont 14 803 espèces sont répertoriées dans AlgaeBase.

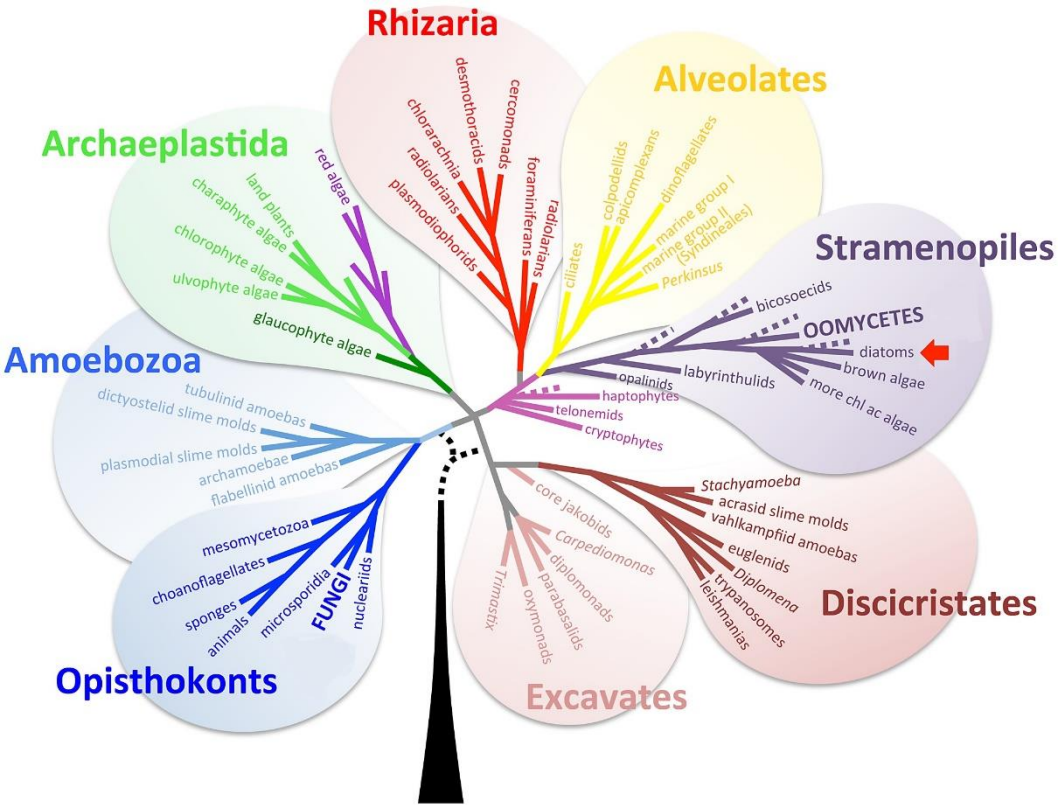

Figure I-1 Arbre de vie positionnant les diatomées dans le groupe des stramenopiles selon lee *et al.,* 2012

Les diatomées sont les seuls organismes unicellulaires à posséder une structure externe siliceuse enveloppant totalement la cellule. Cette enveloppe, nommée frustule, possède une architecture complexe qui définit l'espèce dans la nomenclature. Le frustule est formé de deux thèques emboîtées à symétrie remarquable. Les diatomées se divisent en deux groupes en fonction de la forme de leur frustule : les centriques, à symétrie radiale et les pennées à symétrie bilatérale ou transversale. Les diatomées centrales sont apparues sur terre il y a 150 millions d'années, et sont restées pratiquement inchangées durant tout le tertiaire. Les diatomées pennales sont quant à elles apparues durant l'Eocène. A l'inverse des diatomées centrales, elles ont évolué et leur proportion a fortement augmenté à partir de la fin du miocène pour aujourd'hui surpasser en nombre les centrales. Actuellement, les diatomées centrales tendent à être majoritairement

planctoniques alors que les diatomées pénales sont plus importantes parmi les espèces benthiques. La systématique a permis d'affiner cette classification en divisant les diatomées en 3 classes : les Coscinodiscophyceae (diatomées centrales), les Fragilariophyceae (diatomées pennales non-raphées) et les Bacillariophyceae (diatomées pennales raphées) (tableau I-1).

Tableau I-1 Classification des diatomées

Division	BACILLARIOPHYTA		
CLASSE	Coscinodiscophyceae	Fragilariophyceae	Bacillariophyceae
Sous classe	Thalassiosirophycidae, Coscinodiscophycidae, Biddulphiophycidae, Lithodesmiophycidae, Corethrophycidae, Cymatosirophycidae, Rhizosoleniophycidae, Chaetocerotophycidae	Fragilariophycidae,	Eunotiophycidae, Bacillariophycidae

La particularité des diatomées est l'existence d'une enveloppe siliceuse entourant l'ensemble du contenu cellulaire. Cette enveloppe, ou test, a la structure d'une boîte de pétri. La « base » est nommée hypovalve et le « couvercle » épivalve (Figure I-2). Ces deux structures sont reliées par des bandes intercalaires nommées ceintures connectives. Le frustule est recouvert d'une fine couche organique, le mucilage, qui permet la mobilité de la cellule et son adhésion éventuelle à un substrat ou à d'autres cellules (Kröger *et al*., 1994).

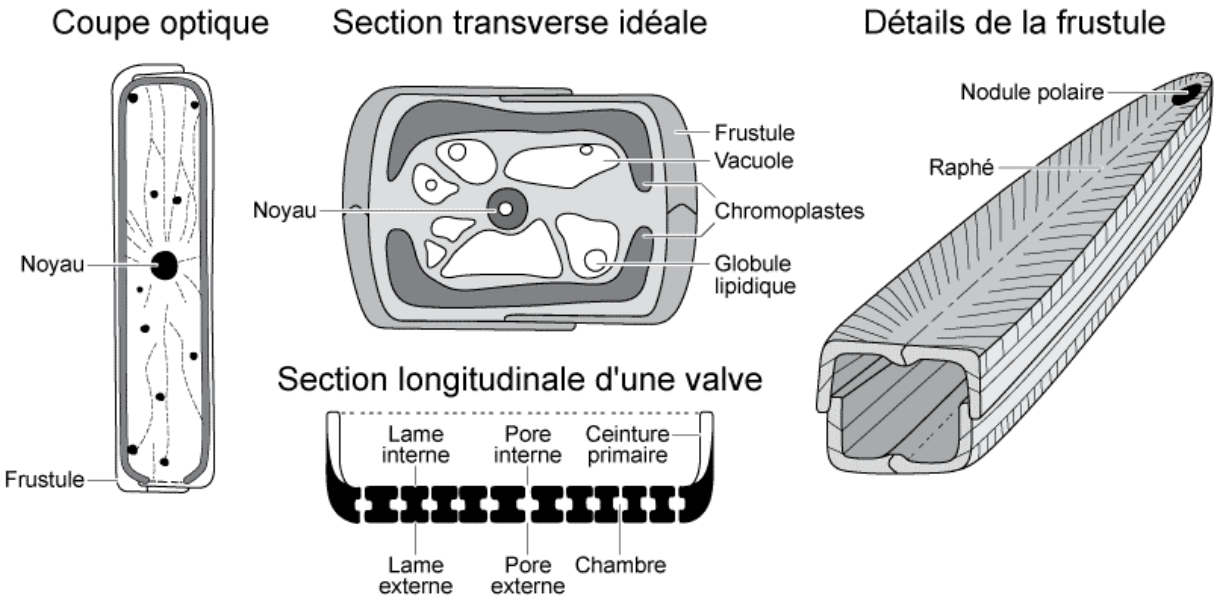

Figure I-2. Détail de la structure du frustule de diatomée **(Mathieu *et al*., 2011)**

Trois grands groupes de diatomées peuvent être distingués selon leur mode de vie :

- Les diatomées épipéliques mobiles qui pour la plupart sont des espèces pennées raphidés migrant dans le sédiment (Fischer *et al*., 1977; Round and Eaton, 1966; Round and Palmer, 1966).
- Les diatomées epipsammiques qui sont pour la plupart des espèces pennées vivant attachées aux grains de sédiment ne possédant pas toujours de raphé.
- Les diatomées tychoplanctoniques qui sont des espèces pennées ou centriques capables de passer une partie de leur cycle de vie dans la colonne d'eau (Trites *et al*., 2005; Vos and De Wolf, 1993) ce dernier groupe reste cependant mal défini.
-

Les diatomées sont des organismes autotrophes qui utilisent l'énergie de la lumière grâce à la chlorophylle *a* et la chlorophylle *c* contenue dans leur chloroplaste par photosynthèse.

2.3 Les mécanismes de la photosynthèse

La photosynthèse est la conversion de l'énergie lumineuse en énergie chimique qui est stockée sous forme de composés carbonés organiques. Pour extraire l'énergie du carbone ou pour l'utiliser comme élément constitutif des molécules organiques, le carbone doit être chimiquement réduit, ce qui demande un investissement en énergie. La photosynthèse peut être écrite sous forme d'une réaction d'oxydo-réduction (Eq. I-1) :

$$CO_2 + H_2O + \text{photons} \leftrightarrow CH_2O + O2 \qquad \text{Eq. (I-1)}$$

CH_2O – chainon constitutif de sucre

La Chl *a*, pigment photosynthétique, catalyse une série de réactions ou l'énergie lumineuse est utilisée pour oxyder l'eau (Eq. I-2) :

$$2H_2O + \text{photons} \rightarrow 4H^+ + 4e + O_2 \qquad \text{Eq. (I-2)}$$

Les réactions chimiques liées à la photosynthèse ont lieu dans les chloroplastes (Figure. I-3), qui contiennent différentes couches de membranes lipoprotéiques et des phases aqueuses. Les membranes lipoprotéiques sont appelées les thylakoïdes. La membrane des thylakoïdes contient des complexes pigments-protéines permettant la captation de la lumière. La phase aqueuse qui entoure les thylakoïdes est nommé le stroma. Les protéines solubles dans le stroma sont utilisées comme réducteur chimique et génère de l'énergie par des réactions biochimiques dans la membrane des thylakoïdes pour réduire le CO_2, NO_2^- et SO_4^{2-}.Le stroma contient des éléments fonctionnels comme l'ADN, les ribosomes, l'ARN et toutes les enzymes nécessaires pour la transcription et la translation du génome des chloroplastes.

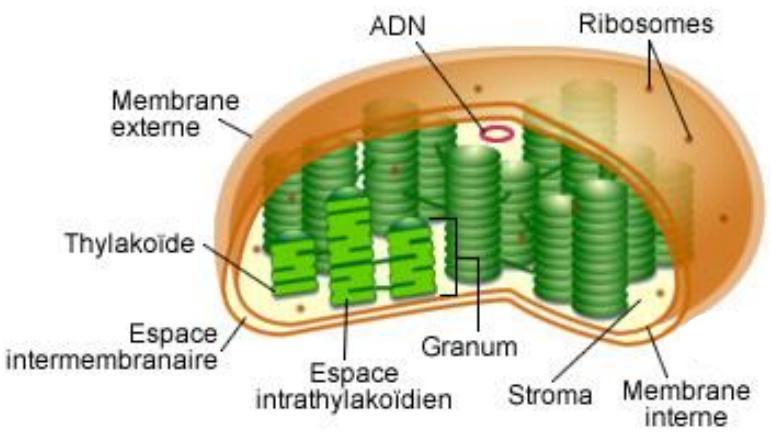

Figure I-3. Schéma de la structure des chloroplastes (http://www.cours-pharmacie.com/biologie-vegetale/la-photosynthese.html, consulté le 05/02/2019)

2.4 La chaine linéaire de transporteurs d'électrons

La première étape de la photosynthèse a lieu dans les thylacoïdes des chloroplastes (Figure. I-4). Elle implique une chaine linéaire de transporteurs d'électrons qui peut être divisée en trois segments. Tout d'abord, les électrons de l'eau situés dans le lumen (espace intrathylakoïdien) sont transférés au PSII via le donneur d'électrons des PSII. Ensuite, les électrons extraient de l'eau vers le PSII sont transférés par un système intermédiaire de transport d'électron impliquant le cytochrome B_6/f. Les électrons passent ensuite à travers des plastocyanines (PC) dans le PSI dans lequel, grâce à un accepteur d'électrons, le nicotinamide adénine dinucléotide phophate (NADPH) est réduit en nicotinamide adenine dinucléotide (NADP). Le transport d'électrons aboutit également à la production d'ATP (molécule très énergétique) via l'ATP synthase qui utilise les H+ accumulés dans le lumen. L'ensemble de ces réactions, qui constituent la conversion de l'énergie lumineuse en énergie chimique, est appelé la photochimie.

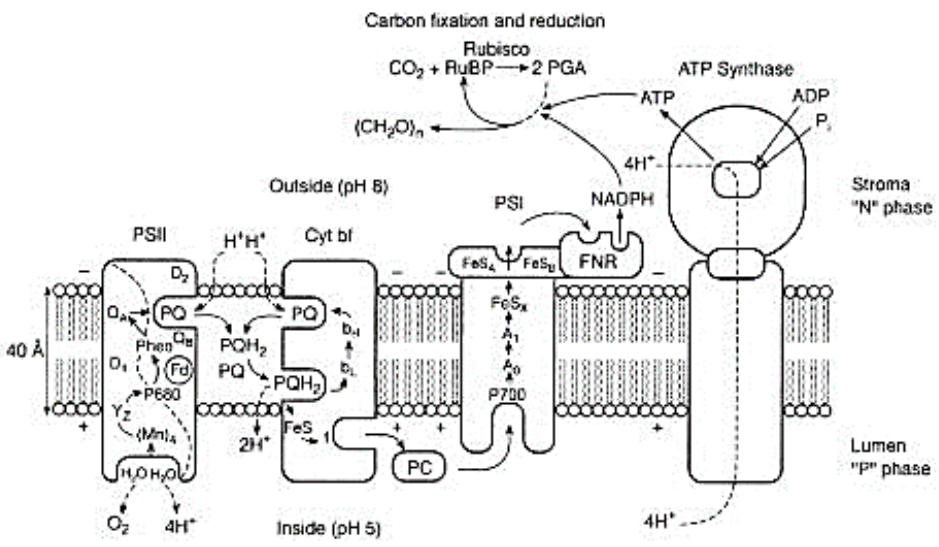

Figure I-4. Schéma d'une coupe transversale d'une membrane de thylakoïde **(Falkowski and Raven, 2013)**. La chaîne de transport d'éléctrons est indiquée par des flèches pleines, le transport de protons par des lignes pointillées. abbréviation : yz, tyrosine qui est le donneur d'éléctron direct du PSII ; P680 et P700, centre de réaction chlorophyllien des PSII et PSI. Pheo : Phéophytine ; QA et QB lien des plastoquinones ; QH2 plastoquinone réduite, cyt bt et cyt bh, forme basse et haute du cytochrome B6F ; FeS centre fer-soufre de Rieske ; f cytochrome f ; pc plastocyanine ; A0 chlorophylle ; A1 phylloquinone ; Fx, Fa, Fnr, centres fer-soufre ; fd, ferrédoxine ; FNR, ferrédoxine/NADP+ oxydoréductase ; NADPH, nicotinamide adenine dinucleotide phosphate ; ADP, adenosine diphosphate ; ATP, adenosine triphosphate ; pi, phosphate inorganisques ; H+ , protons. RuBP, ribulose-1,5-biphosphate ; rubisco, ribulose-1,5-biphosphate carboxylase/oxygenase ; PGA, 3-phosphoglycerate ; (CH20)n, carbohydrate en générale.

2.5 Le cycle de Calvin

La deuxième étape se déroule dans le stroma des chloroplastes et permet la réduction de CO_2, ou des bicarbonates de l'eau $HCO3^-$, sous forme de glucides au travers du cycle de Calvin-Benson qui utilise une partie de molécules d'ATP et de NADPH précédemment produites. Les organismes photoautotrophes incorporent le CO_2 en matière organique en ajoutant 4 électrons et 4 protons à l'atome de carbone ce qui forme des glucides. La réaction nette pour la fixation du carbone peut être écrite sous la forme (Eq. I-3) :

$$CO_2 + 2NADPH + 2H^+ + 3ATP \rightarrow CH_2O + H_2O + 2NADP^+ + 3ADP + 3Pi \qquad \text{Eq. (I-3)}$$

Après la production d'ATP et de NADPH grâce à des réactions dépendantes de la lumière, il y a assez d'énergie chimique accumulée pour le cycle de Calvin-Benson, ce cycle enzymatique ne dépend pas directement de la lumière.

Comme le montre le schéma de la Figure I-5, l'assimilation du CO_2 se fait en trois phases. La première étape fait intervenir une enzyme clé, la Ribulose Biphosphate Carboxylase/Oxygénase (RuBisCO). Cette enzyme incorpore une molécule de CO_2 dans un composé à cinq carbones, le ribulose biphosphate (RuBP) ce qui conduit à la formation d'une molécule instable à 6 carbones qui donnera par la suite deux molécules de 3-phosphoglycérate. La deuxième étape correspond à la réduction du 3-phosphoglycérate en 3-phosphoglycéraldéhyde (G3P). En premier lieu le 3-phosphoglycérate, ou acide phosphoglycérique (APG), est phosphorylé par l'ATP pour donner de l'acide biphospho-glycérique (ABPG) qui sera lui-même réduit par le NADPH + H^+ pour former le 3-phosphglycéraldéhyde (G3P). Le G3P est un sucre constitué de 3 atomes de carbones à l'origine de la synthèse des acides gras (lipides), acides aminés (protéines) et glucides et à la régénération de l'accepteur de CO_2 (ribulose 5-phosphate). La dernière étape correspond à la régénération de l'accepteur de CO_2, le RuBP. La régénération du RuBP se réalise grâce à un ensemble de réactions faisant intervenir des sucres à nombres variés de carbones : fructose (C6), érythrose (C4) et sédoheptulose (C7). A partir de 5 G3P se forment 3 pentoses phosphates RuP qui sont convertis en RuBP grâce à l'ATP. Cette réaction de phosphorylation est catalysée par la phosphate ribulose kinase (PRK). La régénération du RuBP nécessite donc une molécule d'ATP supplémentaire par molécule de CO_2 fixé. Un sixième G3P formé sera exporté vers le cytoplasme de la cellule, ou il servira comme composant de base pour la synthèse des glucides en proportion élevée.

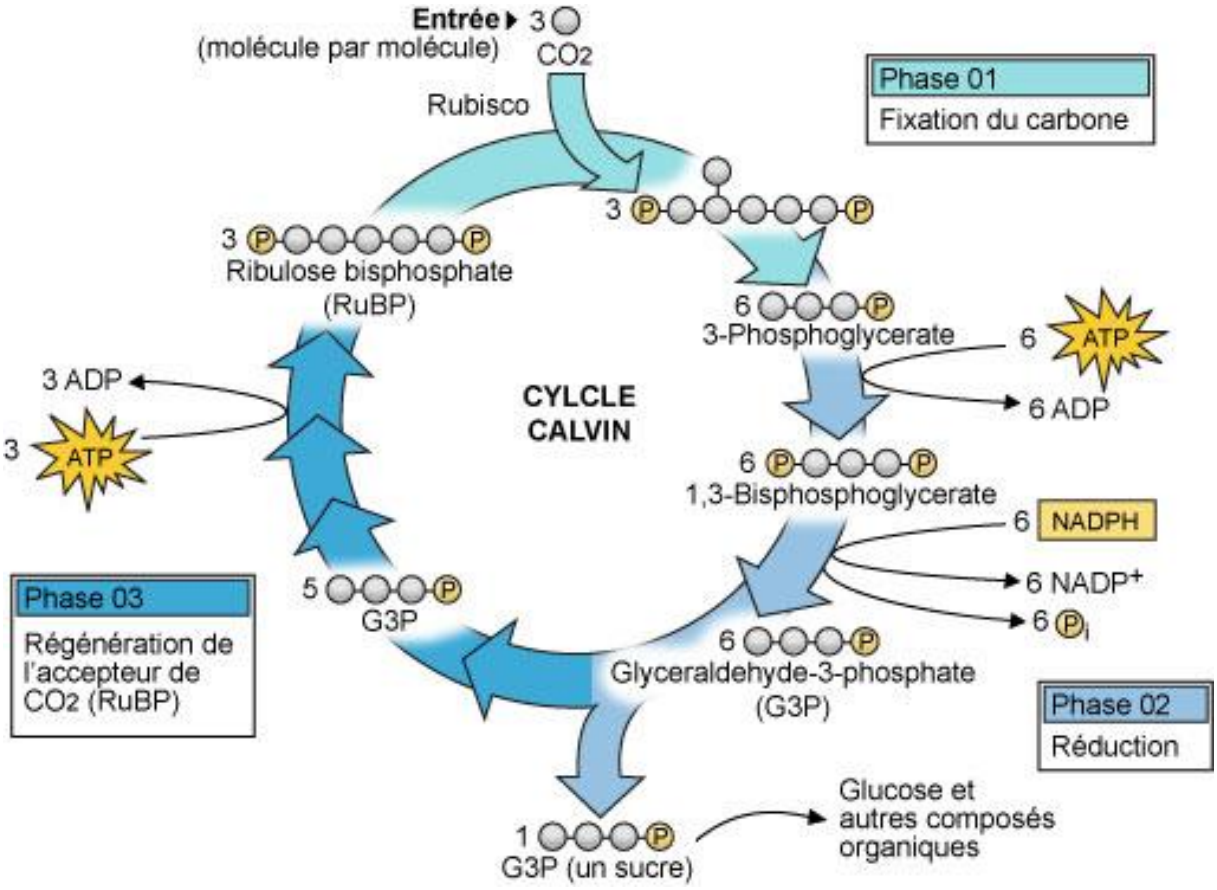

Figure I-5. Représentation schématique du cycle de Calvin (http://www.cima.ualg.pt/piloto/UVED_Geochimie/UVED/site/html/2/2-3/2-3-1/2-3-1-4.html consulté le 05/02/2019, consulté le 05/02/2019)

2.6 La fluorescence de la chlorophylle

A la lumière, tous les organismes photosynthétiques émettent de la fluorescence qui provient essentiellement de la Chl *a* du PS II. La mesure de la fluorescence émise par les cellules renseigne sur l'efficacité de la réaction photosynthétique (Hancke *et al*., 2008) et donc sur l'état physiologique de la cellule. Les mesures de la variation de la fluorescence chlorophyllienne sont possibles grâce aux fluorimètres PAM (Pulse amplitude modulated).

Les méthodes traditionnelles de mesures de biomasses impliquent des échantillonnages destructifs ou au mieux intrusifs pour le système étudié (Consalvey *et al*., 2005). La mesure de

la fluorescence de la Chl *a* est une mesure non-destructive qui peut donner des informations importantes sur l'état de santé cellulaire et le niveau de biomasse de la culture.

Quand la lumière est absorbée par la Chl *a*, il existe trois voix de dissipation de l'énergie : elle peut être réémise par fluorescence, transférée au centre réactionnel du PSII et utilisée pour la photochimie ou dissipée thermiquement par le processus de Quenching non photochimique de la fluorescence de la chlorophylle (NPQ) Figure I-6. En cas de lumière excessive et avant la saturation photosynthétique, le singulet excité de la Chlorophylle *a* peut former des états triplés qui réagissent avec des molécules d'oxygène produisant des dérivés réactifs de l'oxygène (DRO). Toutes ces routes de la dissipation de l'énergie sont en compétition et le mécanisme le plus rapide va désexciter la chlorophylle. La fluorescence de la Chl *a* est émise principalement par l'antenne collectrice du PSII, la modulation de son rendement peut être utilisée comme une mesure de l'activité photosynthétique.

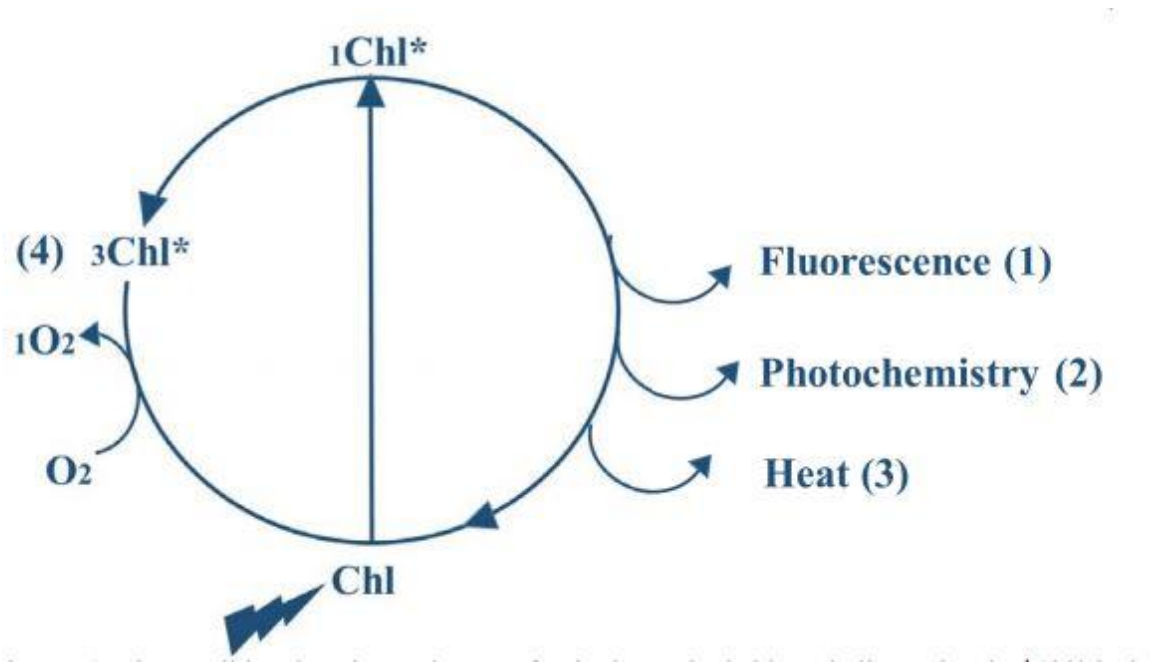

Figure I-6 Schéma des voies de dissipation de l'énergie photosynthétique (Müller *et al.*, 2001)

La fluorescence est la réémission de photons captés sous forme de photons d'un niveau énergétique plus faible. La Chl *a* réémet dans le spectre lumineux rouge. En absence de lumière, les centres réactionnels du PSII sont dit 'ouverts', c'est-à-dire qu'ils sont prêts à recevoir des électrons pour effectuer la séparation de charge. Le niveau de fluorescence est minimal (F0). Si on applique alors un court flash lumineux suffisant pour fermer tous les centres réactionnels PSII (saturating pulse) on atteint une fluorescence maximale (Fm). La différence entre ces deux mesures nous donne le potentiel de fluorescence (Fv = Fm – F0). Le rapport Fv/Fm permet d'évaluer le rendement quantique du PSII qui est communément utilisé pour estimer l'état de santé des organismes photosynthétiques.

3 Culture des diatomées

Les diatomées ont besoin pour croître d'une source lumineuse, d'une source de carbone inorganique et de minéraux. En effet, le carbone est essentiel à la synthèse de toutes les composantes organiques nécessaires à la croissance. Les variations des facteurs environnementaux et nutritionnels jouent un rôle important dans le métabolisme de ces cellules et peuvent impacter sur la production lipidique.

3.1 Facteurs environnementaux

3.1.1 Lumière

La lumière affecte fortement la croissance des microalgues puisque les réactions photosynthétiques dépendent de l'énergie lumineuse reçue par les organites photosynthétiques. La réponse des microalgues à la lumière est le résultat complexe de phénomène de régulation et d'adaptation de la chaîne photosynthétique aux flux lumineux captés. La durée d'acclimatation dépend de la souche et de l'espèce. Généralement, elle varie de quelques heures à quelques jours (7 jours). La cellule s'adapte ainsi aux changements du flux lumineux en changeant la composition et la concentration des pigments de sa chaîne photosynthétique dans

le but d'ajuster l'absorption de la lumière et la conversion de cette dernière pour la synthèse de molécules énergétiques nécessaires à son métabolisme intrinsèque. La luminosité peut varier sous forme d'intensité lumineuse et sous forme de cycle lumineux. Par exemple en condition de lumière saturante, la production lipidique augmente chez *P. tricornutum* (Huete-Ortega *et al*., 2018). Les quantités d'acide gras augmentent avec l'augmentation de l'intensité lumineuse pour *Chaetoceros gracilis* (Mortensen *et al*., 1988). Selon la littérature (Barnett et al., 2015; Brand *et al*., 1981) aucune tendance phylogénétique générale de la réponse à différents cycles lumineux ou intensité lumineuse n'a pu être discernée actuellement. Il semblerait qu'en général, les espèces des régions côtières peuvent se diviser aussi rapidement ou plus rapidement sous une lumière continue que dans un cycle jour nuit 14 :10 h, alors que la plupart des espèces des régions océaniques sont affectées par la lumière continue. Selon (Guihéneuf *et al*., 2008), la concentration de certains acides gras augmente lorsque les cellules de *Skeletonema costatum* sont soumises à un éclairement de saturation (340 µmol de photons m^{-2} s^{-1}).

3.1.2 Température

La température du milieu environnant des microalgues est également un paramètre qui présente une grande influence sur la croissance de ces dernières. En plus de son influence sur les réactions biochimiques intracellulaires (Breuer *et al*., 2013b; Converti *et al*., 2009), la température affecte l'état physiologique de la cellule. Chaque souche a une température optimale de croissance. Chez certaines souches, la température affecte le métabolisme lipidique intracellulaire. A titre d'exemple les taux d'acides gras insaturés sont plus élevés à des températures basses (18 °C) chez la diatomée marine *Chaetoceros gracilis* (Mortensen *et al*., 1988). Quand la température diminue le contenu d'acides gras polyinsaturés augmente alors que la quantité d'acides gras monoinsaturés et saturés diminue. (Pasquet *et al*., 2014) ont démontré que diminuer la température optimise l'accumulation d'EPA et de DHA dans la diatomée marine *Odontella aurita*, alors que la quantité d'acide myristique et palmitique, elle

diminue. Une telle augmentation du taux d'insaturation est un mécanisme d'adaptation qui permet à la cellule de maintenir la fluidité de la membrane lorsqu'elle est cultivée dans des conditions de basse température (Harwood, 1998).

3.1.3 pH

Les réactions biochimiques ainsi que les échanges des substrats entre l'intérieur et le milieu environnant sont hautement dépendants de la valeur du pH (Breuer *et al*., 2013b). A noter que le pH optimal pour la plupart des espèces de diatomées est compris entre 7 et 9 (Wang *et al*., 2012). Le pH joue également sur la dissolution du CO_2 dans le milieu. La variation du pH peut affecter la croissance des microalgues de nombreuses façons. Il peut modifier la disponibilité des formes de CO_2 dans le milieu, des nutriments majeurs et si il devient trop élevé, il peut potentiellement causer des dommages physiologiques (Chen and Gao, 2004). Les concentrations de CO_2, $HCO3^-$ et CO_3^{2-} et le pH sont liés. Quand le pH augmente, les carbonates diminuent (Figure. I-7).

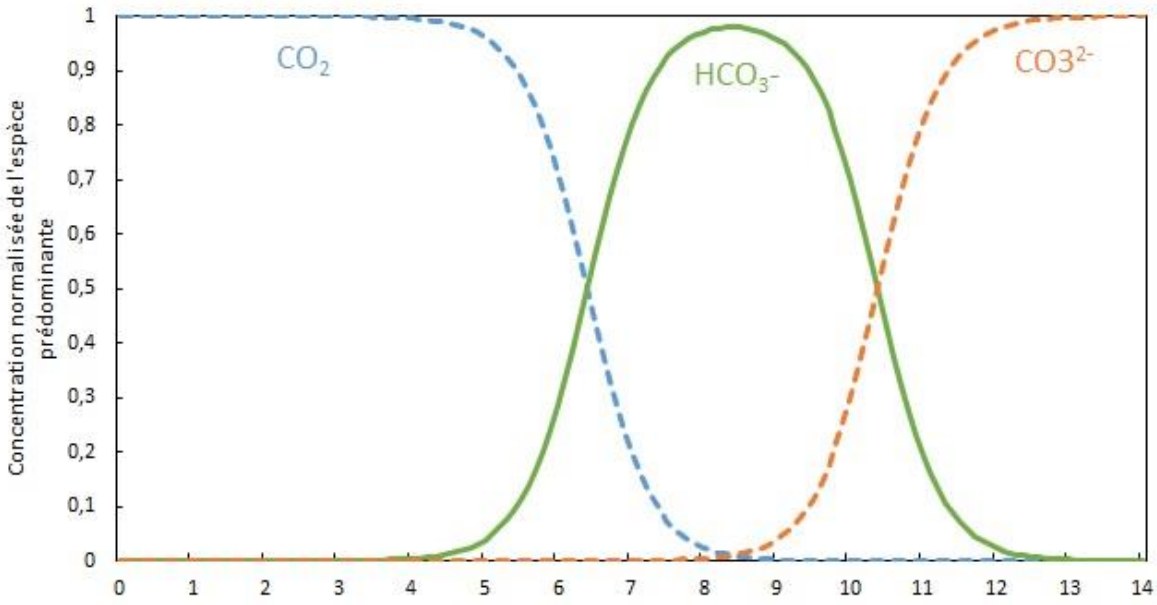

Figure I-7. Evolution des différentes espèces carbonées dissoutes en fonction du pH du milieu (Le Gouic, 2013).

3.2 Facteurs nutritionnels

3.2.1 Azote :

L'azote joue un rôle essentiel dans la synthèse de protéines, chlorophylle et d'enzymes. Il est un des constituants de la chlorophylle, organite central de la photosynthèse. Chez les diatomées, l'azote est principalement apporté sous forme de nitrates NO_3^-. Les diatomées sont aussi capables d'assimiler différentes sources d'azote dissous inorganique comme le nitrite (NO_2), et l'ammonium (NH_4^+) (Dortch, 1982; Vincent, 1992; Waser *et al*., 1998) ou des formes organiques comme l'urée (Antia *et al*., 1991; Lomas, 2004; Syrett *et al*., 1986) et des acides aminés (Antia *et al*., 1991; Flynn and Syrett, 1986; Flynn and Wright, 1986).

3.2.2 Phosphate :

Le phosphate en plus d'être un élément important pour la production de protéines, est un élément essentiel pour la division cellulaire et donc un élément de base nécessaire à la croissance des diatomées.

3.2.3 Silice

La forme principale de silice en solution est l'acide orthosilicique H_4O_4Si (Paasche and Ostergren, 1980). Chez les diatomées, l'acide silicique n'est pas capté à une vitesse constante à travers le cycle cellulaire, mais est absorbé plus rapidement durant la formation du frustule ; la silice ne se retrouve pas uniquement dans le cytoplasme, mais aussi dans des organites comme les mitochondries (Volcani, 1978). La silice est nécessaire pour les diatomées, car elle forme une majeure partie du frustule et est impliquée dans des processus métaboliques diffèrents. En cas d'absence de silice, la division cellulaire cesse, la synthèse de protéines, chlorophylle, et caroténoïdes est inhibée. La photosynthèse et la glycolyse sont réduites (Werner, 1978) la synthèse de lipides est renforcée (Roessler, 1988; Taguchi *et al*., 1987).

3.2.4 Micronutriments

Les micronutriments (K, Mg, Ca, Mn, Cu, Fe) sont indispensables à la croissance des microalgues. Certains d'entre eux interviennent au niveau des réactions biochimiques au sein de la cellule tout en remplissant des rôles de cofacteurs enzymatiques. Par exemple, le fer est un élément indispensable à la synthèse de pigment chlorophyllien. Le magnésium est un constituant des chlorophylles et toute carence d'un de ces deux éléments, affecte directement l'activité photosynthétique de la cellule. Le calcium est quant à lui un élément constitutif de la paroi cellulaire.

3.3 Facteurs technologiques

Différents systèmes de culture existent pour produire des microalgues à grande ou à petite échelle. Les systèmes ouverts sont les plus utilisés à l'échelle industrielle, mais nécessitent des espèces dominantes, robustes et extrémophiles afin d'éviter au maximum les risques de contaminations extérieures. Aujourd'hui très peu d'espèces sont cultivés de manière efficace dans ces systèmes ouverts. Les méthodes développées au cours de cette thèse ont utilisé principalement des systèmes clos. Ces systèmes consistent à cultiver les microalgues dans un milieu totalement séparé du milieu environnant. On parle alors de photobioréacteurs (PBR) (Chisti, 2007a).

3.3.1 Systèmes ouverts

Les systèmes de culture sont dits ouverts lorsqu'il n'y a pas de séparation physique entre la culture et l'environnement extérieur. Dans ces systèmes, le contrôle de la culture (pH, température en particulier) est techniquement difficile. L'évaporation du milieu n'est pas contrôlée et la culture est exposée aux contaminations extérieures.

La surface spécifique a_s (rapport entre surface et volume de culture) de tels systèmes est inférieure à 20 m^{-1} (épaisseur de culture supérieure à 5 cm), menant à de faibles productivités.

Cela est compensé usuellement par une augmentation de la taille de ces technologies. Les volumes mis en jeu dans ce type de systèmes sont alors souvent de plusieurs mètres cubes, et les surfaces peuvent aller jusqu'à plusieurs hectares.

Etant donné l'absence quasi-totale de contrôle sur ces systèmes, leur utilisation est limitée à la production de souches robustes, voire extrêmophiles. La grande majorité de ces systèmes utilise l'énergie solaire du fait de leur grande surface. Très peu de diatomées benthiques sont cultivées dans ces système, mais des études récentes ont démontré la possibilité de cultiver des souches d'*amphora coffeaformis* en raceway (Rajaram *et al*., 2018) (Figure I-8 A) et *Mayamea* sp., une diatomée résistante aux faibles températures (Matsumoto *et al*., 2017) (Figure I-8 B).

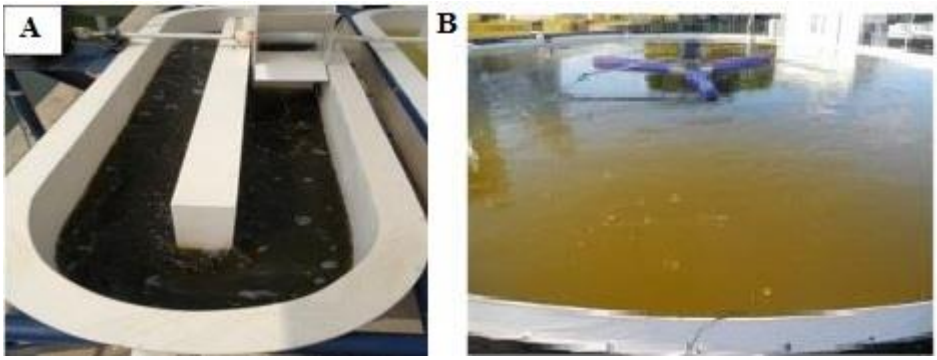

Figure I-8 Culture de *Amphora coffeaformis* en raceway (A) et de *Mayamea* sp. en bassin (B)

3.3.2 Les sytèmes clos

Par rapport aux systèmes ouverts, les systèmes clos permettent de limiter les risques de contamination et par conséquent de cultiver une seule espèce de microalgues, en environnement hautement stérile et contrôlé. Ils offrent également plus de possibilités quant aux éléments de conception (géométrie, matériaux…) et les surfaces spécifiques peuvent être largement augmentées par réduction des épaisseurs de culture, maîtrise de l'apport de lumière et contrôle de l'évaporation du milieu. L'apport de nutriments, le pH et les échanges gazeux ainsi que la température peuvent être également maitrisés. De ce fait, les PBR peuvent compenser un coût plus élevé en investissement et en exploitation par obtention d'une productivité optimisée. Les

cultures de microorganismes photosynthétiques dans les PBR clos sont donc actuellement orientées majoritairement vers la production de molécules à haute valeur ajoutée. Un PBR est donc un système clos à l'intérieur duquel se déroule, en présence d'énergie lumineuse, des interactions biologiques que l'on cherche à contrôler en maîtrisant les conditions de cultures (Figure I-9).

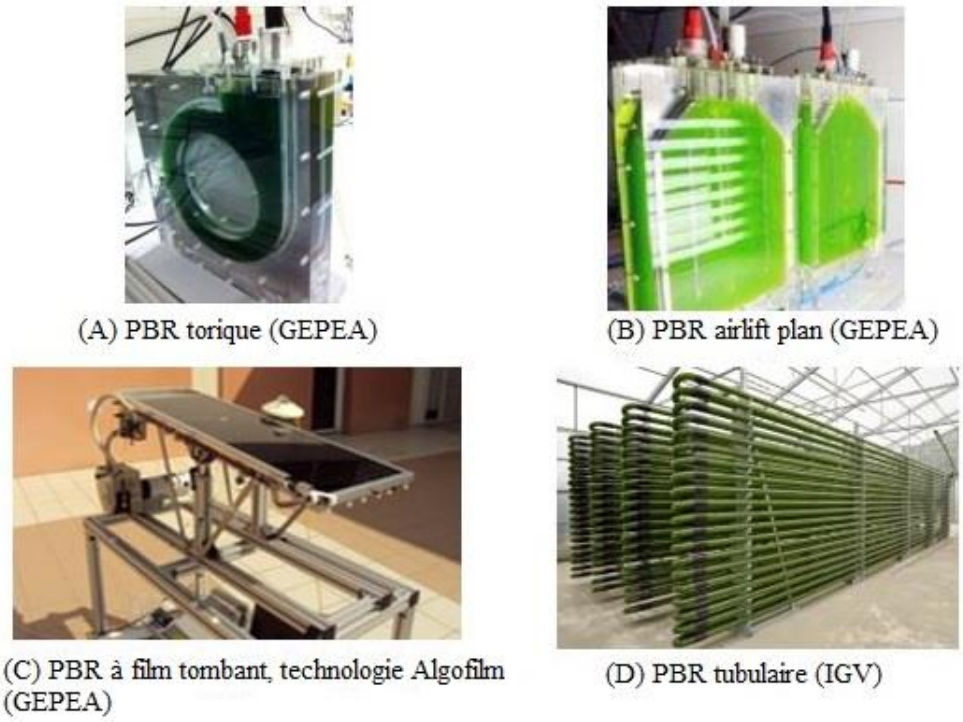

Figure I-9 Exempe de sytèmes de culture clos

4 Potentiel biotechnologique des diatomées.

4.1 La silice

Les diatomées sont les seules microalgues qui peuvent être exploitées pour leur silice. En fonction de l'espèce de diatomée et des conditions de croissance (Csögör *et al.*, 1999) ces frustules possèdent différents types de morphologies et confèrent aux diatomées un mécanisme de protection efficace (Hamm *et al.*, 2003). La silice est transportée dans les cellules par des transporteurs d'acide silicique nommé SIT. De nouveaux frustules doivent être synthétisés

avant la duplication des cellules. La silice est condensée dans des vésicules spéciales qui sont situées proche de la membrane plasmique des cellules en division, s'en suit une exocytose de l'ensemble du frustule. La silice biogénique peut être intéressante dans le domaine de la nanotechnologie. Selon (Parkinson and Gordon, 1999) le frustule peut servir d'abrasif, de déodorants, d'agent décolorant, d'agent de filtration pour purifier l'eau. La « poudre de diatomée » constituée des squelettes fossilisés de différentes espèces d'organismes unicellulaires siliceuses marines et d'eau douce, en particulier les diatomées sont utilisées comme insecticides. Le fait que la structure du frustule est dépendant de l'espèce démontre que sa production est contrôlée génétiquement et qu'il serait possible d'influencer ou même de contrôler ce processus. Cependant, à ce jour, les mécanismes génétiques impliqués dans la production de silice ne sont pas connus.

4.2 Les acides aminés

Les acides aminés à la surface de la peau humaine contribuent à l'hydratation des cellules de la couche cornée en retenant l'eau. Pour apporter de la souplesse et de l'élasticité à la peau, les produits cosmétiques contiennent des acides aminés. Ils sont présents comme substance hydrosoluble dans la couche cornée, ils agissent en tampon et aident à neutraliser les agents alcalins (Derrien *et al*., 1998). De nombreux acides aminés chez les diatomées ont montré des propriétés actives dermatologiquement qui peuvent être potentiellement utilisées dans les produits cosmétiques. Par exemple, Derrien *et al*. (1998) ont montré que l'acide aspartique, en tant qu'acide dominant, et l'isoleucine sont synthétisés par *Chaetoceros calcitrans* et *Skeletonema costatum*, la leucine produite par *C. calcitrans*, ornithine par *S. costatum*, sérine, l'acide glutamique et la tyrosine comme acides dominants par *Thalassiosira sp.* Quatre acides aminés étaient responsables de plus que 60% de la concentration totale dans toutes les espèces examinées : acide aspartique, acide glutamique, arginine et tyrosine. Taraldsvik and Myklestad, 2000 ont montré que la production d'acides aminés était dépendante du pH. La production

d'acides aminés augmentent jusqu'à un pH 8 et diminue drastiquement si cette valeur est dépassée (13.88 fmol.cell^{-1} à pH 8 *vs* 2.51 fmol.cell^{-1} à pH 9.4).

Il existe aussi des acides aminés toxiques comme l'acide domoïque, produite principalement par la diatomée *Nitzschia pungens* qui peut causer des troubles neurotoxiques et en particulier avoir des effets amnésique en agissant sur des antagonistes de l'acide glutamique (Rao *et al*., 1988). L'acide domoïque est un acide tricarboxylique ($C_{15}H_{21}NO_6$) et un antagoniste neuroexcitateur puissant du glutamate, un neurotransmetteur trouvé dans le système nerveux central. Il a longtemps été utilisé dans la médecine traditionnelle comme antihelminthique et présente des propriétés insecticides (Lincoln *et al*., 1990). Cette toxine, produite par *Nitzschia pugens forma multiseries*, a été caractérisée en 1987 au Canada (Bates *et al*., 1989) et a été impliquée dans des contaminations de coquillages et des empoisonnements d'oiseaux (Kotaki *et al*., 2000). La diatomée *Nitzschia navis-varingica* produit également de l'acide domoïque avec un rendement de 1.7 pg. cellule^{-1} ce qui est comparable aux niveau de production de *N. pugens* (Kotaki *et al*., 2000). Des conditions de cultures limitantes, par exemple, une carence en carbone, azote, phosphore ou silice peuvent conduire à une production supérieure d'acide domoïque (Pan *et al*., 1996).

4.3 Les lipides

4.3.1 Définitions des lipides

La diversité des critères utilisés pour caractériser les lipides (propriété physique, structures chimiques, fonctions biologiques) ne permet pas de dégager une classification homogène et universellement admise par l'ensemble des équipes travaillant dans ce domaine. Cependant, la distinction des classes de lipides en lipides polaires (triglycérides, hydrocarbures, stérols) et lipides neutres (glycolipides et phospholipides) semble obtenir un large consensus de la part des lipochimistes. Les acides gras (AG) sont finalement les constituants principaux des lipides puisqu'on les retrouve dans les structures chimiques des triglycérides (TG) des lipides neutres

et dans les glycolipides (GL) et phospholipides (PL) des lipides polaires. Ils seront abordés globalement dans le paragraphe sur les triglycérides.

4.3.2 Les lipides neutres

4.3.2.1 Hydrocarbures, haslène et caroténoïdes

Des effets antibactériens et antifongiques ont été établis dans toutes les classes d'algues et notamment chez les diatomées (Lincoln *et al*., 1990; Pesando, 1990; Viso *et al*., 1987). Les composés antibactériens sont généralement présents parmi un complexe d'acides gras, comme montrés par Viso *et al*. (1987) et Imada *et al*. (1992), mais la plupart des molécules actives n'étaient pas identifiées. L'activité antibactérienne de *Skeletonema costatum* a été démontrée contre des agents pathogènes en aquaculture (Naviner *et al*., 1999), ainsi la croissance d'un agent pathogène du genre Vibrio, pathogène de coquillages ou de poissons, a été inhibée. Des molécules antitumorales sont également synthétisées par les diatomées. Des extraits organiques de *Skeletonema costatum* (Bergé *et al*., 1997) et des extraits aqueux de la diatomée pennée *Haslea ostrearia* (Bergé *et al*., 1999; Rowland *et al*., 2001) ont montré des activités antitumorales in vitro contre des cellules du cancer du poumon chez l'homme et des effets anti-VIH. Wraige *et al*., (1999) ont démontré que de nouvelles molécules hautement ramifiées - les polyènes isoprénoïdes (huiles de sesterpènes polyinsaturés ou haslènes) - synthétisées par des cellules de microalgues de *Haslea ostrearia* étaient responsables de ces activités, les haslènes les plus actifs étant les plus insaturés. Les haslènes sont des hydrocarbures isoprénoïdes hautement ramifiés (HBI) insaturés en C25 qui proviennent apparemment d'un nombre relativement réduit d'espèces de diatomées (Rowland *et al*., 2001). *Haslea ostrearia* synthétise et excrète également un composé hydrosoluble, la marennine, un pigment vert bleu qui est responsable du verdissement des branchies d'huîtres (Robert, 1983).

Les diatomées ont aussi récemment été explorées comme sources de composés bioactifs tels que les caroténoïdes en raison de leur potentiel économique (Xia *et al*., 2013b) et de leur potentiel bénéfique pour la santé (Gong and Bassi, 2016). Les caroténoïdes sont des composés lipophiles de couleur jaune, orange ou rouge et sont les pigments les plus répandus dans la nature (Sasso *et al*., 2012; Varela *et al*., 2015). La plupart des caroténoïdes partagent en commun un squelette hydrocarboné C40 d'unités isoprènes nommés terpénoïdes. Les caroténoïdes, basés sur leurs structures chimiques (Figure I-10), peuvent être divisés en deux catégories :

- Les carotènes, tels que le β-carotène
- Les xanthophylles, telles que la Fucoxanthine

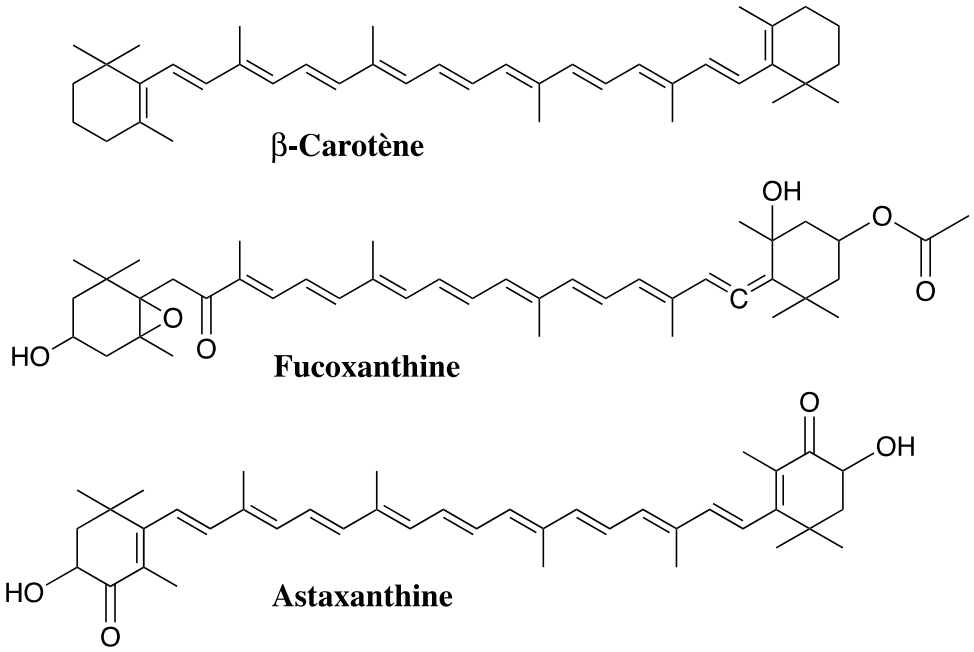

Figure I-10 Structure chimique des caroténoïdes retrouvés majoritairement chez les microalgues

Comme les caroténoïdes sont des antioxydants, ce sont des composés sensibles à la lumière, à l'oxygène et à la chaleur ce qui les rend difficiles à stocker et à manipuler.

Le β-carotène est une source primaire majeure de vitamine A nécessaire aux fonctions de la rétine et agit sur de nombreux types de tissus grâce à son action régulatrice de l'expression des

gènes (Dufossé *et al*., 2005). En outre, le β-carotène aide également à protéger la peau contre le photovieillissement grâce à son activité antioxydante (Murthy *et al*., 2005). Il a également été suggéré que la fucoxanthine pourrait avoir des effets bénéfiques sur la santé chez les humains, notamment des effets anticancéreux, anti-obésité et antidiabétiques, ainsi qu'une activité antipaludique (Peng *et al*., 2011). La demande de caroténoïdes synthétisés naturellement, y compris la fucoxanthine sur le marché mondial a augmenté de façon spectaculaire (Vílchez *et al*., 2011). À l'heure actuelle, la fucoxanthine est principalement produite à partir d'algues brunes comestibles, qui contiennent moins de 1,0 mg/g de poids sec (Xiao *et al*., 2012). Comparativement aux algues, les diatomées telles que *Phaeodactylum tricornutum* sont généralement riches en fucoxanthine dans des conditions contrôlées et pauvres en iode, ce qui en fait d'excellentes candidates pour la production de fucoxanthine (Fu *et al*., 2015). Comparées aux plantes supérieures, les microalgues ont un contenu en caroténoïde spécifique plus élevé. L'astaxantine et le β-carotène peuvent atteindre 50 mg/g dans des conditions de cultures spécifiques des microalgues (Kyriakopoulou *et al*., 2015; Suh *et al*., 2006).

4.3.2.2 Les triacylglycérols

Les triacylglycérols (aussi appelés triacylglycérides, triglycérides ou TAG) sont des glycérides dans lesquels les trois groupes hydroxyle du glycérol sont estérifiés par des acides gras. Ils sont les constituants principaux des graisses animales et de l'huile végétale.

Les huiles de microalgues sont similaires à celles des poissons et des huiles végétales et peuvent donc être considérées comme des sources potentielles pour la production d'huile fossile. Dans les années 1940, des fractions lipidiques représentant 70-85% du poids sec ont été répertoriées dans les microalgues (Iwamoto *et al*., 1955; Spoehr and Milner, 1949). Néanmoins seulement quelques auteurs ont reporté une valorisation des lipides possible à partir des diatomées (McGinnis *et al*., 1997; Sriharan and Sriharan, 1990).

Dans leurs profils d'acides gras, les diatomées sont enrichies d'acides gras à chaîne moyenne ainsi que d'acides gras polyinsaturés à chaîne très longue supérieur à 20C (AGPI-LC), ce qui n'est généralement pas le cas des chlorophytes ni des plantes à fleurs (Guschina and Harwood, 2006). Les acides gras prédominants dans les diatomées sont l'acide myristique (14:0), l'acide palmitique (16:0), l'acide palmitoléique (16:1), le DHA (22 :6) et l'EPA (20: 5). Les acides gras en C18 ne sont habituellement présents qu'à l'état de traces (tableau. 2). Pour la production de biocarburants, les acides gras à chaîne moyenne sont préférables puisqu'ils donnent un biodiesel moins visqueux (Merz and Main, 2014). En outre, la plupart des diatomées ont des teneurs élevées en acide arachidonique AGPI-LC (ARA, 20:4 ω6) et en acide eicosapentaenoïque (EPA, 20: 5 ω3) (Armbrust *et al*., 2004; Hemaiswarya *et al*., 2011; Lebeau and Robert, 2003; Merz and Main, 2014; Ramachandra *et al*., 2009; Spolaore *et al*., 2006) (Figure. I-11).

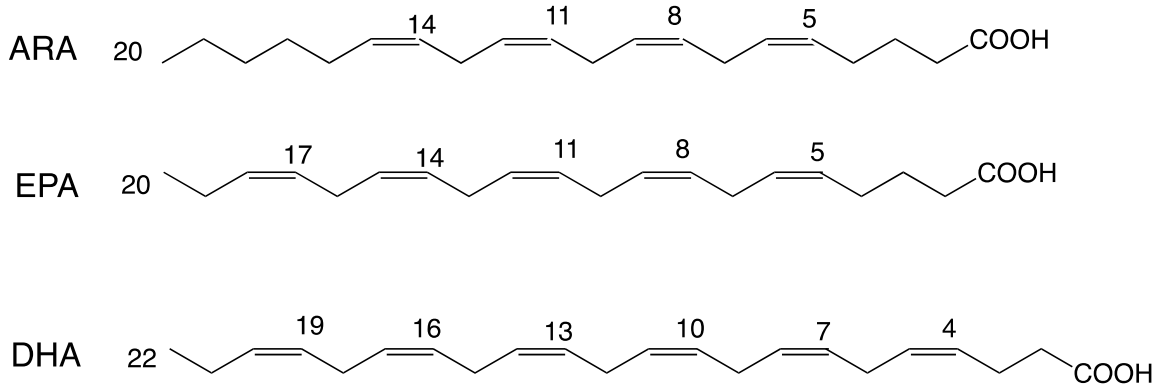

Figure I-11 structure chimique de l'acide arachidonique ARA, de l'acide eicosapentaenoïque (EPA) et de l'acide docosahexaenoïque (DHA).

Skeletonema menzelii et *P. tricornutum* sont des espèces potentielles pour la production commerciale d'EPA et de DHA (Yi *et al*., 2017). Les AGPI-LC sont des acides gras essentiels utilisés dans les industries pharmaceutiques et neutraceutiques. Selon les conditions de croissance, l'âge de culture, etc., les acides gras essentiels ω3 peuvent être contenus dans les triacylglycérols (TAG) en proportions variables d'une espèce à l'autre (Tonon *et al*., 2002).

Selon l'application finale, les TAG peuvent être modifiés pour contenir des niveaux élevés d'acides gras à chaîne moyenne, qui sont plus facilement solubilisables et ont une résistance à l'oxydation, ou peuvent être modifiés pour avoir des niveaux élevés d'AGPI-LC (Yi *et al*., 2017; Zulu *et al*., 2018)

De nombreuses algues sont capables de produire des AGPI-LC, les plus importants pour la santé humaine sont l'acide eicosapentaénoïque (EPA) et l'acide docosahexaénoïque (DHA). Le DHA est un acide gras avec six insaturations et l'EPA un acide gras à cinq insaturations (tableau I-2).

Tableau I-2 Lipides valorisable chez les diatomées

Classe lipidique	composition	représentation	Bioactivité	références
Acide gras	HTA*	16 :3 (n-3)	Antibactérienne	[2-3]
	Acide palmitoléique	16 :1 (n-7)	Antibactérienne	[3], [4], [7]
	Acide stéarique	18 :0	Antimicrobienne	[4], [6]
	Acide ruménique	18 :2 (n-7)	Antimicrobienne	[4], [6-7]
	EPA	20 :5 (n-3)	Anticancéreux, antibactérien, anti-inflammatoire	[4-5], [7]
	DHA	22 :6 (n-3)		[5], [8]
TAG	TAG		Biodiesel	[1]

*Acide Hexadecatrienoique (HTA), d'Ippolito *et al*., 2015 [1]; Desbois *et al*., 2009, 2008 [2,3]; Desbois and Smith, 2010 [4]; Hallahan and Garland, 2005 [5]; Jiang *et al*., 2016 [6]; Kabara *et al*., 1972 [7]; Lafourcade *et al*., 2011 [8]

Le DHA joue un rôle important dans le corps humain, en effet, la matière grise de notre cerveau en est composée à 20 %. Une quantité importante est également présente dans la rétine, nous sommes cependant incapables de produire cette molécule nous-même (Sastry, 1985). Les sources actuelles de DHA sont les huiles de poisson et la viande animale. Il a été démontré que les diatomées telles que *Chaetoceros brevis* et *Thalassiosira weissflogii* peuvent produire du DHA (Boelen *et al*., 2013).

La molécule la plus étudiée est l'acide eicosapentaénoïque (EPA, C20:5 ω3) qui appartient à la catégorie des acides gras polyinsaturés (AGPI). Il a été démontré que l'EPA prévient les maladies coronariennes, l'hyperglycémie, diminue le cholestérol dans le sang, ce qui réduit les risques d'inflammation et de sclérose des artères (Ruxton *et al*., 2004; Swanson *et al*., 2012).

La demande en EPA est d'environ 125 tonnes au Japon et dans le monde entier elle est estimée à 300 tonnes par an (Sánchez Mirón *et al*., 1999). La principale source commerciale d'EPA se situe dans les huiles de poisson et dans les viscères animaux. Les huiles de poisson représentent une source inférieure et inadéquate due à la diminution des populations de poissons, aux variations géographiques et saisonnières impactant la qualité de l'EPA (Varela *et al*., 2015). Il a été démontré que l'EPA provenant des microalgues est de meilleure qualité et plus stable (Belarbi *et al*., 2000). Les diatomées pourraient être une source alternative en EPA. Cette molécule est produite par différentes espèces de diatomées appartenant au genre *Nitzschia*, *Navicula* et *Phaeodactylum* (Borowitzka, 2013; Wen and Chen, 2000). Les diatomées sont une source potentielle d'EPA, car elles poussent vite et produisent en petite quantité d'autres AGPI tel que le DHA et l'acide arachidonique (ARA, 20 :4 ω6), ce qui facilite la récupération des composants (Robles Medina *et al*., 1999). Cependant la production d'EPA est plus faible chez les microalgues par rapport aux bactéries et aux champignons (Bajpai and Bajpai, 1993). Ceci est dû à des taux de croissance faible en conditions photoautotrophes. L'optimisation des capacités de croissance des souches est le meilleur moyen pour rendre les microalgues compétitives en terme de coût.

Alors que l'EPA a été largement étudié, l'acide arachidonique (ARA, 20:4 ω6), un acide gras essentiel, a été beaucoup moins étudié malgré son rôle important en nutrition humaine ; c'est un précurseur de l'activité biologique des prostaglandines et des leucotriènes et un des composants du lait humain (Koletzko *et al*., 1996). Les microalgues peuvent être une alternative aux viscères d'animaux ou aux champignons dans lesquels ce composé est majoritairement prélevé.

4.3.2.3 Les stérols

Les diatomées ont été les plus étudiées en ce qui concerne la composition des stérols. Rampen *et al*, 2010 ont identifié parmi 100 souches, 44 stérols dont 11 sont présents à un niveau supérieur à 10 %. Les stérols sont le plus souvent utilisés comme marqueurs chimiotaxonomique et phylogénétique, car ils peuvent être caractéristiques d'une classe, d'une famille, d'un genre ou même d'une espèce. Les cinq stérols les plus souvent rencontrés chez les diatomées sont décrits dans la Figure I-12. Un certain nombre d'études ont montré que le diatomsterol (24-methylcholesta-5,22-dien-3β-ol) est présent dans plus de la moitié des espèces de diatomées pennées connues (Rampen *et al*., 2010). Les stérols avec une méthylation en C-23 sont aussi produits par différentes espèces de diatomées (Rampen *et al*., 2009). La majorité des diatomées qui ont été étudiées contiennent des stérols C_{28} mais des stérols en C27 ou C29 peuvent être majoritaires dans certains groupes phylogénétiques. Les stérols peuvent avoir des activités cytotoxiques, anti-inflammatoires, antitrypanosomales et antimicrobiennes (Viegelmann *et al*., 2014).

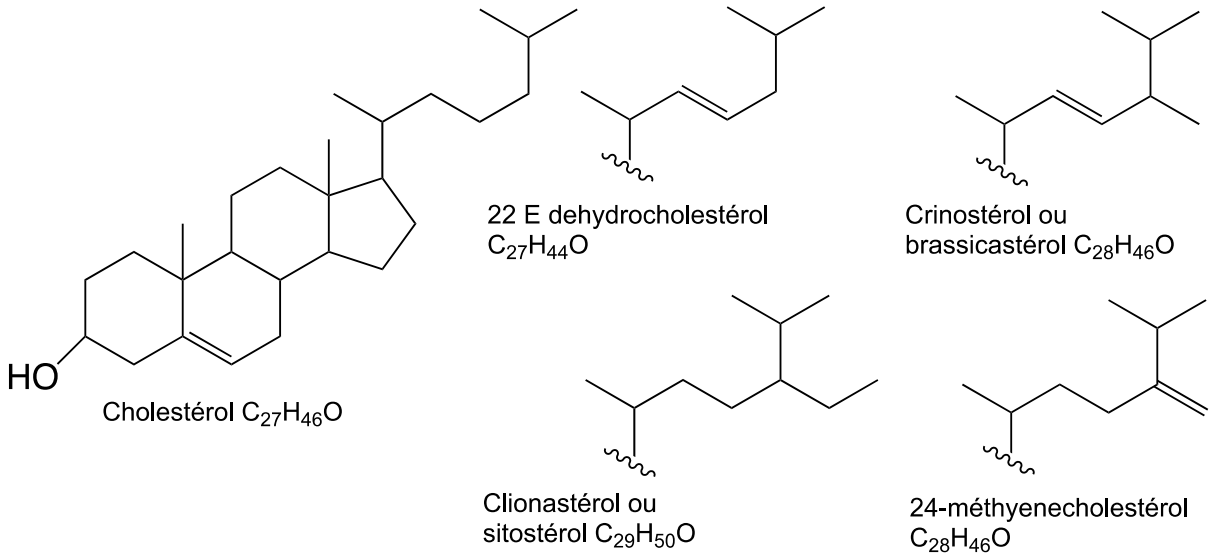

Figure I-12 Structure des stérols majoritaires retrouvés chez les diatomées.

4.3.3 Lipides polaires

4.3.3.1 Glycolipides

Les lipides polaires majoritaires chez les diatomées sont le monogalactosyldiacylglycerol (MGDG), le digalactosyldiacylglycerol (DGDG) et le sulfoquinovosyldiacylglycerol (SQDG). Les glycolipides sont des composants importants localisés principalement dans les chloroplastes, ils possèdent également des activités antivirales, antibactériennes et anti-inflammatoires (Plouguerné *et al*., 2014). Les glycolipides constituent une voie de valorisation intéressante des diatomées. En effet, les glycolipides végétaux sont impliqués dans le processus photosynthétique et à ce titre se distinguent par leur nature des glycolipides animaux ou d'organismes chimioorganotrophes. La présence d'AGPI-LC confère aux microalgues une spécificité forte. L'absence de certains glycolipides dans le domaine des réactifs biochimiques conjuguée à une demande croissante de ces composés, en particulier du sulfoquinovosyldiacylglycérol (SQDG), peut représenter une voie de valorisation à court ou moyen terme. Par ailleurs, le SQDG suscite un vif intérêt en recherche médicale soutenue par l'industrie pharmaceutique, dans la mesure où des activités anti-VIH ont été mises en évidence (Pham and Durand-Chastel, 2003). La Figure I-13 présente les différentes structures de glycolipides rencontrées chez les diatomées.

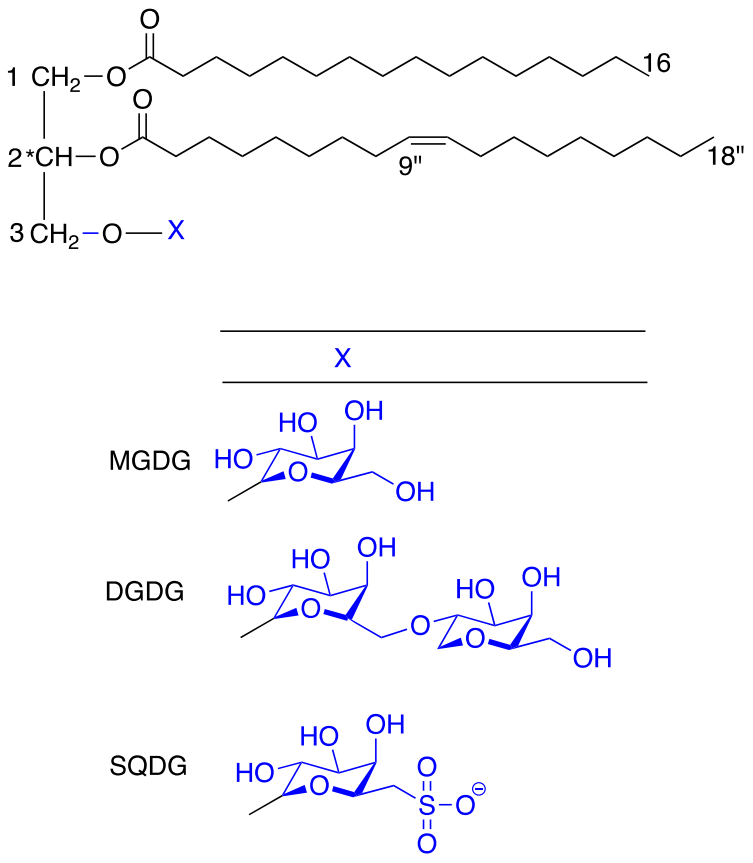

Figure I-13 Structure du monogalactosyldiacylglycérol (MGDG), digalactosyldiacylglycérol (DGDG) et sulfoquinovosyldiacylglycérol (SQDG)

4.3.3.2 Phospholipides

Les phospholipides sont des composés universels des membranes cellulaires qui peuvent être utilisés dans l'alimentaire, la cosmétique et en industrie pharmaceutique pour leur rôle de porteurs d'AGPI (Yi *et al*., 2017). Ces lipides font aujourd'hui l'objet d'une commercialisation importante sous le terme de lécithine qui est un terme générique désignant un mélange de phospholipides à degré de pureté variable. Les applications industrielles des lécithines sont diverses. En effet, les lécithines sont très utilisées en industrie alimentaire en qualité d'auxiliaire technologique, et le soja est l'une des principales sources qui ne nécessite pas de caractérisation de pureté. Leur double polarité hydrophile et hydrophobe, leur confèrent la propriété d'être de bons vecteurs d'acides gras à principes actifs (liposomes, nanoémulsions). Les phospholipides

majoritaires chez les diatomées sont la phosphatidylcholine (PC), la phosphatidylinositol (PI), la phosphatidylsulfocholine (PG) ainsi que le 1-deoxyceramide-1-sulfate et le phosphatidylsulfocholine en quantité plus faible (Anderson *et al*., 1978) (Figure. I-14).

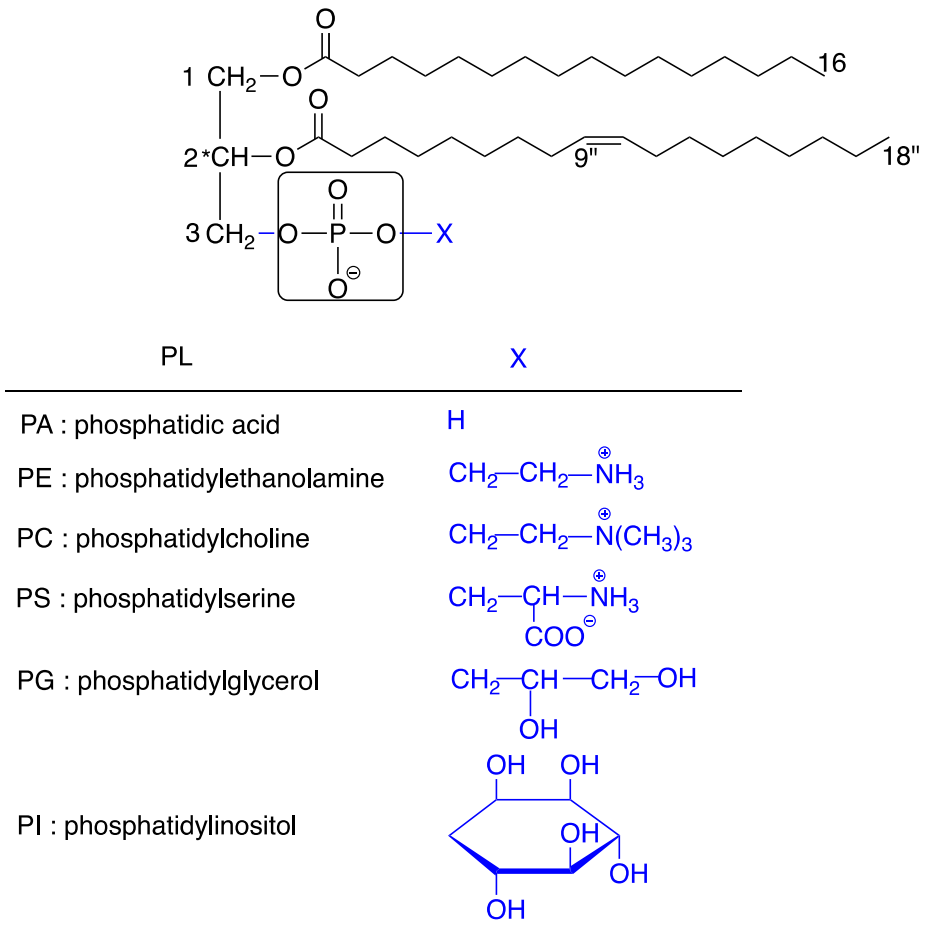

Figure I-14 Structure des phospholipides majoritairement rencontrés chez les diatomées

Les AGPI estérifiés à ces phopholipides confèrent aux microalgues une spécificité intéressante et prometteuse au regard d'autre source. En effet, les phospholipides (notamment la phosphatidylcholine) à estérification en AGPI de type acide AA ou DHA proviennent principalement de sources animales (cerveau de bovins, foie de porc, extrait placentaire) qui sont rejetés en raison des risques liés aux protéines protéases résistantes (EBS, Creutzfeld-Jacob).

5 Le métabolisme lipidique

Nos connaissances sur la manière dont la biosynthèse et le métabolisme des lipides sont organisées, et même régulées chez les diatomées sont encore très limitées par rapport aux animaux, aux plantes ou aux microalgues vertes (Guschina and Harwood, 2006). Des voies eucaryotes et procaryotes de la biosynthèse des lipides ont été identifiées dans les diatomées, comme c'est le cas des plantes à fleurs.

5.1 La synthèse d'acide gras

La synthèse d'acide gras chez les diatomées a lieu dans les plastes ou la malonyl-Coenzyme A (malonyl-CoA) est utilisée comme un substrat (Figure I-15). Grace à l'activité de l'enzyme acide gras synthase (FAS), l'acide gras couplé à la protéine porteuse d'acyle (ACP) est mélangé à travers différentes sous-unités de l'enzyme FAS. Une série d'étapes de condensation et d'élongation catalysées par FAS abouti à la formation de LC-acyl-ACP (principalement 16:0-ACP et 18:0-ACP), qui sont ensuite utilisés dans diverses autres étapes. Les acides gras synthétisés peuvent entrer dans deux voies de synthèse lipidique – la voie procaryote ou eucaryote. Dans le premier cas, les acides gras sont retenus dans le plaste et se lient au glycérol-3-phosphate (G3P), qui subit une estérification en acide lysophosphatidique (lyso-PA), acide phosphatidique (PA) et diacylglycerol (DAG). Enfin, le DAG est incorporé dans les lipides membranaires. Quand les acides gras entrent dans la voie eucaryote, l'acyl-coenzyme A (acyl-CoA) est d'abord hydrolysée par les thioestérases et canalisée vers le pool d'acyl-CoA dans le cytosol par un mécanisme non identifié à ce jour. Les acyl-CoA peuvent également être désaturées et entrer dans diverses voies « eucaryotes » du métabolisme des lipides à la membrane du réticulum endoplasmique. Celles-ci comprennent la formation de AGPI-LC (VLC-PUFA en anglais) et la biosynthèse de TAG, qui est déposée dans des gouttelettes lipidiques.

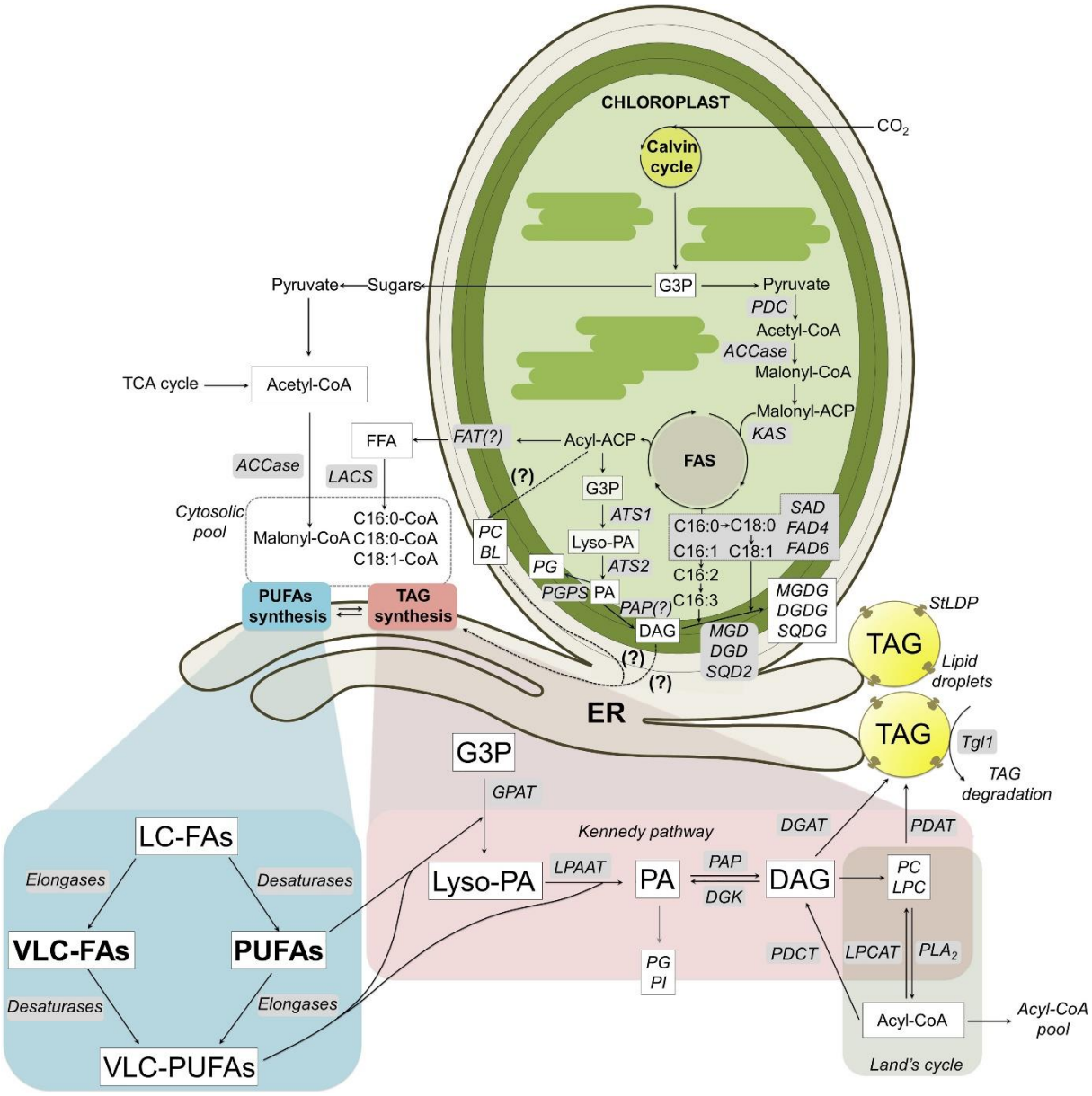

Figure I-15 Représentation schématique des voies de biosynthèses des acides gras ainsi que des voies majeures du métabolisme lipidique dans une cellule de diatomée **(Zulu *et al*., 2018)**

5.2 La synthèse des triglycérides

La synthése des AGPI-LC dans le réticulum endoplasmique commence par la désaturation d'acide oléique plastidique 18 :1 (n-9) en acide linoléique 18 :2 (n-6) qui peuvent entrer dans les voies ω3 ou ω6 (Figure I-16). Une série d'étapes de désaturation et d'élongation aboutit à la formation de AGPI-LC tels que l'acide arachidonique 20 :4 ω6, l'EPA 20 :5 ω3 ainsi que le DHA 22 :6 ω6. Les AGPI-LC nouvellement formés en tant que coenzyme A peuvent être

exporté vers le plaste et incorporées dans les galactolipides. En tant que résidents dans le réticulum endoplasmique, les AGPI-LC pourraient entrer dans le cycle des lands et échanger leurs groupes polaires avec les diacylglycerol (DAG) « procaryotes » et servir de substrat pour les phospholipides : diacylglycerol acyltransferase (PDAT), qui les convertissent en TAG. Alternativement, les AGPI-LC peuvent entrer dans la voie Kennedy et comme les DAG eucaryotes sont converties en TAG par les enzymes acyl-CoA: diacylglycerol acyl transferase (DGAT). Les AGPI-LC contenant des TAG sont emballés dans des gouttelettes de lipides (LD).

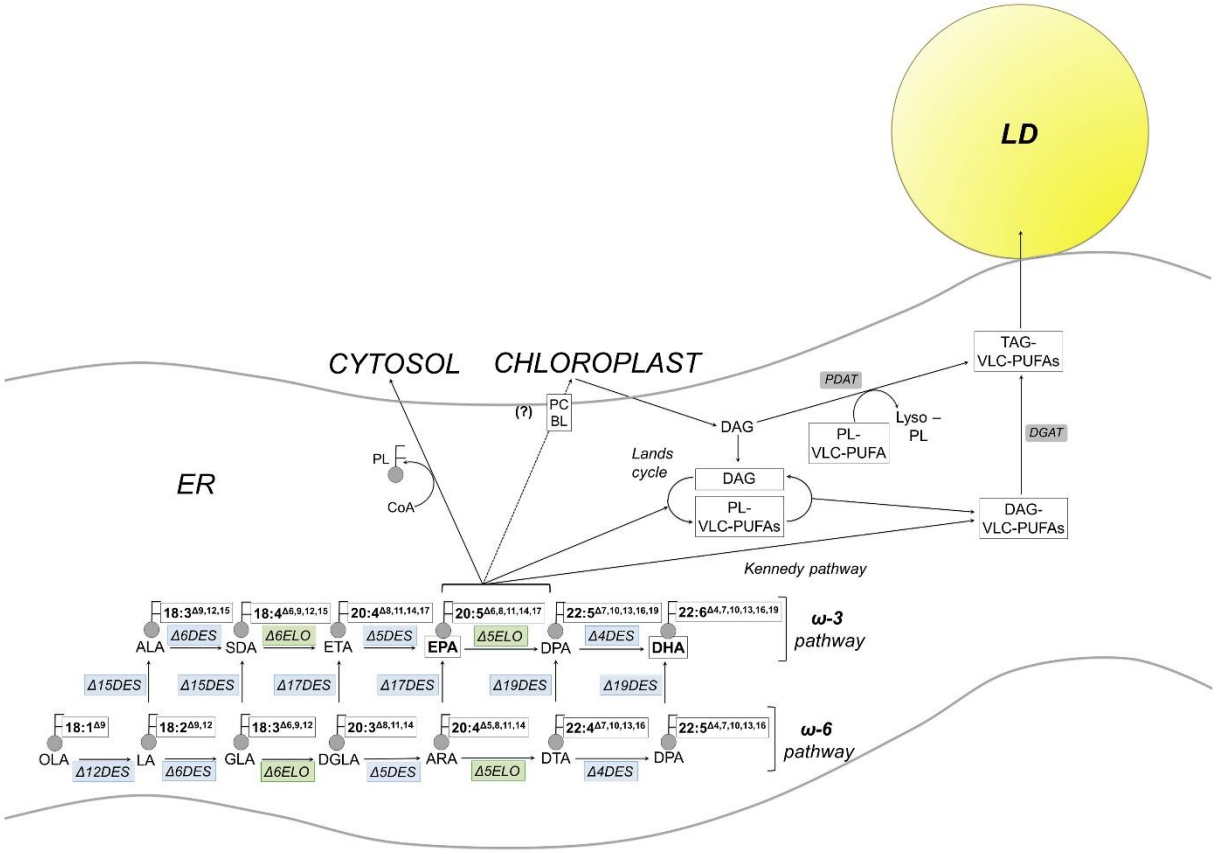

Figure I-16 Représentation schématique de la voie de biosynthèse des triglycérides dans une cellule de diatomée **(Zulu *et al*., 2018)**.

5.3 Facteur stimulant la production de lipides

Sous des conditions de croissance optimales, les microalgues absorbent et utilisent le carbone en condition de prolifération cellulaire et produisent des petites quantités de lipides. Ceux-ci sont essentiellement constitués de phospholipides et de glycolipides, constituants structuraux et fonctionnels des membranes cellulaires. Le taux de triglycérides, qui possède un rôle principal de réserve, est alors très faible. Les microalgues peuvent être soumises à des conditions de stress sous forme de stimulis environnementaux physiques (intensité lumineuse, température) ou chimiques (pH, salinité, limitation en nutriments: azote, phosphate, sulfate ainsi que la silice pour les diatomées), ou plus simplement en phase de vieillissement de culture (Chisti, 2007b; Hu *et al*., 2008; Van Vooren *et al*., 2012). Dans ce cas, une accumulation de réserves carbonées (carbohydrates) ou de lipides, s'il s'agit de microalgues oléagineuses, est généralement observée. Cependant, ces conditions spécifiques ont un impact négatif sur le développement photosynthétique. La limitation en azote est ainsi le facteur nutritionnel limitant le plus fréquemment rapporté pour mener à une accumulation majeure des lipides intracellulaires. Il s'en suit une modification importante du contenu en lipides, en qualité et quantité, en déplaçant le métabolisme lipidique vers la formation et l'accumulation de lipides surtout sous la forme de triglycérides qui peuvent représentent jusqu'à plus de 80% des lipides totaux. De nombreuses études sont disponibles sur le sujet (Breuer *et al*., 2012; Chisti, 2007b; Hu *et al*., 2008; Pruvost, 2011; Pruvost *et al*., 2009; Rodolfi *et al*., 2009). Il en résulte donc une induction de nombreux changements physiologiques dans les microalgues, concomitants avec l'accumulation progressive de lipides. Il y a ainsi une augmentation soudaine du contenu en sucre qui diminue puis demeure constant durant le reste de la culture, et une chute significative de la teneur en protéines (Breuer *et al*., 2012; Pruvost, 2011). En cas de suffisance en azote, le taux de fixation du carbone photosynthétique est de sept à dix fois celui de l'assimilation de l'azote. Sous une limitation en azote, la photosynthèse se poursuit à un taux réduit. En effet, dans les phases

initiales d'une telle carence, avant que la capacité photosynthétique ne soit significativement diminuée, la fixation de carbone est en déséquilibre par rapport à l'assimilation limitée de l'azote pourtant nécessaire à la croissance des microalgues. L'excès de carbone qui en est issu est détourné de la synthèse des protéines dans des composés de stockage tels que les glucides ou les lipides pour les microalgues oléagineuses. Cette accumulation a pour conséquence un stockage du carbone sous forme de triglycérides en réponse au stress qui a également un rôle régulateur au niveau de l'énergétique cellulaire. En effet, en conditions de stress, il y a un excès des électrons qui s'accumulent au niveau de la chaîne photosynthétique de transport d'électrons ce qui mène à une surproduction d'espèces réactives de l'oxygène, qui peuvent provoquer une inhibition de la photosynthèse et des dommages aux lipides membranaires, aux protéines et à d'autres macromolécules. Dans ces conditions, l'induction de la formation des acides gras C18 qui est hautement consommatrice de NADPH, H+ régule la chaîne de transport d'électrons. Il est à noter que cette voie de biosynthèse de triglycérides est généralement coordonnée avec la synthèse des caroténoïdes secondaires dans les microalgues. Ces caroténoïdes (la lutéine et l'astaxanthine chez les chlorophytes) sont estérifiés avec les TAG et séquestrés dans les corps lipidiques cytosoliques. Ils ont un rôle protecteur en réduisant l'excès de lumière frappant le chloroplaste. De plus, cette voie constitue un réservoir de galactolipides et d'acides gras toxiques alors exclus de la membrane en les maintenant sous forme de TAG (Hu *et al*., 2008)

6 Sélection de souches de microalgues

Il existe beaucoup de collections de microalgues à travers le monde, ces algothèques sont répertoriées au sein du World data center for Organisms. Cependant, la Nantes culture collection (NCC) sur laquelle se base cette thèse est la seule collection contenant principalement des diatomées benthiques représentatives de la biodiversité des vasières du littoral atlantique. Le choix d'une souche potentielle pour des applications biotechnologiques dépend de plusieurs critères. Le choix et la mise en culture d'une souche de microalgues qui permettent à la fois

d'obtenir un taux de croissance satisfaisant et un contenu intéressant sur le marché incarnent des critères essentiels. La souche sélectionnée doit posséder autant que possible les caractéristiques suivantes :

1) Productivité élevée de biomasse ;
2) Production élevée du produit valorisé ;
3) Capacité élevée de fixation du $C0_2$ en autotrophie ;
4) Capacité élevée d'utilisation de la lumière en autotrophie ;
5) Capacité de dominance sur les espèces indigènes en système ouvert ;
6) Tolérance à une large gamme de températures suivant les variations diurnes et saisonnières.

Il est extrêmement difficile à ce jour de sélectionner une souche qui réponde à l'ensemble de ces critères. Le choix d'une espèce se fait d'abord en sélectionnant des espèces ayant un taux de croissance cellulaire rapide, pour permettre d'atteindre une forte productivité en biomasse. Ensuite selon le mode de culture et le produit ciblé, d'autres critères entrent en considération : La souche doit être résistante aux conditions de cultures imposées et à la contamination.

Les méthodes de sélection actuelle prennent du temps et sont difficiles à mettre en place, c'est pourquoi durant cette thèse nous nous sommes intéressés à des méthodes de sélection à haut débit aussi bien pour identifier la rapidité de croissance des souches et leur contenu lipidique dans ce cas précis.

7 Conclusion

Depuis les années 1980 l'intérêt des microalgues pour leur potentiel biotechnologique est grandissant (Becker, 1994; Borowitzka, 2013; Chen and Jiang, 2013; Chew *et al*., 2017a; Chisti, 2007b; Larkum *et al*., 2012; Pulz and Gross, 2004; Rodolfi *et al*., 2009). Les applications varient de la production de biomasse destinée à l'alimentation humaine et animale à la production de molécules d'intérêts pour des applications en santé, nutrition, cosmétique et pharmaceutique (Kay and Barton, 1991). Pour la plupart de ces applications, le marché continue de se développer, et ceci avec avec un nombre réduit de souches microalgales expoitées au regard de l'énorme biodiversité de ce groupe de micro-organismes (Davidovich *et al*., 2015). La diversité des microalgues représente l'une des voies les plus prometteuses en matière de découvertes de nouveaux produits et d'applications innovantes.

Le succès de la biotechnologie algale repose principalement sur la sélection de souches possédant des propriétés pertinentes pour des conditions de cultures et la production de produits spécifiques. Un certain nombre de souches de microalgues modèles sont actuellement utilisées pour des applications biotechnologiques, mais les diatomées le sont très peu et représentent un vivier sous-exploité.

La première utilisation notable de diatomée pour une application biotechnologique a été l'utilisation de biomasse fossile pour l'absorption de la nitroglycérine pour créer de la dynamite par Alfred Nobel (Hungerford, 1988).

Les diatomées représentent probablement les producteurs les plus importants de biomasses sur Terre et sont capable d'accumuler des lipides. En raison de leur forte productivité et l'accumulation de lipides, les diatomées représentent une source future pour la production de carburant et d'acides gras originaux (Fu *et al*., 2015; Vílchez *et al*., 2011; Vinayak *et al*., 2015). La thématique de recherche attachée aux diatomées marines benthiques et à leurs productions lipidiques au sein du laboratoire Mer Molécule Santé débute avec ce travail. La Nantes Culture

Collection (NCC), une collection de diatomées marines benthiques conservées au sein du laboratoire depuis plus de 15 ans n'avait encore pas fait l'objet de telle recherche. L'intérêt mondial grandissant pour la découverte de nouvelles souches de microalgues productrices de molécules d'intérêt a motivé ce travail.

La première étape a consisté à mettre en place une méthode de criblage à haut débit pour identifier rapidement les souches avec un potentiel biotechnologique.

Ce criblage a consisté en un premier stade de pré-criblage afin d'identifier dans la littérature les genres et espèces hébergés par la NCC déjà étudiés ou criblés pour leurs potentiels oléagineux, ainsi que ceux inconnus afin de combler le manque de connaissance sur ce groupe.

Ainsi, seuls les genres et espèces non mentionnés dans la littérature pour leur potentiel lipidique et les genres décrits, mais possédant un fort potentiel oléagineux, ou producteurs de molécules originales, ont été sélectionnés pour l'étape de criblage. Le deuxième stade a consisté à la caractérisation du taux de croissance et du taux de lipides des souches sélectionnées dans l'étape de pré-criblage. L'ensemble des résultats de l'étape de criblage sont présentés dans le chapitre suivant.

II- Criblage et sélection rapide des souches de diatomées marines benthiques riches en lipides

Résumé

Ce chapitre présente la méthodologie mise en place pour sélectionner les souches de diatomées benthiques pour la production de lipides d'intérêts. La première partie de ce chapitre comprend une introduction générale précisant la nécessité de développer des procédures innovantes et robustes de criblage de souches. La procédure de criblage ainsi que les différents critères pris en compte pour sélectionner les genres criblés sont expliqués et détaillés dans la deuxième partie. La troisième partie est consacrée à la description des genres présents dans la NCC et fait le point sur les connaissances actuelles existantes au sein de chacun de ces genres. La quatrième partie est consacrée à la description de la méthodologie mise en place pour cultiver, suivre et caractériser les souches sélectionnées. Les résultats obtenus ont fait l'objet d'une publication dans Algal Research et sont présentés à la fin de ce chapitre.

1 Introduction

Depuis une vingtaine d'années, de nombreuses études se sont intéressées à identifier de nouvelles souches de microalgues capables de croître rapidement et d'accumuler un fort contenu lipidique pour des applications en pharmaceutique, cosmétique et pour la production de biocarburants alternatif (d'Ippolito *et al*., 2015; Doan *et al*., 2011; Dunstan *et al*., 1993; Joseph *et al*., 2017; Renaud *et al*., 1999; Volkman *et al*., 1989;F.-Y. Zhao *et al*., 2016). Au sein des microalgues, les diatomées représentent une ressource très accessible puisqu'on les retrouve dans de nombreux habitats (rivière, océans, zone cotière). Les diatomées marines peuvent croître rapidement et stocker de grandes quantités de lipides (Niu *et al*., 2013). Cependant, les diatomées sont très peu étudiées actuellement et constituent un vivier de ressources inéxploité (Gross, 2012). Il est donc nécessaire de développer des techniques de bioprospection afin d'évaluer le potentiel de ces espèces. L'approche de séléction employée dans ce travail s'est concentrée sur l'identification de souches de diatomées pouvant être cultivées à grande échelle et produisant des composés à haute valeur ajoutée.

La Nantes Culture Collection n'ayant jamais fait l'objet de tels travaux auparavant, il a été nécessaire dans un premier temps d'établir une sélection des souches par la littérature pour faire le point sur les connaissances et les utilisations actuelles des souches conservées. Le taux de croissance et le taux de lipides des souches sélectionnées lors de cette étape de pré-criblage ont été évalués dans un second.

La description détaillée de la procédure de criblage est présentée dans le paragraphe suivant.

2 Procédure de criblage

L'approche globale de la procédure de criblage est présentée dans la Figure II-1. L'étape (1) est une étape de pré-criblage correspondant à l'analyse bibliographique des souches conservées dans la collection. Les souches qui ont été sélectionnées sont celles qui ont été peu ou pas décrites dans la littérature et celles possédant un potentiel intéréssant mais étant encore sous-exploités. Les espèces qui n'ont pas été sélectionnées sont celles qui sont décrites comme ayant un potentiel faible de production, une absence de production de molécules à hautes valeurs ajoutées et les espèces déjà décrites et cultivées à grande échelle qui sont sur-représentées dans la littérature.

L'étape de criblage (2) a consisté en la caractérisation du taux de croissance et du taux lipidique des souches sélectionnées en utilisant des techniques rapides, fiables et innovantes. Lors de cette étape, les souches sont cultivées en erlenmeyer de 150 mL, à 16°C sous un flux de lumière continue. Le taux de croissance a été caractérisé en mesurant la fluorescence minimal F0 et le taux de lipides par l'utilisation de la technologie FTIR-HTSXT qui sera présentée par la suite. Les souches possédant un fort taux de croissance et/ou un fort taux de lipides ont été conservées pour l'étape (3) correspondant au criblage approfondi des souches. Cette étape a consisté en la réalisation de test de croissance et de production lipidique des souches en PBR airlift plan de volume 1L qui seront décrits et présentés dans le chapitre 3. Il faut noter que ce volume relativement plus important a permis de caractériser finement le contenu lipidique des souches et ainsi de valider la production de molécules à hautes valeurs ajoutées.

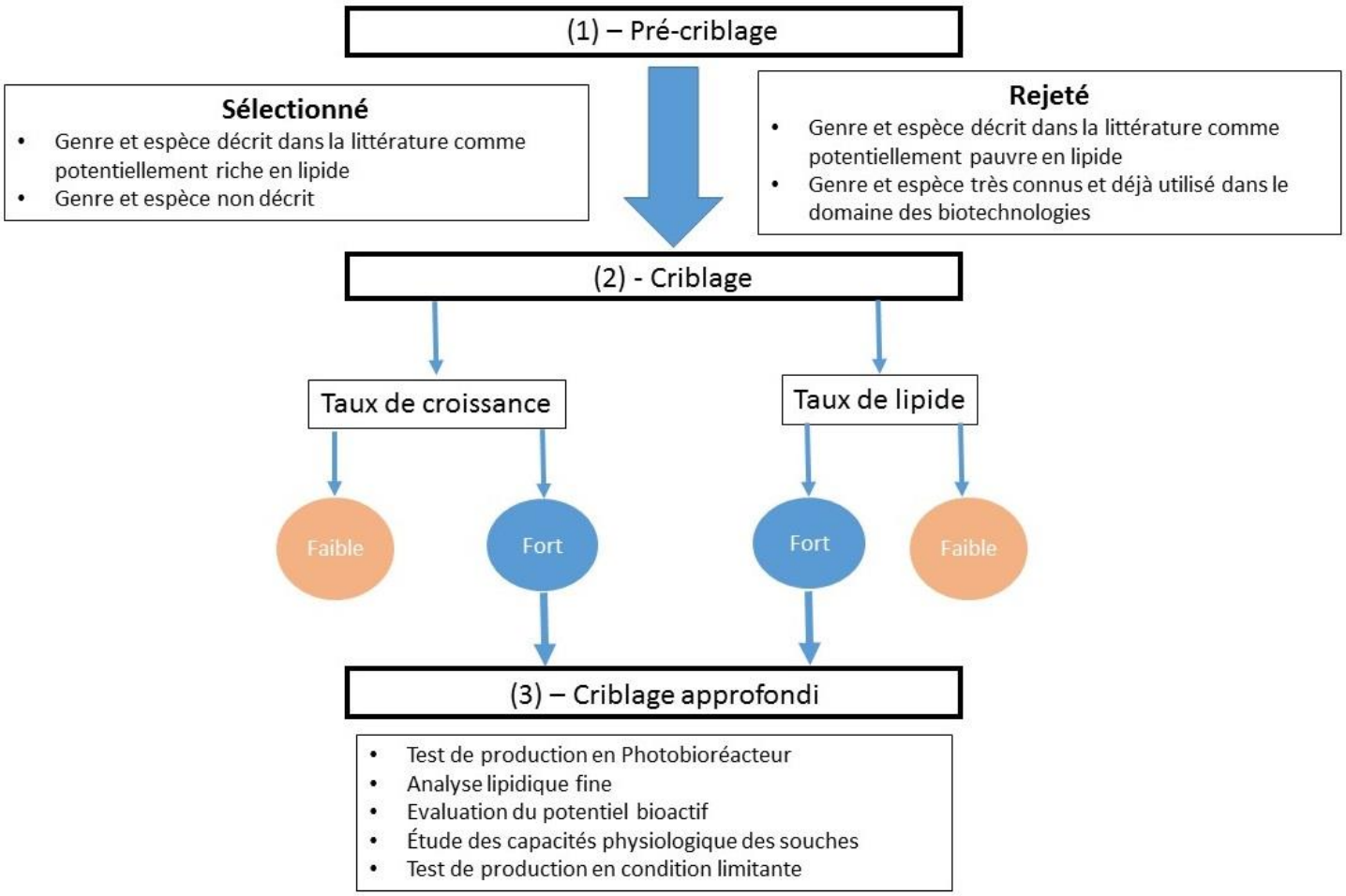

Figure II-1 Représentation schématique de la procédure globale de criblage

3 Algothèque MMS –Sélection des souches criblées

3.1 La Nantes culture collection

La Nantes Culture Collection, ou NCC, est un centre de ressources biologiques, inscrit au World Data Center for Microorganisms' sous la référence « NCC WDCM 856 » depuis 2002. Cette collection a pour originalité d'héberger essentiellement des souches de microalgues appartenant à la classe des diatomées benthiques, le microphytobenthos, ce qu'aucune autre collection à travers le monde ne fait. Elle est constituée de plus de 300 souches, regroupées en plus de 40 genres représentants la biodiversité des vasières du littoral Atlantique. La NCC est un véritable conservatoire du patrimoine local puisque plus de 90 % des souches sont isolées des vasières de la Baie de Bourgneuf, de l'estuaire de la Loire ainsi que des marais Breton-Vendéens et Guérandais.

Les souches utilisées et sélectionnées au sein de la NCC ont été référencées par un code interne (NCC + numéro de la souche). L'identification du matériel biologique a été effectuée principalement par l'analyse morphologique au microscope optique et électronique à balayage. La classification générale des souches est présentée dans le tableau suivant :

Tableau II-1 Classification phylogénétique actuelle pour les genres des souches de diatomées benthiques étudiées (Haeckel, 1878).

Classification phylogénétique actuelle	
Règne	Chromista
Embranchement	Bacillariophyta
Sous-embranchement	Bacillariophytina
Classe	Bacillariophyceae

L'objectif de l'utilisation de la NCC est de savoir si les souches produisent des lipides particuliers d'intérêts économiques et s'il existe un lien entre la biodiversité des diatomées et leur composition biochimique. Une phase de sélection par la bibliographie a été nécessaire pour savoir si les souches conservées dans la NCC avaient déjà été décrites dans la littérature pour leur potentiel lipidique. Au total, 40 genres représentant 101 espèces, soit 134 souches ont été

investigués (tableau II-2). Il s'est avéré que 23 genres (77 espèces, 105 souches) ont été décrits dans la littérature, parmi ces genres seulement 13 genres (42 espèces, 47 souches) ont été sélectionnés. Les souches, dont les genres n'ont jamais été mentionnés dans la littérature pour leur capacité de production lipidique ou de croissance, ont été automatiquement sélectionnées. Cela représente 17 genres (24 espèces, 29 souches). Il est important de différencier le terme espèce et souche, en effet une même espèce a pu être prélevée en différents endroits ou isolée plusieurs fois, de ce fait leur métabolisme de croissance et lipidique peuvent en être impactés. Au sein de la collection, une espèce peut représenter plusieurs souches.

Tableau II-2 Description des ordres et genres de souches de diatomées benthiques présents dans la NCC ainsi que les nombres de souches et d'espèces disponibles.

Ordre	Genres	Espèce (souches)	Littérature[a]
Achnanthales	*Achnanthes*	1 (1)	[11],[12],[44]
	Cocconeis	1 (3)	[6],[25]
Bacillariales	*Cylindrotheca*	2 (4)	[9],[13],[19],[23],[35],[43]
	Nitzschia	23 (25)	[5],[6],[40]
	Pseudonitzschia	1 (1)	-
Chaetocerotales	Chaetoceros	1 (1)	[20],[21],[22],[28],[29],[39]
Cymatosirale	Brockmaniella	1 (2)	-
	Cymatosira	1 (1)	-
	Extubocellulus	1 (1)	[16]
Fragilarirale	Catacombas	1 (1)	-
	Opephora	2 (2)	-
	Tabularia	1 (1)	-
	Staurosira	1 (1)	[15]
Leptocylindrales	Leptocylindrus	1 (2)	-
Licmophorales	Licmophora	1 (1)	-
Lithodesmiales	Helicotheca	1 (2)	-
	Lithodesmium	1 (1)	-
Melosirales	Melosira	1 (2)	[6],[11],[44]
Naviculales	Berkeleya	2 (2)	[4]
	Biremis	1 (3)	[32]
	Caloneis	1 (1)	[11],[44]
	Craspedostauros	6 (7)	-
	Diploneis	1 (1)	[11],[32],[44]
	Fallacia	2 (2)	-
	Gyrosigma	3 (3)	[11],[32]
	Halamphora	1 (1)	-
	Navicula	5 (5)	[6],[11]
	Phaedoctylum	1 (6)	[1],[2],[10],[24],[34],[37],[38],[42]
	Pleurosigma	2 (4)	[11],[26],[44]
Paraliales	Paralia	1 (1)	-
Rhizosoleniales	Rhizosolenia	1 (1)	[3],[33]
Surirellales	Entomoneis	10 (16)	[17],[18]
	Surirella	1 (1)	-
Thallasionematales	Thalassionema	2 (2)	[3],[8],[44]

Thalassiophysales	Amphora	7 (7)	[7],[44]
Thalassiosirales	Conticriba	1 (2)	-
	Skeletonema	1 (3)	[6],[11],[30]
	Thalassiosira	4 (6)	[11],[36]
Triceratiales	Lampriscus	1 (1)	-
	Odontella	5 (9)	[5],[14],[27],[31],[41]

[a] Reference bibliographique : **1**-Alonso *et al*., 2000 ;**2**-Arao *et al*.,1987 ;**3**-Bromke *et al*.,2015 ;**4**-Brown *et al*.,2014 ;**5**-Chen *et al*., 2007 ;**6**-Chen *et al*.,2012 ;**7**-Chtourou *et al*.,2015 ;**8**-Doan *et al*.,2011 ;**9**-Elsey *et al*.,2007 ;**10**-Fajardo *et al*.,2007 ;**11**-Fields and Kociolek.,2015 ;**12**-Guerrini *et al*.,2000 ;**13**-Griffiths and Harrison.,2009 ;**14**-Haimeur *et al*.,2012 ;**15**-Huntley *et al*.,2015 ;**16**-Islam *et al*., 2013 ;**17**-Jauffrais *et al*., 2015 ;**18**-Jaufrais *et al*., 2016 ;**19**-KINGSTON.,2009 ;**20**-Liang *et al*.,2006 ;**21**-McGinnis *et al*., 1997 ;**22**-Mendiola *et al*., 2005 ;**23**-Moura *et al*.,2007 ;**24**-Mus *et al* .,2013 ;**25**-Nappo *et al*.,2009 ;**26**-Nichols *et al*.,1998 ;**27**-Pasquet *et al*.,2014 ;**28**-Pernet *et al*., 2003 ;**29**-Richmond *et al*.,2004 ;**30**-Rodolfi *et al*.,2009 ;**31**-Roleda *et al*.,2013 ;**32**-Scholz *et al*.,2013 ;**33**-Sinninghe Damste *et al*.,1999 ;**34**-Siron *et al*.,1989 ;**35**-Suman *et al*.,2012 ;**36**-Trentacoste *et al*.,2013 ;**37**-Valenzuela *et al*.,2012 ;**38**-Veloso et el.,1991 ;**39**-Wang *et al*., 2014 ;**40**-Wen and Chen.,2000 ;**41**-Xia *et al*., 2013 ;**42**-Xue *et al*.,2015 ;**43**-Ying *et al*.,2002 ;**44**-Zhao *et al*., 2016.

3.2 Les Achnantales

Dans la NCC l'ordre des Achnantales est représenté par deux espèces : *Achnantes brevipes* NCC183 et *Cocconeis scutellum* (NCC209.1, NCC209.2 et NCC209.3).

3.2.1 Achnantes *sp.*

Dans les années 2000, Guerini *et al* ont réalisé le bilan des réponses métaboliques liées à un stress en nutriments chez cette diatomée (Guerrini *et al*., 2000). Cette étude s'est intéressée particulièrement à la production des carbohydrates et des protéines sous un stress nutritif en phosphate et en azote. Cette espèce produit des sucres lorsqu'elle est cultivée en conditions limitantes en particulier lors d'un stress phosphaté. La biomasse atteinte, lorsque les cellules sont cultivées en milieu F/2, est faible (100000 cell. mL^{-1}). La faible biomasse atteinte pour cette espèce a été confirmée par l'étude de Zhao *et al* 2016 avec une biomasse maximale de 0.035 $g.L^{-1}$; cependant, un taux de lipides maximum de 48.61 % est atteint pour cette espèce (F.-Y. Zhao *et al*., 2016). En condition de culture favorable le taux de lipides maximum atteint pour cette espèce est entre 20 et 30 % (Fields and Kociolek, 2015). Aucune molécule avec une activité spécifique n'a été reportée pour cette espèce, elle n'a donc pas été sélectionnée pour le stade de criblage.

3.2.2 Cocconeis sp.

Cocconeis scutellum est une espèce qui produit un ou plusieurs composés responsables de la mort programmée des cellules (apoptose) de la gonade mâle et des glandes androgènes de la crevette *Hippolyte inermis* (Zupo, 2000, 1994; Zupo *et al*., 2007). Cette espèce possède 75 % d'acides gras composés majoritairement d'acides gras saturés (30 %) (Nappo *et al*., 2009). L'espèce *Cocconeis neothumensis* a été cultivée en batch et en photobioreacteurs (Raniello *et al* 2007). Cette espèce est caractérisée par un faible taux de croissance et une adhésion forte au substrat. La composition lipidique de *Cocconeis scutellum* a été caractérisée par (Chen,

2012)cette espèce possède un taux de lipides de 30% en condition normal de culture et a la capacité de produire de l'EPA et du DHA. Cette espèce a été sélectionnée pour l'étape de criblage.

3.3 Les Bacillariales

L'ordre des Bacillariales est représenté par trois genres *Pseudonitzchia americana*, *Nitzschia* sp. et *Cylindrotheca* sp. correspondant à 26 espèces et 28 souches.

Aucune littérature n'existe sur le potentiel de production lipidique de l'espèce *Pseudonitzchia americana*, cette espèce a donc été sélectionnée pour l'étape de criblage.

Le genre *Cylindrotheca* est représenté par deux espèces : *Cylindrotheca closterium* NCC106 et *Cylindrotheca fusiformis* CCMP343. Ce genre est décrit comme ayant un taux de lipides autour de 30 % en condition normale de culture et en condition limitante (Elsey *et al*., 2007; Griffiths and Harrison, 2009). Les taux de croissance des espèces de *Cylindrotheca* sont plus hauts que la plupart des autres espèces de diatomées (KINGSTON, 2009). Cette espèce est déjà utilisée en aquaculture pour la nutrition des larves (Moura Junior *et al*., 2007) . Les espèces de *Cylindrotheca* sont résistantes, faciles à cultiver et à récolter (Suman *et al*., 2012; Ying *et al*., 2002). Cette espèce n'a pas été sélectionnée pour l'étape de criblage, car elle est déjà bien décrite dans la littérature.

Le potentiel lipidique du genre *Nitzschia* a été reporté dans plusieurs études (Chen *et al*., 2007; Chen, 2012; Wen and Chen, 2000). L'espèce *Nitzschia leavis* produit essentiellement des lipides neutres. Elle a été étudiée pour sa production d'EPA. Cette espèce produit majoritairement des triacylglycérol (80 % du total des acides gras) et 37 % des TAG sont composés par de l'EPA. Le taux de lipides pour ce genre varie de 12 à 27 % en condition normale de culture et peut aller jusqu'à 46 % en condition de culture limitante. Parmi les 25 espèces de *Nitzschia*, 6 espèces ont été sélectionnées : *Nitzschia alexandrina* NCC33, *Nitzschia laevis* NCC39, *Nitzschia salinicola* NCC41, *Nitzschia sp B4* NCC114, *Nitzschia sp 5* NCC109.

3.4 Chaetocerotales

Dans la NCC, cet ordre est représenté par l'espèce *Chaetoceros sp 06.1* NCC201. Ce genre a été identifié comme potentiellement producteur de lipides depuis les années 1997 (McGinnis *et al*., 1997). La capacité de croissance et de production lipidique de *Chaetoceros muelleri* a été largement étudiée (Liang *et al*., 2006; McGinnis *et al*., 1997; Mendiola *et al*., 2007; Pernet *et al*., 2003; Wang *et al*., 2014). *C. muelleri* est une des espèces de diatomée marine les plus recommandées à travers le monde pour le nourrissement de larve de crustacés et de mollusques du fait de son fort contenu lipidique et de sa composition en acide gras particulier (Göksan *et al*., 2003; Richmond, 2004). *C.muelleri* a été identifiée comme une des espèces la plus adaptée pour la production de lipide à grande échelle. Elle peut être cultivée dans des bassins extérieurs et intérieurs pour une utilisation commerciale (Becerra-Dórame *et al*., 2010; López-Elías *et al*., 2005). Cette espèce n'a pas été sélectionnée pour l'étape de criblage, car elle a été très largement étudiée.

3.5 Cymatosirale

L'ordre des Cymatosirales est représenté par 3 genres et 3 espèces au sein de la NCC : *Brockmaniella Brockmanii* NCC161 et NCC403, *Cymatosira belgica* NCC208, *Extubocellulus cf cribriger* NCC229.

Aucune littérature n'existe sur le potentiel lipidique de *Brockmaniella Brockmanii* et *Cymatosira belgica*, ces deux espèces ont donc été sélectionnées pour l'étape de criblage.

Le genre *Extubocellulus* est répertorié dans une seule étude (Islam *et al*., 2013), son taux de lipides est estimé à 27 %. Ce genre est composé à 43 % d'acide gras, aucune production d'EPA

ou de DHA n'a été détectés dans cette étude pour ce genre. Au vu du peu de littérature disponible pour ce genre, il a été sélectionné pour l'étape de criblage.

3.6 Fragilariales

L'ordre des Fragilariales est représenté par 4 genres et 5 espèces : *Catacombas sp 1* NCC337, *Opephora sp.2* NCC365, *Opephora sp.1* NCC366, *Tabularia tabulata* NCC338 et *Staurosira* sp. NCC182.

Aucune littérature n'existe sur le potentiel lipidique des genres *Catacombas*, *Opephora* et *Tabularia*. Ces trois genres ont donc été sélectionnés pour la phase de criblage.

Une seule étude existe sur le potentiel lipidique du genre *Staurosira*, cette espèce a été cultivé à grande échelle à Hawaii après une étape de sélection (Huntley *et al*., 2015). Cette espèce est considérée par cette équipe comme potentielle pour la production de biodiesel et de complément alimentaire. Son taux de lipides est estimé à 38 % en condition normal de croissance et à 45 % en condition limitante. Au regard du peu de littérature disponible pour ce genre, cette espèce a été sélectionnée pour l'étape de criblage.

3.7 Melosirales

L'ordre des Melosirales est représenté par une espèce au sein de la NCC : *Melosira nummuloides* NCC25 et NCC25.1.

Le genre *Melosira* a été étudié pour son taux lipidique dans trois études. Son taux de lipides peut varier de 7 à 22 % (Fields and Kociolek, 2015; F.-Y. Zhao *et al*., 2016) et il a été mentionné la production de DHA et d'EPA (Chen, 2012) par *Melosira nummuloides*, elle a donc été sélectionnée pour l'étape de criblage.

3.8 Naviculale

Les Naviculales sont représentés par 11 genres et 25 espèces au sein de la NCC. Trois de ces genres n'ont jamais été décrits dans la littérature : *Craspedostauros* représenté par 6 espèces au

sein de la NCC : *Craspedostauros Brittanicus* NCC195 et NCC199, Craspedostauros sp 1 NCC57 et sp 2 NCC58, *Craspedostauros sp 2* NCC218, *Craspedostauros sp 1* NCC228 et *Craspedostauros sp 06.4* NCC204 ; le genre Fallacia représenté par deux espèces : *Fallacia sp 1* NCC303 et *Fallacia sp 2* NCC304 et le genre *Halamphora* représenté par une espèce : *Halamphora coffeaformis* UTCC58. L'ensemble de ces trois genres ont donc été sélectionnés pour l'étape de criblage.

Au sein de cet ordre, il reste 8 genres décrits dans la littérature. Parmi ces genres, 5 seulement ont été sélectionnés pour l'étape de criblage : *Berkeleya*, *Caloneis*, *Gyrosigma*, *Navicula* et *Pleurosigma.*

3.8.1 Les genres non sélectionnés

Trois genres n'ont pas été sélectionnés pour l'étape de criblage : *Biremis*, *Diploneis* et *Phaeodactylum.*

Biremis est représenté par une espèce au sein de la NCC : *Biremis lucen* (NCC359, NCC360.1, NCC360.2). Le taux de lipides est estimé à 20 % et la production de biomasse est de 829 μm^3 pour l'espèce *Biremis lucen* selon Scholtz *et al*, 2012. Le genre *Diploneis* est représenté par une espèce : *Diploneis sp e9* NCC276. Plusieurs études ont déjà investigué la production de biomasse et de lipides de ce genre (Fields and Kociolek, 2015; Scholz and Liebezeit, 2013; F.-Y. Zhao *et al*., 2016). Sa production lipidique est comprise entre 23 et 27 % du poids sec. La production de biomasse est de l'ordre de 9 889 μm^3. Il a été jugé que ces deux genres, dans l'ordre des Naviculale, n'étaient pas les plus intéressants en terme de taux lipidique moyen, c'est pour cela qu'ils n'ont pas été sélectionnés.

Phaeodactylum est représenté par une espèce au sein de la collection : *Phaeodactylum tricornutum* (NCC45, NCC122.1, NCC159, NCC340, CCAP1052 et CCMP632). Cette espèce a été largement étudiée depuis les année 1990 (Alonso *et al*., 2000; Arao *et al*., 1994, 1987; Fajardo *et al*., 2007; Mus *et al*., 2013; Siron *et al*., 1989; Valenzuela *et al*., 2012; Veloso *et al*.,

1991; Xue *et al*., 2015). *P. tricornutum* est une espèce modèle dans le domaine des diatomées. Cette espèce a la capacité de se développer dans des milieux exempts de silice, elle peut survivre sans produire de frustule siliceux. Le génome de cette espèce a été séquencé et est répertorié dans le diatom EST Database. Cette microalgue est considérée comme une source potentielle pour produire de l'énergie, elle croît rapidement et peut accumuler des lipides entre 20 et 30 % de son poids sec dans des conditions de culture standard. Un stress azoté peut induire une accumulation de lipides jusqu'à 54 % de son poids sec (Chisti, 2007b; Yang *et al*., 2013). Cette espèce a été largement étudiée depuis et a été identifiée comme une microalgue productrice d'EPA (W. Yongmanitchai and Ward, 1991). Cette espèce de par sa popularité n'a pas été sélectionnée pour des études ultérieures.

3.8.2 Les genres sélectionnés

Cinq genres ont été sélectionnés pour l'étape de criblage : *Berkeleya*, *Caloneis*, *Gyrosigma*, *Navicula* et *Pleurosigma*.

Une étude de Brown *et al*, 2014 a identifié un isoprénoide di-insaturé en C25 hautement ramifié (HBI) chez la diatomée *Berkeleya rutilans*. Ces HBI peuvent avoir des activités anti-prolifératives contre le cancer du poumon ainsi que des effets anti-VIH (Wraige *et al*., 1999). Ces isoprenoides particuliers sont connus pour être biosynthétisés par les diatomées et sont une composante commune dans les environnements marins et d'eau douce. Cependant, la capacité qu'ont les diatomées à produire ces hydrocarbures inhabituels est restreinte à seulement quelques espèces qui sont représentées par quatre genres (*Haslea*, *Pleurosigma, Rhizosolenia* et *Navicula*). Le genre *Berkeleya* a été sélectionné pour des études ultérieures.

Le genre *Caloneis* peut produire de 36.3 à 47.4 % de son poids sec en lipides (F.-Y. Zhao *et al*., 2016) Il peut atteindre 38.4 % de son poids sec en conditions de culture limitante (Fields and Kociolek, 2015). Peu d'études existent sur ce genre, il a donc été sectionné pour l'étape de criblage.

Le genre *Gyrosigma* est représenté par 3 espèces au sein de la NCC : *Gyrosigma tenuissimum* NCC258, *Gyrosigma sp 1* NCC411, *Gyrosigma sp 2* NCC412. Son taux de lipides maximum est de 35 % en conditions de culture non-limitante. Cette espèce a une bonne capacité de croissance et peut atteindre un volume de 9.844 μm^3 (Fields and Kociolek, 2015; Scholz and Liebezeit, 2013).

Le genre Navicula représenté par trois espèces : *Navicula sp 1* NCC226, *Navicula sp 2* NCC269 et *Navicula cf ramosissima* NCC449. Différentes espèces de *Navicula* ont été étudiées, ce genre possède une bonne capacité de production de lipides entre 6 à 35% en condition normale de culture et entre 34 à 43% en condition limitante (Fields and Kociolek, 2015). Chen *et al*, 2011 ont mis en évidence la production d'EPA et de DHA pour ce genre.

Le genre *Pleurosigma* est représenté par 2 espèces au sein de la NCC : *Pleurosigma sp 1* NCC339, *Pleurosigma sp 2* NCC404, NCC425 et NCC428. Ce genre a été identifié comme producteur d'HBI (Nichols *et al*., 1988), il peut atteindre un taux de lipides entre 20 et 30 % en condition normale de croissance et jusqu'à 38% en condition limitante (Fields and Kociolek, 2015; F.-Y. Zhao *et al*., 2016).

3.9 Thallassiosirales

Le genre *Skeletonema* est représenté par une espèce au sein de la NCC : *Skeletonema costatum* (NCC60, NCC26 et NCC354). *Skeletonema Costatum* est une espèce bien étudiée qui est déjà utilisée en aquaculture pour nourrir les mollusques. Sa contenance lipidique est de 17 à 21 % du poids sec en condition normale de culture et peut aller jusqu'à 37 % en condition limitante (Chen, 2012; Fields and Kociolek, 2015; Rodolfi *et al*., 2009). Cette algue produit principalement des lipides neutres et également des aldehydes antiprolifériatifs qui peuvent induire un faible taux d'éclosion chez les copépodes (d'Ippolito *et al*., 2004).

Le genre *Thallasiosira* est représenté par quatre espèces au sein de la NCC : *Thalassiossira aestivalis* NCC196, *Thalassiosira pseudonana* CCMP1335, *Thalassiosira punctigera* (NCC98, NCC187) et *Thalassiosira cf punctigera* (NCC277, NCC278). En 2013,

une étude en ingénierie métabolique du catabolisme des lipides a réussi à augmenter le taux de lipides de *T. pseudana* sans compromettre sa croissance (Trentacoste *et al*., 2013). Ce genre possède une contenance lipidique moyenne entre 16 et 22 % en condition normale et jusqu'à 24 % du poids sec en condition limitante (Fields and Kociolek, 2015). La particularité de ce genre est qu'il est facile à manipuler, il a une faible adhésion à la surface du verre, une bonne capacité de croissance dans des conditions de température élevée. Ce genre n'a pas été sélectionné pour l'étape de criblage, son taux de lipides est trop faible par rapport au potentiel d'autre souche de la NCC.

3.10 Triceratiales

Le genre *Lampriscus* est représenté par une espèce au sein de la NCC : *Lampriscus* sp. NCC347. Aucune littérature mentionnant la capacité de production lipidique n'est disponible sur ce genre. Le genre *Odontella* est représenté par 5 espèces : *Odontella aurita* (NCC87, NCC88, NCC116, CCMP5, CCMP15), *Odontella sp 1* NCC43, *Odontella sp 2* NCC44, *Odontella sp 05* NCC164, *Odontella sp austral* NCC356. Le genre *Odontella* a été largement étudié pour sa capacité à produire une grande quantité d'EPA (Chen, 2007; Haimeur *et al*., 2012; Pasquet *et al*., 2014; Roleda *et al*., 2013; Xia *et al*., 2013a). L'espèce *Odontella aurita* est déjà produite à grande échelle comme complément alimentaire destiné à l'alimentation humaine.

3.11 Rhizosoleniales

Le genre *Rhizosolenia* est représenté au sein de la NCC par une espèce : *Rhizosolenia setigera* NCC127. Cette espèce a été identifiée comme productrice d'HBI (Sinninghe Damsté *et al*., 1999). Cette espèce est identifiée comme productrice de lipides, mais son taux n'est pas précisé dans l'étude de Bromke *et al*, 2015. Finalement, peu d'information son disponible sur ce genre, il a donc été sélectionné pour l'étape de criblage.

3.12 Surrirellale

Le genre *Surrirela* est représenté par une espèce au sein de la NCC : *Surirella* sp. NCC270. Aucune information n'est disponible sur son potentiel lipidique dans la littérature. Cette souche a donc été sélectionnée pour l'étape de criblage.

Le genre *Entomoneis* est représenté par 10 espèces au sein de la NCC : *Entomoneis alata* NCC16 et NCC448, *Entomoneis paludosa* (NCC18.1.1, NCC18.1.2, NCC18.2.1 à NCC 18.2.4), *Entomoneis sp 1* NCC350, *Entomoneis sp 2* NCC20, Entomoneis sp 3 NCC351, *Entomoneis sp 4* NCC301, *Entomoneis sp 5* NCC302, *Entomoneis sp 6* NCC335, *Entomoneis BAB2* NCC415, *Entomoneis Neli* NCC445. *Entomoneis paludosa* est une des espèce modèle au laboratoire MMS, sa physiologie a été abondamment étudiée (Jauffrais *et al*., 2016, 2015) mais aucune étude n'a été publiée sur son contenu lipidique précis et sa capacité à produire des molécules d'intérêt. 12 souches d'*Entomoneis* ont donc été sélectionnées pour l'étape de criblage (une souche de chaque espèce, 2 souches d'*Entomoneis paludosa* et les deux souches d'*Entomoneis alata*)

3.13 Thallasionematales

Le genre *Thallasionema* est représenté au sein de la NCC par deux espèces : *Thalassionema frauenfeldii* NCC135 et *Thalassionema sp Austral* NCC355, Ce genre est identifié comme peu productif en terme de lipide (3 % DW) (Bromke *et al*., 2015; Doan *et al*., 2011; F.-Y. Zhao *et al*., 2016) il n'a donc pas été sélectionné pour l'étape de criblage.

3.14 Thallassiophysales

Le genre *Amphora* est représenté par 7 espèces différentes dans la NCC : *Amphora acutiuscula* NCC216, *Amphora sp05* NCC169, *Amphora sp b1* NCC260, *Amphora sp B2* NCC261, *Amphora AC16* NCC410 et *Amphora sp AE8* NCC413. Ce genre a été identifié comme potentiellement intéressant pour produire du biodiesel. C'est un genre qui sédimente rapidement et qui peut donc être récolté à moindre coût. Son taux de lipides varie de 21 à 28 % en condition normale de croissance et peut aller jusqu'à 40 % en condition de culture limitante (Fields and Kociolek, 2015; F.-Y. Zhao *et al*., 2016). Cette microalgue pourrait être valorisée dans d'autres domaines comme l'aquaculture ou l'alimentation animale selon Chtourou *et al*., 2015. Ce genre a été sélectionné pour l'étape du criblage du fait de son fort potentiel et de la forte diversité d'espèces présentes dans la collection.

3.15 Autres ordres : Leptocylindrales, Licmophorales et Lithodesmiales

L'ordre des Leptocylindrales est représenté par une espèce au sein de la NCC : *Leptocylindrus danicus* (NCC205 et NCC206). L'ordre des Licmophorales par une espèce : *Licmophora sp. 1* et l'ordre des Lithodesmiales par deux espèces : *Lithodesmium sp austral* NCC59 et *Helicotheca thamesis* (NCC59, NCC60). Aucune littérature n'existe sur le potentiel lipidique de ces espèces, elles ont donc été sélectionnées pour l'étape de criblage.

4 Souches sélectionnées

Les 40 genres hébergés par la NCC (101 espèces, 134 souches) ont été investigués dans la littérature. Des informations sur le contenu lipidique de 23 genres (77 espèces, 105 souches) ont été retrouvés dans la littérature mais aucune pour 17 genres (24 espèces, 29 souches). Parmi les souches décrites dans la littérature, 13 genres ont été sélectionnés, ce qui représente 42 espèces et 47 souches. Avec les 17 genres non étudiés dans la littérature, un total de 30 genres (66 espèces, 76 souches) a été sélectionné pour l'étape de criblage (Figure. II-2).

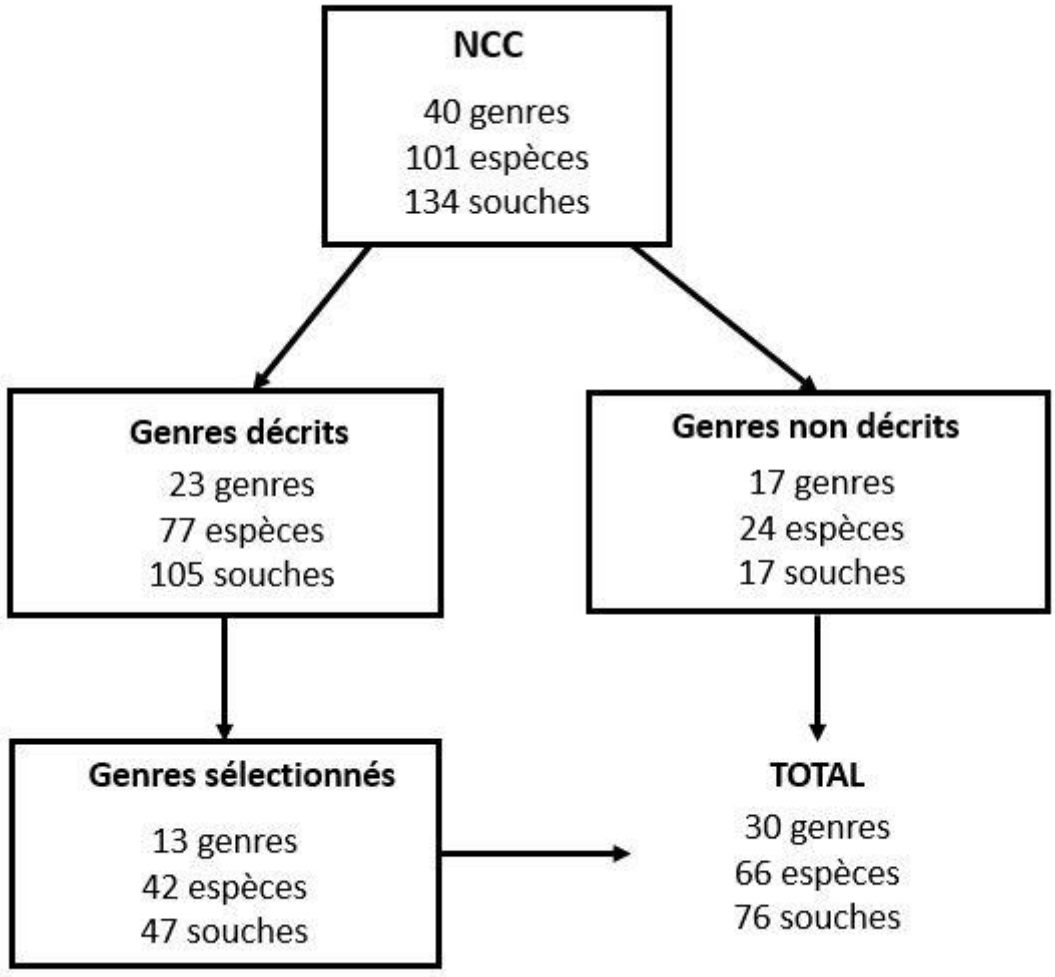

Figure II-2 Bilan schématique des différentes étapes de sélections des souches par la littérature

La majorité des souches sélectionnées (tableau II-3) ayant été isolées au cours de différentes campagnes, principalement en baie de Bourgneuf et sur l'estuaire de la Loire, elles sont représentatives de la diversité retrouvée sur les vasières des côtes Atlantique françaises. Les souches sont conservées en culture stock, en plus de celles en chambre de culture de la collection. Pour cela, des ballons de 500 mL remplis de 250 mL d'eau de mer enrichie (F/2, Guillard) sont ensemencés et les cultures repiquées toutes les 5 semaines. Elles sont conservées à une luminosité de 100 µmol.photons.m^{-2}.s^{-1}, à une température de 16 °C et sous un cycle lumineux jour/nuit (14-10H).

Tableau II-3 Souches sélectionnées et citées dans les différents chapitres

Ordre	Famille	Genre et espèces	Code NCC	Zone d'échantillonnage
Achnantales	Cocconeidaceae	*Cocconeis scutellum 1*	NCC209.1	France, NW Atlantic coast
		Cocconeis scutellum 2	NCC209.2	France, NW Atlantic coast
		Cocconeis scutellum 3	NCC209.3	France, NW Atlantic coast
Bacillariales	Bacillariaceae	*Nitzschia alexandrina*	NCC33	France, NW Atlantic coast
		Nitzschia sp. 5	NCC109	France, NW Atlantic coast
		Nitzschia laevis	NCC39	France, NW Atlantic coast
		Nitzschia salinicola	NCC41	France, NW Atlantic coast
		Nitzschia sp B4	NCC114	France, NW Atlantic coast
		Pseudonitzschia americana	PNA06 KER	France, NW Atlantic coast
Cymatosirales	Cymatosiraceae	*Extubocellulus cf cribriger*	NCC229	France, NW Atlantic coast
		Brockmaniella brockmanii 1	NCC161	France,NW Atlantic coast
		Brockmaniella brockmanii 2	NCC403	France,NW Atlantic coast
		Cymatosira belgica	NCC208	France, NW Atlantic coast
Fragilariales	Fragilariacea	*Staurosira sp 06 cf elliptica*	NCC182	France, NW Atlantic coast
		Opephora sp. 1	NCC366	France,NW Atlantic coast
		Opephora sp. 2	NCC365	France,NW Atlantic coast
		Catacombas sp 1	NCC180	France,NW Atlantic coast
		Tabularia tabulata	NCC338	France,NW Atlantic coast
Leptocylindrales	Leptocylindraceae	*Leptocylindrus danicus 1*	NCC205	France,NW Atlantic coast
		Leptocylindrus danicus 2	NCC206	France,NW Atlantic coast
Licmophorales	Licmophoraceae	*Licmophora sp. 1*	NCC253	France,NW Atlantic coast
Lithodesmiales	Lithodesmiaceae	*Lithodesmium sp Austral*	NCC353	Australia,, Moreton bay
		Helicotheca thamesis 1	NCC59	France, Mediterranean sea
		Helicotheca thamesis 2	NCC60	France,NW Atlantic coast
Melosirales	Melosiraceae	*Melosira nummuloides 1*	NCC25	France,NW Atlantic coast
		Melosira nummuloides 2	NCC25.1	France,NW Atlantic coast
Naviculales	Amphipleuraceae	*Halamphora coffeaeformis*	UTCC58	Canada, NW Pacific coast
	Berkeleyaceae	*Berkeleya rutilans*	NCC210.2	France,NW Atlantic coast
		Berkeleya sp 1	NCC309	France, Mediterranean sea
	Sellaphoraceae	*Fallacia sp. 1*	NCC303	Greenland, east coast
		Fallacia sp. 2	NCC304	Greenland, east coast
	Naviculaceae	*Caloneis sp 1*	NCC180	France, NW Atlantic coast
		Craspedostauros britannicus	NCC195	France, NW Atlantic coast
		Craspedostauros sp. 1	NCC228	France, NW Atlantic coast
		Craspedostauros sp. 2	NCC218	France, NW Atlantic coast
		Craspedostauros sp. 3	NCC57	France, NW Atlantic coast
		Craspedostauros sp. 4	NCC58	France, NW Atlantic coast
		Craspedostauros sp 5	NCC204	France, NW Atlantic coast
		Craspedostauros britannicus	NCC199	France, NW Atlantic coast
		Navicula sp. 1	NCC113	Maroc, Oum R'bia estuary
		Navicula sp. 2	NCC226	France, NW Atlantic coast
		Navicula sp Z4	NCC224	France, NW Atlantic coast
		Navicula sp e1	NCC269	France, NW Atlantic coast
		Navicula cf ramosissima	NCC449	France, NW Atlantic coast
	Pleurosigmataceae	*Gyrosigma sp 1*	NCC411	France, NW Atlantic coast
		Gyrosigma sp 2	NCC412	France, NW Atlantic coast
		Gyrosigma tenuissimum	NCC258	France, NW Atlantic coast
		Pleurosigma sp K	NCC339	France, NW Atlantic coast

		Pleurosigma sp LM	NCC404	France, NW Atlantic coast
		Pleurosigma sp BC1	NCC423	France, NW Atlantic coast
		Pleurosigma sp BC7	NCC425	France, NW Atlantic coast
		Pleurosigma sp BC15	NCC428	France, NW Atlantic coast
Paraliales	Paraliaceae	*Paralia sulcata*	NCC177	France, NW Atlantic coast
Rhizosoleniale	Rhizosoleniaceae	*Rhizosolenia setigera*	NCC127	France, NW Atlantic coast
Surirellaes	Entomoneidaceae	*Entomoneis alata 1*	NCC16	France, NW Atlantic coast
		Entomoneis alata 2	NCC448	Portugal, NW Atlantic coast
		Entomoneis sp. 5	NCC302	France, NW Atlantic coast
		Entomoneis sp. 2	NCC20	France, NW Atlantic coast
		Entomoneis sp. 7	NCC445	France,,NW Atlantic coast
		Entomoneis paludosa	NCC18.1.1	France, NW Atlantic coast
		Entomoneis sp. 4	NCC301	France, NW Atlantic coast
		Entomoneis paludosa	NCC18.2.1	France, NW Atlantic coast
		Entomoneis sp. 6	NCC335	France, Mediterranean sea
		Entomoneis sp. 1	NCC350	France, Mediterranean sea
		Entomoneis sp. 3	NCC351	France, Mediterranean sea
		Entomoneis sp BAB2	NCC415	France, NW Atlantic coast
	Surirellaceae	*Surirella sp. 1*	NCC270	France, NW Atlantic coast
Thalassiophysales	Catenulaceae	*Amphora sp. 1*	NCC260	France,NW Atlantic coast
		Amphora sp. 2	NCC169	France,NW Atlantic coast
		Amphora acutiuscula	NCC216	Viet Nam, South east coast
		Amphora sp. B2	NCC261	France, NW Atlantic coast
		Amphora sp. AC16	NCC410	France, NW Atlantic coast
		Amphora sp. AE8	NCC413	France, NW Atlantic coast
Thalassiosirales	Thalassosiraceae	*Conticriba weissflogii*	CCMP1336	USA, NE Atlantic coast
		Conticriba weissflogii	NCC133	Maroc, Oum R'bia estuary
Triceraticales	Triceratiaceae	*Lampriscus* sp.	NCC347	France, Mediterranean sea

5 Développement d'une méthode de criblage à haut débit pour évaluer le potentiel lipidique des diatomées marines benthiques

Les souches sélectionnées lors de l'étape de pré-criblage ont été cultivées en erlenmeyers de 150 mL, sous un flux de lumière continue (127 µmol.photons.m^2.s^{-1}) à une température de 16 °C. Le milieu de culture utilisé est le milieu F/2 (Guillard, 1975). Parmi les 66 espèces sélectionnées, 33 espèces ont été cultivées avec succès. Parmi ces 33 espèces, 15 ont été étudiées pour la première fois. Une méthode simple et fiable a été mise en place pour caractériser la cinétique de croissance des souches. Une analyse semi-quantitative pour déterminer le taux de lipides a été développée. Les mesures de cinétique de croissance ont été obtenues en mesurant quotidiennement la fluorescence minimale (F0). Le taux de lipides a été quantifié en utilisant la spectroscopie infrarouge sur cellules entières et sur extrait lipidique brut. Les résultats indiquent que cette méthode peut être utilisée directement sur cellules entières malgré la présence de silice liée au frustule qui peut interférer dans l'acquisition du signal infrarouge. Les résultats suggèrent que le taux de lipides est dépendant de l'espèce et varie de 3.7 % à 30.5 % du poids sec. Six espèces, parmi les 33 explorées, présentent un taux de lipides supérieur à 15 % du poids sec et 11 possèdent un taux de lipides variant de 10 % à 15 % du poids sec. Cette étude a permis d'identifier 5 espèces de diatomées (*Amphora* sp. NCC169, *Nitzschia* sp. NCC109, *Nitzschia alexandrina* NCC33, *Opephora* sp NCC366 and *Staurosira* sp. NCC182) possédant un taux de lipidique superieur à 15 % du poids sec et/ou une productivité en biomasse supérieur à 0.20 g.L.j^{-1}. Cette étude a fait l'objet d'une publication dans le journal Algal Reasearch et est présentée ci-dessous.

Algal Research 39 (2019) 101425

Contents lists available at ScienceDirect

Algal Research

journal homepage: www.elsevier.com/locate/algal

Lipids in benthic diatoms: a new suitable screening procedure

Short title: Screening and rapid selection of lipid rich benthic diatoms

Eva Cointet[1], Gaëtane Wielgosz-Collin[1], Vona Méléder[1], Olivier Gonçalves[2*]

[1] Université de Nantes, Laboratoire Mer Molécules Santé, EA 21 60, BP 92208, 44322 Nantes, France

[2] Université de Nantes, GEPEA, UMR CNRS-6144, Bât.CRTT, 37 Boulevard de l'Université, BP406, F-44602 Saint-Nazaire Cedex, France

5.1 Abstract

The selection of suitable and indigenous microalgae species is a fundamental requirement in developing added-value bioactive compounds recoverable in the food, health, and cosmetics markets. In this work, an integrated screening approach was developed to characterize the lipid rate of 33 diatom species (including 15 species studied for the first time) belonging to 16 genera from the Nantes Culture Collection, with the main objective of discovering bioactive lipid producers. For that purpose, a simple reliable method for establishing growth kinetics of strains and semi-quantitative analysis of lipid rates was developed. Growth kinetics measurements were achieved by daily minimal measurement fluorescence (F0) whereas lipid rate analyses were performed by high-throughput Fourier Transform Infrared spectroscopy on entire cells and lipid extracts. Results indicated that the method could be used directly on entire cells in spite of the presence of silica for the FTIR approach (due to frustule). The total lipid rate was species-dependant and ranged from 3.7% to 30.5% DW. Six strains out of 33 were found to present a higher total lipid rate superior to 15% DW, and 11 showed medium lipid rates ranging

from 10% to 15% DW. The results revealed that five diatom species i.e. *Amphora* sp. NCC169, *Nitzschia* sp. NCC109, *Nitzschia alexandrina* NCC33, *Opephora* sp NCC366 and *Staurosira* sp. NCC182 presented interesting growth capabilities and should be further investigated as potential sources for their original lipid rate.

Keywords: FTIR spectroscopy, growth kinetics, benthic Diatoms, lipid rate, bioactive fatty acids.

Abbreviation

ATR:	Attenuated Total Reflectance
AW:	Ash weight
DW:	Dry weight
DHA:	Docosahexaenoic acid
EPA:	Eicosapentaenoic acid
FA:	Fatty acid
F0:	Minimum chlorophyll fluorescence
HTSXT-FTIR:	Fourier-transform infrared spectroscopy high-throughput screening extension
LED:	Late exponential day
LED biomass:	Biomass corresponding to culture harvest days
MUFA:	Monounsaturated fatty acid
NCC:	Nantes Culture Collection
NDVI:	Normalized Difference Vegetation Index
N:	Nitrogen
PFD:	Photon flux density
PAM:	Pulse amplitude modulation
PAR:	Photosynthetically active radiation
PUFA:	Polyunsaturated fatty acid
ρ :	Reflectance
SD :	Standard deviation
SFA:	Saturated fatty acid
TAG:	Triacylglycerol

µmax: Maximum growth rate

5.2 Introduction

In the last two decades, a large body of research has focused on finding new strains of microalgae capable of producing high lipid content for a wide range of applications including pharmaceutical, cosmetics and alternative biofuels (Borowitzka, 2013; Khan *et al*., 2018; Mata *et al*., 2010; Spolaore *et al*., 2006). In the kingdom of microalgae, diatoms are very accessible resources, since they are ubiquitously found in most aquatic environments (rivers, oceans, coastal areas). They constitute a unicellular eukaryotic group with a typical species-specific siliceous cell wall (also known as frustule). They present different life-forms that could be benthic (microphytobenthos) or planktonic (phytoplankton). Marine diatoms can grow quickly and store large amounts of lipids (Niu *et al*., 2013). Their lipids are mainly composed of a neutral fraction with traces of sterols and polar lipids (Yi *et al*., 2017). Neutral lipids constitute the reserve fraction, with triacylglycerol (TAG) accounting for more than 60% of the total lipids (Artamonova *et al*., 2017). Their PUFAs are mainly composed of eicosapentaenoic acid (EPA, C20:5 n-3) (Chew *et al*., 2017b) but some strains were also found to present docosahexaenoic acid (DHA, C22:6 n – 3) (Dunstan *et al*., 1993). The biosynthesis of the lipids varies within the different diatom species, their growth stages, and environmental parameters (Chen, 2012; Chuecas and Riley, 1969). Previous studies (Artamonova *et al*., 2017; Chew *et al*., 2017b; Dunstan *et al*., 1993; Niu *et al*., 2013; Yi *et al*., 2017) have demonstrated their ability for lipid production, more specifically for the PUFA fraction (DHA and EPA), recognized for its broad spectrum bioactivities (anti-carcinogenic, immune modulation, anti-diabetic, anti-obesity and anti-thrombotic properties) (Nagao and Yanagita, 2005). Unfortunately, the Diatoms group is poorly studied and constitutes therefore an underexploited resource (Gross, 2012) even if the number of their genera and species is estimated to be between 250 and 100,000 (Lebeau and Robert, 2003). Bioprospecting efforts should therefore be encouraged in order to assess this

potential. Basically, bioprospecting would be achieved if the identified microalgae could be exploited at an industrial scale for their biomass or their high value lipid compounds (Mata *et al*., 2010). Therefore, during the screening approach, specific focus should be performed on the efficient identification of the appropriate microalgae strains, i.e. those characterized by high productivity (biomass and lipids), high resistance to contamination and high tolerance to a wide range of environmental parameters (Chisti, 2007b; Dempster and Sommerfeld, 1998; Hu *et al*., 2008; Huntley *et al*., 2015). Native species adapt to local environmental changes and should be thus resilient and competitive enough regarding these criteria. However, systematic estimation of the growth rates requires a time-consuming series of measurements in order to estimate biomass evolution. The cell count approach is among the most widely used. Alternatively, other parameters could be measured as proxy for the cell numbers, if it could be shown to be linearly correlated. Typical proxy measurements are *in vivo* fluorescence (Vyhnalek *et al*., 1993), optical density and biomass direct estimation (such as dry weight, pigment content) (Steinman *et al*., 2017) and *in vivo* or in solvent spectroscopy (Méléder *et al*., 2003). The concentrations of protein, carbohydrates and lipids in cultures could also be used as proxy measures depending of the robustness of their linear relationship with either cell numbers or biomass. Finally, the cell number is recognized as being a robust reference method if "counting methods" are easily available and could be applied to a given biological system. Only *in vivo* fluorescence and spectroscopy seem to be faster than cell counting and are easy to use. For these reasons, one of the objectives of this study is to test both techniques as an alternative to counting in the screening process. Conventional methods used for lipid determination, systematically require solvent extraction and gravimetric determination. These methods are time consuming, need extensive manipulations, use high amounts of biomass (10-15 mg (Akoto *et al*., 2005)) and have a low throughput screening rates. Consequently, a faster measurement of the lipid content is needed (Cooksey *et al*., 1987). As for counting methods, alternative approaches exist, that

can be roughly classified into invasive and non-invasive techniques. Fluorescent based technologies are the most commonly used and require fluorescent dyes like Bodipy. However, it is an indirect measure that has several issues such as sample preparation before staining, careful choice of dye especially in microalgae due to the presence of chlorophylls within chloroplasts, leading to non-quantitative information (Koreivienė, 2017). Vibrational spectroscopy such as Raman (Jaeger *et al*., 2016) could be a good alternative for investigating lipid content since it can image and chemically identify the lipids without labelling. However, autofluorescence signals from the chloroplast will overwhelm the Raman signal. Increasing the acquisition time or incident power can solve this issue, although irreversible photo damage may result, leading to loss of the semi-quantitative information, limiting therefore its use in the context of high-throughput screening. Infrared spectroscopy has advantages over the above techniques, since it limits photodamage, is not influenced by autofluorescence, and presents robust systems such as high-throughput screening for chemical spectra acquisition for large quantities of samples. Coat *et al.* demonstrated (Coat *et al*., 2014) that it was robust and sensitive enough to quantify the lipids and that directly on entire microalgae cells. The second objective of this study was to test this technique as an alternative to gravimetric determination of lipid content.

In the present work, we propose to explore the potential for original lipid sourcing of the benthic diatoms hosted in the Nantes Culture Collection (NCC) bank. First – to identify the NCC strains that could potentially produce interesting fatty acids – a bibliographic inventory of current and past knowledge of the principal genus and species hosted in the NCC bank was conducted. It focused on the families of molecules with high added value for pharmacology, health, nutrition, and cosmetics such as PUFAs, taking also into account the influence of cultural conditions (Fan *et al*., 2014; Metzger and Largeau, 2005). The selected species were then, investigated to gain basic knowledge on their biological characteristics, to highlight their chemo diversity (in terms

of protein, carbohydrates, silica and lipid rates), and finally on their potential for high-value fatty acid molecule biosynthesis. To select the most promising NCC strains, an original workflow was developed, integrating different steps including the analysis of the NCC strain growth and their rapid biochemical profiling through HTSXT-FTIR. The results obtained in the present study are discussed hereafter.

5.3 Material and methods

5.3.1 Strains cultivation

Diatom strains from the NCC were selected and cultivated in 250 mL Erlenmeyer flasks filled with 150 mL of F/2 culture medium, enriched in silica using 0.47 µm filtered natural sea water (Guillard, 1975; Guillard and Ryther, 1962). Vitamins and carbonates were added before autoclave sterilization (Autoclave Vertical Lequeux AUV 100L), salinity was adjusted at 28 and pH was fixed at 7.8 to reduce nutrient precipitation. Inoculation of each strain was performed from the stock cultures with an initial concentration of 30 000 cells.mL^{-1}. The diatom strains were thus grown at 16°C with a photon flux density (PFD) of 127 µmol photons m^{-2} s^{-1} provided under continuous light to the bottom of flasks by flat led pannel (LP EPURE-Chateaugiron, France).

5.3.2 Growth parameter estimations

To retrieve the growth parameters on the screened strains, the growth rate (µmax in day^{-1}) and the end of the exponential phase were identified. The growth rate identifies the faster growing strains. The end of the exponential phase, known to be the period of lipid accumulation (Yang *et al*., 2013), identifies the harvest day for lipid analyses. These parameters were retrieved using daily biomass estimation. All erlen flasks and stir bars were autoclaved. Before sampling, flasks were agitated by magnetic stirring for 2 minutes allowing cell and nutrient homogenization and aggregate destruction.

Alternative techniques were tested to replace the cell counting by hemocytometer (here Neubauer; n ≥ 300) which is a time-consuming technique.,

- Minimum chlorophyll fluorescence measurement (F0) by fluorometry PAM (Water-PAM, Waltz, Germany). This parameter, proportional to Chl *a* content, was used as a proxy of the vegetal biomass (Honeywill *et al*., 2002). Measurements were made directly on the microalgal suspension.

- Reflectance (ρ) of the cells by spectroradiometry (Jaz, Ocean Optics, USA) in the PAR domain (400-700 nm). Reflectance values were used to calculate the Normalized Difference Vegetation Index (NDVI) following the equation. (1), known to be proportional to Chl *a* content and used as a biomass proxy (Méléder *et al*., 2003). Measurements were made on filtered microalgae using CML microfiber filters with a 25 mm diameter and a 0.7 µm pore diameter and a 25mm Whatman filter funnel.

$$NDVI = \frac{\lambda 750 - \lambda 675}{\lambda 750 + \lambda 675} \qquad \text{eq. (1)}$$

With λ750: maximal reflectance wavelength, and λ675: Chl *a* absorption wavelength

Daily measurements were performed on each sample of culture to follow the growth kinetics (at the beginning of the growth phase and during three days, between 3 mL and 5 mL of cultures were sampled, and then 2 mL until the end of the growth). To extract and compare the growth parameters from the alternative techniques and the cell count approach, the Gompertz model (Gompertz, 1825) was used to fit the growth data (equation. 2) using MATLAB software. It consisted of a latency phase followed by an exponential phase and a stabilization of the curve at its maximum phase.

$$f(x) = A \times e^{-e(\mu max \times \frac{e^1}{A} \times (\lambda - x) + 1)} \qquad \text{eq. (2)}$$

With *A*: maximum cell concentration in the natural logarithm of the biomass (number of cells. mL^{-1}, F0 or NDVI); µmax: Maximum growth rate (day^{-1}); λ : Latency (days).

The *A* parameter allows calculation of the biomass ($LED_{biomass}$) obtained at the late exponential day (LED) (equation. 3). This corresponded to the harvest day for the lipid analyses.

$$LED_{biomass} = exp(A + log(Bmin)) \quad \text{eq. (3)}$$

With *Bmin* = Initial biomass (number of cells.mL^{-1}, F0 or NDVI); $LED_{biomass}$ = biomass of the late exponential day (cell.mL^{-1}, F0 or NDVI)

The comparison of the three thechniques, and the selection of the fastest one to estimate the growth parameters was done using a panel of 6 very different strains, chosen for their different growth kinetics and their different morphology (aggregate of cells, cells in chains or solitary cells) : *Amphora* sp. 1 NCC260, *Entomoneis* sp. 1 NCC350, *Entomoneis* sp. 6 NCC335, *Entomoneis paludosa* NCC18.2, *Extubocellulus cribriger* NCC229 and *Navicula* sp. 2 NCC226.

5.3.3 Diatom strain characterisation

At the end of the exponential phase (LED), when the cells were harvested for HTSXT-FTIR analyses (see §5.3.4), several analysis were perforemd to collect more information about the strains:

- the cell length and the width were estimated using the image of light microscopy (OLYMPUS CH40, ×400; n=150).

- the dry weight (DW) of the biomass was estimated by filtering 150 mL of algal suspension through a microfiber filter, Whatman 47 mm diameter, 0.7 μm pore. The filters containing the cells were washed using 10 mL of ammonium formiate (3%) to the remove salt. The wet filters were frozen at -80°C and freeze-dried under a vacuum. DW (g.L^{-1}) and µmax (day^{-1}) were then used to estimate the strain productitivty (Px) in g.L^{-1}.day^{-1} (equation. 4).

$$Px = \mu max \times DW \quad \text{eq. (4)}$$

- the strains total lipid rate was assessed by gravimetric assay, to compare it to the infrared semi-quantitative measurments (HTSXT-FTIR, see § 5.3.4). Biomass filtered, washed and freeze-dried for dry weight estimation were used for lipid content estimation. The filters were macerated in flasks using 100 mL of solvent per gram of biomass (dichloromethane-methanol (1:1 V/V)) (Bligh and Dyer, 1959). Maceration at ambient temperature was performed for 24H on a vibrating tray (Edmund Bühler GmbH, SM-30). After maceration, the mixture was filtered on pleated filters, 190 mm diameter, 10µm pore, to remove the filter debris and the silica fragments. The filtrates were transferred into a separatory funnel with 20 mL of distilled water and shaken for 5 min. The lipid fraction (organic phase) was then separated from the separatory funnel, dried using an anhydrous sodium sulfate salt, filtered, evaporated and weighed to obtain the crude lipid extract (CLE) value. Total lipid rate (TLR) was finally expressed in % of the DW (equation. 5).

$$TLR = \frac{CLE}{DW} \times 100 \qquad \text{eq. (5)}$$

- the silica content of the cells was also determined to ensure the normalization of the FTIR semi-quantitative results (see § 4.3.4). Cultures were harvested by filtering new 150 mL of the algal suspension using the same recovery cell procedure used for dry weight estimation. Filters were then freeze-dried, weighed (DW) and heated at 400°C for four hours in a muffle oven and weighed (AW) and the silica proportion evaluated in % of DW by equation. 6 :

$$Silica\ content = \frac{AW}{DW} \times 100 \qquad \text{eq. (6)}$$

5.3.4 Molecular profiles measured by infrared spectroscopy

The FTIR spectra acquisition on entire cells was performed according to Coat *et al*. 2014 recommendations (Coat *et al*., 2014). It consisted in concentrating the cells up to 10^6 - 10^8 cells.mL^{-1} by centrifugation (10 000g for 5 min) using Sigma 3K30 centrifuge. The supernatant was removed, and the pellet resuspended in an ammonium formiate isotonic solution (68 g.L^{-}

[1]). This process was repeated twice to wash out the cells from the growth medium in order to avoid medium contribution on the FTIR spectra. The cells were thus resuspended in 1mL in an isotonic solution. Ammonium formiate solution prevents cell lyses during washing (Breuer *et al*., 2013a). For the FTIR spectra acquisition, a Bruker tensor 27 FTIR spectrometer equipped with a HTSXT plate reader module coupled to OpusLab v 7.0.122 software (Bruker Optics, Germany) was used. Rinsed cell aliquots of 5 µL were deposited on a 384 well microplate, void-dried in a vacuum desiccator for at least 24 hours. FTIR spectra were then recorded in transmission mode directly on the microplate loaded with the dried samples. This method was chosen since it is fast and non-invasive on intact diatom cells, their biochemical signatures expressed in term of total lipids, total proteins and total carbohydrates superimposed partially with the silica signal of the diatom frustul. To confirm the whole cells FTIR spectra results, estimation of the lipid rate was also performed on crude lipid extract, using attenuated total reflectance sampling system (ATR), that was more suitable forcrude organic extracts. For the acquisition of the ATR spectra, 10 µL of crude lipid extract (see §5.3.3 (Bligh and Dyer, 1959)) were deposited directly on the Bruker tensor 27 FTIR spectrometer lens. The absorbance spectra were all collected between 4 000 cm^{-1} and 700 cm^{-1} with 30 scans and averaged. The spectra were analyzed by relatively straightforward methods such as peak ratios or integral ratios (León *et al*., 2014). The lipid signature was associated to the CH_2-CH_3 signal (~3000 – 2800 cm^{-1}) and the ester bond (Eb) signal (~1740 cm^{-1}). The carbohydrate signature was associated to the C-O-C signal of the polysaccharides (~1200-900 cm^{-1}) (Zeroual *et al*., 1994). The protein signature was associated to the amide II band (~1540 cm^{-1}) of the N-H of the amides associated to the proteins. The silica signature was associated to the Si-O signal of the silicate frustule (~1068 cm^{-1}) (Williams and Fleming, 1980). To estimate the relative content of the lipids, carbohydrates and proteins, their respective peak heights (i.e. ester bond + (CH_2 + CH_3), ~1159 cm^{-1} and amide II) were standardized to the silica peak (Schaub *et al*., 2017) (equation 7). For

the crude lipid extract spectra, the ratio used for that purpose was the ester bond and the CH_2 + CH_3 signals standardized with the total spectrum area (equation 8). FTIR and ATR ratio were expressed in arbitrary units abundance (a.u).

$$\text{FTIR} = \frac{Peak\ height\ (S)}{Silica\ peak\ high} \qquad \text{eq. (7)}$$

S = lipids (eb+(CH_2+CH_3)) or carbohydrates (~1159 cm^{-1}) or amide II (~1540 cm^{-1})

$$\text{ATR} = \frac{Peak\ area\ (eb+CH_2+CH3)}{Total\ spectra\ area} \qquad \text{eq. (8)}$$

5.3.5 Data processing

The Pearson product-moment correlation was carried out to test the positive correlation between the growth curves obtained with the cell count (Cells.mL^{-1}), fluorescence (F0) and reflectance (NDVI).

Comparison of the growth rate and LED estimated from the three techniques for the selected species were performed using ANOVA when the data presented normal distribution or the Kruskal – Wallis test when the data distribution was not normal. It was systematically followed by the Tuckey post hoc test. The ANOVA was also performed on the growth rate (µmax), production (Px) and lipid rate (TLR) results to identify the strains with the highest performance. A multivariate correspondence analysis was performed on the FTIR ratio normalized by silica for lipids, protein and carbohydrates to assess the dispersion of the biochemical information across the screened species and to identify if strains could be classified according to this information. This method was chosen since it analyzes binary, ordinal and nominal data without distributional assumptions (unlike traditional multivariate techniques) and also to preserve the categorical nature of the variables. The correspondence analysis provided a unique graphical display showing how the variable response categories were related (Sourial *et al*., 2010).

The Pearson product-moment correlation was used to test the correlation between the calculation methods using the FTIR spectra semi-quantitative information with the total lipid

quantification reference method (the gravimetric approach). The Pearson product-moment correlation and the comparison of the growth parameters were carried out using SigmaStat 3.1 software. The Past3 software was used for the correspondence analysis approach. All experiments were performed in triplicate.

Finally, all the information and tests were combined and used for the validation of the screening methodology to characterize the diatom strains of the NCC and the selection of candidates presenting the best potential in terms of growth capabilities and lipid rates.

5.4 Results

5.4.1 Determination of the growth parameters

The latency, exponential and stationnary phases were observable whatever the technique used to establish the growth curve for the 6 strains selected for their different kinetic behaviour (Fig. II-3). Moreover, the cell count, NDVI and F0 data were all correlated (Tab.II-4) confirming the same growth pattern. Cell count and NDVI were positively correlated (p<0.001) as cell count and F0 (p<0.001). R values for the NDVI varied from 0.70 to 0.90 and for F0 measurements from 0.60 to 0.93.

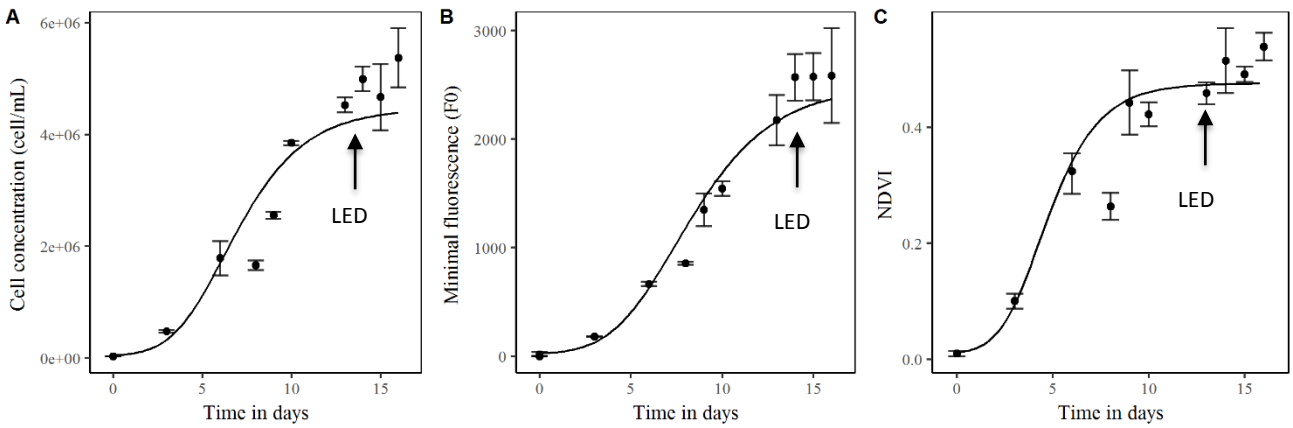

Figure II-3 Example of growth curves measured for *Amphora* sp 1 NCC260 by (A) cell count, (B) fluorometry PAM (F0) and (C) radiometry (NDVI). Points corresponding to cell concentration according to time. Line curves corresponding to the Gompertz model fitted to cell concentration as a function of time. n=3, vertical bar = SD. The arrows indicate the late exponential day estimated by the Gompertz model.

Table II-4 Pearson product correlation between radiometry (NDVI) and cell count and fluorometry PAM (F0) and cell count. Correlation was significant (p <0.001)

Species	NDVI	F0
Amphora sp. 1 NCC260	0.90	0.93
Entomoneis paludosa NCC18.2	0.86	0.82
Entomoneis sp. 1 NCC335	0.86	0.81
Entomoneis sp. 6 NCC350	0.80	0.60
Extubocellulus cf cribriger NCC229	0.70	0.90
Navicula sp. 2 NCC226	0.80	0.78

There were no significant differences ($p > 0.05$) between the technique used to estimate the growth rate (µmax) and the late exponential day (LED) for the six tested species, except for the µmax value estimated for *Entomoneis paludosa* (Tab. II-5). For example, *Amphora* sp. 1 reached the late exponential phase at the day c.a. 13 (LED, Fig. II-3, Tab. II-5) with a mean µmax of c.a. 0.81 (Tab. II-5). At this time, the maximum biomass was reached by the cell count indicator with $4.5 \pm 0.2 \times 10^6$ cells.mL^{-1} by PAM fluorometry with F0 values 2785 ± 609, and by radiometry with NDVI reaching 0.47 ± 0.05. Because the fluorimetry is used extensively for the measurement of extracted Chl *a*, for the estimation of the phytoplankton Chl *a in vivo* (Lorenzen, 1966; Vyhnalek *et al*., 1993) and do not need filtration of high amounts of culture (contrary to NDVI), it was selected as an fast and reliable alternative approach to the cell count to determine the growth rates of all selected diatom strains in this study. Regarding *Entomoneis paludosa*, a new experiment using only PAM measurments, in the same culture conditions but without counting and NDVI estimation were conducted. µmax values obtained were 0.52, 0.55, 0.55, leading to an average value of 0.54 ± 0.016. A second statistical test performed on these new data concluded no significant difference for µmax and LED ($p = 0.47$).

Table II-5 Values of the growth parameters (maximum growth rate, µmax (in d^{-1}) and late exponential day, LED (in days)) retreived from the Gompertz model using six species employed for the comparison of the cell count approach with two alternative techniques: Fluorometry PAM and radiometry. The calculated P value corresponded to the ANOVA test except for the (*) values that were obtained using the Kruskal-Wallis test. N=3, independent measurements, ± SD.

Species	Techniques	µmax (day^{-1})	LED (day)	P value (µmax)	P Value (LED)
Amphora sp. 1 NCC260	Cell count	0.76 ± 0.10	13 ± 1	P=0.8	P=0.16*
	Pam	0.78 ± 0.30	14 ± 1		
	Spectroradiometer	0.88 ± 0.25	12 ± 2		
Entomoneis paludosa NCC18.2	Cell count	0.50 ± 0.03	12 ± 1	P≤ 0.05[1]	P=0.07*
	Pam	0.95 ± 0.23[1]	10 ± 0		
	Spectroradiometer	0.47 ± 0.01	10 ± 0		
Entomoneis sp. 6 NCC335	Cell count	0.53 ± 0.10	14 ± 1	P=0.27	P=0.14*
	Pam	0.54 ± 0.12	12 ± 1		
	Spectroradiometer	0.32 ± 0.14	12 ± 2		
Entomoneis sp. 1 NCC350	Cell count	0.24 ± 0.01	16 ± 2	P=0.29	P=0.09
	Pam	0.37 ± 0.12	14 ± 1		
	Spectroradiometer	0.35 ± 0.06	14 ± 1		
Extubocellulus cf cribriger NCC229	Cell count	0.68 ± 0.04	14 ± 1	P=0.10	P=0.14
	Pam	0.81 ± 0.01	9 ± 0		
	Spectroradiometer	0.83 ± 0.07	10 ± 3		
Navicula sp. 2 NCC226	Cell count	0.91 ± 0.04	8 ± 0	P=0.42*	P=0.78*
	Pam	1.02 ± 0.23	8 ± 2		
	Spectroradiometer	0.87 ± 0.02	9 ± 2		

[1] Entomoneis paludosa µmax value for the second run was 0.54 and associated P value was 0.47

5.4.2 Diatom strain characteristics

Among the 68 screened strains, 33 were cultivated successfully and 36 did not grow (supplementary data S1). This information is reported in Tab. II-6, (with the NCC reference, the sampling location, the cell size, the LED, the growth rate, the silica content, the DW and lipid rate). Globally the cell length varied from 58 ± 14 µm (*Craspedostauros* sp. 2 NCC218) to 4.8 ± 0.7 µm (*Extubocellulus cf cribriger* NCC229). The cell width varied from 22.6 ± 4.1 µm (*Lithodesmium sp* NCC353) to 2.9 ± 0.4 µm (*Fallacia* sp. 1 NCC303). The end of the exponential phase, corresponding to the harvest day (LED), varied from day 6 for *Surirella* sp. 1 NCC270 to day 16 for *Craspedostauros britannicus* NCC228 and *Navicula* sp. 1 NCC113 (ANOVA, $p < 0.001$). Three groups were therefore identified depending on their growth rate: group A, included *Nitzschia alexandrina* NCC33 and *Entomoneis* sp. 5 NCC302 with respective growth rates of 1.89 ± 0.10 and 1.50 ± 0.18 day^{-1}, group B with 13 species (i.e 40%

of the total number of strain) presented a growth rate ranging from 1.19 ± 0.08 to 0.81 ± 0.09 day^{-1} and group C with 18 species (54%) had a growth rate below 0.8 day^{-1} with a minimum at 0.22 ± 0.05 day^{-1}.

To ensure the standardization of the FTIR results for inter species comparison purposes, the total silica rate was evaluated for the 33 species. It showed a significant difference (ANOVA, $p < 0.01$), where five species (i.e. 15% of the total number of strains) had a silica content of c.a. 40% of the dry weight with a maximum of 46.11 ± 4.58% for *Entomoneis* sp 1 NCC350. Three species (i.e. 9% of the total number of strains) presented a silica content of c.a. 23% of the dry weight with a minimum of 22.9 ± 2.6% for *Conticriba weissflogii* CCMP1336. In the other species, representing more than 75% of the total number of strains, the differences were not significant (ANOVA, $p = 0.055$), supporting a stable silica content situated at around 35% DW. The dry weight (DW) biomass values of the assessed strains ranged from 0.502 ± 0.039 $g.L^{-1}$ (*Craspedostauros britannicus* NCC195) to 0.065 ± 0.001 $g.L^{-1}$ (*Entomoneis* sp. 3 NCC351). For three strains (9% of the total number of strains) the DW was greater than 0.30 $g.L^{-1}$. For 27 strains (81%) the biomass was greater than 0.10 $g.L^{-1}$ but lower than 0.30 $g.L^{-1}$. For the three remaining strains (9%) the biomass was lower than 0.10 $g.L^{-1}$.

The lipid rate estimated with the gravimetric method ranged from 30.5 ± 0.7% DW (*Nitzschia* sp. 5 NCC109) to 3.7 ± 1.1% DW (*Brockmaniella brockmanii* NCC161). For three strains (9%) the lipid rate was greater than 20% DW. For 14 strains (42%) the lipid rate was greater than 10% DW. In the remaining 16 strains (48%) the lipid rate was lower than 10% DW.

Biomass productivity varied substantially among the tested strains (Fig. II-4A) and ranged from 0.36 ± 0.02 $g.L^{-1}.day^{-1}$ (*Nitzschia alexandrina* NCC33) to 1.4 ± 0.3 × 10^{-2} $g.L^{-1}.day^{-1}$ (*Entomoneis* sp. 3 NCC351). The results were found to be statistically different among those strains (ANOVA, $p< 0.001$). Finally, the strains were clustered into three groups according to the following parameters (Fig. II-4): group 1 with productivity between 0.35 ± 0.02 and 0.19 ±

0.04 $g.L^{-1}.day^{-1}$; group 2 with productivity ranging from 0.17 ± 0.08 to 0.09 ± 0.02 $g.L^{-1}.day^{-1}$; group 3 with lower productivity ranging from $7.5 \pm 0.4 \times 10^{-2}$ to $1.4 \pm 0.3 \times 10^{-2}$ ($g.L^{-1}.day^{-1}$). The most productive strains were those exhibiting the highest µmax associated to the highest DW. But they did not correspond to the richest in terms of total lipid rate (Fig. II-4B).

Table II-6 Characteristics and sampling locations of the investigated diatoms species. All data were obtained by experimental measurements. N=3, independent measurement, ± SD. (Chen *et al*., 2007 [1]; Chisti, 2007b [2]; Chtourou *et al*., 2015 [3]; Dalay *et al*., 2014 [4]; De la Pena, 2007 [5]; Fields and Kociolek, 2015 [6]; Griffiths and Harrison, 2009 [7]; Huntley *et al*., 2015 [8]; Islam *et al*., 2013 [9]; Jauffrais *et al*., 2016, 2015 [10-11]; Johansen *et al*., 1987 [12]; Knuckey *et al*., 2002 [13]; Renaud *et al*., 1999[14]; Scholz and Liebezeit, 2013 [15]; Sheehan *et al*., 1998 [16]; Slocombe *et al*., 2015 [17]; Soares *et al*., 2013 [18]; Viriyayingsiri *et al*., 2016 [19]; Wen and Chen, 2000 [20]; F.-Y. Zhao *et al*., 2016 [21])

Species	NCC strain identification	Sampling location	Cell size (µm)		LED (day)	µmax		Silica content (%)	Biomass ($g.L^{-1}$)	TLR (% DW)	Ref
			Length	Width							
Nitzschia alexandrina	NCC33	*France, NW Atlantic coast*	11.0 ± 1.2	3.7 ± 0.4	11 ± 0	1.89 ± 0.10	A	27.2 ± 3.8	0.189 ± 0.004	12.7 ± 3.2	[1,2,4,7,12,14,16,20,21]
Entomoneis sp. 5	NCC302	*France, NW Atlantic coast*	22.4 ± 3.5	15.0 ± 2.2	9 ± 0	1.50 ± 0.18		38.9 ± 0.7	0.132 ± 0.025	6.9 ± 2.4	[10,11,13,18,19]
Entomoneis sp. 2	NCC20	*France, NW Atlantic coast*	30.5 ± 4.6	18.5 ± 3.2	8 ± 0	1.19 ± 0.08		34.3 ± 2.8	0.244 ± 0.042	10.3 ± 2.7	[10,11,13,18,19]
Staurosira sp.	NCC182	*France, NW Atlantic coast*	6.9 ± 1.4	5.5 ± 1.2	8 ± 2	1.17 ± 0.09		28.9 ± 5.1	0.262 ± 0.084	25.1 ± 1.2	[8]
Fallacia sp. 1	NCC303	*Greenland, east coast*	6.4 ± 0.7	2.9 ± 0.4	12 ± 2	1.12 ± 0.14		37.4 ± 4.5	0.154 ± 0.016	14.2 ± 1.9	-
Fallacia sp. 2	NCC304	*Greenland, east coast*	6.4 ± 0.8	3.1 ± 0.4	12 ± 0	1.07 ± 0.15		31.8 ± 4.9	0.265 ± 0.028	9.2 ± 3.3	-
Entomoneis sp. 7	NCC445	*France, NW Atlantic coast*	10.4 ± 1.5	4.1 ± 0.7	9 ± 2	1.02 ± 0.05		41.4 ± 2.9	0.122 ± 0.005	10.2 ± 2.8	[10,11,13,18,19]
Entomoneis paludosa	NCC18.1.1	*France, NW Atlantic coast*	18.4 ± 3.3	10.7 ± 1.9	11 ± 1	0.96 ± 0.03		37.8 ± 4.0	0.130 ± 0.016	5.3 ± 0.3	[10,11,13,18,19]
Entomoneis sp. 4	NCC301	*France, NW Atlantic coast*	23.9 ± 3.4	17.3 ± 2.2	7 ± 1	0.92 ± 0.14		26.7 ± 3.9	0.171 ± 0.012	6.7 ± 1.5	[10,11,13,18,19]
Pseudonitzschia americana	PNA06 KER	*France, NW Atlantic coast*	6.6 ± 0.8	4.5 ± 0.5	9 ± 2	0.89 ± 0.09	B	36.4 ± 0.6	0.099 ± 0.019	5.7 ± 1.6	-
Surirella sp. 1	NCC270	*France, NW Atlantic coast*	6.8 ± 1.3	5.0 ± 1.6	6 ± 1	0.85 ± 0.31		33.7 ± 3.5	0.173 ± 0.033	19.3 ± 2.8	-
Navicula sp. 2	NCC226	*France, NW Atlantic coast*	9.1 ± 1.3	5.6 ± 0.7	8 ± 2	0.82 ± 0.05		41.4 ± 1.5	0.131 ± 0.015	8.7 ± 2.5	[2,6,12,15,16,21]
Opephora sp. 1	NCC366	*France, NW Atlantic coast*	5.4 ± 0.8	3.7 ± 0.8	14 ± 1	0.82 ± 0.16		37.8 ± 8.4	0.233 ± 0.010	11.5 ± 3.1	-
Entomoneis paludosa	NCC18.2.1	*France, NW Atlantic coast*	18.8 ± 1.8	11.2 ± 2.5	12 ± 1	0.81 ± 0.05		36.0 ± 3.9	0.150 ± 0.003	7.3 ± 1.0	[10,11,13,18,19]
Extubocellulus cf cribriger	NCC229	*France, NW Atlantic coast*	4.8 ± 0.7	3.9 ± 0.5	9 ± 0	0.81 ± 0.09		33.7 ± 2.3	0.155 ± 0.003	14.2 ± 4.8	[9,13,17]
Amphora sp. 1	NCC260	*France, NW Atlantic coast*	9.8 ± 1.3	3.7 ± 0.5	13 ± 0	0.78 ± 0.30		36.2 ± 2.6	0.176 ± 0.041	18.5 ± 4.2	[3,5,6,15,21]
Conticriba weissflogii	CCMP1336	*USA, NE Atlantic coast*	15.6 ± 2.5	10.8 ± 1.4	12 ± 0	0.59 ± 0.15		22.9 ± 2.6	0.277 ± 0.035	7.2 ± 1.7	-
Brockmaniella brockmanii	NCC161	*France, NW Atlantic coast*	9.2 ± 2.4	4.3 ± 0.6	10 ± 0	0.58 ± 0.01		37.5 ± 0.2	0.185 ± 0.025	3.7 ± 1.1	-
Craspedostauros britannicus	NCC195	*France, NW Atlantic coast*	37.8 ± 8.8	11.0 ± 2.2	9 ± 0	0.53 ± 0.09		44.7 ± 0.1	0.502 ± 0.039	8.2 ± 1.8	-
Conticriba weissflogii	NCC133	*Morocco,Oum R'bia estuary*	14.3 ± 1.7	12.1 ± 1.7	7 ± 0	0.53 ± 0.08		34.6 ± 1.2	0.181 ± 0.015	6.4 ± 0.7	-
Licmophora sp. 1	NCC253	*France, NW Atlantic coast*	20.0 ± 3.9	12.4 ± 1.6	11 ± 0	0.51 ± 0.02		37.8 ± 5.7	0.161 ± 0.049	13.5 ± 1.1	-
Amphora sp. 2	NCC169	*France, NW Atlantic coast*	9.0 ± 1.2	5.8 ± 1.2	13 ± 3	0.48 ± 0.14		33.8 ± 4.8	0.157 ± 0.024	16.0 ± 2.6	[3,5,6,15,21]
Craspedostauros sp. 1	NCC228	*France, NW Atlantic coast*	55 ± 14	14.9 ± 4.2	16 ± 4	0.46 ± 0.22	C	25.2 ± 0.7	0.384 ± 0.042	5.6 ± 1.4	-
Craspedostauros sp. 2	NCC218	*France, NW Atlantic coast*	58 ± 14	13.6 ± 3.4	12 ± 0	0.45 ± 0.18		26.0 ± 4.1	0.178 ± 0.047	5.9 ± 1.4	-
Cymatosira belgica	NCC208	*France, NW Atlantic coast*	5.6 ± 0.6	4.7 ± 0.7	12 ± 0	0.44 ± 0.12		35.5 ± 3.4	0.118 ± 0.043	14.6 ± 3.0	-
Amphora acutiuscula	NCC216	*Viet Nam, South east coast*	10.0 ± 1.0	5.6 ± 0.8	11 ± 0	0.43 ± 0.07		32.4 ± 0.7	0.144 ± 0.041	13.7 ± 5.1	[3,5,6,15,21]
Lithodesmium sp	NCC353	*Australia, Moreton bay*	29.3 ± 5.4	22.6 ± 4.1	9 ± 1	0.43 ± 0.02		34.1 ± 6.1	0.129 ± 0.006	7.1 ± 2.9	-
Navicula sp. 1	NCC113	*Morocco,Oum R'bia estuary*	17.1 ± 2.9	5.1 ± 1.2	16 ± 0	0.42 ± 0.02		25.0 ± 1.0	0.168 ± 0.035	23.1 ± 6.4	[2,6,12,15,16,21]
Entomoneis sp. 6	NCC335	*France, Mediterranean Sea*	13.9 ± 1.9	7.7 ± 1.9	12 ± 1	0.38 ± 0.03		36.8 ± 4.7	0.226 ± 0.036	3.7 ± 1.1	[10,11,13,18,19]
Entomoneis sp. 1	NCC350	*France, Mediterranean Sea*	29.0 ± 4.0	17.5 ± 2.7	14 ± 0	0.36 ± 0.13		46.1 ± 4.6	0.098 ± 0.048	8.8 ± 0.1	[10,11,13,18,19]
Craspedostauros britannicus	NCC199	*France, NW Atlantic coast*	31.2 ± 3.2	8.8 ± 1.6	12 ± 2	0.35 ± 0.14		40.0 ± 2.9	0.421 ± 0.053	12.5 ± 1.2	-
Nitzschia sp. 5	NCC109	*France, NW Atlantic coast*	33.1 ± 4.1	10.1 ± 1.5	12 ± 1	0.31 ± 0.05		23.0 ± 1.5	0.239 ± 0.026	30.5 ± 0.7	[1,2,4,7,12,14,16,20,21]
Entomoneis sp. 3	NCC351	*France, Mediterranean Sea*	16.6 ± 3.7	12.3 ± 3.0	13 ± 0	0.22 ± 0.05		38.6 ± 5.8	0.065 ± 0.001	13.3 ± 4.6	[10,11,13,18,19]

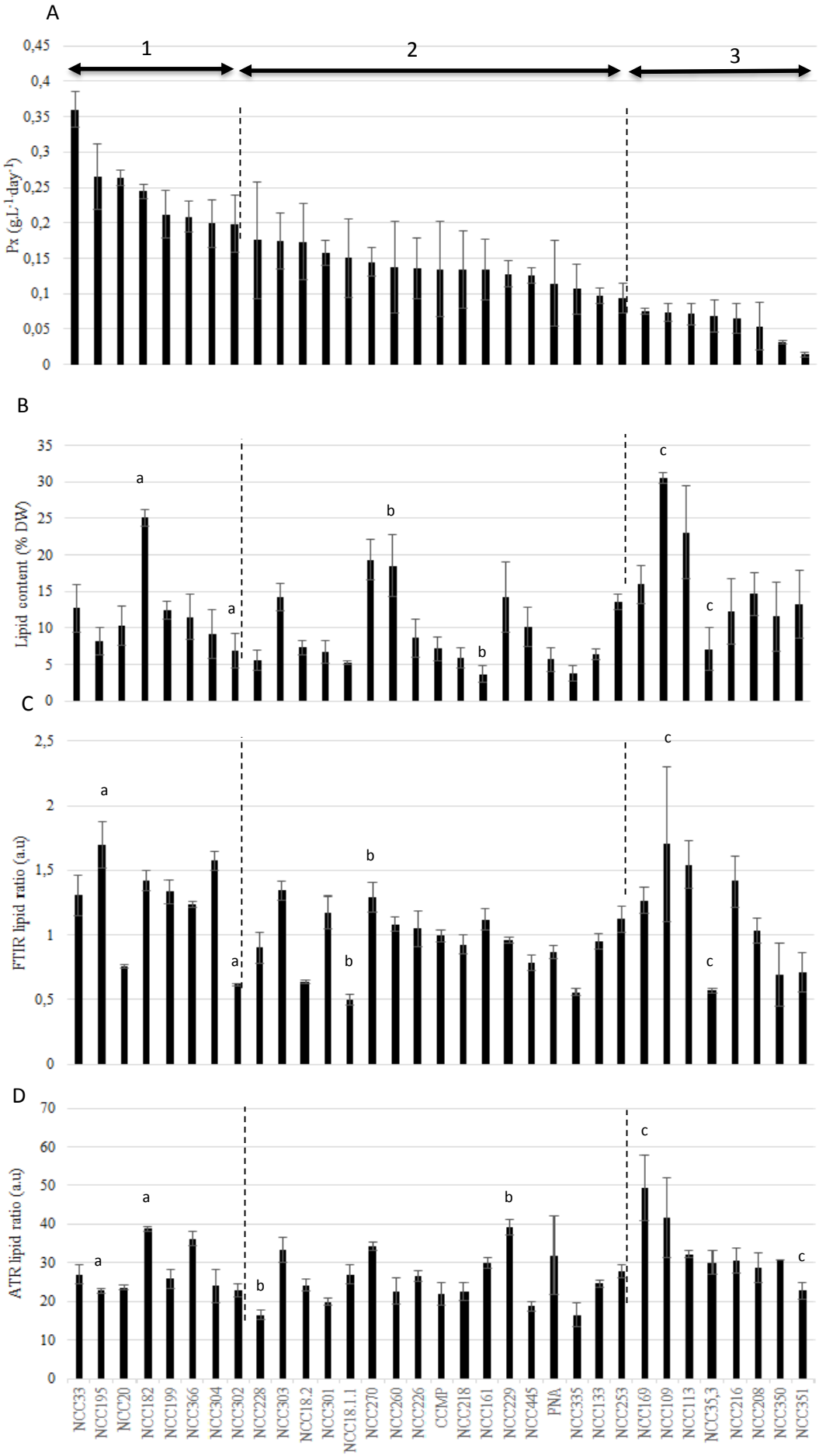
A
1
2
3
Px (g.L-1.day-1)
B
Lipid content (% DW)
C
FTIR lipid ratio (a.u)
D
ATR lipid ratio (a.u)
NCC33
NCC195
NCC20
NCC182
NCC199
NCC366
NCC304
NCC302
NCC228
NCC303
NCC18.2
NCC301
NCC18.1.1
NCC270
NCC260
NCC226
CCMP
NCC218
NCC161
NCC229
NCC445
PNA
NCC335
NCC133
NCC253
NCC169
NCC109
NCC113
NCC35,3
NCC216
NCC208
NCC350
NCC351

Figure II-4 Values of the parameters measured for the screened strains includes strain productivity (A), lipid rates as measured with the gravimetric method (B), lipid ratio measured semi-quantitatively by the FTIR approaches, [(eb+CH3+CH3)/si] (C) and [area eb+CH2+CH3)/Total area] multiplied by 100 for scaling purposes (D). Notations a, b, and c correspond to the maximum and minimum values for groups 1, 2 and 3. N=3, independent measurements, ± SD

5.4.3 FTIR analysis

5.4.3.1 FTIR spectrum interpretation

HTSXT-FTIR analysis was performed on the 33 assayed species (Tab. II-6, supplementary data S2). The lipid rate was associated to three main signals on the recorded spectra (Fig. II-5A), i.e. through the two vibrations of the fatty acid carbon chains (ν CH_2 and ν CH_3) (ν C-H ~ 2923 and 2852 cm^{-1}) (Coat *et al*., 2014) and of the ester bond function (Eb) (ν C=O ~ 1750 cm^{-1}) (Giordano *et al*., 2001). The other major bands corresponded to the principal cellular components such as the proteins (the amide I band ν C=O ~1650 cm^{-1}; the amide II band δ N=H ~1540 cm^{-1}), the nucleic acids (ν P=O ~1230 cm^{-1}) and the carbohydrates band superimposed on the silica band (~900 – 1200 cm^{-1}). For details see Wagner *et al*., 2010 (Wagner *et al*., 2013). Whereas the infrared signature obtained on the whole cells showed superimposed bands of silica and carbohydrates at 1078 cm^{-1} (Fig. II-5A) the signature obtained on the crude lipid extract (Fig. II-5B) did not exhibit this band, but a well defined ester bond (Eb) band at 1750 cm^{-1} and well-defined bands for the CH_2-CH_3 signature at 3000-2800 cm^{-1}.

The lipid ratio estimated from the FTIR data measured on the entire cells (Fig.II-4C) ranged from 1.70 ± 0.59 (*Nitzschia* sp. 5 NCC109) to 0.49 ± 0.04 (*Entomoneis paludosa* NCC18.1.1). It was thus possible to cluster the assessed strains into three groups. Group 1 showed a maximum ratio at 1.69 ± 0.18 for *Craspedostauros britannicus* NCC195 and a minimum at 0.61 ± 0.01 for *Entomoneis* sp 5 NCC302, group 2 showed a maximum ratio at 1.34 ± 0.07 for *Fallacia* sp 1 NCC303 and a minimum at 0.49 ± 0.04 for *Entomoneis paludosa* NCC18.1.1 and group 3 showed a maximum ratio at 1.70 ± 0.59 for *Nitzschia* sp NCC109 and minimum at 0.56 ± 0.02 for *Lithodesmium sp* NCC35.3.

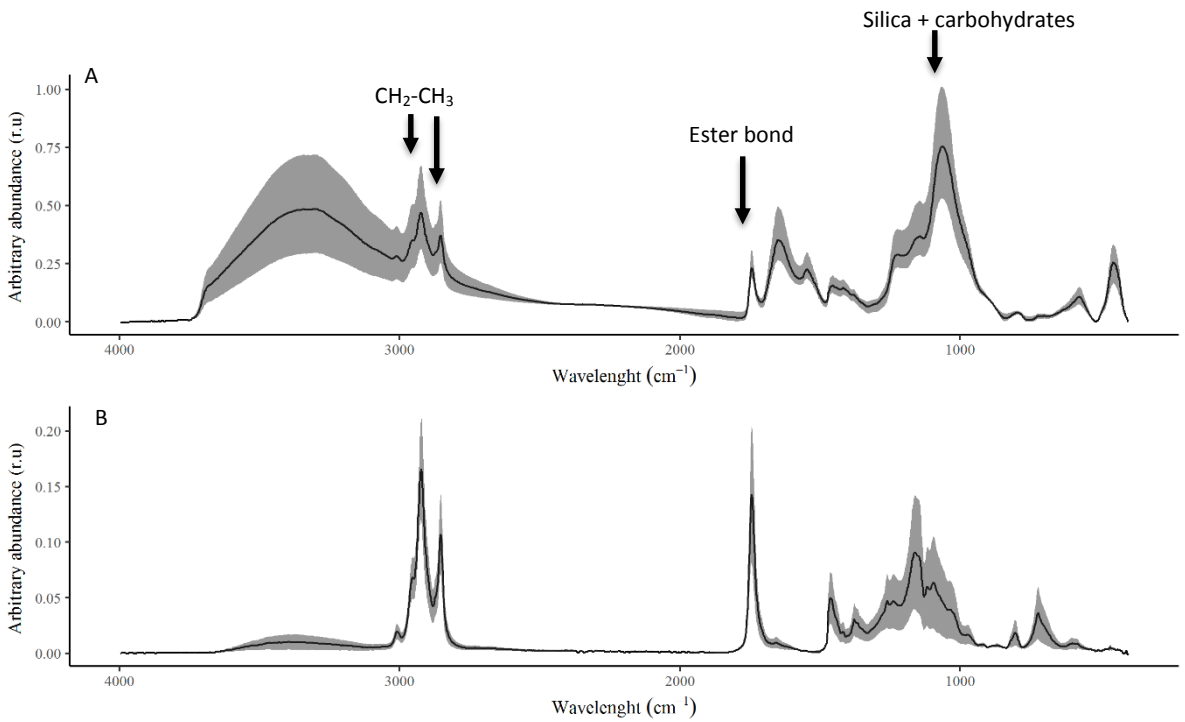

Figure II-5 Example of averaged FTIR spectra recorded on entire cells or on the corresponding lipid extract. (A) *Staurosira* sp NCC182 FTIR signature recorded on the entire cells and (B) *Staurosira* sp NCC182 FTIR signature recorded on a crude lipid extract. The grey area corresponds to the variation of the FTIR signal associated to the standard deviation for n=3 independent measurements.

The lipid ratio estimated from the FTIR data recorded on the lipid extracts (Fig.II-4D) ranged from 49.3 ± 8.5 (*Amphora* sp. 2 NCC169) to 16.5 ± 3.1 (*Entomoneis* sp. 6 NCC335). Three groups were also proposed regarding this criterion, group 1 showed a maximum ratio at 38.84 ± 0.63 for *Staurosira* sp. NCC182 and a minimum ratio at 22.8 ± 1.8 for *Entomoneis* sp. 5 NCC302, group 2 a maximum ratio at 39 ± 2 for *Extubocellulus* sp. NCC229 and a minimum at 16.5 ± 1.2 for *Craspedostauros britannicus* NCC228 and group 3 with a maximum ratio at 49.3 ± 8.3 for *Amphora* sp. 2 NCC169 and a minimum at 23 ± 2 for *Entomoneis* sp. 3 NCC351. The silica amount did not appear to significantly impact on the lipid FTIR signature except in three species for which the FTIR lipid ratio fell between the two FTIR signature sampling methods (i.e. on entire cells or on lipid extract). These were Craspedostauros *brittanicus*

NCC195, *Navicula* sp. 4 NCC113 and *Conticriba weissflogii* CCMP1336. For the other species with different silica content, the lipid signature remained stable in both FTIR sampling methods.

5.4.3.2 Multivariate analysis of the FTIR spectra recorded on entire cells

In order to assess the main differences in terms of biochemical composition among the 33 screened strains, a correspondence analysis approach using the lipid, protein and carbohydrate bands normalized to the silica amounts was performed. The resulting map (Fig. II-6) is a classification of the data on two main dimensions. Dimension 1 represents 81% of the initial information and could be associated to the variation of the lipid composition of the assessed strains, ranging from the lowest to the highest amount of total lipids from right to left on the map. Two strains, *Staurosira* sp. NCC182 and *Amphora* sp. 2 NCC169 presented the highest amount in total lipids. Along dimension 2, representing 19% inertia, the strains associated to that dimension were mainly opposed on the basis of their protein and carbohydrate content. *Craspedostauros* sp. 2 NCC218 was rich in proteins, whereas in *Brockmaniella brockmanii* NCC161 the main fraction was associated to the carbohydrates.

These results indicate that the 2 most notable differences or largest deviations in the sample were observed first between *Staurosira* sp. NCC182, *Amphora* sp. 2 NCC169 and the other species for their lipid rates, and secondly between the strains *Craspedostauros* sp. 2 NCC218, *Brockmaniella brockmanii* NCC161 and the other species by their respective protein and carbohydrate composition. This analysis summarizes the main biochemical characteristics of the strains hosted in the NCC bank in a single step. Although the distance between the macromolecular content and the species were not mathematically defined, their closeness on the map could be used as a guideline to interpret their biochemical characteristics: the squares correspond to the strains particularly rich in lipids, the triangles, the strains rich in carbohydrates and the dots, the strains particularly rich in proteins.

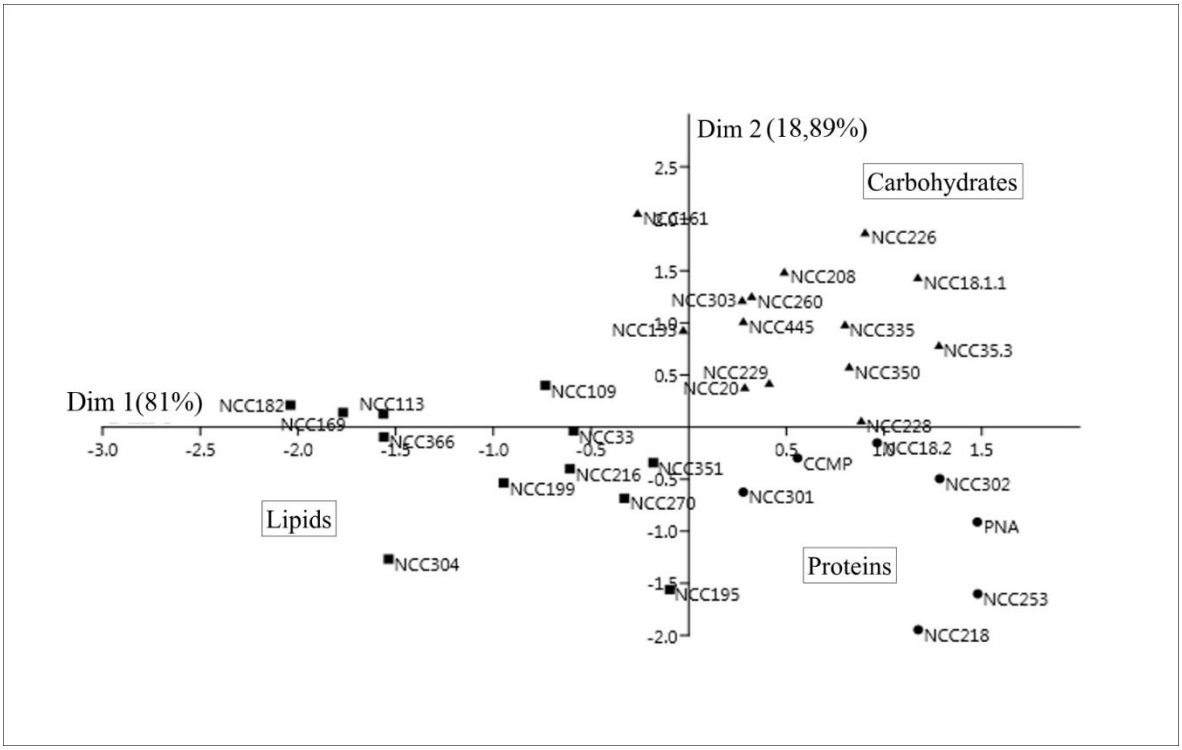

Figure II-6 Correspondence analysis map calculated on the basis of the macromolecular content as evaluated by FTIR on all the assayed strains of the NCC. N=3 independent measurements.

5.4.3.3 Comparison of the lipid amounts estimated by the gravimetric method and the FTIR approaches.

A significant positive correlation was found for all the techniques (gravimetric and FTIR) ($p < 1.10^{-7}$) with a Pearson correlation score R superior to 0.53. For the 33 analyzed species, 14 presented a high lipid ratio (> 12% DW) using the gravimetric measurements: *Nitzschia alexandrina* NCC33, *Staurosira* sp. NCC182, *Fallacia* sp. 1 NCC303, *Surirella* sp. 1 NCC270, *Extubocellulus cf cribriger* NCC229, *Amphora* sp. 1 NCC260, *Licmophora sp.1* NCC253, *Amphora sp. 2* NCC169, *Cymatosira belgica* NCC208, *Amphora acutiuscula* NCC216, *Navicula* sp. 1 NCC113, *Craspedostauros britannicus* NCC199, *Nitzschia* sp. 5 NCC109 and *Entomoneis sp.3* NCC351 (Fig. II-4B, Fig. II-7). The FTIR method applied on entire cells identified 12 species rich in lipids (FTIR lipid ratio > 1.20) with nine species identified in common with the gravimetric method: NCC33, NCC182, NCC303, NCC270, NCC169, NCC216, NCC113, NCC199 and NCC109 (Fig. II-4C, Fig. II-7). FTIR for the lipid extract analyses identified 12 species rich in lipids (ATR lipid ratio > 30) with eight species identified in common with the gravimetric approach: NCC182, NCC303, NCC270, NCC229, NCC169, NCC216, NCC113 and NCC109 (Fig II-4D, Fig. II-7).

The correspondence analyses (Fig.II-6) performed on the FTIR profiles obtained in the entire cells gave supplementary information and identified seven species particularly rich in lipids: NCC182, NCC270, NCC169, NCC113, NCC366, NCC109 and NCC33. These species were also identified by the gravimetric method with the exception of NCC366, only identified by the FTIR method on crude lipid extract.

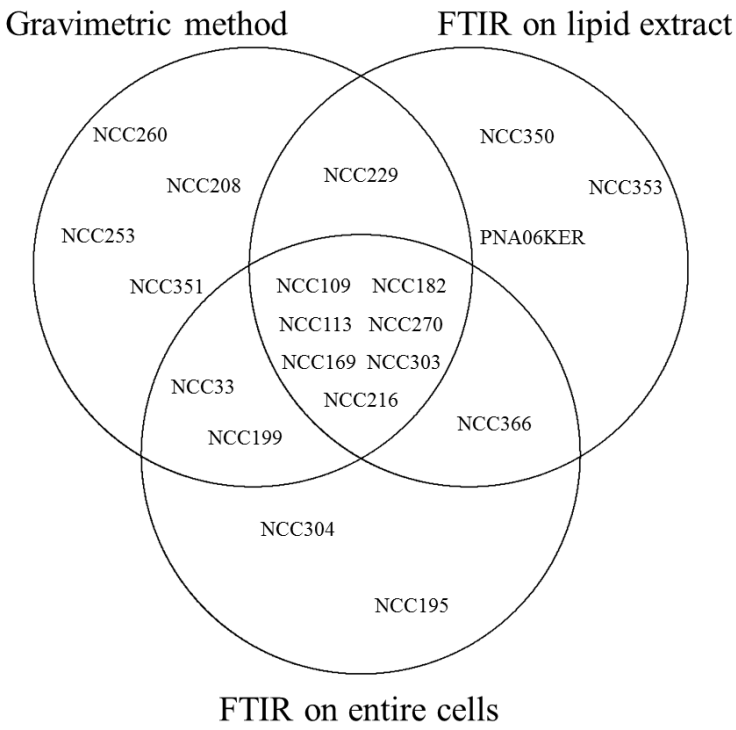

Figure II-7 Venn diagram showing the degree of overlap among the different approaches used to identify the lipid rich diatoms. In the gravimetric method circle, 14 strains were identified as rich in lipids: 4 only with this method (NCC260, NCC208, NCC253, NCC351), one strains were also identified as rich and lipid by the FTIR on lipid extract (NCC229), and two strains were also identified as rich in lipids by the FTIR on entire cells (NCC33, NCC199). One strain was identified by FTIR on lipid extract and FTIR on whole cells (NCC366) and seven strains were identified as rich in lipids by all three methods (NCC109, NCC182, NCC113, NCC270, NCC169, NCC303, NCC216).

5.4.4 Strain selection

The selection of the strains exhibiting both high biomass productivity and high lipid rates, was performed using whole sample distribution based on the lipid rates as estimated by the FTIR approaches, gravimetry and strain biomass productivity as estimated by the fluorometry. On the boxplots summarizing this data (Fig. II-8), the colored dots represent the species with the highest potential for biotechnology applications based on lipid molecules: *Nitzschia alexandrina* NCC33, *Staurosira* sp NCC182 and *Opephora* sp NCC366 presented a lipid ratio whatever the considered technique and productivity above the median. *Amphora* sp 2 NCC169 and *Nitzschia* sp 5 NCC109 were also identified with an above median lipid ratio, but with lower productivity. Both these species were finally selected for their high lipid rate, even though their productivity needs to be improved.

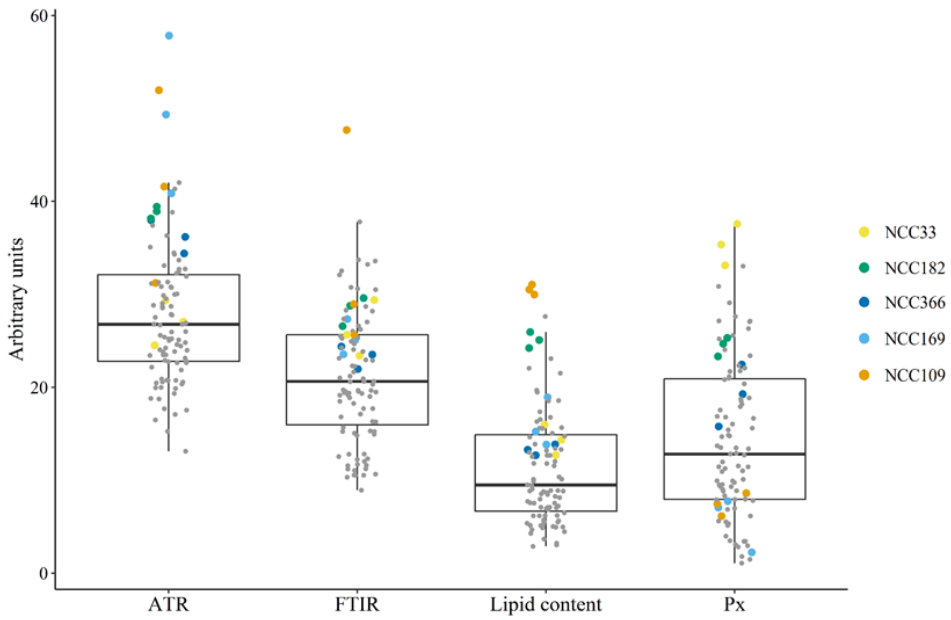

Figure II-8 Boxplots summarizing the sample distribution criteria as measured with FTIR methods, gravimetry for the lipid rate and flurorimetry for productivity. FTIR data was expressed in arbitrary units. Lipid rate in %DW and Px in $g.L^{-1}.day^{-}.^{1}$ FTIR results were multiplied by 20 for scaling purposes. The Px was multiplied by 100 for scaling purposes. 33 strains were assayed in independent biological triplicates.

5.5 Discussion

5.5.1 Determination of growth by fluorimetry

In this study a rapid and precise method for the estimation of cell abundance was needed to efficiently establish the growth parameter of over 60 benthic diatom species. The use of microscope counting chambers is slow, tedious and imprecise. The use of particle counters is feasible only for those phytoplankton species within a certain size range that do not form chains and have long appendages (Brand *et al*., 1981). *In vivo* fluorescence has been successfully used in the past to monitor the growth of phytoplankton culture (Gilstad and Sakshaug, 1990; Honeywill *et al*., 2002; Lorenzen, 1966; Steinman *et al*., 2017; Vyhnalek *et al*., 1993). *In vivo* fluorescence measurement is rapid, sensitive and can be used with all types of diatoms cell structures, i.e. on solitary cells such as *Entomoneis* and *Navicula* genera and on chain-forming diatoms, such as *Extubocellulus* genus or aggregates of cells such as *Amphora* genus. However, *in vivo* fluorescence is a measurement of the increase in chlorophyll and chlorophyll per cell varies greatly with light intensity and cellular nutritional status so it can only be used to measure growth when culture conditions are constant. Changes in light and other culture conditions can lead to a change in chlorophyll a content. In this case F0 will also change, introducing a bias in growth rate estimation. Reflectance can also be used to monitor the diatom growth rate, as demonstrated in this study; the NDVI was highly correlated with the cell count as *in vivo* fluorescence (R> 0.70). Méléder *et al*, 2003 (Méléder *et al*., 2003) have already demonstrated this correlation on monospecific benthic diatom cultures with *Entomoneis paludosa* and *Navicula ramosissima*. Compared to fluorometry this technique required more culture sampling and a filtration step which took longer to set up. Fluorometry was more sensitive than spectroradiometry and required less material, which made it ideal for very low amounts of biomass. *In vivo* fluorometry demonstrated several advantages: ease of use, real-time measurement, non-destructive sampling.

5.5.2 Determination of the lipid rate by FTIR

The total lipid evaluation by gravimetry has been used for more than 50 years (Breil *et al*., 2017), but this technique is clearly not compatible with screening efforts involving large numbers of samples because of processing time required particularly in the extraction phase. Furthermore, large volumes of samples are systematically needed for the measurements. It also requires sufficient amounts of dried biological sample, thus making it unsuitable for high frequency monitoring of small scale microalgal cultivation. Feng *et al*., (2013) (Feng *et al*., 2013) suggested that the presence of chlorophyll could also affect the accuracy of the method. In comparison to conventional chemical analysis, FTIR spectroscopy presented striking advantages due to its high reliability, sensitivity and speed of the measurement (Wagner *et al*., 2013). An IR spectrometer coupled to a microtiter plate reader open the possibility of high throughput analysis of a few nanograms of cell material (Stehfest *et al*., 2005). Coat *et al*, (2014) (Coat *et al*., 2014) demonstrated that the repeatability of FTIR signal reached excellent values (10%), but only for a limited range of analyzed quantities of matter (10^6 to 10^8 cells. mL^{-1}).

In the present study we have demonstrated that FTIR was a suitable technique to evaluate the lipid ratio of diatoms. The use of the FTIR technique was even more rapid, due to the use of direct fresh biomass. The results obtained on entire cells and lipid crude extracts were similar, suggesting that measurement on entire cells did not improve the lipid quantification. Measurement on whole cells could be considered sufficient to get a first idea on their intracellular lipid rate. In addition, removing the silica did not seem necessary in view of the present results to improve the lipid semi-quantification.

However, there are some limitations with this non-invasive technique. Even though the FTIR results between entire cells and crude extracts were similar, we did not obtain a perfect linear correlation with the traditional lipid extraction. Nevertheless, the FTIR method has the

advantage of simultaneously detecting the relative amount of lipids, carbohydrates and proteins, even though those components overlapped, implying a certain degree of inaccuracy. The different steps required for the lipid extraction can also produce a bias in the evaluation of the lipid quantity, added to the inaccuracy of weighing of the lipid matter, making it less precise than the spectrometric approach. The heterogeneity observed in the present FTIR results could be also associated to the utilization of different strains (33 strains in the current study). These are not described in the previous studies evaluating lipid quantification with FTIR where only one species was used (Coat *et al*., 2014; Dean *et al*., 2010; Schaub *et al*., 2017). FTIR did not differentiate polar/apolar lipids, or the different types of fatty acids produced by the strains. Lipid analysis by chromatographic techniques coupled to mass spectrometry will be needed to further identify the presence of interesting molecules like EPA or DHA. Nevertheless, the present study opens the way to rapid and reliable semi-quantification of total amounts of intracellular lipids in diatoms using a fast, non-invasive approach.

5.5.3 Method assessments

This study highlighted the efficiency of PAM and FTIR measurements as fast techniques to characterize both the growth and lipid content of microalgae (Tab.II-7). The use of PAM fluorometry was three times faster than cell counting. Where 15 minutes were necessary to count 3 samples (8.25 hours for 99 samples) and 10 minutes to measure reflectance by spectroradiometry (5.5 hours for 99 samples), only 5 minutes were necessary to measure F0 by PAM fluorometry (2.75 hours for 99 samples).

Table II-7 Evaluation of three methods for algal growth kinetic determination

Evaluation index	Counting	NDVI	PAM
Cultivation scale	Large	Large–small	Large–small
Monitoring frequency	High	Medium	High
Sample state	Liquid	Filtered	Liquid
Volume consumed	5 - 1 mL	5- 3 mL	>1 mL
Time consumed	8.25 h	5.5 h	2.75 h
Equipment	Counting chambers	Spectroradiometer	PAM fluorometer
Reliability	Low	High	High

For lipid extraction, dichloromethane methanol solvent is usually used (Bligh and Dyer, 1959; Li *et al*., 2014; Mubarak *et al*., 2015; Xu *et al*., 2013). Even though extraction was very effective, this method is known to have environmental and health risks (Mubarak *et al*., 2015). Moreover, it is expensive: for 99 extractions, 10 L of each solvent was necessary costing 234 € (9.68 €/L of methanol and 13.72 €/L of dichloromethane (Fischer Scientific). The time necessary for the lipid extraction using Bligh and Dyer method was time-consuming (Tab. II-8) due to the time needed for maceration and lipid separation. 5.5 weeks were necessary to perform the extraction of 99 samples (ca. 7920 hours). Nile red, a lipid soluble fluorescent dye, is commonly used to evaluate the lipid content of animal cells, microorganisms, and especially microalgal strains. Required time to perform spectrophotometric measurements with Nile red and Bodipy was evaluated at 10 mins per sample (measurement before and after Nile red or Bodipy application) and 25 to 40 mins incubation time was necessary after application of Nile red or Bodipy before reading spectrophotometric values (Feng *et al*., 2013; Xu *et al*., 2013). In comparison FTIR is a fast and eco-friendly technique. Two plates of 384 well were necessary to evaluate the lipid content for the 33 strains (each strain needed 15 wells with 5 wells per replicate). It took 30 seconds to read each well to obtain the FTIR spectra leading to ca. and 4 hours to read an entire plate.

Table II-8 Evaluation of three methods for algal lipid content determination

Evaluation index	Gravimetric	FT-IR	Nile Red / Bodipy 505/515
Cultivation scale	Large	Large–small	Large–small
Monitoring frequency	Low	Medium	High
Sample state	Dried	Liquid	Liquid
Biomass consumed	100 mg	5 µL of 1.0 mg mL^{-1}	3 mL of OD_{680} 0.4
Time consumed	>50 h	8 h	25 h
Equipment	Nitrogen evaporator	FT-IR	FS & FM [a]
Accuracy	Total lipid	Total lipid	Neutral lipid

[a] Fluorescence spectrophotometer and Fluorescence microscopy

Nile red and Bodipy 505/515 staining are powerful quantification tools in terms of time and cost of biomass (De la Hoz Siegler *et al*., 2012; Mutanda *et al*., 2011), high throughput quantification method of lipids with Nile red or Bodipy 505/515 fluorescence can hardly been seen as a method for screening different species of microalgae, as the staining protocol is species specific. The significant disadvantages of Nile red were its limited photostability, interference with chlorophyll (Chen *et al*., 2009; Laurens and Wolfrum, 2012), and difficulty of permeation for some species. Bodipy 505/515 produced a better marker than Nile red for visualizing neutral lipid content in fluorescence microscopy (Cooper *et al*., 2010; De la Hoz Siegler *et al*., 2012) but some authors have reported disadvantages with these techniques such as background fluorescence of the dye in the medium and failure to quantify neutral lipids between rich and low oil strains. When microalgae were cultured on a large scale with a low-frequency monitoring requirement, any of the three methods could be adopted, although gravimetric determination might be preferable as it was an absolute method for quantification of both crude and neutral lipids without the need of specialized equipment. For the general laboratory culture of microalgae, the FT-IR method for simultaneous characterization of total lipid, carbohydrate and protein content and the Nile Red method for both neutral lipid content

and location can be used, both of which are relative quantification methods, but require special equipment.

Although these analyses demonstrate that FTIR and Nile Red were equally effective at measuring lipid accumulation, FTIR was likely to be a more efficient tool for this purpose because of its much faster analysis time and high reproducibility of results (Murdock and Wetzel, 2009). Furthermore, FTIR may also be more suitable than Nile Red for efficiently detecting large increases in lipid concentration. Nile Red does not appear to be efficient at accurately quantifying lipid concentration above 20 mg/ml (Chen *et al*., 2009) while FTIR can efficiently detect linear lipid concentration changes up to at least 250 mg (Dreissig *et al*., 2009). Measurements with FTIR were more precise because of the technical quintuplicate performed for the acquisition of spectra.

5.5.4 Screening for lipid rich benthic diatom strains

The aim of this study was to investigate the growth characteristics and the lipid rates of the benthic marine diatom species hosted in the NCC bank in order to evaluate their potential for original lipid bioproducts of potential economic interests. First, a selection based on the genera identified in the literature was applied. Among the 134 strains hosted by the NCC, corresponding to 40 genera and 101 species, 23 genera (corresponding to 77 species, 105 strains in the NCC) were largely studied (Chen *et al*., 2007; Chisti, 2007b; Dalay *et al*., 2014; Fields and Kociolek, 2015; Huntley *et al*., 2015; Knuckey *et al*., 2002; Renaud *et al*., 1999, 1995; Scholz and Liebezeit, 2013; Slocombe *et al*., 2015; F.-Y. Zhao *et al*., 2016) Among these 23 genera, only 13 genera (42 species, 47 strains) with high productivity and/or producing high lipid quantities were selected for the current study. Among these 47 strains, only 18 strains, (6 genera, 17 species) grew successfully. Among the NCC's 40 genera, 17 genera (corresponding to 24 species, 29 strains) were not previously reported in the literature in terms of productivity or ability to produce lipids or added value molecules. Thus, the 29 strains corresponding to

these 17 genera were also selected and assayed for the current study. Among these strains, 15 strains (13 species, 10 genera) did successfully grow. Finally, at the end of this first screening step based on the growth rates, 33 strains (18 previously described and 15 that have never been described before in the literature) were selected for the second step of the screening process. As reported in the supplementary data S1, 43 strains failed to grow which may be associated to shear stress; some species like *Rhizosolenia setigera* cells were broken during agitation.

The second step consisted in the determination of the lipid rate on the selected strains. In microalgae, it can typically vary from 1 to 85% of the dry weight under adverse conditions (Borowitzka and Borowitzka, 1988; Chisti, 2007b; Spoehr and Milner, 1949). Factors such as temperature, irradiance and most markedly nutrient availability have been shown to affect both lipid composition and lipid rate (Guschina and Harwood, 2006; Hu *et al*., 2008; Roessler, 1990). In general, high irradiance stimulates TAG accumulation (Roessler, 1990), while under low irradiance, the polar lipids (phospholipids and glycolipids), structurally and functionally associated to cell membrane, are preferentially synthesized (Hu *et al*., 2008). The lipid rate found in the current study for the *Amphora* genus was similar to that estimated by Renaud *et al*., (1999) (Renaud *et al*., 1999). The authors proposed 19% DW *vs.* 14 to 19% DW in the current study. This similarity could be explained by the similar culture conditions for light and nutrient although the temperature was different (25°C *vs* 16°C in the current study). According to Chtourou *et al*., 2015 (Chtourou *et al*., 2015), the temperature could be an important factor for *Amphora* genus lipid rate which can achieve lipid rates up to 24% of DW at 20°C. Media enrichment could also be an important factor: *Amphora* cells grown in media enriched with macronutrients and trace metal can also achieve lipid rates up to 32% under low light conditions (11.4 µmol photon m^{-2} s^{-1}) (De la Pena, 2007) or under nitrogen deficiency (Fields and Kociolek, 2015). These factors could be used as guideline to improve lipid production of the selected *Amphora* strains hosted in the NCC. The biomass measurements for the *Amphora*

genus in Zhao *et al.* study were in accordance with our results. The authors found 0.13 $g.L^{-1}$ vs. 0.16 $g.L^{-1}$ in the current study. According to their measured lipid productivity, the *Amphora* genus appeared to be a good candidate for lipid based potential applications.

The lipid rate found in our study for the *Nitzschia* genus was similar to the results found by Renaud *et al*., (1999) for one species but very different for *Nitzschia sp 5* NCC109 in the current study. They found a lipid rate of between 13 and 16% DW for the *Nitzschia* genus. In the present study, *Nitzschia alexandrina* NCC33 showed a lipid rate of 13% DW but for *Nitzschia sp 5* NCC109 it was estimated up to 30% DW. However, this rate could only be found for *Nitzschia* genus under nitrogen or silica deficiency increasing up to 45-47% DW (Griffiths *et al*., 2012; Johansen *et al*., 1987; Sheehan *et al*., 1998). Since the amount of nitrogen was not monitored in the culture, it is possible that nitrogen depletion occurred, explaining the high lipid rate measured for *Nitzschia sp 5* NCC109. Further analysis for this strain is necessary to establish whether this was due to the absolute lipid richness of the strain, or to a bias in culture conditions.

The biomass found for the *Nitzschia* genus in Zhao *et al.* (2016) was lower than the measurements in the present study. The biomass estimated in the current study ranged from 0.07 to 0.14 $g.L^{-1}$ vs. 0.19 to 0.23 $g.L^{-1}$. This difference could be due to the light/dark cycle culture conditions, suggesting that under continuous light the biomass production would be more significant for this specific genus (Brand and Guillard, 1981).

It has been demonstrated that the species with a lipid rate of 30% DW and productivity under non-optimized conditions of around 0.30 $g.L^{-1}$ could be potential strains for lipid production (Chisti, 2007b; Williams and Laurens, 2010). In the present study *Nitzschia sp 5* NCC109 had the highest lipid rate, 30.51% DW, Nitzschia *alexandrina* NCC33 with the highest productivity 0.35 $g.L^{-1}$. Both strains were thus selected as candidates for further analyses to assay their potential for lipid-based applications.

The *Navicula* genus also presented a lipid rate for the 2 tested species of between 9% and 23% DW. Zhao *et al*, (2016) found a lipid range from 5 to 30% for 3 *Navicula* species (*Navicula ramosissima*, *Navicula molli* and *Navicula halophia*) and Scholz *et al*, (2013) between 18-25% for 6 *Navicula* species (*Navicula digito-radiata*, *Navicula forcipata*, *Navicula gregaria*, *Navicula perminuta*, *Navicula phyllepta* and *Navicula salinicola*). The data were estimated in spite of very different culture conditions (dark night cycle at 600 µmol photons.m^{-2}.s^{-1}). This observation is important, since for that specific genus, the observed variability in the range of lipid rate for the different tested species is the same regardless of the culture conditions used. The biomass measurements found by Zhao *et al*., (2016) for the *Navicula* genus are in accordance with the present study, ranging from 0.10 to 0.17 g.L^{-1} vs. 0.13 to 0.17 g.L^{-1} suggesting that this genus could produce the identical biomass quantity under light/dark cycle or continuous light.

The lipid rate found for the *Extubocellulus* genus in Slocombe *et al*., (2015) was 23% DW and the biomass equalled 0.06 g. L^{-1}. The lipid rate for this genus, 15% DW in the actual study was lower but the biomass obtained was higher 0.16 g.L^{-1}. The culture was grown under light/dark cycle in the Slocombe *et al*. study suggesting that this genus could grow better under continuous light but produce more lipids under light/dark cycle. Wahidin *et al*., (2013) (Wahidin *et al*., 2013) found the same trend for the microalgae genus *Nannochloropsis*.

Knuckey *et al*, (2002) found 27% DW of lipid rate for the *Entomoneis* genera. In the present study 9 strains of *Entomoneis* presented lipid rates ranging from 3 to 13% DW. In the Knuckey *et al*, (2002) study the pH and the nutrients were monitored. The culture conditions were identical to the present study (continuous light, 120 µmol photons.m^{-2}.s^{-1}). It is therefore possible, that for this genus a nutrient limitation occurred and instead of enhancing the lipid production, it has diminished it. It has been reported that this species produces EPA which is interesting for nutraceutical products (Knuckey *et al*., 2002).

In this study the species with the highest lipid rate (~20 %) and the greatest biomass productivity (up to 0.24 $g.L^{-1}.day^{-1}$) was *Staurosira* sp NCC182. This species was similar in productivity to the marine microalgae *Nannochloropsis* sp. with productivity higher than 0.21 $g.L^{-1}.day^{-1}$ and reached a total lipid rate of 30% DW, when cultivated in batch mode under continuous light and reached 68% DW of lipid production under nitrogen deprivation (Rodolfi *et al*., 2009). *Nannochloropsis* sp. was investigated for algal biofuel production due to its ease of growth and high oil rate. *Staurosira* sp was grown in raceway ponds by Huntley *et al*., (2015) and the lipid quantification demonstrated that these strains could reach a lipid rate of 45.5% DW under low N content. In the present study, *Staurosira* sp. NCC182 presented all the characteristics (good productivity and oil content) to be produced on a large scale and was considered to be one of the most promising candidates for lipid-based applications.

Even if the microalgae oil yield is strain-dependent it is generally superior to other vegetable crops (Chisti, 2007a; Williams and Laurens, 2010). Oil content in Corn, Hemp, Soybean, Sunflower or Palm oil varied from 18 (Soybean) to 44% DW (Corn). Christie *et al*., (2007) demonstrated that microalgae with a lipid rate up to 30% of DW could produce 58 L/Ha of oil and microalgae up to 70% of DW could produce 136 L/Ha of oil. Corn can produce 172 L/Ha, soybean 446 L/Ha and oil palm 5950 L/Ha but require a lot of land for production: 1540 M/Ha for Corn, 594 M/Ha for Soybean and 45 M/Ha for oil palm. Microalgae production only requires 2 to 5 M/Ha. In the NCC collection *Nitzschia sp 5* NCC109 and *Staurosira sp NCC182* had all the mandatory features to be grown on a large scale: good productivity and high lipid rate. In the present study, *Nitzschia alexandrina* NCC33 had the highest productivity in the NCC collection (0.36 $g.L^{-1}.day^{-1}$) and presented a lipid rate superior to 10% DW. Despite its low productivity of 0.08 $g.L^{-1}.day^{-1}$, *Amphora sp 2* NCC169 was chosen for its lipid rate, superior to 15% DW. These 4 strains were selected for further analyses and to improve their productivity and lipid rate with the objective of supplying new resources for lipid based

applications. *Entomoneis paludosa* was also selected despite its low lipid rate since it was already characterized for its ability to produce EPA.

Among the strains not described in the literature, the measured lipid rate ranged from 3 to 20% DW and productivity from 0.05 to 0.27 $g.L^{-1}.day^{-1}$. Only one genus was selected for further study: *Opephora sp 1* NCC366. This species showed a mandatory balance between relatively high biomass productivity (0.23 $g.L^{-1}$) and a high intracellular lipid rate (above 10% DW).

5.6 Conclusion

In this work, we focused on developing an easy to use screening method to explore the NCC bank for diatom strains with the highest relative lipid content. The experimental results showed that the combined use of water-PAM to estimate strain growth kinetics and FTIR on whole cells to estimate the semi-quantitative strain macromolecular content and more specifically lipids, could be rapid, reliable and accessible techniques. The developed methodology opens the way to a systematic, fast, and convenient screening of microorganisms (microalgae in this proof of concept). Moreover, the sensitivity and specificity of the method makes it suitable for a reasonable amount of biomass. This method could also be used in systematic studies for the optimization of culture conditions and to measure the influence of the environment on the metabolic plasticity of the assessed organism. Using this screening approach, 5 strains hosted in the NCC bank were selected for their high productivity and high lipid rate: Nitzschia alexandrina NCC33, Staurosira sp NCC182, Opephora sp 1 NCC366, Nitzschia sp 5 NCC109 and Amphora sp 2 NCC169. The lipid rate achieved by theses strains reached a maximum of 30% DW in the assayed cultivation conditions.

In order to improve the lipid quantity, the selected strains could be grown under different culture conditions. The impact of light, temperature and nutrients, especially nitrogen, could be assayed both in terms of lipid productivity and ecophysiology to ensure the highest growth rate possible.

Once optimal conditions are found for those strains, the production in photobioreactors could be tested and productivity and lipid rates evaluated, in order to estimate quantitatively if the selected strains can compete with the best ones found in the literature (de Souza *et al*., 2018; Liang *et al*., 2018; Shuba and Kifle, 2018). Finally, depending on their oil quality and original lipid activities, those strains may constitute new and original genetic resources that could have potential interesting applications (biodiesel, pharmaceutical, etc.).

Acknowledgements

This work was supported by the regional Atlantic Microalgae research program (AMI), funded by the Pays de la Loire region. We also express our sincere thanks to GEPEA staff in particular Remy Coat and Delphine Kucma for support and advice on the FTIR spectrometer.

Conflict of interest

The authors declare that there is no conflict of interest. No conflicts, informed consent, human or animal rights are applicable to this work.

Author's contribution

Eva Cointet, Gaëtane Wielgosz-Collin, Vona Méléder and Olivier Gonçalves designed and supervised the research. Eva Cointet, Gaëtane Wielgosz-Collin, Vona Méléder and Olivier Gonçalves conducted experiments. Eva Cointet, Gaëtane Wielgosz-Collin, Vona Méléder and Olivier Gonçalves analyzed and interpreted the data and drafted the manuscript. Eva Cointet, Gaëtane Wielgosz-Collin, Vona Méléder and Olivier Gonçalves critically reviewed the manuscript. All authors read and approved the final version of the manuscript.

6 Conclusion

La méthodologie développée dans cet article ouvre la voie pour le criblage systématique, rapide, accessible et fiable des microalgues avec l'utilisation combinée de la fluorescence modulée (PAM), pour évaluer la cinétique de croissance des souches, et de la spectroscopie infrarouge (FTIR) sur cellules entières, pour estimer de façon semi-quantitative le contenue lipidique des souches. De plus, ce travail a permis d'explorer pour la première fois la diversité des diatomées marines benthiques, hébergées au sein de la NCC. Cinq espèces à fort potentiel ont été sélectionnées : *Amphora* sp. 2 NCC169, *Nitzschia alexandrina* NCC33, *Nitzschia* sp. 5 NCC109, *Staurosira* sp. NCC182 et *Opephora* sp.1 NCC366. Le taux maximum de lipides atteint pour ces souches est de 30 % du poid sec. Il est important de préciser que *Entomoneis paludosa* NCC18.2 a été sélectionnée comme sixième espèce malgré son faible taux de lipides, car elle est utilisée depuis longtemps au sein du laboratoire pour de nombreuses études, c'est une espèce modèle. Elle sera utilisée comme témoin dans la suite de l'étude qui est l'optimisation des conditions et des modes de cultures sur les capacités de croissance et de production lipidique des souches benthiques. Cette optimisation s'est faite via des tests de croissance en photobioréacteur (PBR) airlift plan dont les résultats font l'objet du chapitre suivant.

III- Etude de la croissance et de la production lipidiques des souches sélectionnées cultivées en photobioréacteur airlift

1 Contexte de l'étude

L'utilisation des diatomées en biotechnologie est actuellement en développement. A ce jour seulement neuf genres de diatomées (*Skeletonema*, *Thalassiosira*, *Phaeodactylum*, *Chaetoceros*, *Cylindrotheca*, *Bellerochea*, *Actinocyclus*, *Nitzschia*, *Cyclotella*) sont cultivés et utilisés à des fins industrielles (Lebeau and Robert, 2003) notamment en raison du manque de systèmes de culture disponibles pour leurs exploitations. La nécessité d'une production et d'une utilisation de cultures monoalgales a conduit à la mise en place de PBR expérimentaux de culture d'algues en circuit fermé. L'intensification du développement de ces systèmes s'est renforcée à la fin des années 1980, à la suite de l'intérêt général porté au développement de PBR de tailles commerciales (Krichnavaruk *et al*., 2007; Pulz, 2001; Tredici, 2004). Les caractéristiques de fonctionnement de ces systèmes comprennent la capacité de régulation et de contrôle de paramètres de culture importants, notamment la température, la teneur en CO_2 et le contrôle de la contamination (Pulz, 2001). Quelques espèces de diatomées importantes pour l'aquaculture ont été cultivées avec succès dans ces systèmes comme par exemple les espèces : *Chaetoceros calcitrans* (Krichnavaruk *et al*., 2007, 2005), *Skeletonema costatum* (Granum and Myklestad, 2002), *Phaeodactylum tricornutum* (Fernández *et al*., 2000; Molina *et al*., 2000). L'une des principales caractéristiques de la croissance des diatomées benthiques est qu'elles forment des biofilms sur le substrat. Les habitudes de vie typiques de ces diatomées les rendent difficiles à cultiver dans les systèmes de culture traditionnellement utilisés, orientés vers le maintien des algues en suspension. Contrairement à la plupart des microalgues actuellement produites commercialement (e.g *Chlorella*, *Spirulina* et *Dunaliella*) qui se développent dans des conditions très sélectives avec peu de problème de contamination par d'autres microalgues ou protozoaires, les diatomées ne possèdent pas cet avantage sélectif et doivent être cultivées de façon axénique dans des systèmes clos (Borowitzka, 1999). Les systèmes clos peuvent être

des PBR placés en extérieur ou intérieur et incluent par exemple l'utilisation de sacs, de PBR tubulaires ou plats. Dans ces derniers, la diffusion de la lumière à l'intérieur du réacteur est plus efficace que dans des bassins placés en extérieur ; le milieu est homogène, les échanges de gaz sont également plus importants et la température est contrôlée ce qui permet d'obtenir une biomasse plus élevée ce qui réduit les coûts de récolte.

L'objectif de cette étude est d'évaluer le potentiel d'utilisation d'un PBR airlift plat pour la culture massive de diatomées benthiques (Figure III-1). Cinq espèces de diatomées benthiques identifiées précédemment pour leurs capacités à produire et accumuler des lipides : *Amphora* sp. NCC169, *Nitzschia alexandrina* NCC33, *Nitzschia* sp. NCC109, *Opephora* sp. NCC366 et *Staurosira* sp. NC182 et un témoin *Entomoneis paludosa* NCC18.2 ont donc été cultivées dans des conditions hautement contrôlées en PBR airlift plat. Les cultures ont été réalisées en batch, le milieu de culture a été enrichi de façon à obtenir 1g/L de biomasse à la fin de la phase exponentielle. La cinétique de croissance ainsi que le contenu lipidique ont été analysés pour chaque espèce. Les résultas obtenus font l'objet d'un article en cours de soumission dans le journal Algal Research et sont présentés ci-dessous.

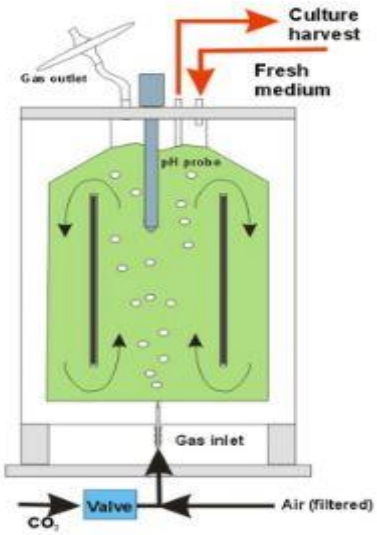

Figure III-1 Schéma du photobioréacteur airlift utilisé en mode batch dans l'étude (Pruvost *et al.*, 2011)

2 Evaluation du potentiel de production de lipides de six diatomées benthiques cultivées dans un PBR airlift

Assessing the lipids production potential of six benthic diatoms grown in airlift PBR

Eva Cointet[1], Elise Séverin[1], Aurélie Couzinet-Mossion[1], Vona Méléder[1], Olivier Gonçalves[2], Gaëtane Wielgosz-Collin[1*]

[1] Université de Nantes, Laboratoire Mer Molécules Santé, EA 2160, BP 92208, 44322 Nantes, France

[2] Université de Nantes, GEPEA, UMR CNRS-6144, Bât.CRTT, 37 Boulevard de l'Université, BP406, F-44602 Saint-Nazaire Cedex, France

2.1 Abstract

Diatoms have been emerging as a major source for the production of bioactive compounds. Marine diatoms can store high amounts of lipids and grow quickly. Unfortunately, they are barely studied and underexploited resources. The current work objective is to promote microalgae strains from a new and original origin never before investigated: intertidal mudflats. Benthic diatom strains were isolated and hosted in the Nantes Culture Collection (NCC). After a high-throughput screening on 76 pre-screened strains, six were selected for their high biomass and/or lipid productivity: *Amphora* sp., *E. paludosa*, *N. alexandrina*, *Nitzschia* sp., *Opephora* sp. and *Staurosira* sp. These benthic diatom strains were cultivated in airlift photobioreactor for the first time. Their lipid class composition, fatty acid and sterol distribution were studied using thin-layer chromatography and gas chromatography mass spectrometry (GC-MS). Total lipid production varied from 41%DW (*Staurosira* sp.) to 11.4%DW (*Amphora* sp.). Neutral lipid amounts varied from 23% (*Amphora* sp.) to 76% (*Staurosira* sp.) of the total lipids. Glycolipids ranged from 18% (*Staurosira* sp.) to 59% (*Opephora* sp.) of the total lipids. Phospholipids accounted for 6% (*Staurosira* sp.) to 26% (*Amphora* sp.) of the total lipids. Some qualitative and quantitative differences were identified in fatty acid and sterol composition in the different

analyzed strains. *Staurosira* sp. seems to be the most promising strain in terms of lipid production and most particularly in triacylglycerol production. *E. paludosa* produced phytosterols and eicosapentaenoic acid (EPA), compounds that could be recoverable in pharmaceuticals industries. *N. alexandrina* produced squalene and low saturated fatty acid which could be interesting in nutraceutical industries as antioxidants.

Keywords: Benthic diatoms, Nantes Culture Conditions, Bioactive lipid diversity, Airlift photobioreactor, fatty acids, Eicosapentaenoic acid

Abbreviations

CLE: Crude lipid extract
DGDG: Digalactosyldiacylglycerols
DHA: Docosahexaenoic acid
DW: Dry weight
EPA: Eicosapentaenoic acid
FA: Fatty acid
FAME: Fatty acid methyl ester
FFA: Free fatty acid
GC-MS: Gas chromatography mass spectrometry
GL: Glycolipids
HC: Hydrocarbons
LEP: Late exponential phase
Lz: Optical depth
MGDG: Monogalactosyldiacylglycerols
MUFA: Monounsaturated fatty acid
NAP: *N*-acyl pyrrolidides
NCC: Nantes Culture Collection
NL: Neutral lipids
PAR: Photosynthetically active radiation
PBR: Photobioreactor

PFD: Photon flux density

PL: Phospholipids

PMMA: Polymethyl methacrylate

PUFA: Polyunsaturated fatty acid

Px: productivity

q_o: Incident light flux

RT: Retention time

SQDG: Sulfoquinovosyl diacylglycerols

TAG: Triacylglycerols

TLC: Thin layer chromatography

TLR: Total lipid rate

µmax: Maximum growth rate

2.2 Introduction

Marine diatoms are able to store high amounts of lipids and to grow quickly (Niu *et al*., 2013). Their lipids are mainly composed of a neutral fraction with traces of sterols and polar lipids (Yi *et al*., 2017). Neutral lipids constitute the reserve fraction, with triacylglycerol (TAG) accounting for more than 60% of the total lipids (Artamonova *et al*., 2017). Their polyunsaturated fatty acids (PUFAs) are mainly composed of eicosapentaenoic acid (EPA, 20:5 n-3) (Chew *et al*., 2017b) but some strains were also found to present docosahexaenoic acid (DHA, 22:6 n-3) (Dunstan *et al*., 1993). The biosynthesis of the lipids varies within the different diatom species, their growth stages, and environment (Chen, 2012; Chuecas and Riley, 1969). Previous studies (Artamonova *et al*., 2017; Chew *et al*., 2017b; Dunstan *et al*., 1993; Niu *et al*., 2013; Yi *et al*., 2017) have demonstrated their ability for lipid production, more specifically for the PUFA fraction (DHA and EPA), recognized for its broad-spectrum bioactivities (anti-carcinogen, immune modulator, anti-diabetic, anti-obesity, anti-thrombotic and anti-atherogenic) (Nagao and Yanagita, 2005).

The use of diatoms in biotechnology is currently under development. To date only a few diatom species have been grown and used for industrial purposes because of the lack of cropping systems available for their exploitation. The need for high production and use of monoalgal crops has led to the establishment of experimental units for tubular and tubular closed-circuits for seaweed cultivation called photobioreactors. The intensification of the development of these systems was reinforced in the late 1980s following the general interest in the development of commercial sized photobioreactors (Krichnavaruk *et al*., 2007; Pulz, 2001; Tredici, 2004). Operating characteristics of these systems include the ability to control important parameters such as temperature, hydrodynamics, contamination control and CO_2 regulation (Pulz, 2001). Some diatom species used in the aquaculture market have been successfully cultured in these systems, for example species like *Chaetoceros calcitrans* (Krichnavaruk *et al*., 2007, 2005), *Skeletonema costatum* (Granum and Myklestad, 2002) and *Phaeodactylum tricornutum* (Fernández *et al*., 2000; Molina *et al*., 2000). One of the main features of benthic diatom growth is their capacity to form biofilms on the substrate. The habits of life, typical of these diatoms, make them difficult to cultivate in systems traditionally used, oriented towards the maintenance of algae in suspension. Unlike most commercially produced microalgae (*Chlorella* sp., *Spirulina* sp., *Dunaliella* sp.) that develop under very selective conditions with little problem of contamination by other microalgae or protozoa, diatoms do not have this selective advantage and must be grown axenically in closed systems (Borowitzka, 2013). Photobioreactors can be placed indoors or outdoors and include the use of bags, tubular reactors or flat reactors. Because of the photoautotrophic status of the majority of diatoms, microalgal cultures suffer from limitation of light diffusion, the use of airlift PBR copes with this matter because of the circulatory flow in the system which helps prevent cell precipitation and enhanced light utilization efficiency (Monkonsit *et al*., 2011). In tubular or flat photobioreactors, the scattering of light inside the reactor is more efficient, medium is homogeneous, gas exchanges are more

significant and temperature is controlled, which makes it possible to obtain higher biomass, thus reduceing harvesting costs.

In our previous study (Cointet *et al*., 2019), strains were selected in relation to the amount of lipids found within the crude lipid extract (CLE) by HTSXT-FTIR analysis. This technique being only quantitative and not qualitative, it was impossible to determine the fatty acid (FA) composition in TAG, glycolipids (GL) and phospholipids (PL). Gas chromatography coupled with mass spectrometry (GC-MS) analyses were thus conducted on the six species previously selected. This method is commonly applied to the analysis of lipids and more particularly FAs and sterols (Davoodbasha *et al*., 2018; Gladu *et al*., 1991; Subhash *et al*., 2017; Tanaka *et al*., 2017). To complete the lipid analysis data, the CLEs were separated into lipid classes by open column chromatography on silica gel. This fractionation technique used conventionally with three solvents of increasing polarity, separates NLs (CH_2Cl_2), GLs (acetone) and PLs (MeOH). This fractionation make it possible to determine the proportions in lipids within each class and to be able to analyze the fractions (Berge *et al*., 1995; Chen, 2007; Hubert *et al*., 2017). These fractions can be analyzed by TLC by comparing their references with that of specific controls (Hubert *et al*., 2017; Subhash *et al*., 2017). The fractions can be injected in GC-MS in free state (sterols), acetylated (sterol acetate) or after TAGs saponification, GLs hydrochloric methanolysis and FA derivation into FAME and NAP (Delattre *et al*., 2016; Hubert *et al*., 2017; Medina *et al*., 1998; Sabia *et al*., 2018; Viron *et al*., 2000).

The first objective of this study is to evaluate the potential of using airlift photobioreactor (PBR) to assess industrial potential of the selected strains. In this study, six benthic diatom species: *Amphora* sp., *Entomoneis paludosa*, *Opehora* sp., *Nitzschia alexandrina*, *Nitzschia* sp. and *Staurosira* sp. were studied for their ability to produce and accumulate lipids expressed in terms of productivity in a highly controlled airlift PBR. Other limiting factors, such as nutrients, pH, temperature, bioturbation must be taken into account. In the PBR system used in this study, pH

was controlled with a pH probe and a fed-batch strategy, with daily supplementation of bicarbonate and silica, developed to ensure no nutrient limitation. The second objective was to precisely measure lipid classes and identify original compounds with the aim of evaluating their productivity.

2.3 Materials and Methods

2.3.1 Cultivation conditions

The six benthic strains, *Amphora* sp. NCC169, *Entomoneis paludosa* NCC18.2, *Nitzschia alexandrina* NCC33, *Nitzschia* sp. NCC109, *Opephora* sp. NCC366 and *Staurosira* sp. NCC182 were obtained from the Nantes Culture Collection (NCC). Each strain was grown using enriched natural seawater medium (F/2 medium)(Guillard, 1975), filtered sterilized (0.2 µm) to avoid nutrient precipitation often occurring when autoclaving is used. 50 mL of culture stock was treated with 2 mL Antibiotic Antimycotic Solution (SIGMA-ALDRICH) for 48 H, followed by re-suspension in 150 mL sterile culture solution to ensure the absence of bacteria and/or protozoa during PBR growth. Stock cultures were maintained in 250 mL Erlenmeyer flasks filled with 150 mL medium at 20 °C under continuous light of 127 µmol.photons.m^{-2}.s^{-1}. Inoculation in the PBR was carried out at a concentration dependent on the starter (250 mL reconcentrated before inoculation). During PBR growth 21 mg of silica (Na_2SiO_3, $5H_2O$) and 200 mg of sodium bicarbonate ($NaHCO_3$) were added daily to ensure no nutrient limitation. Medium used was a modified F/2 (Table III-1) filtered sterilized (0.2 µm). In the PBR, cultivation conditions were pH = 7.8, T = 20 °C under continuous light of 127 µmol.photons.m^{-2}.s^{-1}.

Table III-1 Airlift PBR F/2 medium composition.

Element		Final concentration $g.m^{-3}$
Nitrate	$NaNO_3$	750
Phosphate	NaH_2PO_4	170
Trace metals	Na_2EDTA	5.06
	$FeCl_3,6H_2O$	3.15
	$MnCl_2,4H_2O$	0.18
	$ZnSO_4$	0.01
	$CoCl_2,6\ H_2O$	0.01
	$CuSO_4,5\ H_2O$	0.01
	$Na_2MoO_4,\ 2\ H_2O$	63×10^{-4}
Vitamins	Thiamine	0.10
	Cyanocobalamine	5×10^{-4}
	Biotin	5×10^{-4}

* EDTA: Ethylenediaminetetraacetic acid

2.3.2 Airlift Photobioreactor description

A flat-panel airlift PBR was used for experiments. The light supplying device was placed in front of the PBR perpendicular to its optical surface. The light source was a LED panel (Effilux) placed parallel to the front side of the PBR at the same height as the PBR. Air was injected at the bottom for culture mixing. The PBR consisted of three parts: the central where air was injected (riser) and two lateral parts for culture recirculation (downcomer). This ensured good mixing condition and prevented cell sedimentation. PBR volume was 1 L with a depth of culture Lz = 30 mm (perpendicular to the optical surface). The illuminated surface to volume ratio of the reactor was equal to 33.3 m^{-1}. The PBR was built in transparent polymethyl methacrylate (PMMA) except for the back side which was in stainless steel for reactor cooling by ambient air blowing (fan). The PBR was eqquiped with a complete loop of sensors and automations for microalgal culture, namely temperature, pH and gas injections (CO_2 and air). pH was regulated by automatic injection of CO_2 and temperature by ambient air blowing. The PBR was sterilized 30 min prior to all experiments with a 5 mM peroxyacetic acid solution. Batch cultures were realized in chemostat mode under continuous light illumination. The incident light flux qo or photon flux density (PFD) was measured in the 400–700 nm wavelength (photosynthetically active radiation, PAR) for different distances between PBR and tubes using a flat cosine

quantum sensor (Li-190SA, Li-COR, Lincoln, NE). The incident light flux was obtained by averaging sensor measurements for 12 different locations on the PBR front. A variation of less than 10% was observed showing a homogeneous illumination of the PBR's optical surface. A PFD value of qo = 127 µmole.m^{-2}.s^{-1} was applied in all experiments.

2.3.3 Analytical methods

2.3.3.1 Growth

Daily, 2 mL of culture samples were fixed with lugol and counted (n ≥ 300) using Neubauer hemocytometer and an optical microscope (OLYMPUS CH40, ×400). Following Cointet *et al* (2019), maximum growth rates (µmax in day^{-1}) were determined by fitting growth kinetic data with a Gompertz model using Matlab software (Equation 1) (Cointet *et al*., 2019):

$$f(x) = A \times e^{-e(\mu max \times \frac{e^1}{A} \times (\lambda - x) + 1)} \quad \text{(Eq.1)}$$

with A: maximum cell concentration in the natural logarithm of the biomass; µmax: Maximum growth rate (day^{-1}); λ: Latency (days).

Growth was also monitored by measuring the optical density (OD) daily at 680 nm using a spectrophotometer (JASCO V-630).

2.3.3.2 Pigments

To estimate Chlorophyll a (Chl a) in %DW, 2 mL of culture were sampled and centrifuged at 11200 g for 5min each day until the end of growth. After supernatant removal, pigments were extracted by adding 2 mL of methanol (99.9%) on the pellet. To remove cell debris, methanol suspension was centrifuged for 5min at 11200 g. Absorbance at 665 and 632 nm were measured by spectrophotometer (JASCO V-630) on the clean supernatant to calculate pigment content, expressed in %DW following Equation 2 (Ritchie, 2006):

$$Chl\ a = \frac{13.26 \times A665 - 2.68 \times A632}{DW} \times 100 \quad \text{(Eq.2)}$$

2.3.3.3 Nutrients

3 mL of culture was sampled daily and until late exponential pahse (LEP) to analyze the remaining nitrate and phosphate concentrations in the medium. These two nutrient concentrations were determined using anion chromatography (DIONEX-120, anionic column IonPAC AS14A with SRS). Eluent was an 8 mM Na_2CO_3 and 1mM $NaHCO_3$ solution with a flow of 1mL/min.

2.3.3.4 Dry Weight

At the end of the exponential phase, cultures were harvested and filtered on previously weighted filters, Whatman GF/F, 47 mm diameter, 0.7 µM pore. Filters containing cells were washed using 10 mL ammonium formiate (68 $g.L^{-1}$) to remove salt. Wet filters were frozen at –80 °C and freeze-dried under vacuum for 24 H. Dry weight (DW in $g.L^{-1}$) and µmax (day^{-1}) were then used to estimate strain productivity (Px) in $g.L^{-1}.day^{-1}$ (Equation 3)

$$Px = \mu max \times DW \quad \text{(Eq. 3)}$$

2.3.3.5 Lipids

Total lipids were extracted from freeze-dried biomass using a modified method of Bligh and Dyer (Bligh and Dyer, 1959). Two macerations at room temperature were carried out with 100 mL of solvent per gram of biomass (Dichloromethane (CH_2Cl_2)/Methanol (MeOH) 1:1 (v/v)) for 24 H on a vibrating tray (Edmund Bühler GmbH, SM-30). Mixtures were then filtered to obtain delipidified biomass. Organic phases were then washed by adding 40% of the volume of 0.9% KCl solution. Organic phases were combined, dried over anhydrous Na_2SO_4 and then evaporated to dryness under N_2 to obtain the crude lipid extract (CLE) and estimated Total lipid rate (TLR) (Equation 4)

$$TLR = \frac{CLE}{DW} \times 100 \quad \text{(Eq. 4)}$$

2.3.4 Lipid analyses

2.3.4.1 Thin layer chromatographic analysis

Thin layer chromatography (TLC) on CLE was performed using silica plate on an aluminium support (20 cm×20 cm, 0.2 mm, Alugram®Sil G/UV254, Macherey-Nagel). Fractions were applied (10 µL with a concentration of 1mg.mL^{-1}) to the thin layer chromatography plate with standardized micropipettes for elution. Mobile phase was adapted according to sample structure and polarity (Table 2). Different controls were used to characterize extract composition. After migration, a specific revealer was used to highlight the sample composition. (Table III-2).

Table III-2 TLC: mobile phases, controls and revealers used according to analyzed fractions**.**

Types of fractions	Mobile phase	Controls	Revealer
Neutral lipids	Hexane/Diethyl ether/Acetic acid (50/50/0.75 v/v/v)	Sesame oil Cholesterol/Cholesterol acetate	UV / Vanillin
Glycolipids (according to polarity)	CH_2Cl_2/MEOH (90/10 v/v) CH_2Cl_2/MEOH (80/20 v/v)	Spinach	Vanillin/Orcinol

2.3.4.2 Fractionation in lipids classes

Lipid classes were separated on open silica gel column chromatography, column size and amount of silica used depended on CLE mass to be fractionated (1g of CLE for 20 g of silica). Lipids were eluted using CH_2Cl_2 for neutral lipids (NL), acetone for glycolipids (GL) and MeOH for phospholipids (PL) as successive mobile phases.

2.3.4.3 Fatty acid and sterol analyses

Fatty acids and unsaponifiable fractions (sterols, hydrocarbons…) were analyzed as described previously (Kendel *et al*., 2013). Briefly, unsaponifiable matter was acetylated using acetic anhydride and pyridine, giving a mixture containing sterol acetates. Free fatty acids (FFA) were obtained after saponification with 2 M ethanolic potassium hydroxide (1.5 H at 80 °C under reflux) of CLE or after hydrochloric methanolysis (1.5 H at 80 °C under reflux in a MeOH/distilled water/concentrated hydrochloric acid 29:4:3, v/v/v) for GL. Fatty acid methyl esters (FAME) were obtained by methylation of FFA (40 min at 80 °C, under reflux in 6% hydrochloric MeOH). FAME were then converted into *N*-Acyl pyrrolidides (NAP) (60 min at 80 °C under reflux in a pyrrolidine/acetic acid mixture 5:1 v/v). FAME and NAP, free and acetylated sterols were then analyzed by gas chromatography coupled with mass spectrometry (GC-MS) (supplementary data S6 and S7).

2.3.4.4 Gas chromatography coupled with mass spectrometry (GC-MS)

Samples (1 $mg.mL^{-1}$ in CH_2Cl_2) were analyzed by GC-MS, Hewlett Packard HP 7890-GC system/HP 5975C – 70 ev) equipped with an HP-5^{MS} column (30 m × 0.25 mm × 0.25 µm, Sigma-Aldrich). Injector and detector temperatures were set at 250 and 280 °C, respectively. Helium carrier gas had a flow rate of 1 mL/min. Oven temperature was programmed at 170°C (4 min), then 3 °C/min up to 300°C for 10 min (cycle = 57.33 min); for NAP, at 200 °C (4 min), then 3 °C/min up to 310°C for 20 min (cycle = 60.67 min); for sterols and sterols acetate, at 200 °C (4min) then 3 °C/min up to 310°C, for 25 min (cycle=61.67 min) for FAME analyses. Injected volume was 1 µL in splitless mode and the solvent delay was 4 min. To identify and quantify the FAMEs, sterols and sterol acetates, identifications were confirmed by comparing mass spectra and retention data with those previously reported and with those obtained from commercial standards. Amount of sterols can be expressed as a % of total sterol or as a % of total lipid rate (%TLR) following Equation 5:

$$Sterols\ \%\ TLR = \%\ total\ sterols \times \frac{Unsaponifiable\ weight}{CLE} \quad \text{(Eq. 4)}$$

2.4 Results

2.4.1 Growth

The growth of the six species grown in Airlift PBR is shown in Figure III-2. *Amphora* sp. and *Opephora* sp. did not support growth in Airlift PBR. *N. alexandrina*, *E. paludosa*, *Nitzschia* sp. and *Staurosira* sp. support growth. A lag phase was only present for *E. paludosa*. The Chl *a* content (%DW) varied during growth as shown in Figure III-3. Chl *a* content increased with growth for *N. alexandrina* and *Staurosira* sp. This results can be explained by the increase of biomass leading to a decrease of incident light achieving cells. For *E. paludosa* and *Nitzschia* sp. Chl *a* content was on average constant over time. Evolution of Chl *a* content for *Opephora* sp. and *Amphora* sp. was not calculated hence these species did not grow in the PBR.

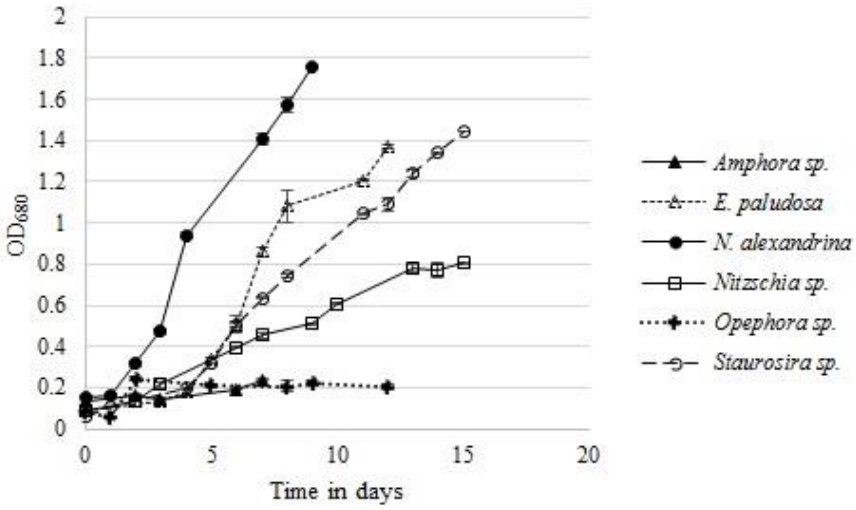

Figure III-2 Growth curves of the six species grown in airlift PBR

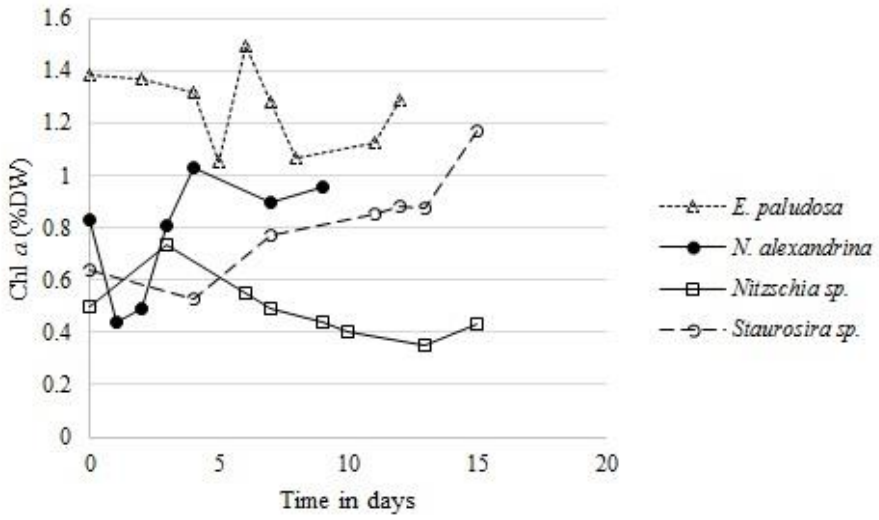

Figure III-3 Evolution of the Chl *a* content in function of time for *E. paludosa*, *N. alexandrina*, *Nitzschia* sp. and *Staurosira* sp.

2.4.2 Nutrients

As expected, phosphate and nitrate concentrations available in the medium decreased with time (Figure III-2, Table III-3). *Staurosira* sp. had a maximal nutrient concentration at J0 with 142 mg.L^{-1} of phosphate and 510 mg.L^{-1} of nitrate. Growth stoppage for all species when concentrations under 62 mg.L^{-1} of phosphate and 224 mg.L^{-1} of nitrate were achieved. However these results suggest that all species were not nutrient limited in the PBR.

Table III-3 Phosphate [PO_4^{3-}] and nitrate [NO_3^-] concentration for the six species between J0 and late exponential phase (LEP)

Species	[PO_4^{3-}] (mg.L^{-1})		[NO_3^-] (mg.L^{-1})	
	J0	LEP	J0	LEP
Amphora sp.	117	64	449	302
E. paludosa	108	63	507	107
N. alexandrina	91	66	448	96
Nitzschia sp.	77	45	430	138
Opephora sp.	85	26	381	243
Staurosira sp.	142	62	510	224

2.4.3 Growth kinetics

Table. III-4 summarizes growth parameters (µmax and LEP), cell concentrations (minimum and maximum cells in cell.mL^{-1}), biomass (g.L^{-1}) and the productivity obtained for each species. Highest productivity and growth rates were obtained for *N. alexandrina* (0.80 g.L.day^{-1} and 0.69 day^{-1} respectively). Highest biomass was reached for *Staurosira* sp. (1.60 g.L^{-1}). The two species *E. paludosa* and *N. alexandrina* achieved the same biomass at the end of growth (1.16 g.L^{-1}). Lowest biomasses were obtained for *Amphora* sp. (0.23 g.L^{-1}) and *Opephora* sp. (0.31 g.L^{-1}). Small differences between minimum and maximum cell numbers for *Amphora* sp. demonstrates that this species did not develop at all in the PBR as shown in Figure III-2.

Table III-4 Growth parameters, biomass and productivity obtained for the six species studied

Species	µmax (day^{-1})	LEP (day)	Minimum cells (cell.mL^{-1})	Maximum cells (cell.mL^{-1})	Biomass (g.L^{-1})	Productivity (g.L.day^{-1})
Amphora sp.	-	-	1 126 666	1 485 555	0.23	-
E. paludosa	0.46	11	281 111	3 976 666	1.16	0.53
N. alexandrina	0.69	8	1 175 555	38 533 333	1.16	0.80
Nitzschia sp.	0.39	13	74 444	1 088 888	0.83	0.32
Opephora sp.	0.18	9	536 111	3 466 666	0.29	0.05
Staurosira sp.	0.44	13	311 111	7 493 333	1.60	0.62

2.4.4 Lipid analyses

Total lipid rate (TLR) obtained after extraction was variable according to the species studied (Table III-5). *Staurosira* sp. had the highest lipid content with 40.9% DW. *Nitzschia* sp. produced lipid levels of more than 20%. The other species had a lipid content under 16%. CLE composition was obtained after saponification allowing to have on one side the unsaponifiable (analyzed free and then acetylated by GC-MS) and on the other the FAs (derivatives in FAME and NAP for GC-MS analysis).

CLE composition was variable according to the species studied. CLE of *E. paludosa* and *Amphora* sp. were composed of more than 20% of unsaponifiable content. Conversely, levels

of unsaponifiable content were low for *Nitzschia* sp. (6.4%). CLE of the other 3 species were composed of 12 to 14% of unsaponifiable content.

Table III-5 Biomass (g.L^{-1}), CLE (mg), TLR (% dry weight) and unsaponifiable content (% CLE) obtained after extraction for the six species studied. Remarkable values in bold.

Strains	**Biomass (g.L^{-1})**	CLE (mg)	**TLR (%)**	Unsaponifiable (% CLE)
Amphora sp.	0.23	21.3	11.3	25.4
E. paludosa	**1.16**	100.2	12.3	20.7
N. alexandrina	**1.16**	131.9	15.7	14.0
Nitzschia sp.	0.82	133.6	**20.8**	6.4
Opephora sp.	0.29	30.4	14.3	13.3
Staurosira sp.	**1.60**	524.4	**40.9**	12.0

2.4.5 Lipids class fractionation

The CLE of the six species were fractionated into lipid classes and chromatographed on an open silica gel column (Figure III-4., supplementary data S3). *Staurosira* sp. was the only diatom to produce predominantly NL (>76%). *Nitzschia* sp. and *E. paludosa* produced NL in lower proportion at 59.1% and 46.7% respectively. The other species mainly produced GLs. TLC analysis of the fractions allowed determination of their composition by comparison with the controls. It was possible to estimate the different proportions of lipid classes by weighting the fractions. PLs classes were not characterized because they were too difficult to identify. With regards to NLs, TAGs were mainly present in *Staurosira* sp. (71%). FFAs were above 11% in *E. paludosa* and *N. alexandrina*. In the GLs fractions, pigments and Monogalactosyldiacylglycerols (MGDG) were above 30% in *Amphora* sp. and *Opephora* sp. Digalactosyldiacylglycerols (DGDG) were higher than 16% in *E. paludosa*, *N. alexandrina* and *Opephora* sp. Sulfoquinovosyl diacylglycerols (SQDG) were over 10% in *Amphora* sp. PLs were present to a lesser extent in *Staurosira* sp. (6%) and more than 15% in *N. alexandrina* and *Amphora* sp.

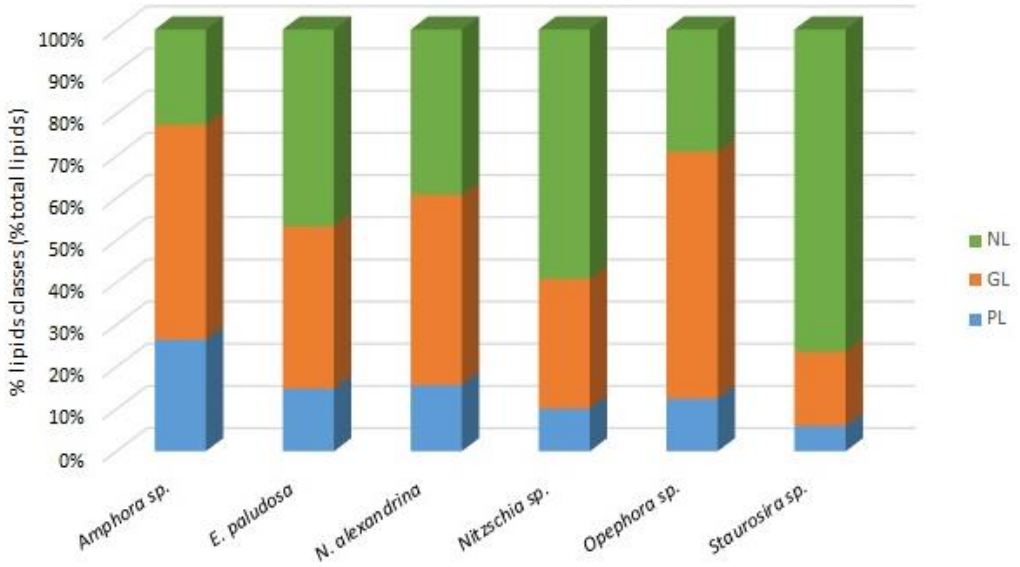

Figure III-4 Neutral lipids (NL), glycolipids (GL) and phospholipids (PL) distribution in the six species studied.

2.4.6 Analyses of unsaponifiable fraction by GC-MS

As shown in Figure III-5, composition of the unsaponifiable fractions was different depending on the species. Indeed, phytol was present in the 6 species in different amounts. The highest amount of phytol was obtained for *Opephora* sp. with 40.4% of unsaponifiable fraction and *Nitzschia* sp. with 26.6% (supplementary data S4). The amount of phytol for the other species was under 20%. Not all species studied produced hydrocarbons (HC). The highest HC amount was for *Amphora* sp. (16.1%) and *Opephora* sp. (18.2%). Among these HC, squalene was only quantifiable in *N. alexandrina* and represented 1.9% of the unsaponifiable. The analysis of sterols in each species was related to the total lipid rate (TLR) (Equation 4). Several species profiles emerge according to the variety of sterols (Figure III-6).

Species with low variability in sterol composition were *Amphora* sp. which contains mainly 24-Ethylcholesta-5,22*E*-dien-3β-ol at 62.2% (15.8% TLR), *Nitzschia* sp. which contains mainly 24-Ethylcholest-5-en-3β-ol at 59.2% (3.8 % TLR) and 10.7% of 24-Methylcholest-5-en-3β-ol (0.7% TLR). *Staurosira* sp. contains mainly Cholesta-5,22-dien-3β-ol at 45.8% (5.5% TLR)

and 24-Methylcholesta-5,22*E*-dien-3β-ol at 34.6% (4.2%TLR). Three strains have a profile of more than 4 different sterols: *E. paludosa* with 61.1% of 24-Ethylcholest-5-en-3β-ol (12.6% of TLR), 28.7% of 24-Ethylcholesta-5,22*E*-dien-3β-ol, 2.2% of 24-Methylcholest-5-en-3β-ol and a ketone at 2.3%.

N. alexandrina contains 6 different sterols, the major being Cholesta-5,22-dien-3β-ol with 30.8% (4.31% TLR). 24-Ethylcholest-7,22*E*-en-3β-ol was the most abundant sterol in *Opephora* sp. with 16.3% (2.2% TLR). The two species with the lowest amount of total sterols within CLE were *Opephora* sp. (5.21% TLR) and *Nitzschia* sp. (4.5%TLR).

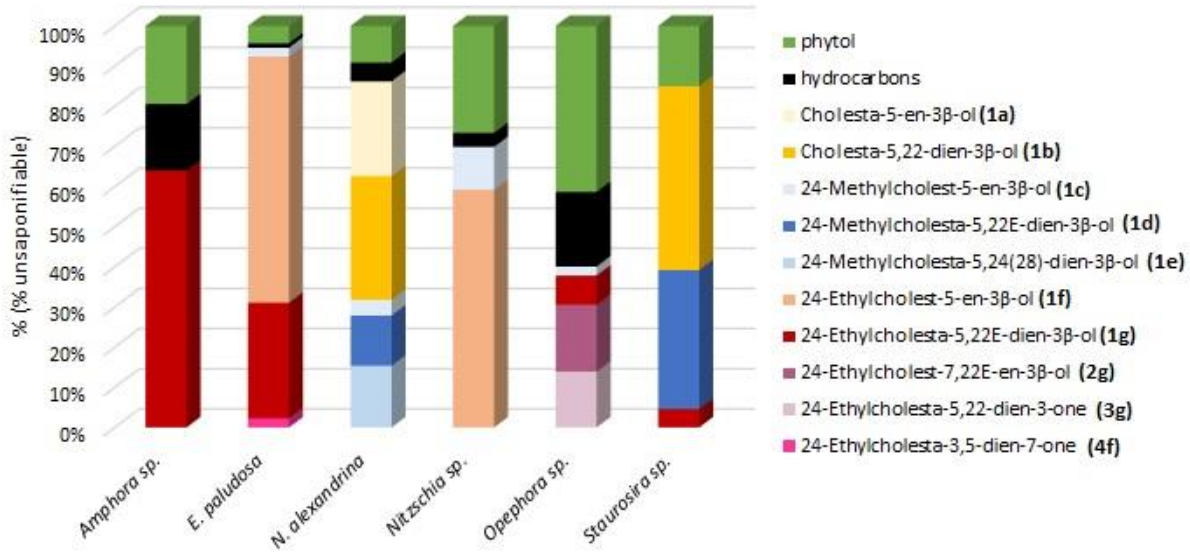

Figure III-5 Unsaponifiable composition of the 6 species (for annotations in bold see Figure. III-6)

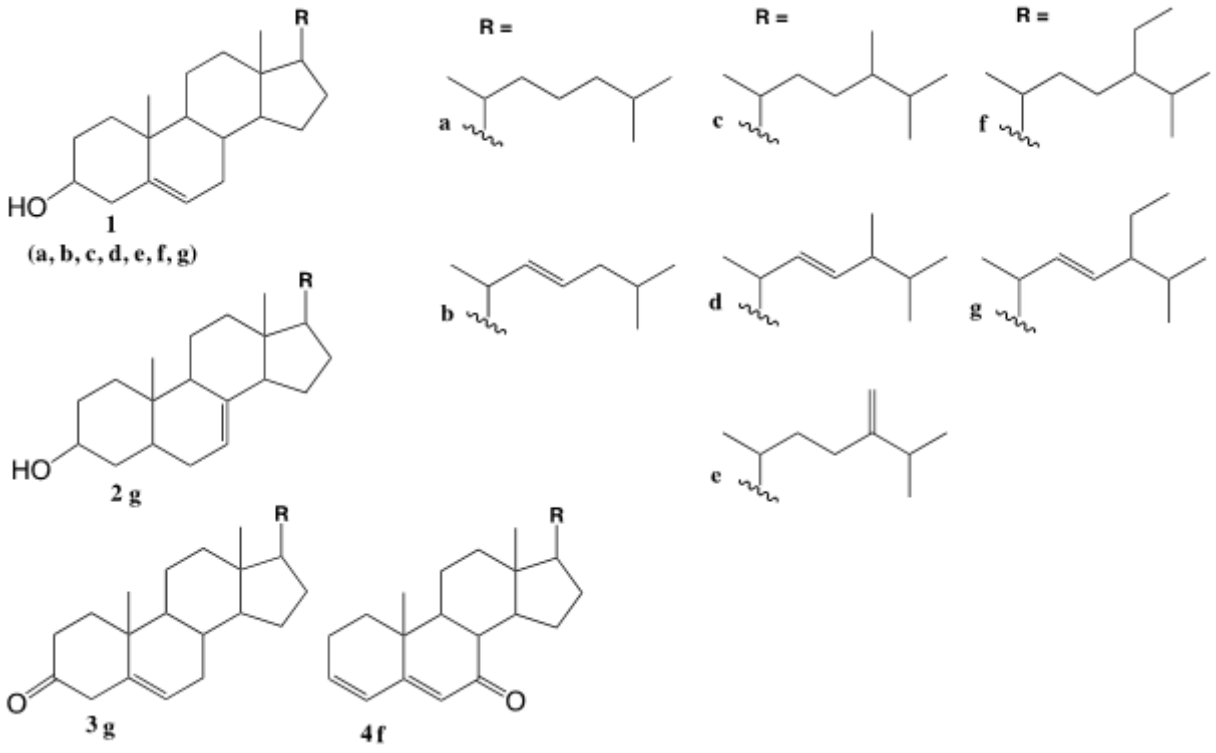

Figure III-6 Sterols analyzed in the six diatom species

2.4.7 Total fatty acid composition for the six species

Fifteen FA were identified in the six species and the percentages are presented in Figure III-7 and Supplementary data S5. Variability in the quality of FAs was observed, with the presence in different proportions of saturated and unsaturated FAs depending on the species. All the species produced more unsaturated than saturated FA especially *N. alexandrina*, *Opephora* sp., and *Staurosira* sp. Species as *Nitzschia* sp., *Opephora* sp. and *Staurosira* sp. produced more than 50% of MUFAs. Two species produced more than 18% of PUFAs, namely *E. paludosa* and *N. alexandrina*. Major FAs in the six species were palmitoleic acid (9-16:1), followed by palmitic acid (16:0) and myristic acid (14:0). Palmitoleic acid was produced less in *E. paludosa* compared to the other species. However, this species produced a greater amount of myristic acid (14:0) and EPA than the other species. Moreover, this species was the only one to produce nervonic acid (24:1). On the 15 characterized FAs, 11 were common to the six species. 6,9,12-hexadecatrienoic acid was produced by three species (*Amphora* sp., *Nitzschia* sp. and *Staurosira* sp.). 6,9-hexadecadienoic acid was also produced by three species (*E. paludosa*, *N. alexandrina* and *Opephora* sp.). 5,9,12-octadecatrienoic acid was produced by four species (*Amphora* sp., *E. paludosa*, *Opephora* sp. and *Staurosira* sp.).

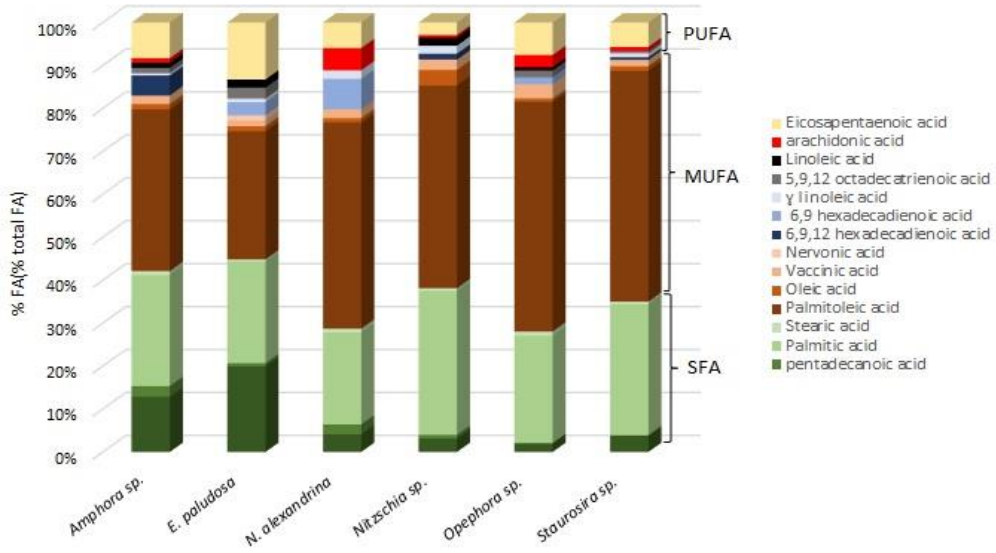

Figure III-7 Fatty acid composition of the six species studied after CLE saponification

2.5 Discussion

2.5.1 Biomass and lipid content

Each diatom had species specific characteristics. Cultivation methods impact differently on biomass production. Silva-Aciares *et al*. (2008) compared the growth of six diatom species (including *Amphora* and *Nitzschia* genera) with two different airlift photobioreactors (Silva-Aciares and Riquelme, 2008). In Silva-Aciares *et al*. study; variations in the amount of biomass were observed between the 6 species but also for the same species cultivated in two different airlift. Some adhesive species such as the genus *Amphora*, produce more biomass in a system with of a rough PVC surface, called PBB airlift (PBR bristles) rather than in a conventional system with constant movement (1.28g.L^{-1} *vs* 1.08 g.L^{-1}). However, the genus *Nitzschia* produced more biomass in an airlift without a PVC plate (2.26 vs 2.02 g.L^{-1}) and supported the suspension in the airlift very well. This variability of production relating to diatom characteristics was also found in the present study for *Amphora* sp. and *Opephora* sp. These species have the lowest biomass production rate (0.23 g.L^{-1} and 0.29 g.L^{-1}). Scanning electron

microscopy culture analysis showed that these species develop in clusters. They are therefore disturbed by the continuous movement in the PBR. The use of PBB airlift with PVC allowing the adhesion of cells could be tested to optimize biomass production for these two diatom species. In airlift PBR, cultures were not phosphate, nitrogen, carbons or silica depleted. However growth could stop because of light limitation (Sánchez Mirón *et al*., 2002) and/or lack of other compounds (vitamins, trace metals etc.) (Croft *et al*., 2005; Gao *et al*., 2013). In fact, chl *a* content increased for *N. alexandrina* and *Staurosir*a sp. suggesting a decrease of light achieving cells (Sánchez Mirón *et al*., 2002).

Total lipid content obtained for all six species produced in airlift differs from our previous study (Cointet *et al*., 2019a) (Figure 7). Four species produced more lipids when grown in Airlift PBR compared to the Erlenmeyer flask (*E. paludosa*, *N. alexandrina*, *Opephora* sp. and *Staurosira* sp.) while two species produced fewer lipids (*Amphora* sp. and *Nitzschia* sp.). These results can be explained by an increases in temperature parameter which was 20°C in the present study and 16°C in our previous study. As shown by de Castro Araújo *et al*. (2005) a temperature increase of five degrees can increase lipid content (de Castro Araújo and Garcia, 2005). As demonstrated by Chen *et al*. (2012) culture conditions impact lipid production (Chen, 2012). They compared the lipid production of 10 diatom genera including 2 used in the present study (*Amphora* and *Nitzschia*). Species were grown under greenhouse or incubator during summer and winter. Summer temperatures ranged from 25 to 34.5 °C and from 14 to 22.5 °C during winter. Light intensity in the summer greenhouse ranged from 47 to 969 µmol.photons.m^{-2}.s^{-1} and from 13 to 360 µmol.photons.m^{-2}.s^{-1} in the winter greenhouse. Temperature in the incubator was 24°C, with a light intensity of 122 µmol.photons.m^{-2}.s^{-1} under 12:12 light:dark cycle. Lipid content variation was observed for the different species studied depending on the culture conditions. For example, the genus *Amphora* had a higher lipid content in the greenhouse in summer than in winter (45% *vs.* 33%) and a lipid level of 39% when grown in an incubator. Conversely,

Nitzschia genus produced more lipids when grown in the greenhouse in winter (38%) than in summer (33%) but still produced more lipids in the incubator (42%). These results are not in aggreements with our study as the two species seem to produce more lipids under 16°C. However, in Chen *et al* study the range of temperature and light variations in the greenhouse may explain the difference. Moreover, the application of a light-dark cycle may improve lipid production for these species. The incubator temperature was higher than in the airlift PBR which may explain why these species produce more lipids.

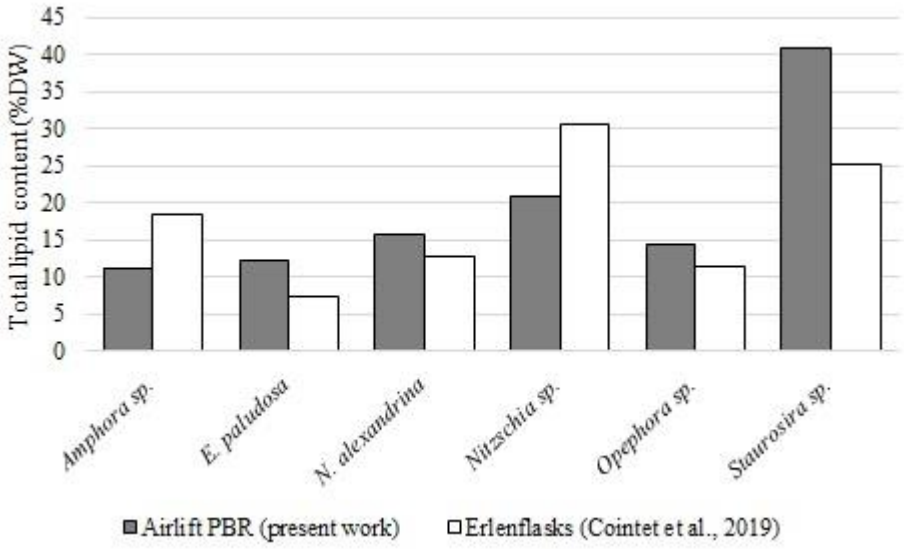

Figure III-8 Total lipid content in airlift and an Erlenmeyer flask (Cointet *et al*., 2019) for the six species studied.

Increases in biomass and lipid production can be explained by cell stress induced by CO_2 (Medina *et al*., 1998), temperature (Dunstan *et al*., 1993), the culture medium used and/or nutrient composition (Dunstan *et al*., 1993; Schnurr and Allen, 2015) as well as the achievement of late exponential phase (Lebeau and Robert, 2003; Sharma *et al*., 2012). In the present study, *Staurosira* sp. was the only species to produce a total lipid content of higher than 35%. The three interesting species in terms of biomass production and lipid content were *N. alexandrina* (15.7%), *Nitzschia* sp. (20.8%) and *Staurosira* sp. (40.9%).

2.5.2 Lipids analyses

2.5.2.1 Lipids classes analyses

It has been reported that GLs are predominantly produced during the exponential phase and TAGs during the stationary phase (Bergé and Barnathan, 2005). The amount of GLs mainly produced in *Opephora* sp. can be explained by the microscopic cell structure. As they need to grow in clusters, the continuous movement created by the airlift disrupts biomass production. It is therefore possible to assume that growth is longer, and the stationary phase is never reached, hence the higher amount of GLs (58.5%) and lower lipid storage (NLs) (29.0%). A single publication dealing with *Staurosira* sp. lipid production for biodiesel exists (Huntley *et al*., 2015). In this study, Huntley *et al* demonstrated that *Staurosira* sp. can be grown at large scale because of a high lipid content (37.8%DW) which is in accordance with our study. However, they do not highlight the biochemical composition of this species. Its significant production of TAG (71%) could be interesting for the cosmetology market. It could also be interesting for biodiesel production since currently developed biofuels are composed of a larger amount of MUFA than PUFA. Biodiesel is produced by TAG transesterification with MeOH, and is a substitute for petroleum diesel. Biodiesel FA saturation has better oxidative stability but poorer flow properties. PUFA have better flow properties but are sensitive to oxidation. MUFA are therefore the most suitable for biodiesel (Sabia *et al*., 2018). *Staurosira* sp. is therefore an excellent candidate for the valorization of its lipids in biodiesel. FA are found in different proportions in polar lipids. As described in the literature, GLs and PLs of algae have anti-inflammatory, anti-cancer and antimicrobial activity (da Costa *et al*., 2017; Plouguerné *et al*., 2013). It would be interesting to test different GLs and PLs cellular models found in the six species according to their quantity and their structural profile, in order to define their potential activity.

2.5.2.2 Unsaponifiable analyses

Unsaponifiable analyses (phytol, HC, sterols) of the six species showed a composition with 4.3 to 40.4% of phytol. This molecule is a degradation product of chlorophyll (Ponomarenko *et al*., 2004). Phytol is also present as a free molecule, playing a role in diatom photosynthesis and photoprotection (Stonik and Stonik, 2015). Chlorophyll concentration varies according to the species, which explaines phytol content variability between species (Massé *et al*., 2004; Yao *et al*., 2015; Zapata *et al*., 2011). Unsaponifiable content was also composed of HC and squalene, which is a sterol precursor, in low quantities (1-4% TLC). These molecules are commonly found in diatoms (Grossi *et al*., 2004; Nichols *et al*., 1988; Volkman and Hallegraeff, 1988; Yao *et al*., 2015). Their presence may be explained by certain FA decarboxylations (Volkman *et al*., 1994). Sterols are found in all organisms (Blunt *et al*., 2011), including macro and microalgae (Hamed *et al*., 2015; Thompson Jr, 1996). They are present in all taxonomic groups of diatoms. The most common sterols found in diatoms belong to the Δ5 series (Figure. 5) (Stonik and Stonik, 2015). With regard to the sterols found in the six species analyzed, the basic structure is indeed cholesterol (Δ5 unsaturation).

Sterols in diatoms are described as being mostly composed of 28 carbons but certain phylogenetic groups synthetize 27 or 29 carbon sterols, which is in accordance with the present study and consistent with the biosynthetic pathway. Sterol classification is therefore in some cases an aid to the phylogenetic diatom classification (Stonik and Stonik, 2015). A study conducted by Rampen *et al* (2010) on 106 diatom strains highlighted the presence of 44 sterols and 2 steroidal ketones (Rampen *et al*., 2010). The 9 sterols characterized in the GC-MS analyses are found among the 44 sterols described. Sterol quantity and quality can be variable between two species belonging to the same genus (Geng *et al*., 2017; Rampen *et al*., 2010) as seen for *N. alexandrina* and *Nitzschia* sp. in the present study. Other studies described the same kind of sterols, present or absent according to the species studied and in variable concentrations

(Barrett *et al*., 1995; Gladu *et al*., 1991; Nappo *et al*., 2009; Nichols *et al*., 1988; Ponomarenko *et al*., 2004; Sharma *et al*., 2012; Yao *et al*., 2015).

Sterol proportions found in the Rampen *et al*. (2010) study for *E. paludosa* (previously *Amphiprora paludosa*) differs in the present study. Indeed, 24-methylcholesta-5,22*E*-dien-3β-ol was found at 27% of total sterols in the Rampen *et al*. study but only in trace amounts in the present study. Moreover, 24-methylcholest-5-en-3β-ol (14%) and 24-ethylcholesta-5,22*E*-dien-3β-ol (55%) were found in higher concentrations in Rampen *et al*. than in the present work (2.2% and 28.7% of total sterols respectively). Conversely, Rampen *et al*. found lower concentrations of 24-ethylcholest-5-en-3β-ol than in this study (4% *vs.* 61.1%). In the present study *Amphora* sp. was composed of almost 100% of 24-ethylcholesta-5,22*E*-dien-3β-ol against 88% to 96% and 4 to 9% of 24-ethylcholest-5-en-3β-ol in the literature (Barrett *et al*., 1995; Gladu *et al*., 1991; Rampen *et al*., 2010). These differences can be explained by the fact that within the same genus, species produce sterols in different ways (Volkman and Hallegraeff, 1988). The *E. paludosa* species produced more sterols than the others (19.5% TLC). The *N. alexandrina* species is interesting for the production of recoverable squalene in cosmetology.

2.5.2.3 Fatty acid analyses

In diatoms, FA proportions range from 0.2% to 35% of total FAs according to the species (Dunstan *et al*., 1993; Medina *et al*., 1998; Nichols *et al*., 1993; Sabia *et al*., 2018; Viso and Marty, 1993; Yao *et al*., 2014). In comparison with other algae, diatoms are described as enriched in myristic acid (14:0) (4 to 32%) and produce less stearic acid (18:0) (Hildebrand *et al*., 2012). They produce more PUFA with 16 and 18 carbons and more EPA compared to green algae (Thompson Jr, 1996). These results are in agreement with our study. The FA analysis of 17 diatoms species (including 6 *Nitzschia* species and 2 *Amphora* species) (Levitan *et al*., 2014) made it possible to highlight the predominant FAs. Palmitic and palmitoleic acids as well as EPA were mainly found in the 17 species. FAs found to a lesser extent were myristic, 6,9-

hexadecadienoic, linoleic, oleic, vaccinic and 6,9,12 hexadecatrienoic acids. These results were consistent with our study. Some species of *Nitzschia* produce less EPA than others of the same genus, which could explain the difference between *N. alexandrina* (5.4%) and *Nitzschia* sp. (2.8%) (Levitan *et al*., 2014). All the species in the present study had proportions of unsaturated FAs higher than 50%, which remains consistent with the study of Dunstan *et al*. (1993) which analyzed FAs in 14 diatom species (Dunstan *et al*., 1993). However, quantities of these FAs was different. Proportions of saturated FA was higher for the six species studied here: 26 % to 42.5% *vs.* 17.5 to 36.6% in the Dunstan *et al*. study. It was the same for MUFA (31.8-54.2% *vs.* 20.6-27.2%). FA proportions are thus independent of the species. After CLE analyses, *Nitzschia* sp. produced the lowest EPA level. The two species *Amphora* sp. and *E. paludosa* produced higher EPA content. EPA was found in different amounts in all six species (2.8 to 12.6% of total FAs). The species which produced more EPA was *E. paludosa* (12.6%). This species contained more EPA than Atlantic salmon (6.5%) or *Chlorella vulgaris* microalgae (0.46%) but slightly less than the brown algae *Laminaria* sp. (16.2%) (Hamed *et al*., 2015).

PUFA play a role in cell membranes by providing fluidity and flexibility. Long chain PUFA play a role in heart health, especially n-3 (EPA). It stabilizes atherosclerotic plaques by reducing the infiltration of immune and inflammatory cells. They may be usefull in preventing cardiovascular diseases. Several studies have described the effect of these FA against prostate cancer or adenocarcinoma. They are also found to reduce interleukins levels, which cause pain in rheumatoid arthritis (Bergé and Barnathan, 2005). EPA is recommended in diets for patients with psoriasis, to reduce the formation of pro-inflammatory factors. Decreasing these factors may play a role in lowering the risk of developing asthma attacks. Consumption of DHA and EPA is also recommended during pregnancy to supplement the intake for mother and child (Lebeau and Robert, 2003; Matsunaga *et al*., 2005)

2.6 Conclusion

Six species were grown in airlift PBR and their precise lipid composition was determined. Results showed that in terms of biomass productivity *N. alexandrina*, *Staurosira* sp. and *E. paludosa* are the most promising. However, in terms of lipid content *Staurosira* sp., *Nitzschia* sp. and *N. alexandrina* are the most productive. In terms of biochemical diversity, the species which produced interesting chemical compounds were not easily grown in the photobioreactor. Despite interesting sterol production for *Amphora* sp. and interesting quantities of GLs for *Opephora* sp., these two species produced little biomass and lipids in the airlift PBR. To recover these compounds, other photobioreactor designs such as flat pannel must be tested. However, the culture method developed in this study demonstrated that three of the six species can be easily grown in this system. Moreover, their biochemical compounds can be recoverable for different industrial purposes. *Entomoneis paludosa* is an interesting species for sterol and EPA production. *Nitzschia alexandrina* produces squalene and few SFAs. *Staurosira* sp. produces high amounts of TAG with a large proportion of MUFA. *Nitzschia* sp. produces high amounts of biomass and lipids but does not produce glycolipids or particularly interesting recoverable fatty acid so this species was not selected for future analyses.

Acknowledgements

This work was supported by the regional Atlantic Microalgae research program (AMI), funded by the Pays de la Loire region. We also express our sincere thanks to Ms Raphaëlle Touchard (GEPEA) for support and advice for the utilization of the Airlift PBR.

Conflict of interest

The authors declare that there is no conflict of interest. No conflicts, informed consent, human or animal rights are applicable to this work.

Author contributions

Eva Cointet, Elise Séverin, Aurélie Couzinet-Mossion, Vona Méléder, Olivier Gonçalves and Gaëtane Wielgosz-Collin designed and supervised the research. Eva Cointet, Elise Séverin, Aurélie Couzinet-Mossion, Vona Méléder, Olivier Gonçalves and Gaëtane Wielgosz-Collin conducted experiments. Eva Cointet, Elise Séverin, Aurélie Couzinet-Mossion, Vona Méléder, Olivier Gonçalves and Gaëtane Wielgosz-Collin analyzed and interpreted the data and drafted the manuscript. Eva Cointet, Elise Séverin, Aurélie Couzinet-Mossion, Vona Méléder, Olivier Gonçalves and Gaëtane Wielgosz-Collin critically reviewed the manuscript. All authors read and approved the final version of the manuscript.

3 Conclusion

Le fractionnement des EBLs et l'analyse des différentes classes de lipides a permis d'estimer la qualité des lipides des 6 diatomées marines benthiques cultivées en PBR airlift plat. *Entomoneis paludosa* NCC18.2 semble être la plus intéressante pour la production de stérols et d'EPA, *Nitzschia alexandrina* NCC33 pour la production de squalène et d'une faible proportion d'AG saturés et *Staurosira* sp. NCC182 pour la production en TAG. Malgré une production de stérols supérieur à 62.2 % de la fraction insaponifiable, *Amphora* sp. NCC169 produit seulement 0.23 $g.L^{-1}$ de biomasse et 11.3 % du poids sec en lipides. *Opephora* sp. NCC366 produit 58.5 % de glycolipides, mais produit seulement 0.29 $g.L^{-1}$ de biomasse et 13.3 % du poids sec en lipides lorsqu'elle est cultivée en airlift. *Nitzschia* sp. NCC109 produit 0.82 $g.L^{-1}$ de biomasse et 20.8% du poids sec en lipides ce qui est intéressant en terme de production, mais elle ne produit pas de glycolipides ou d'acides gras particuliers valorisables, elle n'a donc pas été sélectionnée pour la suite de l'étude.

Les deux espèces séléctionnées pour la suite de l'étude car possédant une production de biomasse supérieur à 1 $g.L^{-1}$ et un production lipidique supérieur à 20 % du poids sec ainsi qu'une diversité lipidique valorisable en santé sont *N. alexandrina* et *Staurosira* sp.

E. paludosa a également été conservée pour la suite de l'étude du fait de sa production en biomasse supérieur à 1$g.L^{-1}$ et puisqu'elle produit des acides gras valorisable en santé.

Les fractions de lipides neutres (TAG) et glycolipides (MGDG, DGDG et SQDG) des trois espèces sélectionnées dans ce chapitre : *E. paludosa* NCC18.2, *N. alexandrina* NCC33 et *Staurosira* sp NCC182 ont été testées pour leur bioactivité potentielle sur cellules cancéreuses et leur capacité antibactérienne. Les résultats obtenus sont présentés dans le chapitre suivant.

IV- Evaluation du potentiel bioactif des fractions lipidiques extraites de trois espèces de diatomées marines benthiques

1 Contexte de l'étude

Cette étude a demontré la capacité des diatomées marines benthiques à produire de nombreux composés valorisables industriellement. Parmi, les lipides valorisables détectés, les glycolipides sont considérés comme une source importante d'acides gras insaturés. Ces glycolipides sont localisés dans la membrane des chloroplastes et des thylacoïdes et sont d'importantes molécules signals et régulatrices (Harwood and Guschina, 2009; Siegenthaler and Murata, 2006). Ils sont riches en acides gras C16 et C18 saturés et insaturés et contiennent souvent des acides gras polyinsaturés comme l'EPA par exemple. Les glycolipides comprennent trois classes majeures : les monogalactosyldiacylglycérol (MGDG), les digalactosyldiacylglycérol DGDG et les sulfonoquinovosyldiacylglycérol (SQDG). Leurs compositions en acide gras dépendent directement des conditions de cultures. Certaines de ces fractions possèdent des composés à hautes valeurs ajoutées avec des activités antitumorales, antibactériennes et anti-inflammatoires et sont également important en nutrition (Plouguerné *et al*., 2014). Afin d'estimer les activités biologiques des lipides issus des diatomées marines benthiques et pouvoir utiliser ces souches comme nouvelles sources de composés transformables en principes actifs, la bioactivité des produits extraits de ces microalgues ont été testés. Dans ce chapitre, les activités antibactériennes sur des souches à gram négatif et à gram positif, ainsi que le potentiel anti-prolifératif sur des cellules cancéreuses du sein et du poumon, ont été évaluées sur les fractions glycolipidiques extraites des trois espèces de diatomées sélectionées dans le chapitre précédent : *E. paludosa*, *N. alexandrina* et *Staurosira* sp. Lors de cette étude les diatomées ont été cultivées en ballon de 25 L dans des conditions de cultures controlées en lumière et température, mais non en élément nutritif comme cela est le cas en PBR airlift. Cette méthode de culture en plus grand volume a été choisi car elle permet d'obtenir la quantité nécessaire en composés chimiques pour réaliser les tests de bioactivités mais

également de tester la production de composés valorisables en se rapprochant le plus possible des conditions de cultures utilisées actuellement à l'échelle industrielle. Les résultats de cette étude sont présentés ci-dessous et font l'objet d'une publication en préparation à soumettre dans Marine Drugs.

2 Antibacterial and antiproliferative activity against breast cancer and lung cancer cell line of extracted lipid fraction from three benthic diatoms species

marine drugs

MDPI

Article

Antibacterial and Antiproliferative activity against breast cancer and lung cancer cell lines of extracted lipid fraction from three benthic diatom species.

Eva Cointet[1], Olivier Gonçalves[2], Elise séverin[1], Aurélie Couzinet-Mossion[1], Fatima Lakdhar[3], Samira Etahiri[3], Lucie Ory[1], El-Hassan NAZIH[1], Christos Roussakis[4], Vona Méléder[1], Gaëtane Wielgosz-Collin[1*]

1. University of Nantes, Faculty of Pharmaceutical and Biological Sciences, MMS-EA 2160, Institut Universitaire Mer et Littoral FR3473 CNRS, 9 rue Bias BP 53508, 44035 Nantes Cedex1, France.
2. Université de Nantes, GEPEA, UMR CNRS-6144, bât. CRTT, 37 boulevard de l'Université, BP406,F-44602 Saint-Nazaire Cedex, France.
3. University Chouaib Doukkali, Faculty of Science, Laboratory of Marine Biotechnology and Environment, BP 20, El Jadida, Morocco.
4. IICIMED/ERATU, Cancer du poumon et Cibles Moléculaires, Faculté de Pharmacie, Université de Nantes, 1 rue Gaston Veil, BP 53508, F-44035 Nantes Cedex 01, France.

e-mail address: eva.cointet@univ-nantes.fr (E.C); olivier.goncalves@univ-nantes.fr (O.G); elise.severin@gmail.com (E.S); aurelie.couzinet-mission@univ-nantes.fr (A.C.M); fatima19862008@hotmail.fr (F.L); setahiri@hotmail.com (S.E);lucie.ory@univ-nantes.fr (L.O); el-hassane.nazih@univ-nantes.fr (E.H.N); christos.roussakis@univ-nantes.fr (C.R); vona.meleder@univ-nantes.fr (V.M); gaetane.wielgosz-collin@univ-nantes.fr (G.W.C.)*

* Correspondence: gaetane.wielgosz-collin@univ-nantes.fr ; Tel.: +33-276-645-081

Received: date; Accepted: date; Published: date

2.1 Abstract

Potential antibacterial and antiproliferative activity against breast and lung cancer cell lines were investigated in three original marine benthic diatom species : *Entomoneis paludosa*, *Nitzschia alexandrina* and *Staurosira* sp. Cultures were grown in 25 L flasks to obtain molecular compounds in sufficient amount to conduct bioactivity tests. Lipid content obtained with this culture method was compared to the lipid content obtained from airlift PBR culture to

ensure that there was no loss of major compound production. Lipid content varied from 9.6%DW (*E. paludosa*, flask) to 40.9% DW (*Staurosira sp*., airlift). Neutral lipids were mainly produced by *Staurosira sp*. under both culture methods and representing 75% of total lipids. For *E. paludosa* SFA were mainly produced in flasks (50.1% vs 42.5%) whilst MUFA proportion was more important in airlift (31.8% vs 16.3%). *N. alexandrina* produced more TAG in flasks than in airlift (71.6% vs 39.2%). For all species and all culture methods, major fatty acids were 9-16:1, 16:0, 14:0 and 5,8,11,14,17-20:5 (EPA). Larger EPA quantities of 12.6% and 9.6% of total fatty acids were produced by *E. paludosa* (airlift) and *N. alexandrina* (flask) respectively. Antibacterial activity against *B. subtilus* was detected for *Staurosira sp.* DGDG fraction. Antiproliferative activity against the MCF-7 breast cancer cell line was detected for *E. paludosa* glycolipid fraction, *N. alexandrina* DGDG fraction and for *Staurosira sp.* DGDG and MGDG fractions. Antiproliferative activity against the NSCLC-N6 lung cancer cell line was discovered for *N. alexandrina* DGDG fraction and *E. paludosa* SQDG fraction.

Keywords: Glycolipid; *Staurosira* sp ; *E. paludosa* ; *N. alexandrina*, antibacterial activity ; MCF-7 cell ; NSCLC-N6 cell

Abbreviation :

AtB:	Antibacterial
ATCC:	American Type Culture Collection
CLE:	Crude Lipid Extract
DGDG:	Digalactosyldiacylglycerol
DMSO:	Dimethylsulfoxyde
DMEM:	Dulbecco's Modified Eagle Medium
DW:	Dry Weight
FA:	Fatty Acid
FFA:	Free Fatty Acid
FAME:	Fatty acid methyl ester
GC-MS:	Gas Chromatography Mass Spectrometry
GL:	Glycolipid
MUFA:	Monounsaturated Fatty Acid
MGDG:	Monogalactodiacylglycerol
NAP:	N-*acyl* pyrrolidide
NL:	Neutral lipid
PL:	Phospholipid
PUFA:	Polyunsaturated Fatty Acid
SFA:	Saturated Fatty acid
SQDG:	Sulfonoquinovodiacylglycerol
TAG:	Triacylglycerol

2.2 Introduction

Cancer, inflammation and the evolution of antibiotic-resistant pathology, together with other human diseases, are continuously stimulating the search for new bioactive molecules from natural sources. Unlike drug discovery on land, marine drug discovery is a relatively new field which began in the 1940s with the advent of scuba diving and new sampling technologies that allowed scientists to systematically probe the oceans for useful therapeutics. The number of potential compounds isolated from marine organisms now exceeds 28.000 with hundreds of

new compounds being discover every year (Blunt *et al*., 2011). However, despite the number of compounds isolated from marine organisms and the biological activity attributed to many of them, those that have either been marketed or are under development are relatively few (Jaspars *et al*., 2016). Most of these natural products have been isolated from Porifera (sponges) and Chordata (including ascidians) but these macroorganisms are often difficult to cultivate and there may be problems to obtain a sustainable supply of these compounds of interest without ecologically impacting natural populations. More recently there is great interest in exploring the biotechnological potential of microorganisms such as microalgae since they are easier to cultivate, have short generation times and represent a renewable and still poorly explored resource of drug discovery (Guedes *et al*., 2013; Mimouni *et al*., 2012; Nigjeh *et al*., 2013; Samarakoon *et al*., 2013).

Diatoms are the most abundant and diverse group of microalgae (Kooistra *et al*., 2007). They can exist both as single cells or as a chain of connected cells. They exist in both saline and fresh water (Sumich and Morrissey, 2004). They constitute a unicellular eukaryotic group with a typical species-specific siliceous cell wall (Drum and Gordon, 2003; Munn, 2011). Diatoms also have communication capabilities where they can send chemical signals between and within cells to protect themselves from predators (Vardi, 2008). Microalgae and particularly diatoms are severely underrepresented compared to marine bacteria, porifera, molluscs, seaweeds and other marine microorganisms in the search of novel, bioactive marine compounds (Ingebrigtsen *et al*., 2016); Nevertheless, a wide range of bioactivities have been discovered in microalgae in the last 60 years (Borowitzka, 2013). This includes antibacterial, antibiofilm, anticancer, antioxydative and anti-inflammatory activities. Compounds produced by diatoms like free fatty acids (FFAs), oxylipins and photosynthetic pigments or their derivatives, show promising antibacterial activities(Smith *et al*., 2010). For example, chlorophyll derivatives have proven to have antibacterial activity against gram positive and gram negative bacteria (HANSEN, 1973;

Jørgensen, 1962). *Phaeodactylum tricornutum* fucoxanthine from pigment fraction had proven to have anti-cancer, antioxidant and anti-inflammatory effects (Kim *et al*., 2012; Peng *et al*., 2011). Digalactosyldiacylglycerol (DGDG) and sulfoquinovosyldiacylglycerol (SQDG) from glycolipids fraction in *Stephanodiscus* sp. have been proven to have anticancer and antioxidant effects (Talero *et al*., 2015). Searching for bioactive compounds can be done in many ways, *e.g.* by bioassay-guided isolation, chemistry-guided isolation and genomic mining. However, the focus of the present study was only on bioassay-guided isolation with extracted and fractionated samples being tested on different bioassay, namely antibacterial and anti-cancer.

Diatoms reproduce quickly in the right conditions and are thus easy to grow in a high rate (Talero *et al*., 2015) compared to higher plants (de Morais *et al*., 2015). Diatoms are autotrophic so the only requirement for cultivation are inorganic compounds, such as CO_2, salt and solar energy (de Morais *et al*., 2015). However, it seems like various cultivation conditions can cause the metabolic pathway to be turned on and off and consequently trigger the production of various compounds (Ingebrigtsen *et al*., 2016). Nutrient composition is an important factor which can be manipulated in a series of ways, for example with lack/excess of important nutrients; mass *vs* small scale cultivation etc. These various conditions can potentially trigger diatoms to produce natural products for self-protection. For example, production of polyunsaturated fatty acids (PUFAs) or neutral lipids can be stimulated and optimized under nitrogen and phosphate deficiency (Řezanka *et al*., 2012). In this study, three benthic diatom species have been grown at large scale under different conditions. Each species was grown in 25 L flask, under continuous illumination without pH control and without limiting nutrient stress in a classic natural seawater F/2 medium and they were also grown, in a previous study (Cointet *et al*, 2019b), in 1 L Airlift photobioreactor (PBR) with pH control and with limiting nutrient stress in a modified natural seawater F/2 medium. Lipid fractions extracted from the flask cultures were compared with those obtained from airlift, to ensure the same molecular

production. Biomass was harvested, lipids were extracted and fractionated. In order to assess the potential antibacterial activity and antiproliferative activity against human cancer cells (breast and lung) of the molecular compound extracted, only the lipid fractions obtained from flask cultures were tested to ensure a sufficient quantity of these compounds. The first objective of this study is to try a scale-up in a culture less controlled than in airlift PBR to get closer to the growing conditions currently being carried out on a larger scale. This semi-mass culture conditions made it possible to obtain chemical materials in larger quantities than in airlift PBR to be biologically tested and highlight the structural analysis. However, before conducting the bioactivity test the objective of this study is also to ensure that there is no major compounds loss between the semi-mass culture and the airlift PBR culture conditions.

2.3 Results and discussion

2.3.1 Biomass production and lipid rate

Biomass production was ten times higher in airlift than in flasks (Table IV-1). However, maximum biomass harvested was from *E. paludosa* when grown in a flask (5.048 g). Biomass harvested for *Staurosira* sp. was higher in a flask but the use of the PBR made it possible to produce almost the same amount in less volume (1.62 *vs* 1.28 g). Total lipid rate between species varied from 9.61% (*E. paludosa*) to 28.8% (*Staurosira* sp.) in flask cultures and from 12.3% (*E. paludosa*) to 40.9% (*Staurosira* sp.) in airlift.

Crude lipid extract (CLE) composition obtained after saponification made it possible to separate unsaponifiable (analyzed free in GC-MS and then acetylated) from fatty acids (derived in FAME then NAP for GC-MS analysis). CLE was composed by more than 20% of unsaponifiable in *E. paludosa* and *N. alexandrina* when grown in flasks.

The culture grown in a flask made it possible to obtain a larger CLE than the one obtained in airlift. CLE obtained from flask culture can be more easily fractionated and tested for their bioactivity potential.

Table IV-1 General data of the CLEs according to the culture mode.

	Entomoneis paludosa		*Nitzschia alexandrina*		*Staurosira* sp.	
	Flask	Airlift	Flask	Airlift	Flask	Airlift
Biomass (g)	5.05	0.81	1.48	0.84	1.62	1.28
Biomass (g/L)	0.20	1.16	0.11	1.16	0.12	1.60
CLE (mg)	485	100.2	253.3	131.9	467.5	524.4
TLR (%)	9.61	12.3	17	15.7	28.8	40.9
unsaponifiable (% CLE)	24.0	20.7	25.0	14.0	3.1	12.0

2.3.2 Lipid class fractionation

CLE for all species were fractionated into lipid classes by normal phase chromatography on silica gel column (Table IV-2). Neutral lipids (NL) were mostly produced by *Staurosira* sp. for both culture modes. For *E. paludosa* and *N. alexandrina* neutral lipids were mostly found in flasks : 50.9 *vs* 46.6% for *E. paludosa* and 71.6 *vs* 39.2% for *N. alexandrina*.

Glycolipid (GL) amounts varied from 16.0% (*Staurosira* sp., flask) to 45.1 % (*N. alexandrina*, airlift). *N. alexandrina* produced more GL when grown in airlift than in a flask (45.1 *vs* 23%). GL amounts were constant between culture modes for *E. paludosa* and *Staurosira* sp.

Table IV-2 Lipid classes of *E. paludosa*, *N. alexandrina* and *Staurosira* sp. for both culture modes.

	% lipid classes (% total lipids)					
	Entomoneis paludosa		*Nitzschia alexandrina*		*Staurosira* sp.	
	Flask	Airlift	Flask	Airlift	Flask	Airlift
Neutral lipids	50.9	46.6	71.6	39.2	74.8	76.4
Glycolipids	36.1	38.5	23.6	45.1	16.0	17.6
Phospholipids	13.0	14.9	4.8	15.7	9.2	6.0

2.3.3 Analyses of unsaponifiable fraction by GC-MS

The composition of the unsaponifiable CLE fraction was analyzed (data not shown). Bioactivity potential was not tested because they represent only a small fraction of the neutral lipids. However as seen in the previous study, sterol composition between airlift and flasks was the same but in different proportion. The majority of sterols found in the three species were cholesta-5-en-3β-ol, cholesta-5,22-dien-3β-ol, 24-methylcholest-5-en-3β-ol, 24-methylcholesta-5,22*E*-dien-3β-ol, 24-ethylcholest-5-en-3β-ol and 24-ethylcholesta-5,22*E*-dien-3β-ol.

2.3.4 Total fatty acid compositions

Fatty acids (FA) analyzed after saponification were represented by triacyglycerol (TAG) fatty acids, glycolipids (GL) and phospholipids (PL) (Table IV-3). Crude lipid extract fatty acid proportions were variable between species and culture modes. Variability in the quality of fatty acids was observed with the presence in different amounts of saturated and unsaturated fatty acids depending on the species.

Saturated fatty acid (SFA) production between airlift and flask culture modes was constant. Among unsaturated fatty acids, monounsaturated fatty acids (MUFA) were produced by *N. alexandrina* and *Staurosira* sp. in the same proportion. The only difference was for *E. paludosa* that produced less MUFA in a flask than in PBR (16.3 *vs* 31.8%) inducing an increase in SFA in the flask for this species. Polyunsaturated fatty acid (PUFA) production between airlift and flask culture modes was constant for all species.

Major fatty acids were palmitoleic (9-16:1), palmitic (16:0) and myristic (14:0) acids followed by eicosapentaenoic acid (5,8,11,14,17–20:5). Palmitoleic acid and EPA production was more important in airlift than in a flask for *E. paludosa* (11.6 *vs* 28.3%) and (12.6 vs 8.4%) while for *N. alexandrina*, EPA was preferentially produced in a flask than in airlift (9.6 *vs* 5.4%).

Similar fatty acid diversity was observed between both culture modes used in this study for all species, confirming that there was no loss of information even if culture conditions were less controled. However, major differences between composition of lipid classes was found for *N. alexandrina*. Culture in flask induces larger neutral lipid production than in airlift for this species (71.6 % *vs* 39.2 %). A lack of nutrients or pH increases may induce in this species an increase in TAG production, which are an abundant storage product. Microalgal TAGs are generally characterized by both SFA and MUFA (Sharma *et al*., 2012). Indeed, *N. alexandrina* produced more SFA and MUFA when grown in a flask than in airlift PBR. Under unfavorable environmental or stress conditions diatoms alter their lipid biosynthesis pathways toward the formation and accumulation of neutral lipids, mainly in the form of TAG, enabling diatoms to endure these adverse conditions (Praveenkumar *et al*., 2012; Yang *et al*., 2013; Yeh and Chang, 2011).

Tableau IV-3 Fatty acids of *E. paludosa*, *N. alexandrina* and *Staurosira* sp. for both culture modes.

Fatty acid	Formula	% FA (% total FA)					
		E. paludosa		*N. alexandrina*		*Staurosira* sp.	
		Flask	Airlift	Flask	Airlift	Flask	Airlift
Saturated FA							
Myristic Acid	14:0	**19.3**	**18.9**	4.1	3.7	2.1	3.7
Pentadecanoic acid	15:0	1.7	0.7	1.1	2.1	0.5	Tr
Palmitic acid	16:0	**27.6**	**22.4**	**25.7**	**19.4**	**29.6**	**29.4**
Stearic acid	18:0	0.6	0.5	0.6	0.8	0.6	0.6
Σ SFA		50.1	42.5	31.5	26.0	32.9	33.7
Monounsaturated FA							
Palmitoleic acid	9-16:1	**11.6**	**28.3**	**42.0**	**43.5**	**48.3**	**51.8**
Oleic acid	9-18:1	0.8	1.1	ND	0.9	3.4	1.0
Vaccinic acid	11-18:1	0.8	1.3	1.8	1.9	1.9	1.4
Nervonic acid	24:1	0.5	1.1	ND	ND	ND	ND
Σ MUFA		16.3	31.8	53.2	46.3	53.9	54.2
Polyunsaturated FA							
6,9 Hexadecadienoic acid	6,9-16:2	1.8	2.9	2.7	6.4	ND	ND
6,9,12 Hexadecadienoic acid	6,9,12-16:3	2.4	ND	ND	ND	0.5	0.6
ɣ Linoleic acid	6,9,12-18:3	0.6	0.8	1.3	1.8	1.2	0.9
5,9,12 octadecatrienoic acid	5,9,12-18:3	1.4	2.4	ND	ND	1.0	0.5
Linoleic acid	9,12-18:2	1.0	1.8	ND	Tr	0.8	Tr
Arachidonic acid	5,8,11,14-20:4	ND	Tr	1.4	4.7	0.9	0.9
Eicosapentaenoic acid	5,8,11,14,17-20:5	**8.4**	**12.6**	**9.6**	**5.4**	**6.1**	**5.5**
Σ PUFA		16.3	20.5	15	18.7	12.9	8.4

Tr : traces < 0.5% ; ND : Not detected

2.3.5 Bioactivity assay

Different fractions of NL and GL obtained for all species and semi-mass culture modes were tested for biological activity. All fractions were tested for their antimicrobial activity against *B. subtilus*, *S. aureus* (Gram-positive bacteria) and *E. coli* (Gram-negative bacteria). Antiproliferative activity against breast (MCF-7) and lung cancer cell lines (NSCLC-N6 and A549) were also evaluated.

2.3.5.1 Crude lipid extract fractionation

CLE extract for the three species were fractionated and composition was identified by thin layer chromatography (Table IV-4). Bioactivity tests were carried out on the fractions enriched in a single type of compound and when the available quantity made it possible to predict a structural elucidation. According to the literature, GL fractions are known for their potential bioactivity (Ammar Al-Fadhli *et al*., 2006; Takashi Morimoto *et al*., 1993, 1995; Murakami *et al*., 2003a; Cheng-Jung Tsai and Sun Pan, 2012). GL fractions for the three species were tested for their antibacterial potential (AtB) and antiproliferative bioactivity on breast and lung cancer cells. The high lipid content for *Staurosira* sp. made it possible to perform bioactivity test on many fractions. Similarly, since *N. alexandrina* has a high TAG content, this fraction has also been evaluated.

Tableau IV-4 CLE fractionation of *E. paludosa*, *N. alexandrina and Staurosira* sp.

Species	Fractions	Name	%	Composition	Test performed
E. paludosa	Neutral lipid	D1Ep	5.7	HC and TAG	-
		D2Ep	3.4	TAG	-
		D3Ep	42,8	FFA, phytol and sterols	-
	Glycolipid	A1Ep	13.8	Pigment	-
		A2Ep	13.5	MGDG	AtB/ breast and lung cancer
		A3Ep	4.8	DGDG	AtB/ breast and lung cancer
		A4Ep	5.0	SQDG	AtB/ breast and lung cancer
	Phospholipid	M1Na	14.6		-
N. alexandrina	Neutral lipid	D1Na	48.6	TAG	AtB/ lung cancer
		D2Na	23.0	FFA and sterol	-
	Glycolipid	A1Na	4.9	Pigment	-
		A2Na	7.2	MGDG and pigment	-
		A3Na	2.0	DGDG	AtB/ breast and lung cancer
		A4Na	1.7	DGDG	AtB/ breast and lung cancer
		A5Na	3.3	DGDG	AtB/ breast and lung cancer
		A6Na	4.3	SQDG	AtB/ breast and lung cancer
	Phospholipid	M1Na	4,8		-
Staurosira sp.	Neutral lipid	D1St	1.8	HC and TAG	-
		D2St	54.5	TAG	AtB/ lung cancer
		D3St	18.5	HC and sterol	-
	Glycolipid	A1St	3.0	Pigment	AtB
		A2St	0.6	Fucoxanthine	AtB
		A3St	8.9	MGDG	AtB/ breast cancer
		A4St	3.3	DGDG	AtB/ breast and lung cancer
		A5St	0.2	SQDG	AtB/ breast and lung cancer
	Phospholipid		9.2		-

2.3.5.2 Antimicrobial activity against human pathogenic bacteria

Antimicrobial activity of neutral lipid and glycolipid fractions were tested against a wide spectrum of human pathogenic bacteria and efficiency was evaluated according to the mean of the inhibition diameter of three replicates (Table IV-5). Generally, a moderate antimicrobial activity was observed against all bacteria. Highest inhibition zone (19.7 mm) was observed at 25.5 µg/mL on *B. subtilus* and was from a DGDG fraction (A4St) of *Staurosira* sp. Neither NL and GL fractions had an antibacterial activity superior to streptomycin standard antibacterial compounds. Inhibition zones did not increase in a dose depend manner for all tested bacteria.

Glycolipid DGDG fraction has the most antibacterial activity for all species on *B. subtilus* at a concentration of 25.5 µg/mL (A3Ep, A4Na, A4St).

Only moderate antibacterial activity was detected on *S.aureus* and *E. coli* and it was with a SQDG (A5St) and a DGDG (A4St) fraction from *Staurosira* sp. TAG (D2St) and Pigments (A1St) fractions from *Staurosira* sp. showed antibacterial activity on both gram positive bacterial strains (*B. subtilus* and *S. aureus*). These results suggest that the direct use of total lipid content can be interesting for antibacterial property. Antibacterial activity from *Nitschia* genus has already been reported by Kellam and Walker (1989) (Kellam and Walker, 1989). Our results are in accordance with this study in which antibacterial activity was detected on *S. aureus* and *B. subtilis* and no antibacterial activity was detected on *E. coli*. However, in Kellam and Walker, 1989 lipids were not fractionated in classes, antibacterial activity was evaluated on bacteria exposed directly with CLE.

E. coli has proved to be the least susceptible bacterium to inhibition by algal extract in many studies (Hornsey and Hide, 1974; Reichelt and Borowitzka, 1984).

It has already been reported that microalgal products such as pigments, phenols, terpene and/or indoles possesse a wide spectrum of biological activity (antifungal, antimicrobial, antiviral, antiprotozoa, antiplasmodial, anti-inflammatory or anti-oxidative) (Abedin and Taha, 2008; Bellou *et al*., 2014; Guedes *et al*., 2013; Pina-Pérez *et al*., 2017; Ulmann *et al*., 2017). Some microalgae like *Chlorella* or *Arthrospira* are used for their lipid production in cosmetics for skin products, hence some diatoms (*Cylindrotheca closterium*, *Chaetoceros* sp., *Odontella aurita*, *Stephanodiscus* sp.) producing carotenoids, phytosterols, vitamins or antioxidants (Bellou *et al*., 2014; Berthon *et al*., 2017; Mimouni *et al*., 2012). In the present study, TAG and GL antibacterial properties from *Staurosira* sp. were discovered, which comes to complete the knowledge of the action of lipophilic compounds other than lipids already well described in the litterature. An oil (CLE) containing hydrocarbons with lipophilic vitamins like carotenoids,

tocopherol and squalene, TAGs, phytosterol and polar lipids (GL and PL) can be intersting to produce active substances recoverable in cosmetics.

Tableau IV-5 Inhibition zone (mm) for antimicrobial activity of different species fraction obtained from different culture modes against three human pathogenic bacteria at 25.5 and 50 µg/mL and streptomycin (standard antibacterial treatment) n=3.

Species	Fraction	Quantity	*B. subtillus*	*S. aureus*	*E. coli*
E. paludosa	A2Ep	22.5	14±1	10.3±0.6	-
		50	13±0	12 ± 1	-
	A3Ep	22.5	**18.3 ± 1.5**	10 ± 1	-
		50	**14.7 ± 0.6**	12.7 ± 0.6	-
	A4Ep	22.5	13.3 ± 1.5	9.7 ± 0.6	12.7 ± 0.6
		50	14 ± 0	13.3 ± 0.6	11 ± 1
N. alexandrina	D1Na	22.5	13.7 ± 2.1	13.7 ± 1.2	8 ± 1
		50	**16.3 ± 1.5**	13.3 ± 1.2	8.3 ± 0.6
	A3Na	22.5	16.3 ± 1.5	10.7 ± 1.2	9.3 ± 1.2
		50	11.7 ± 0.6	11.3 ± 0.6	-
	A4Na	22.5	**17.3 ± 2.5**	9 ± 0	-
		50	**14.7 ± 0.6**	9.7 ± 0.6	-
	A5Na	22.5	10.3 ± 0.6	12 ± 0	10 ± 1
		50	10.3 ± 0.6	8 ±0	-
	A6Na	22.5	**16 ± 1.7**	9 ± 0	-
		50	13.3 ± 0.6	14 ± 0	11.7 ± 1.5
Staurosira sp.	D2St	22.5	14 ±2	12.3 ± 0.6	8.7 ± 0.6
		50	**15.7 ± 0.6**	**15 ± 0**	-
	A1St	22.5	**15 ± 1.7**	11.7 ± 0.6	9 ±0
		50	**15.7 ± 0.6**	13 ±1	-
	A2St	22.5	12.3 ± 0.6	10 ± 0	-
		50	11.7 ±0.6	11 ± 0	9 ± 0
	A3St	22.5	**15 ± 1**	12 ± 0	9 ±1
		50	**15 ±0**	11.7 ± 0.6	11 ± 1
	A4St	22.5	**19.7 ± 0.6**	13.3 ± 1.2	10 ± 1
		50	16.3 ± 1.2	14 ±1	**13.7 ± 1.5**
	A5St	22.5	13.7 ± 1.5	**14 ± 1**	-
		50	**16 ±0**	**14.7 ± 0.6**	-
Streptomycin		22.5	23.5 ±2.4	27.8 ±0.5	26.8 ± 1.7
		50	27 ± 0	26.8 ± 1	25.3 ± 0.5

2.3.5.3 Antiproliferative actitivity against breast cancer cell lines (MCF-7)

To evaluate potential anti-proliferative activity of the different fraction of glycolipids obtained for the three species studied, viability of the MCF-7 breast cancer cell line after treatment with MGDG, DGDG or SQDG was assessed using MTT assays. The dose level ranging from 50 to 100 µM.mL^{-1}.

For *E. Paludosa* MGDG (A2Ep), DGDG (A3Ep) and SQDG (A4Ep) fractions reduced cell viability (Figure IV-1). Significant reduction of cell viability of 42 ± 3%, 30±2%, 37.6±0.8% was observed for MGDG (A2Ep), DGDG (A3Ep) and SQDG (A4Ep) respectively at a concentration of 50 µg.mL^{-1}. Reduction of cell viability was more important when using a concentration of 100 µg.mL^{-1} (p<0.01) for the SQDG (A4Ep) fraction with a significant reduction of cell viability of 28.2 ± 0.3%. Conversely, reduction of MCF-7 cell viability was stronger when using a concentration of 50 µg.mL^{-1} of MGDG (A2Ep) fraction (p<0.001). No significant differences appeared, when cells were submitted to both concentrations, on cell viability for the DGDG (A3Ep) fraction (p=0.13).

For *N. alexandrina* only the DGDG (A3Na) fraction showed a significant reduction of cell viability on cancer cells at a concentration of 100 µg.mL^{-1} (Figure IV-1). Reduction of cell viability was stronger under 100 µg.mL^{-1} DGDG (A3Na) fraction exposure (p<0.001).

For *Staurosira* sp., the two fractions with the most activity on breast cancer cells were MGDG (A3St) and DGDG (A4St) fractions (Figure IV-1). For these two fractions reduction of cell viability was more important with a 100 µg.mL^{-1} concentration (p<0.001 and p<0.05). Maximum reduction of cell viability with DGDG fraction was 22.30 ±1.14% and 29.09 ±1.72% MGDG fraction.

The three tested fractions inducing cell viability under 25% was the DGDG fractions for the three species (A3Ep, A3Na and A4St).

Glycolipids fraction bioactivity can be associated with the presence of EPA as biologically active fatty acid. Nappo *et al*. (2012) found an antiproliferative activity from *Cocconeis scutellum* EPA fraction on breast carcinoma (BT20) however active concentration was not specified (Nappo *et al*., 2012). The authors concluded that it is not yet clear whether EPA is the only factor involved in the apoptosis of BT20 cells of if there is a synergic association among different compounds in the same fraction. Antiproliferative activity from *Chaetceros calcitrans* EtOH extract has been reported by Nigjeh *et al*. (2013) on the MCF-7 breast cancer cell line with a concentration of 3.0 µg.mL^{-1} (Nigjeh *et al*., 2013). However, composition of the EtOH extract is no precised in this study. To our knowledge these two diatoms are the only ones tested for antiproliferative activity on breast cancer cell lines (Martínez Andrade *et al*., 2018).

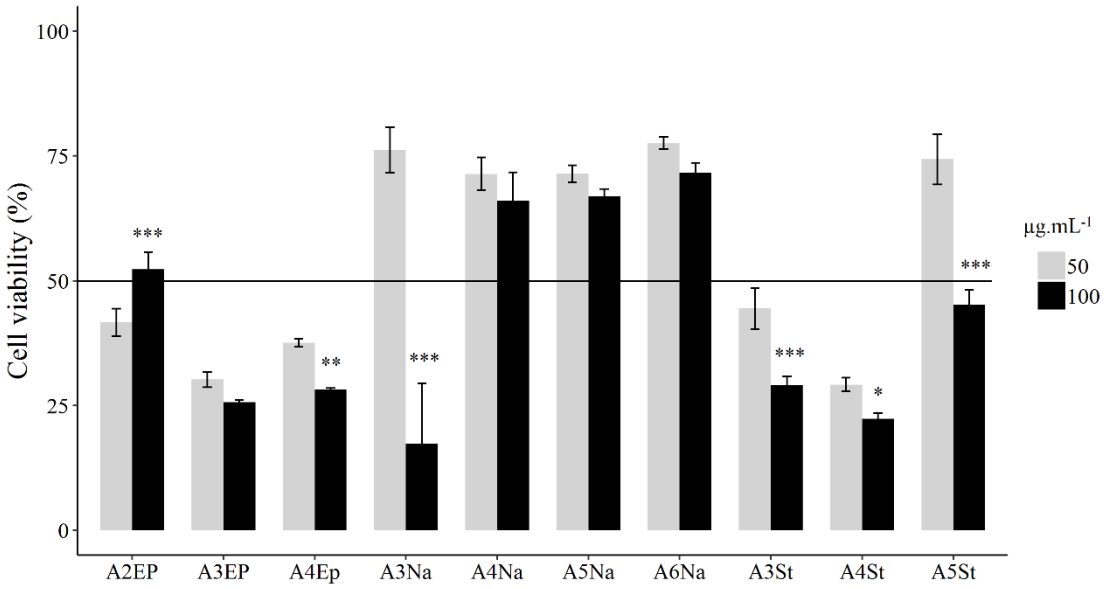

Figure IV-1 MCF-7 breast cancer cell viability evaluation on cells treated with fractions obtained from the three species under two concentrations: 50 µg.mL^{-1} and 100 µg.mL^{-1} during 72 h. (n=3).* $p<0.05$;** $p<0.01$;*** $p<0.001$.

2.3.5.4 Antiproliferative activity against Lung cancer cell lines

To evaluate potential anti-proliferative activity of the different fractions of glycolipids obtained for the three species studied, viability of NSCLC-N6 and A549 lung cancer cell lines after treatment with MGDG, DGDG or SQDG was assessed using MTT assays (Figure IV-2).

For *E. Paludosa*, DGDG (A3Ep) and SQDG (A4Ep) fractions showed a significant activity on NSCLC-N6 cells with IC_{50} = 26 ± 2 µg.mL^{-1} and 17.8 ± 0 µg.mL^{-1} for DGDG and SQDG fractions respectively. For *N. alexandrina*, the DGDG (A4Na) fraction showed a significant activity on NSCLC-N6 and A549 cells with IC_{50} = 15 ± 2 µg.mL^{-1} and 8 ± 0.1 µg.mL^{-1} respectively. The DGDG (A5Na) fraction from *N. alexandrina* showed a significant activity on NSCLC-N6 cells with IC_{50} = 17 ± 2 µg.mL^{-1}. TAG and glycolipid fractions obtained from *Staurosira* sp. showed no potential antiproliferative activity on both lung cancer cell lines.

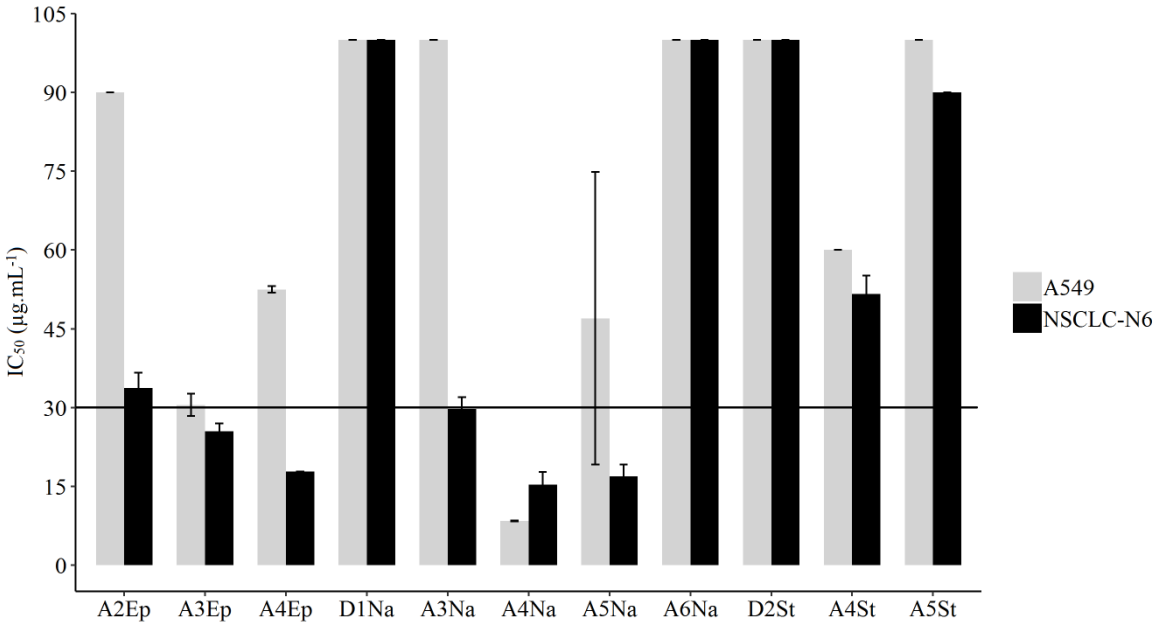

Figure IV-2 Cytostatic activity of the different fractions from the three studied diatoms to lung cancer cell lines NSCLC-N6 and A549. IC_{50} is the concentration of fraction required to reduce the cancer cell concentration by 50% compared to untreated controls after 72 h (n=3).

Polyunsaturated aldehydes (PUAs) from three diatoms (*Thalassiosira rotula*, *Skeletonema costatum* and *Pseudonitzschia delicatissima*) have been reported to possesse antiproliferative activity against the A549 lung cancer cell line at a concentration of 11 to 17

µg.mL^{-1} (Sansone *et al*., 2014). Aqueous extract from *Chlorella sorokiniana* possessed an antiproliferative activity against A549 and CL1-5 lung adenocarcinoma with a concentration of 0.016 to 1 µg.mL^{-1} (Lin *et al*., 2017). To our knowledge these diatoms are the only ones tested on lung cancer cell lines. In the literature, only *Haslea ostrearia* haslene aqueous extract (3.8 to 14.4 µg.mL^{-1}) exhibit in vitro and in vivo activities against the NSCLC-N6 human lung cancer cell line (Rowland *et al*., 2001). Currently, only aqueous extracts from diatoms have been tested for antiproliferative activity. The GL fraction from diatoms was tested for potential antiproliferative activity on lung cancer cell lines for the first time. Our study demonstrated the potential antiproliferative activity of the GL fraction on the NSCLC-N6 cell line. This particular GL property had already been described by Kendel *et al*. (2013) (Kendel *et al*., 2013). In this study, GL were extracted from *Ulva armoricana* (Chlorophyta) and *Soliera chordalis* (Rhodophyta). The MGDG fraction isolated from *S. chordalis* showed an antiproliferative effect on the NSCLC-N6 lung cancer cell line with an IC_{50} of 23 µg.mL^{-1}. The DGDG fraction isolated from *U. amoricana* showed an antiproliferative effet on the NSCLC-N6 cell line with an IC_{50} of 24 µg.mL^{-1}. Even if these compounds were extracted from two macroalgae it is possible that the same structural molecules can be found in the GL fraction from diatoms. Our study confirms the potential bioactivity of GL on lung cancer cells.

In many macroalgae or microalgae, biological activity from MGDG exhibit anti-tumor effects, and from SQDG as well (C.-J. Tsai and Sun Pan, 2012). In the freshwater green alga *Chlorella vulgaris* MGDG and DGDG showed high anti-tumor promoting effects on human lymphoblastoid *in vitro* without showing any cytotoxicity (T. Morimoto *et al*., 1995).

SQDG exhibits also high biological activity (T. Morimoto *et al*., 1993), antitumor activity (T. Morimoto *et al*., 1995; Murakami *et al*., 2003b), and protection against cell death (Matsufuji *et al*., 2000; Murakami *et al*., 2003b), inhibitory activities against DNA polymerase (Hanashima *et al*., 2000; Murakami *et al*., 2002; Ohta *et al*., 2000, 1999, 1998), telomerase (Eitsuka *et al*.,

2004), angiogenesis (Matsubara *et al*., 2005). Also, recently characterised novel galactoglycerolipids have anti-microbial activity (A. Al-Fadhli *et al*., 2006).

2.4 Materials and Methods

2.4.1 Diatoms cultures

Entomoneis paludosa NCC18.2, *Nitzschia alexandrina* NCC33 and *Staurosira* sp. NCC182 were obtained from the Nantes Culture Collection (NCC). These strains were grown in 1L Airlift PBR and in 25L Flasks. Diatom strains were grown at 16°C under a photon flux density (PFD) of 127 µmol.photons.m^{-2}.s^{-1} in both conditions. Medium was a modified F/2, natural seawater filter sterilized and enriched with nutrients. F/2 medium used in Flasks and Airlift are presented in Table IV-6. Flasks were filled with 17 L culture medium and were sterilized by autoclave (20 min, 121 °C), salinity was adjusted at 28, pH was fixed to 7.8 to reduce nutrient precipitation. For 1 L airlift cultures, medium was agitated by a sterile airflow. pH was fixed to 7.8 with a CO_2 influx. Medium used in airlift was filter sterilized (0.2 µm) and salinity was adjusted at 28. Inoculation was performed at a concentration dependent on the starter (1L for the Flask and 250 mL for airlift).

Tableau IV-6 Airlift PBR and flask medium composition

Element		Final concentration $g.m^{-3}$	
		Flask	Airlift
Bicarbonate	$NaHCO_3$	80	*
Nitrate	$NaNO_3$	75	750
Phosphate	NaH_2PO_4	5	170
Metal	Na_2EDTA**	4.36	5.06
	$FeCl_3,6H_2O$	3.15	3.15
	$MnCl_2,4H_2O$	0.18	0.18
	$ZnSO_4$	0.022	0.010
	$CoCl_2,6\ H_2O$	0.010	0.010
	$CuSO_4,5\ H_2O$	0.010	0.010
	$Na_2MoO4,\ 2\ H_2O$	63×10^{-4}	63×10^{-4}
Silica	$Na_2SiO_3,\ 9\ H_2O$	30	*
Vitamin	Thiamine	0.1	0.1
	Cyanocobalamine	5×10^{-4}	5×10^{-4}
	Biotine	5×10^{-4}	5×10^{-4}

* Feed batch were conducted every day with 21 mg of silica (Na_2SiO_3, $5H_2O$) and 200 mg of bicarbonate ($NaHCO_3$).

** EDTA: Ethylenediaminetetraacetic acid

2.4.2 Biomass, lipid extraction and separation of lipid classes

2.4.2.1 Dry weight

When the end of the exponential phase occurred, cultures were harvested and filtered on previously weighted Whatman GF/F, 47 mm diameter, 0.7 µM pore filters. Filters containing cells were washed using 10 mL ammonium formiate (68 $g.L^{-1}$) to remove salt. Wet filters were frozen at –80 °C, freeze-dried under vacuum during 24 H and weighted to estimate the DW (in $g.L^{-1}$).

2.4.2.2 Lipids

Total lipid rate was assessed by gravimetric assay. Biomass filtered, washed and freeze-dried for dried weight estimation were used for lipid content estimation. The filters were macerated in flasks using 100 mL of solvent per gram of biomass (dichloromethane-methanol (1:1 v/v)) (Bligh and Dyer, 1959). Maceration at ambient temperature was performed for 24 H on a vibrating tray (Edmund Bühler GmbH, SM-30). After maceration, the mixture was filtered on

pleated 190 mm diameter, 10 µm pore filters, to remove the filter debris and the silica fragments. The filtrates were then extracted by adding 40% of the volume in a KCl 0.9% solution in a separatory funnel. The organic phase was combined, dried over anhydrous sodium sulfate and then evaporated to obtain the CLE. Total lipid rate was evaluated following equation 1:

$$TL = \frac{CLE}{DW} \times 100 \qquad \text{Eq (1)}$$

2.4.3 Lipids analyses

2.4.3.1 Fractionation in lipid classes

Lipid classes were separated on open silica gel column chromatography, column size and amount of silica used depending on CLE mass to be fractionated (1g of CLE for 20 g of silica). Lipids were eluted using CH_2Cl_2 for NL, acetone for GL and MeOH for PL as successive mobile phases (Figure IV-3). Fractions were used to assess antibacterial activity and antiproliferative activity on breast and lung cancer cell lines respectively.

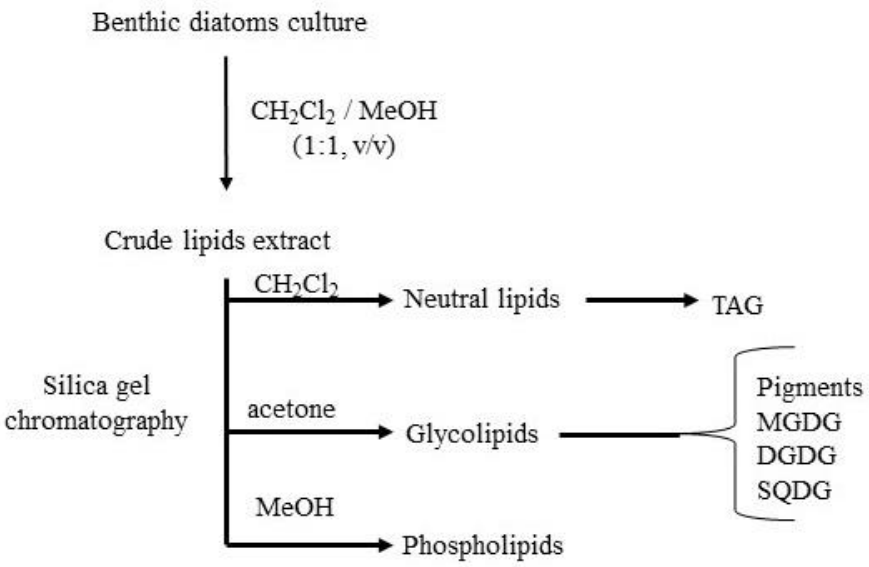

Figure IV-3 Schematic outline of the experimental protocol for lipid classes assessment

2.4.3.2 Fatty acid and sterol analyses

Fatty acids and unsaponifiable fractions (sterols, hydrocarbons…) have been analyzed as described before (Kendel *et al*., 2013). Briefly, unsaponifiable matter was acetylated using acetic anhydride and pyridine, giving a mixture containing sterol acetates. Free fatty acids (FFA) were obtained after saponification with 2 M ethanolic potassium hydroxide (1.5 H at 80 °C under reflux) of CLE or after hydrochloric methanolysis (1.5 H at 80 °C under reflux in a MeOH/distilled water/concentrated hydrochloric acid 29:4:3, v/v/v) for GL. Fatty acid methyl esters (FAME) were obtained by methylation of FFA (40 min at 80 °C, under reflux in 6% hydrochloric MeOH). FAME were then converted into *N*-Acyl pyrrolidides (NAP) (60 min at 80 °C under reflux in a pyrrolidine/acetic acid mixture 5:1 v/v). FAME and NAP, free and acetylated sterols were then analyzed by gas chromatography coupled with mass spectrometry (GC-MS).

2.4.3.3 Gas Chromatography-Mass Spectrometry Analysis (GC-MS)

Samples (1 mg.mL^{-1} in CH_2Cl_2) were analyzed by GC-MS, Hewlett Packard HP 7890-GC system/HP 5975C – 70 ev) equipped with an HP-5^{MS} column (30 m × 0.25 mm × 0.25 µm, Sigma-Aldrich). Injector and detector temperatures were set at 250 and 280 °C, respectively. Helium carrier gas had a flow rate of 1 mL/min. For FAME analyses, temperature of the oven was programmed at 170°C (4 min), then 3 °C/min up to 300°C for 10 min (cycle = 57.33 min); for NAP, at 200 °C (4 min), then 3 °C/min up to 310°C for 20 min (cycle = 60.67 min); for sterols and sterols acetate, at 200 °C (4 min) then 3 °C/min up to 310°C, for 25 min (cycle=61.67 min). Injected volume was 1 µL in splitless mode and the solvent delay was 4 min. To identify and quantify the FAMEs, sterols and sterols acetate, identifications were confirmed by comparing mass spectra and retention data with those previously reported and with those obtained from commercial standards. NAP analyses made it possible to position the double bonds in addition to the FAMEs results. Chromatogram peak areas were analyzed and quantified using WSEARCH32 software.

2.4.4 Antibacterial activity against human pathogens

The strains used to evaluate the antimicrobial activity were obtained the American Type Culture Collection (ATCC). Gram-positive bacteria were *Staphylococcus aureus* (ATCC 25923) and *Bacillus subtillus* (CIP 104717). Gram-negative bacteria were *Escherichia coli* (ATCC 10536). The technique used for the evaluation of the antibacterial activity of the various extracts was that of diffusion in an agar medium, using 6 mm diameter cellulose disks, according to the technique described by Bauer *et al.* (1966). The extracts that were tested were dissolved in a minimum volume of solvent (dichloromethane) and cellulose disks were imbibed with different concentrations. After solvent evaporation, the disks were placed on the surface of a Petri dish previously seeded with 5mL of bacteria suspension (0.2 × 10^4 bacteria/mL) and placed at 37 °C for 24 h. Two different concentrations 25.5 and 50 µg/mL were tested. Disks

with the standard Streptomycin at same concentrations were used as control. The results were obtained by measuring the diameter of the inhibition zone for each disk and expressed in millimeters. The antibacterial effectiveness of the extracts was evaluated according to the following scale: Ø ≤ 8 mm: Non-significant antibacterial activity, 8 < Ø ≤ 12 mm: Moderate antibacterial activity, 12 < Ø ≤ 14 mm: Significant antibacterial activity, Ø > 14 mm: Very important antibacterial activity.

2.4.5 MTT Cell viability assay

The MTT test is widely used as a rapid and sensitive method for screening anticancer drugs as well as for the evaluation of the cytotoxicity of new molecules. The main advantages of the MTT test are its simplicity, speed and automatic reading results with a microplate spectrophotometer. The yellow reagent used is tetrazolium salt MTT (3- (4,5-dimethylthiazol-2-yl) -2,5-diphenyl bromide tetrazolium, ref Sigma M5655-16) which is reduced by succinate dehydrogenase mitochondrial active living cells, in formazan, a purple precipitate. The amount of precipitate formed is proportional to the amount of living cells (but also to the metabolic activity of each cell). These formazan crystals are then dissolved in isopropanol for lung cells and in DMSO for breast cancer cells.

Human breast cancer MCF-7 cells were purchased from the European Collection of Animal Cell Cultures (ECACC, Salisbury, UK). 3-(4,5-Dimethyl-2-thiazolyl)-2,5-diphenyltetrazolium bromide (MTT) and phorbol 12-myristate 13-acetate (PMA), were purchased from Sigma Aldrich (Saint Quentin Fallavier, France). 7-Aminoactinomycin D (7-AAD) was obtained from BD Biosciences (San Jose, CA, USA). Uptilight US Blot HRP substrate was from Interchim (Montlucon, France). All other reagents were purchased from Sigma Aldrich. MCF-7 cells were cultured at 37 °C in a humidified incubator with 5% CO_2 in DMEM medium supplemented with 0.1% fetal bovine serum (FBS) and 1%

penicillin/streptomycin. Viability of MCF-7 was tested in 96-well plate at density 10^4 cells per well in 200 µL of culture medium and allowed to adhere overnight. Then the seeding medium was removed and cells were treated with fractions at 50 µM and 100 µM diluted in 0.1% BSA containing medium for 72 h. For the MTT assay, 50 µL MTT (at 2.5 mg/mL) was added to each well. The mixture was further incubated for 4 h at 37 °C and the liquid in the wells was removed thereafter. Dimethyl sulfoxide (DMSO 200 µL) was then added to each well to solubilize the formazan product and the absorbance was read at 570 nm using a Spectra MAX 190 spectrophotometer, Molecular Devices. The relative cell viability was expressed as a percentage of the control that was not treated with fractions.

2.4.6 Antiproliferative activity against human lung cancer cells

The antiproliferative activity of TAG and GL fractions obtained from the three species studied was evaluated. The NSCLC-N6 (Roussakis *et al*., 1991) lung cancer cell line derived from a human non-small-cell bronchopulmonary carcinoma (moderately differentiated, rarely keratinized, classified as T2N0M0) and the A549 cell line was obtained from ATCC collection reference CCL-185 from National Cancer Institute bank lines (NCI) were used for all experiments. Both cell lines were cultured in RPMI 1640 medium with 5% fetal calf serum, to which were added 100 IU penicillin.mL^{-1}, 100 µg streptomycin.mL^{-1} and 2 mM glutamine at 37 °C in an air/carbon dioxide athmosphere (95:5, v/v). Cytotoxicity was determined by continuous drug exposure. Experiments were performed in 96 well microtiter plates (10^5 cell.mL-1 for NSCLC-N6 and 2×10^4 cell.mL^{-1} for A549). Cell growth was estimated by a colorimetric assay based on the conservation of tetrazolium dye (MTT) to a blue formazan product by living mitochondria (Mosmann, 1983). The procedure were repeated eight times for each concentration. Control growth was estimated from 8 determinations. Optical density at 570 nm corresponding to solubilized formazan was read for each well on Titertek MultisKan MKII.

2.5 Conclusion

Bioactive compounds from marine benthic diatoms have been poorly investigated. Most studies have been done on microalgal extracts or fractions obtained using low resolution methods such as liquid-liquid partitioning or solid phase extractions. This study confirms previous results that showed the interest of GL fractions as potential usefully therapeutic agents (Lauritano *et al*., 2016). Here we analyzed the cytotoxicity of GL fractions from three original marine diatoms species. DGDG fractions from *E. paludosa*, *N. alexandrina* and *Staurosira* sp. showed potential antibacterial activity on gram positive bacteria *B. subtilus*. TAG, pigments and GL fractions from *Staurosira* sp. showed potential antibacterial activity on *B. subtilus* suggesting the direct use of CLE as antibacterial agent. DGDG fraction from *E. paludosa* and *Staurosira* sp. showed potential antiproliferative activity against the MCF-7 breast cancer cell line. MGDG, DGDG and the SQDG fraction from *E. paludosa* and DGDG fraction from *N. alexandrina* showed potential antiproliferative activity against the NSCLC-N6 lung cancer cell line. However, despite the total elucidation of these biological activities their structure and diversity are far for being fully recognized which prevents the full exploitation of the biotechnological potential of these diatoms. In order to establish the glycolipidomic profile, it is necessary to obtain qualitative and quantitative informations on the numerous molecular species present in each MGDG, DGDG and SQDG fractions. Nuclear Magnetic Resonance methods (Da Costa *et al*., 2016) or modern mass spectrometry technologies provide access to the structural characterization of glycolipids (Yao *et al*., 2015) and will be applied soon to all the tested fractions.

Acknowledgments:

This work was supported by the regional Atlantic Microalgae research program (AMI), and funded by the Pays de la Loire region.

Conflicts of Interest: The authors declare no conflict of interest.

Author Contributions: E.C. as Ph. D. student was implicated in all experimental stages including diatom collection, sample preparation and data exploitation. G.W.C. supervised result exploitation. F.L and S.E conducted antibacterial experiements. L.O and E.H.N conducted bioactivity tests on the MCF-7 lung cancer cell line. C.R conducted bioactivity experiments on NSCLC-N6 and A549 lung cancer cell lines. E.C and E.S contributed in lipid extractions, lipid class separations and chemical derivatizations, and performed the GC/MS analyses. A.C.M conducted the data exploitation of the mass analysis. G.W.C., O.G. and V.M. initiated and conducted the research project and they have been supervisors of E.C thesis work. They were responsible for writing, arranging and checking the manuscript. All authors read and approved the final manuscript.

3 Conclusion

Les tests de bioactivités menés dans cette étude montrent que les trois espèces sélectionnées précédemment possèdent des activités antibactériennes et/ou antiprolifératives. En effet, les fractions DGDG extraites de la souche *Staurosira* sp. possèdent une action antibactérienne contre une bactérie à gram positif (*B. subtilus*). L'ensemble des fractions glycolipidiques extraites de la souche *E. paludosa* présentent des activités antiprolifératives contre la lignée MCF-7 du cancer du sein ainsi que la fraction DGDG extraite de la souche *N. alexandrina*. Les fractions MGDG et DGDG de *Staurosira* sp. possédent également une activité antiproliférative sur cette lignée cancereuse. Une activité antiproliférative sur les cellules de la lignée NSCLC-N6 du cancer du poumon a également été découverte sur les fraction DGDG et SQDG provenant de *N. alexandrina* et *E. paludosa* respectivement.

Cependant, malgré les propriétés bioactives intéressantes des GL, leur structure et leur diversité sont loin d'être entièrement connues, ce qui empêche la pleine exploitation du potentiel biotechnologique de ces microalgues. Afin de pouvoir identifier précisément la structure de la molécule possédant une bioactivité potentielle des analyses complémentaires sont nécessaires. Afin d'établir le profil glycolipidomique de ces diatomées, il est nécessaire d'obtenir des informations qualitatives et quantitatives sur les nombreuses espèces moléculaires présentes dans chacune des classes MGDG, DGDG et SQDG. Les méthodes de spectroscopie par résonnance magnétique (RMN) (Da Costa *et al*., 2016) ou les technologies modernes en spectrométrie de masse permettent d'accéder à la caractérisation structurelle des glycolipides (Yao *et al*., 2015) et seront appliquées prochainement sur l'ensemble des fractions testées.

Le fort potentiel bioactif des souches de diatomées marines benthiques ayant été identifié dans ce chapitre, il a semblé important de caractériser les conditions de cultures favorisant leur production lipidique, mais surtout favorisant la composition lipidique vers des classes à fortes

valeurs ajoutées et/ou fortement bioactives. Cette caractérisation fait l'objet du prochain chapitre.

V- Etude de l'effet de l'intensité lumineuse et de la limitation en azote sur les capacités photosynthétiques et la production lipidique chez *E. paludosa*, *N. alexandrina* et *Staurosira* sp.

Chapitre V – Etude de l'effet des conditions de culture sur les capacités photosynthétiques et la production lipidique

1 Contexte de l'étude

Les conditions de cultures ont un rôle important dans la composition moléculaire des microalgues. En effet, des études récentes ont montré que la quantité et la qualité des lipides produits peuvent varier en fonction des modifications des conditions de cultures (concentration en nutriments, température et intensité lumineuse)(Gao *et al*., 2013; Huete-Ortega *et al*., 2018; Schaub *et al*., 2017) . Par exemple, lorsque l'espèce *Botryococcus braunii* est soumise à un stress nutritif et/ou photo-oxydant le taux de lipides peut augmenter jusqu'à 40 % du poids sec (Chisti, 2007b; Ruangsomboon, 2012). De la même façon, les espèces de diatomées comme *Phaeodactylum tricornutum*, *Chaetoceros muelleri* and *Navicula saprophila* subissant une limitation en nutriment modifient leur composition cellulaire ; la limitation en azote peut entraîner une diminution de la teneur en protéines et une augmentation relative du stockage des glucides et/ ou des lipides (Chelf, 1990; McGinnis *et al*., 1997; Mus *et al*., 2013; Yang *et al*., 2013). La limitation en azote peut également entraîner une diminution du taux de croissance et de l'efficacité photosynthétique. L'intensité lumineuse a laquelle sont soumise les cultures peut également affecter la production primaire, les protéines et d'autres fonctions cellulaires. Afin de déterminer les conditions de cultures favorisant la production de lipides d'intérêt, les trois espèces utilisées dans le chapitre précédant ont été soumises à différentes intensités lumineuses : 30 µmol photons.m^{-2}.s^{-1} (LL) ; 100 µmol photons.m^{-2}.s^{-1} (ML) and 400 µmol photons.m^{-2}.s^{-1} (HL) et différentes concentrations d'azote 882 µM (N+) and 88,2 µM (N-). Les effets de ces conditions de cultures ont été évalués sur leur taux de croissance, leur capacité photosynthétique et leur accumulation de lipides intracellulaires ainsi que la composition de la fraction lipidique. L'objectif principal de cette étude est d'obtenir une teneur élevée en lipides et principalement en acides gras originaux tout en maintenant un bon état physiologique. Les résultats de cette étude font l'objet d'un article soumis à la revue PLOS One présenté ci-dessous.

2 Lipid prodcution and fatty acid quality impacted by photosynthetic efficiency of three original benthic diatoms strains selected for biotechnology applications

Lipid production and fatty acid quality impacted by photosynthetic efficiency of three original benthic diatom strains selected for biotechnology applications.

Eva Cointet[1, *], Gaëtane Wielgosz-Collin[1], Gaël Bougaran[2], Vony Rabesaotra[1], Olivier Gonçalves [3], Vona Méléder[1]

[1] Université de Nantes, Laboratoire Mer Molécules Santé, EA 21 60, BP 92208, 44322 Nantes, France

[2] PBA-IFREMER, rue de l'Ile d'Yeu, BP 21105, 44311, Nantes cedex 03, France

[3] Université de Nantes, GEPEA, UMR CNRS-6144, Bât.CRTT, 37 Boulevard de l'Université, BP406, F-44602 Saint-Nazaire Cedex, France

2.1 Abstract

Microalgae biotechnology has gained considerable importance in recent decades. Applications range from simple biomass production for food and feed to valuable products for fuel, pharmaceuticals, health, biomolecules and materials relevant to nanotechnology. However, literature on microalgae high value compounds reveals little exploration of the wider microalgae biodiversity because of a perception that there is little to be gained in terms of biomass productivity by examining new strains. However, without diversity, biotechnology applications are currently limited for innovation. Using microalgae diversity is a very promising way to match species and processes for a specific biotechnology application. In this framework, three benthic marine diatom strains (*Entomoneis paludosa* NCC18.2, *Nitzschia alexandrina* NCC33 and *Staurosira* sp NCC182) were selected for their lipid production and growth capacities. Using PAM fluorometry and FTIR spectroscopy, this study investigated the impact of nitrogen repletion and depletion as well as light intensity (30, 100, 400 µmol.photons.m^{-2}.s^{-1}) on their growth, photosynthetic performance and macromolecular content, with the aim to

increase the quality of their lipid composition. Results suggest that under HL and nitrogen limitation, photosynthetic machinery is negatively impacted leading cells to reduce their growth and accumulate lipids and/or carbohydrates. However, increasing lipid content under stressful conditions does not imply increase in the production of lipids of interest : PUFA, ARA and EPA production decreases. Culture conditions to optimize production of such fatty acids for these three original strains lead to an adequacy between economical and ecophysiological constraints: low light and no nitrogen limitation.

Keywords: Benthic diatoms, nutrient limitation, FTIR spectroscopy, PAM fluorometry, lipids.

Abbreviation:

ARA:	Arachidonic acid
CAR:	Carotenoids
Chl *a*:	Chlorophyll a
Cj:	Conjugated
CLE:	Crude lipid extract
DW:	Dry weight
Eb:	Ester bond
Ek:	Photoacclimation parameter
EPA:	Eicosapentaenoic acid
FA:	Fatty acid
FAME:	Fatty acid methyl ester
Fv/Fm:	Maximum quantum efficiency
HL:	High light
HTSXT-FTIR:	Fourrier-transform infrared spectroscopy high-throughput screening extension
LL:	Low light
LP:	Lipid productivity
LR:	Lipid rate
ML:	Middle light
MUFA:	Monounsaturated fatty acid
ND:	Not detected
PAM:	Pulse amplitude modulated
PSII:	Photosystem II
PUFA:	Polyunsaturated fatty acid
rETR:	Relative electron transport rate
RLC:	Rapid light curve
SFA:	Saturated fatty acid
TAG:	Triacylglycerol
μ:	Specific growth rate
UFA:	Unsaturated fatty acid

2.2 Introduction

The attention in the production of microalgae for biofuels, feedstock and for added value compounds is increasing; several thousand species of microalgae, including diatoms have now been screened for lipid production (Cointet *et al*., 2019; d'Ippolito *et al*., 2015; Doan *et al*., 2011; Dunstan *et al*., 1993; Joseph *et al*., 2017; Renaud *et al*., 1999; Volkman *et al*., 1989; F. Zhao *et al*., 2016). It is essential to identify suitable strains of microalgae for mass cultivation and improve the lipids content. Previous studies have shown that the quantity and quality of lipids can vary as the result of changes in growth condition i.e., nutrient concentrations (Gao *et al*., 2013; Huete-Ortega *et al*., 2018; Mortensen *et al*., 1988; Roessler, 1988; Shifrin and Chisholm, 1981; Wichien Yongmanitchai and Ward, 1991), temperature (Dempster and Sommerfeld, 1998; Schaub *et al*., 2017; Sriharan and Sriharan, 1990) and light intensity (Brown *et al*., 1996; Huete-Ortega *et al*., 2018; Mortensen *et al*., 1988; Schaub *et al*., 2017; Shifrin and Chisholm, 1981). It has been found that oil levels of 20-50% of dry weight are quite common in microalgae, though this varies from species to species, and can reach up to 90% of dry mass when cells are subject to physiological stress conditions or unfavorable environment, such as nutrient limitation or photo-oxidative stress (Spolaore *et al*., 2006). Furthermore, nutrient stress, e.g., nitrogen deprivation, phosphorus starvation and iron supplementation can enhance the lipid content in many microalgae species (Bondioli *et al*., 2012; Converti *et al*., 2009; Liu *et al*., 2008; Roleda *et al*., 2013). Nitrogen limitation or deprivation is a strategy widely used to elicit this response. Lipids biosynthesis varies within the different diatom species, their growth stage and the environments parameters (Chen, 2012; Chuecas and Riley, 1969).

Nutrient availability is of considerable importance to the growth and primary production in microalgae. For diatoms, typical nutrient limitation in nature include nitrogen, phosphorus, and silicate (Berges *et al*., 1996). Diatom cells undergoing nutrient limitation change their cellular composition; nitrogen limitation can lead to a decrease in protein content and a relative increase

in carbohydrate and/or lipid storage (Giordano *et al*., 2001; Hildebrand *et al*., 2012). Nitrogen limitation can also result in a decrease in growth rate and photosynthetic efficiency (Berges *et al*., 1996; Berges and Falkowski, 1998; Geider *et al*., 1993; Parkhill *et al*., 2001). The biochemical changes measured in microalgae are linked with the changes of physiological parameters and are known to be species-specific. Photosynthetically active radiation can also affect primary production, protein synthesis and other cellular functions (Brown *et al*., 1996; Quigg and Beardall, 2003; Vassiliev *et al*., 1994).

In the selection of the most adequate species or strains for bioactive lipid production, many parameters should be considered, such as the ability of microalgae to grow in a wide range of environmental conditions. In this study, three benthic marine diatom species: *Entomoneis paludosa* NCC18.2, *Nitzschia alexandrina* NCC33 and *Staurosira* sp. NCC182, never studied before excepted by Cointet *et al*, (2019) (Cointet *et al*., 2019), were selected for their high growth capacity, high lipid productivity and/or capacity to produce interesting molecular compounds. They are studied here to characterize their photosynthetic capacity and enhanced their lipid productivity. Different light conditions were applied: 30 µmol photons.m^{-2}.s^{-1} (LL) ; 100 µmol photons.m^{-2}.s^{-1} (ML) and 400 µmol photons.m^{-2}.s^{-1} (HL) in combination with different nitrogen concentrations : 882 µM (N+) and 88,2 µM (N-). The aim of this study is to determine the effects of changing nitrogen concentration and light condition on their growth rate, photosynthetic capacity and intracellular lipid accumulation. Cell composition and lipid production are evaluated using Fourier transform infrared spectroscopy (FTIR) analysis performed on whole cell samples and lipid extracted samples respectively. It is well established that the change in macronutrients in the environments will results in the change of cellular macromolecular composition (Dean *et al*., 2010; Giordano *et al*., 2001). FTIR offers the potential to measure the macromolecular composition (proteins, lipids and carbohydrates) simultaneously in the single sample (Beardall *et al*., 2001a). This method requires low biomass,

is very sensitive and rapid. Pulse amplitude modulated (PAM) fluorometry is a valuable tool to detect physiological stress and photosynthetic efficiency both in terrestrial plants (Juneau *et al*., 2005) and microalgae (Baker, 2008; White *et al*., 2011). General PAM parameters include maximum quantum efficiency (Fv/Fm), alpha (α), relative electron transport rate (rETR) and light saturation (Ek). Fv/Fm is used to estimate physiological stress and the Fv/Fm value phytoplankton in non-stressed conditions ranges from 0.6 to 0.7. Also Fv/Fm value decreased in nutrient stressed cultures, and is relatively constant in non-stressed culture (White *et al*., 2011). The parameter α is the initial slope of the light curve and reflects the utilization efficiency of light energy. The rETR is the electron transport rate, which is related to the overall photosynthetic performance of the diatoms (Juneau *et al*., 2005). Ek is a measure of the onset of light saturation and can be calculated by the ratio betwenn rETRmax and α. In this study, strains photosynthetic performances are assessed by evaluating Fv/Fm and Ek parameters. The main goal of this study is to achieved a high lipid content while maintaining a good physiological state with a lower financial cost. To ensure good lipid quality, lipid extracts were finally transesterified to highlight fatty acid (FA) composition.

2.3 Materials and Methods

2.3.1 Diatom cultures and experimental design

The three strains, *Entomoneis paludosa* NCC18.2, *Nitzschia alexandrina* NCC33 and *Staurosira* sp. NCC182 were obtained from the Nantes Culture Collection (NCC). Each strain was grown using artificial seawater medium (Sunda and Huntsman, 2004) enriched with F/2 medium major nutrients. This artificial medium allowed to control initial nutrient and other element amounts (Table V-1), avoiding natural composition variability of natural sea-water (Sunda and Huntsman, 2004). Two different media were used for experimentation: N+ and N- with respective initial $NaNO_3$ amounts : 882 µM and 88.2 µM (Table V-1). Before inoculation, medium was sterilized by filtration (0.2 µm) to avoid nutrient precipitation often occurring with

autoclaving. Culture stocks were acclimated and maintained in 250 mL erlenflasks filled with 150 mL medium N+ under different light conditions (30 – 100 – 400 µmol photons m^{-2} s^{-1}) respectively low, medium and high light (LL, ML and HL) during 5 weeks. A light dark cycle was applied (14-10H), and temperature maintained at 16°C. To prevent pH augmentation due to diatom growth (Dubinsky and Rotem, 1974), cultures were gently bubbled with continuous sterile filtered air (Sartorius, 0.2 µm PTFE) and aseptic glass delivery tube by air compressor.

Table V-1 Artificial seawater medium composition

Elements		Final concentration (µM)
Anhydrous salt	NaCl	336×10^3
	Na_2SO_4	28.8×10^3
	KCl	9.3×10^3
	$NaHCO_3$	3.3×10^3
	KBr	840
	H_3BO_3	48.5
	NaF	71.5
Hydrous salt	$MgCl_2.6H_2O$	54.6×10^3
	$CaCl_2.2H_2O$	10.5×10^3
	$SrCl_2.6H_2O$	63.8
Major nutrients	$NaH_2PO_4.H_2O$	36.2
	$NaNO_3$	882 (N+) or 88.2 (N-)
	$Na_2SiO_3.9H_2O$	106
	Trace metal solution (F/2)	1 mL
	Vitamin solution (F/2)	1 mL

To start experimentation, inoculation of fresh medium was done using cells from stock cultures centrifuged (5 min at 3500 *g*) and washed with N- artificial seawater medium to avoid salt concentration. Initial concentration of cells was fixed at 30.000 cells.mL^{-1} in 150 mL sterilized medium for both media: 88,2 µM (N-) or 882 µM (N+), and cultures were exposed to the three light conditions: LL, ML and HL. Samples were collected daily for growth rate estimation by cell counting until reaching stationary growth phase. During exponential growth phase, photosynthetic parameters of strains (the maximum PSII quantum efficiency, Fv/Fm and the light saturation parameter Ek) were estimated using PAM-fluorometery (Ralph and Gademann, 2005). Thus the culture volume to harvest 10^7 cells were sampled and centrifuged (10 min at 4500 *g*) for biochemical composition determination: pigment composition by

spectrophotometry (Ritchie, 2006) and protein, carbohydrate and lipid composition by HTSXT-FTIR (Cointet *et al*., 2019). Total amounts of cells in culture were harvested by filtration (0.7 µm) to estimate DW and proceed to lipid extracting according to Blight and Dyer (Bligh and Dyer, 1959). Media free of cells were recuperated during filtrations to estimate nutrient composition using a DIONEX ion-chromatography (Bougaran *et al*., 2010).

2.3.2 Nutrients

Before inoculation, 50 mL of fresh medium were sampled, as well as during the cell harvesting process by filtration, 50 mL of filtered medium were frozen at -80°C for conservation until measurement of nitrogen, phosphate and silica content. Residual phosphate (PO_4^{3-} µM) and nitrate (NO_3^- µM) concentrations were analyzed according to the method described by Aminot and Kérouel (2007). After being thawed, samples were centrifuged (10 min at 3000 *g*) and colorimetric assays were carried out using the supernatant on a AA3 autoanalyzer (SEAL Analytical®) which allows automatic nutrient determination by continuous flow spectrophotometry. Determination of PO_4^{3-} with this method relies on the reaction of molybdate with antimony. This reaction leads to the formation of the phosphomolybdic complex which is then reduced by ascorbic acid to form a blue compound, the measurement of which was carried out at λ= 820 nm. Nitrate is initially reduced to NO_2 using a cadmium column treated with copper and in the presence of two reagents (ammonium chloride and hydroxide sodium). Total NO_2 is then determined by reaction with sulfanilamide, to produce a diazo that reacts in turn with N-naphtyl-thlenediamine in an acid medium and gives a pink coloration, assayed at λ=540nm. Residual silica (SiO_3^{2-} µM) was determined by colorimetric assay according to Hansen & Koroleff 1999 (Hansen and Koroleff, 1999) based on the formation of silicomolybdic acid, which was then reduced to produce an intense blue color assayed at 870 nm. Nutrient consumption by cells during growth was calculated as the difference between starting and final concentrations for each major nutrient (-NO_3^-, -PO_4^{3-}, -SiO_3^{2-}). Ammonium (NH_4^+ µM) was

also analyzed at the end of the growth, because it is known to be produced by bacteria and can be utilized by diatoms for growth (Amin *et al*., 2015). This nutrient was measured to estimate its potential use by cells and its possible interaction with nitrogen conditions tested. NH_4^+ was analyzed with the colorimetric indophenol blue method adapted to seawater assayed at 630 nm (Koroleff 1970) directly on medium free of cells without freezing (Koroleff, 1970) because ammonium was unstable in the samples so they has to be processed in the shortest time possible (Aminot and Kérouel, 2004). Final NH_4^+ concentration was used to know if a production occured during growth.

2.3.3 Growth rate estimation

Daily triplicate samples of 2 mL were fixed with lugol and counted ($n \geq 300$) using a Neubauer hemocytometer and an optical microscope (OLYMPUS CH40, ×400). Following Cointet *et al* (2019), maximum cell concentration (A expressed in log) and latency time (λ in day) were determined by fitting growth kinetic data with a Gompertz model using Matlab software (Equation 1):

$$f(x) = A \times e^{-e(\mu max \times \frac{e^1}{A} \times (\lambda - x) + 1)} \quad \text{(Eq.1)}$$

with A: maximum cell concentration in the natural logarithm of the biomass; μmax: Maximum growth rate (day^{-1}); λ: Latency (days).

The relative growth rate (day^{-1}) was calculated following Eq. 2, where N_{t1} is the number of cells on the first day of the exponential phase ($=t_1$), N_{t2} is the number of cells at the end of the exponential phase ($=t_2$), and T (days) is the interval between t_1 and t_2.

$$\mu = \frac{1}{T(lnN_{t2} - lnN_{t1})} \quad \text{(Eq.2)}$$

2.3.4 Determination of photosynthetic parameters

During the exponential growth phase ("mid" sampling), and at the end of the growth, when the stationary phase was reached ("end" sampling), 2 mL aliquot of the culture were sampled for photosynthetic parameter estimations using the cuvette version of Water-PAM fluorometer (Walz GmbH, Effeltrich, Germany). Aliquot was first dark adapted for 1 hour, and then introduced into the 10 mm quartz glass cuvette of the PAM fluorometer controlled by WinControl-3 software. Maximum PSII quantum efficiency (Eq. 3) was then measured using a 600 ms saturating pulse (2500 µmol photons.m^{-2}.s^{-1}):

Where F0 is the minimum fluorescence yield for dark adapted cells, Fm, the maximum fluorescence yield for dark adapted cells during the saturating flash and Fv the variable fluorescence.

$$Fv/Fm = (Fm-F0)/Fm \qquad \text{(Eq.3)}$$

To provide detailed information on the overall photosynthetic performance of the microalgae (Ralph and Gademann, 2005), RLCs were constructed using nine 30s incremental irradiance steps (0, 38, 52, 77, 121, 179, 259, 391 and 580 µmol photons $m^{-2}s^{-1}$) and calculating relative electron transport rate (rETR, Eq.4) through PSII for each level of actinic light (Beer *et al*., 1998):

$$rETR = \left(\frac{F'm-F}{F'm}\right) \times PAR \times 0.5 \qquad \text{(Eq.4)}$$

where PAR was the actinic irradiance (=Photosynthetic Active Radiation from 400 to 700 nm), (F'm-F)/F'm was the effective quantum yield of PSII with F, the fluorescence yield for a given PAR intensity, F'm the maximum fluorescence for a given PAR intensity during the saturating flash and 0.5 was a multiplication factor based on the assumption that 50% of the absorbed quanta are distributed to PSII (Beer *et al*., 1998).

rETR value data were fitted using the Eilers and Peeter model (Eilers and Peeters, 1988) in order to obtain the initial slope (α), the light saturation parameter (Ek) and the maximum relative electron transport rate (rETRmax). Ek was derived from rETRmax and α (Eq. 5):

$$Ek = rETRmax/\alpha \qquad (Eq.5)$$

2.3.5 Pigment composition

To estimate Chlorophyll a (Chl a) and the total amount of carotenoids pigments (Car) per cell, 2 mL of culture were sampled and centrifuged at 11200 g. for 5min at the end of the growth. After supernatant removing, pigments were extracted by adding 2 mL of methanol (99.9%) on the pellet. To remove cell debris, methanol suspension was centrifuged for 5min at 11200 g. Absorbance at 665, 632 and 480 nm were measured by spectrophotometer (SHIMADZU, UV-1900) on the clean supernatant to calculate pigment content, expressed in pg.cell^{-1} following (Ritchie, 2006):

$$Chl\ a = \frac{13.26 \times A665 - 2.68 \times A632}{Number\ of\ cells} \times 10^6 \qquad (Eq.\ 6)$$

$$Car = \frac{4 \times A480}{Number\ of\ cells} \times 10^6 \qquad (Eq.\ 7)$$

2.3.6 Lipids analyses

2.3.6.1 Fourrier transform infrared spectroscopy (FTIR)

FTIR spectra acquisition was performed according to Coat *et al*, 2014 recommendations (Coat *et al*., 2014) adapted by Cointet *et al*. 2019 for diatom benthic strains. Sample preparation and the FTIR device are detailed in Cointet *et al*. 2019a. FTIR spectra were recorded in transmission mode on 5µL dried harvesting cells (10^7 cells.mL^{-1}) allowing to quickly obtain their biochemical signatures expressed in terms of total lipids, total proteins and total carbohydrates. Absorbance spectra were collected between 4 000 cm^{-1} and 700 cm^{-1} with 30 scans and were averaged. The spectra were analyzed by integral ratios method (León *et al*., 2014). The lipid

signature was associated with the ester bond (Eb) signal (~1740 cm^{-1}), whereas the carbohydrates signature was associated to the C-O-C signal of the polysaccharides (~1200-900 cm^{-1}) [37] and the protein signature was associated to the amide II bond (~1540 cm^{-1}) of the N-H of the amids associated to the proteins. To estimate the relative content of the lipids, carbohydrates and proteins, their respective integral area was standardized with the total spectrum area and expressed in arbitrary units (a.u) as recommended by Cointet *et al*. 2019 (Eq. 7).

$$\text{FTIR} = \frac{Peak\ area\ (s)}{Total\ spectra\ area} \qquad \text{(Eq.7)}$$

Where s = lipids (~1740 cm^{-1}) or carbohydrates (~1159 cm^{-1}) or amide II (~1540 cm^{-1})

2.3.6.2 Gravimetry

Finally, biomass dry weight was estimated by filtering the remaining algal suspension (47 mm, 0.7 µm pore diameter). Filters with cells were washed using 10 mL of ammonium formiate (68 $g.L^{-1}$) to remove salt, frozen at -80°C, freeze-dried and weighted (DW in mg). Crude lipid extract (CLE in mg) was estimated following Cointet *et al*, 2019, Lipid content was evaluated (LC in $mg.L^{-1}$). Lipid rate (LR) and lipid productivity (LP) were finally calculated:

$$\text{LR} = \frac{CLE}{DW} \times 100 \qquad \text{(Eq. 8)}$$

With CLE and DW expressed in mg

$$\text{LP} = LC \times \mu \qquad \text{(Eq. 9)}$$

With LC expressed in $mg.L^{-1}$ and µ in day^{-1}

2.3.6.3 Fatty acid composition

Fatty acid composition was determined by direct transesterification. A mixture of 800 µL hydrochloric methanol 7.5% and 100 µL chloroform were added to the CLE and heated at 80°C during 5 H. After the reaction was complete, the samples were cooled to room temperature and mixed with 500 µL hexane, which allowed phase separation. The organic phase, which contained fatty acid methyl ester (FAME), was collected, dried using an anhydrous sodium sulfate salt, filtered and evaporated using nitrogen. FAME was analyzed using a gas chromatograph mass spectrometry (GC-MS; Hewlett Packard HP 7890 – GC System / Agilent Technologies, Santa Clara, CA, USA) linked to a mass detector (HP 5975C – 70 eV). The Sample was injected (1µL injection volume) into a SLB^{TM}-5ms column (60 m × 0.25 mm × 0.25 µm). The carrier gas was helium at a flow rate of 1mL.min^{-1}. The injector and detector temperatures were set at 250°C and 280°C, respectively, and the temperature column was programmed with a temperature held at 170°C for 4 min and then increasing to 300 °C at 3 °C.min^{-1}. To identify and quantify the FAME, each FA identification was confirmed by comparing mass spectra and retention data with a library build from previous analyses and commercial standards. Chromatogram peak areas were analyzed and quantified using WSEARCH32 software

2.3.7 Data processing

Data are expressed as mean of each triplicate ± standard deviation (SD). Two-way ANOVA with a 5% significant level were carried out after checking normality and homogeneity using Shapiro-Wilk and equal variance tests. Tuckey's least significant test was used to determine which experimental conditions were significantly different. All statistical analyses were carried out using SigmaPlot software.

2.4 Results

2.4.1 Nutrients

Initial major nutrient concentrations (Table V-2) were respected for both media (N+ and N-) and for all species. For *E. paludosa* and *N. alexandrina*, in N+ conditions, nitrate consumption (NO_3^-) was higher under HL and ML than under LL ($p<0.001$) (Table V-3). As expected, all the NO_3^- available in the medium (~83 µM) under HL, ML and LL conditions for N- conditions was consumed. For *Staurosira* sp., the same amount of nitrogen was consumed in LL, HL and ML in N+ conditions ($p=0.30$), however as for the two other species, nitrogen consumption was higher in N+ than in N- conditions ($p<0.05$).

For *E. paludosa*, as for nitrogen, more phosphate was consumed in N+ conditions under HL and ML conditions than under LL ($p<0.001$). However, the same amount of phosphate was consumed in N+ and N- conditions ($p=0.05$). For *N. alexandrina*, phosphate concentration available in the medium was very low at the end of the experimentation (< 5µM) in all tested conditions. These results suggested a phosphate limitation at the end of the experiment for all tested conditions. However, phosphate consumption was higher under N+ than under N- for HL ($p<0.01$) and ML conditions ($p<0.05$). For *Staurosira* sp. less than half of the phosphate concentration available in the medium was consumed. Phosphate consumption decreased with light and was the highest under HL whatever nitrogen conditions ($p<0.001$). For all species and conditions tested silica and ammonium were present in trace amounts at the end of the experiment. All the silica available in the medium was consumed at the end of the experiment for each condition and each species. Presence of a low concentration of NH_4^+ suggests that low production occurs which did not modify our nitrogen culture condition.

For *E. Paludosa*, NO_3^- and PO_4^{3-} consumption was impacted by light. Nutrient consumption was more important under HL and ML. For *N. alexandrina* consumption was mainly impacted

by nitrogen concentration. For *Staurosira* sp., only NO_3^- consumption was impacted by nitrogen concentration, consumption was the same whatever the light.

Table V-2 Initial major nutrient concentration at the start of the experiment for all species and for both culture media (N+ and N-)

	NO_3- (µM)		PO_4^{3-} (µM)		SiO_3^{2-} (µM)	
	N+	N-	N+	N-	N+	N-
E. paludosa	828.54	83.56	37.31	36.31	117.08	114.89
N. alexandrina	868.63	74.53	37.54	37.73	111.04	108.33
Staurosira sp.	894.66	81.62	39.59	39.34	117.70	116.87

Table V-3 Nutrient consumption at the end of the experiment (triplicate mean ± SD) for all species and culture conditions and the corresponding two-way ANOVA results (n=3). Significance levels: *** for P<0.001; ** for P<0.01 and * for P<0.05. LOD = Limits of detection.

Species	Statistical results	Light	Nitrogen	NO_3^- (µM)	PO_4^{3-} (µM)	NH_4^+ (µM)	SiO_3^{2-} (µM)
E. paludosa		LL	N+	285.86 ± 57.79	19.45 ± 2.55	0.08 ± 0.10	116.18 ± 0.86
			N-	83.37 ± 0.04	23.50 ± 0.22	< LOD	114.51 ± 0.12
		ML	N+	430.89 ± 33.12	28.81 ± 0.89	2.71 ± 1.43	116.84 ± 0.15
			N-	83.42 ± 0.04	25.45 ± 0.62	0.64 ± 0.40	114.79 ± 0.18
		HL	N+	458.83 ± 28.47	27.61 ± 2.35	2.89 ± 0.80	116.52 ± 0.61
			N-	82.14 ± 1.58	22.15 ± 0.83	0.50 ± 0.81	114.27 ± 0.55
	Two-ways ANOVA						
	Light conditions		P	<0.001***	<0.001***	0.004**	0.245
	Concentration of N		P	<0.001***	0.049	0.001*	<0.001***
	Interaction		P	<0.001***	<0.001***	0.05	0.598
N. alexandrina		LL	N+	212.18 ± 40.72	36.46 ± 1.34	< LOD	108.29 ± 4.22
			N-	73.23 ± 1.86	36.69 ± 1.14	< LOD	108.33 ± 0.02
		ML	N+	322.96 ± 63.24	36.73 ± 0.10	2.31 ± 1.34	111.04 ± 0.01
			N-	73.78 ± 0.11	34.60 ± 1.91	< LOD	108.33 ± 0.01
		HL	N+	334.11 ± 57.97	37.09 ± 0.14	1.18±2.04	111.04 ± 0.01
			N-	73.30 ± 1.76	35.51 ± 0.59	< LOD	108.33 ± 0.01
	Two-ways ANOVA						
	Light conditions		P	0.034*	0.155	0.176	0.329
	Concentration of N		P	<0.001***	0.004**	0.029*	0.05
	Interaction		P	0.035*	0.031*	0.176	0.321
Staurosira sp.		LL	N+	82.19 ± 14.57	13.91 ± 0.48	0.30 ± 0.53	117.43 ± 0.42
			N-	80.72 ± 0.20	14.33 ± 0.48	< LOD	117.08 ± 0.47
		ML	N+	142.00 ± 54.80	18.22 ± 0.98	< LOD	117.63 ± 0.16
			N-	79.96 ± 0.57	16.59 ± 1.35	< LOD	117.15 ± 0.63
		HL	N+	156.44 ± 83.17	19.89 ± 0.73	0.75 ± 1.30	116.73 ± 0.99
			N-	79.56 ± 2.62	19.32 ± 0.40	0.35 ± 0.61	117.63 ± 0.12
	Two-ways ANOVA						
	Light conditions		P	0.30	<0.001***	0.543	0.805
	Concentration of N		P	0.033*	0.145	0.383	0.931
	Interaction		P	0.28	0.136	0.527	0.095

2.4.2 Growth

For *E. paludosa*, growth rate (μ) was higher under N+ than under N- condition for ML ($p<0.05$) and HL ($p<0.01$) (Table V-4). No significant difference in LL was detected between N+ and N- ($p=0.77$) (Fig. 1A). Maximum biomass (A) was the highest under N+ condition whatever the light condition ($p<0.01$). Latency phase (λ) was impacted by light condition ($p<0.01$): it was longer for LL condition but without significant effect due to nitrogen level ($p=0.824$). These results can be explained by NO_3^- and PO_4^{3-} consumption: namely, more nitrogen has been consumed in N+ under HL and ML, allowing higher growth rate and biomass, whereas under LL, light intensity was not enough to allow efficient growth, in comparison to ML and HL (Table V-4), inducing a lower consumption of nutrients (Table V-4).

For *N. alexandrina* growth rate (μ) increased with light intensity whatever the nitrogen levels ($p<0.001$). There was a significant difference in maximum biomass (A in log) for light conditions ($p<0.05$): HL and LL conditions showing respectively the lowest and the highest values ($p<0.05$). On the other side, there was no significant differences between growth parameters due to nitrogen condition ($p=0.646$), even if a drop in cell concentration in N- medium for HL and ML conditions occurred at the end of the growth (Fig. V-1B). As for *E. paludosa*, latency phase (λ) was longer under LL conditions whatever the nitrogen concentration ($p<0.001$). These results showed that the impact of light prevailed on the impact of nitrogen in terms of growth. Even if nitrogen consumption was higher under N+, it did not affect the growth. The other hypothesis was that phosphate limitation occurred in N+ and N- conditions. All the available phosphate was consumed, which could have limited growth in the same way, whatever the nitrogen concentration, and explain the drop observed under N- conditions. Under LL condition, the low growth induced a later limitation than under HL and ML, due to slower nutrient consumption.

For *Staurosira* sp. there was no significant difference for growth rate between light conditions (p=0.21) and nitrogen concentration (p=0.64). Mean growth rate was 0.56 ± 0.08 day^{-1} for all tested conditions. As for *E. paludosa*, maximum biomass (A) was the highest under N+ conditions whatever light levels (p<0.05). Contrary to *E. paludosa* and *N. alexandrina*, latency phase (λ) was not impacted by culture conditions (p=0.29) and occurred during 2.52 ± 0.79 days for all tested conditions. As for *E. paludosa* more nitrogen was consumed under N+ conditions which explaines the higher biomass obtained. However, no marked trend in growth appears for *Staurosira* sp., in contrary to *E. paludosa* where growth was more conditioned by N concentration (Fig V-1A) and to *N. alexandrina* where growth was more conditioned by light (Fig V-1B). For *Staurosira* sp., there was no significant difference in growth except at the end of the growth were biomass decreased under N- conditions (Fig V-1C).

Table V-4 Growth rate (μ in day^{-1}), maximum cell concentration (A in log) and latency time (λ in day) (triplicate mean ± SD) for all species and culture conditions and the corresponding two-way ANOVA results (n=3). Significance levels: *** for P<0.001; ** for P<0.01 and * for P<0.05. Remarkable value in bold: for details see text.

Species	Statistical Results	Light	Nitrogen	μ (day^{-1})	A (log)	λ (day)
E. paludosa		LL	N+	0.29 ± 0.06	**2.56 ± 0.12**	**2.84 ± 0.47**
			N-	0.30 ± 0.01	2.26 ± 0.10	**2.80 ± 0.71**
		ML	N+	**0.35 ± 0.01**	**2.48 ± 0.02**	1.45 ± 0.28
			N-	0.30 ± 0.02	2.00 ± 0.11	1.70 ± 0.65
		HL	N+	**0.37 ± 0.01**	**2.61 ± 0.38**	1.65 ± 0.16
			N-	0.28 ± 0.02	2.33 ± 0.15	1.26 ± 0.60
	Two Way Anova					
	Light conditions		P	0.090	0.114	<0.001***
	Concentration of N		P	0.003**	<0.001***	0.824
	Interaction		P	0,020*	0.597	0.582
N .alexandrina		LL	N+	**0.67 ± 0.02**	4.62 ± 0.09	**4.38 ± 0.07**
			N-	**0.73 ± 0.02**	4.65 ± 0.30	**4.42 ± 0.08**
		ML	N+	1.05 ± 0.10	4.41 ± 0.17	3.45 ± 0.38
			N-	0.83 ± 0.11	4.61 ± 0.25	1.51 ± 0.52
		HL	N+	1.05 ± 0.07	4.16 ± 0.16	3.56 ± 0.09
			N-	1.16 ± 0.13	4.40 ± 0.20	2.65 ± 0.41
	Two Way Anova					
	Light conditions		P	<0.001***	0.037*	<0.001***
	Concentration of N		P	0.694	0.131	<0.001***
	Interaction		P	0.012*	0.646	<0.001***
Staurosira sp.		LL	N+	0.69 ± 0.18	**2.81 ± 0.96**	2.65 ± 0.14
			N-	0.61 ± 0.08	1.75 ± 0.13	2.60 ± 0.31
		ML	N+	0.46 ± 0.05	**2.50 ± 0.56**	1.65 ± 0.50
			N-	0.56 ± 0.24	2.08 ± 0.05	2.66 ± 0.16
		HL	N+	0.49 ± 0.12	**2.35 ± 0.19**	2.22 ± 1.51
			N-	0.57 ± 0.04	1.80 ± 0.47	3.37 ± 0.69
	Two Way Anova					
	Light conditions		P	0.217	0.674	0.293
	Concentration of N		P	0.647	0.012*	0.054
	Interraction		P	0.497	0.499	0.296

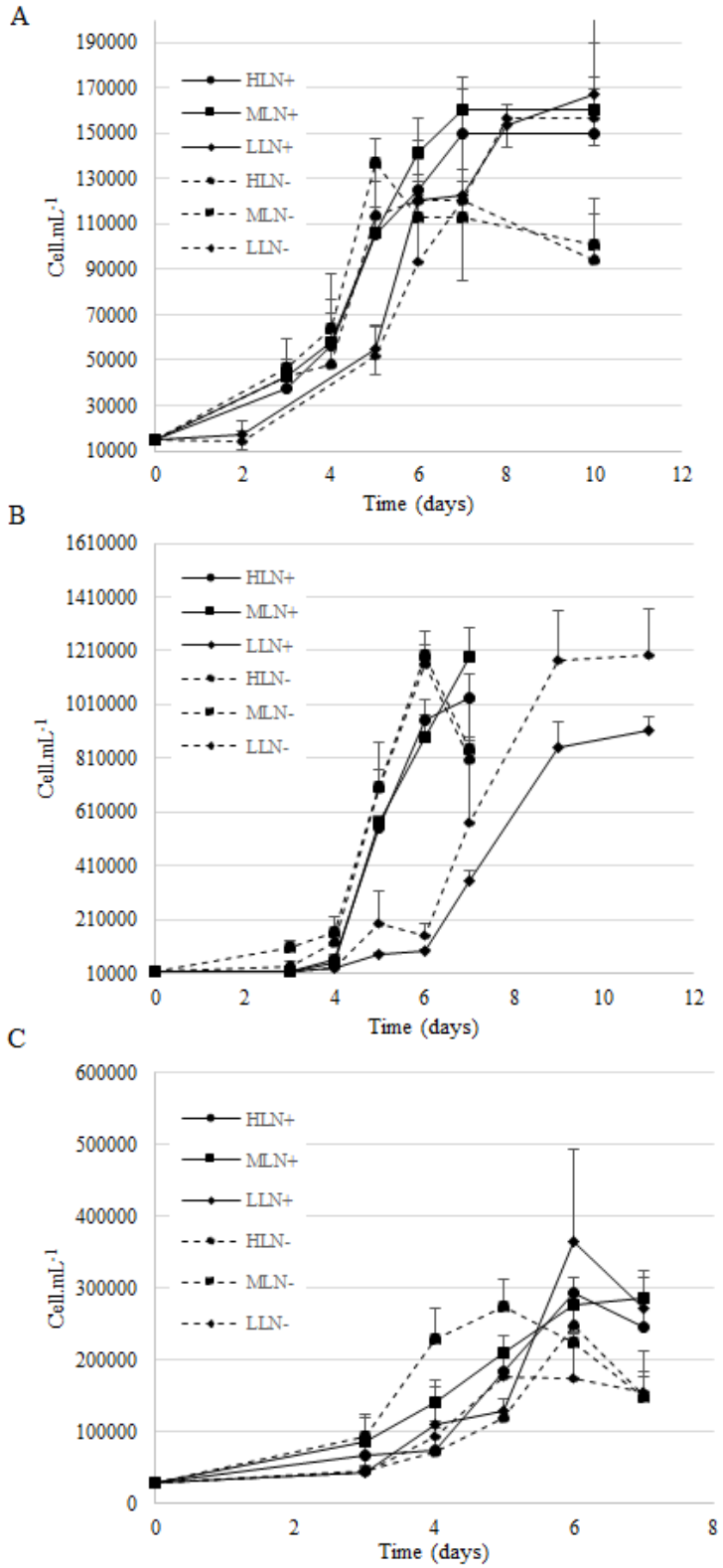

Figure V-1 Growth curves expressed in cell.mL^{-1} of *E. paludosa* (A), *N. alexandrina* (B) and *Staurosira* sp. (C) as a function of time under different light (LL, ML, HL) and nitrogen (N+, N-) conditions.

2.4.3 Photosynthetic performance

For all species, Fv/Fm was higher in LL photoacclimated cultures ($p<0.001$) and higher in N+ medium ($p<0.001$) during mid and end of growth (Figures V-2-4). Fv/Fm was around 0.6 for all species at mid growth except for the HL conditions for *Staurosira* sp. where Fv/Fm was around 0.5 in N+ conditions and 0.4 in N- conditions (Figure 4).

For *E. paludosa* (Figure. V-2A), during mid growth, Fv/Fm values were all superior to 0.58 ± 0.01. It was the same for *N. alexandrina* (Figure. V-3A) where all Fv/Fm values were mainly superior to 0.59 ± 0.01. These results indicated that during mid growth, cells were not stressed by the culture conditions, meaning that all major nutrients were available in the medium, even for *N. alexandrina* for which a limitation by phosphate was suggested (Table V-3). For *Staurosira* sp. (Figure. V-4A) Fv/Fm values tend to decrease with light and with lack of nitrogen ($p<0.001$). Highest Fv/Fm value was obtained under LL and N+ (0.61 ± 0.01) and lowest for HLN- (0.47 ± 0.01).

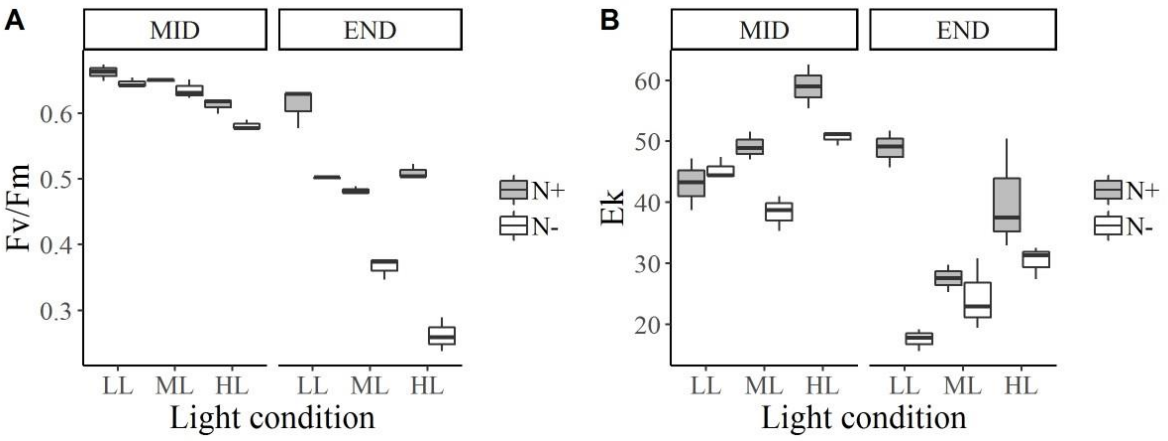

Figure V-2 Box and whisker plots for *E. paludosa* photosynthetic parameters: maximum PSII quantum efficiency, Fv/Fm (A) and maximum light saturation parameter, Ek (B) for each culture condition and for two growth stages: exponential growth phase (mid) and stationary phase (end).

At the end of the growth, for *E. paludosa*, Fv/Fm value was lower under N- than N+ whatever light conditions (p<0.001) and dropped by 54.89 ± 4.78% for HL, 42.25 ± 3.84% for ML and 22.38 ± 0.75% for LL. There was a significant interaction between light conditions and nitrogen concentration (p<0.001). The stronger was the light and lower was the nitrogen concentration, lower was the Fv/Fm value. As for growth, these results can be explained by nutrient consumption and demonstrate the effect of nitrogen limitation on cells.

For *N. alexandrina* (Figure.V-3A), Fv/Fm decreased between mid and end of growth for all conditions (p<0.001) and Fv/Fm was higher under LL whatever nitrogen concentration (p<0.001) as for *E. paludosa*. However no significant difference between N+ and N- for HL and ML was detected (p=0.62). Even though cell concentration was higher under LL in N- condition (Figure V-1), Fv/Fm value suggested that they were, more stressed under N- than N+ conditions (p<0.01). This can be explained by the accumulation of two nutrient limitations (nitrogen and phosphate) under N-, whereas only phosphate was limited under N+ (TableV-3). These nutrient limitations can also explain why no difference between N+ and N- conditions was detected for ML and HL, nitrogen limitation and phosphate limitation can probably have the same effect on cells and trigger a stress.

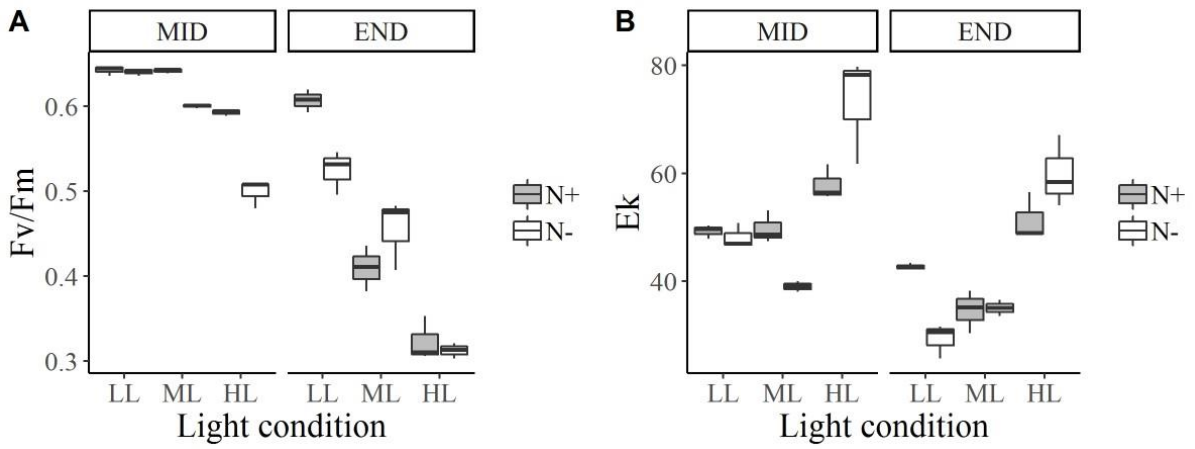

Figure V-3 Box and whisker plots for *N. alexandrina* photosynthetic parameters: maximum PSII quantum efficiency, Fv/Fm (A) and maximum light saturation parameter, Ek (B) for each culture condition and for two growth stages: exponential growth phase (mid) and stationary phase (end).

For *Staurosira* sp. (Figure V-4A), as for *E. paludosa*, the Fv/Fm value droped between mid and end of growth especially under N- conditions ($p<0.001$). The Highest Fv/Fm value was under LL watever nitrogen concentration ($p<0.001$). These results can be explained by nitrogen consumption inducing a stressing nitrogen limitation during growth.

Ek parameters, which is an indicator of the state of photoacclimation of the cells, was as expected, always higher under HL ($p<0.001$) for all species. This result indicates that cultures were well photoaclimated. As a results of stress, induced by nutrient consumption and growth, this parameter decreased between mid and end of growth ($p<0.001$). This decrease can be induced by cells autoshading which implies a decrease in the brightness reaching the cells. Ek value was higher under HL for *Staurosira* sp. (133.3 ± 35.8) compared to *E. paludosa* (59 ± 3.6) and *N. alexandrina* (65.68 ± 10.74). These results can be explained by the fact that this species tends to be more in suspension in the medium than the other which increases the light reaching the cells.

.

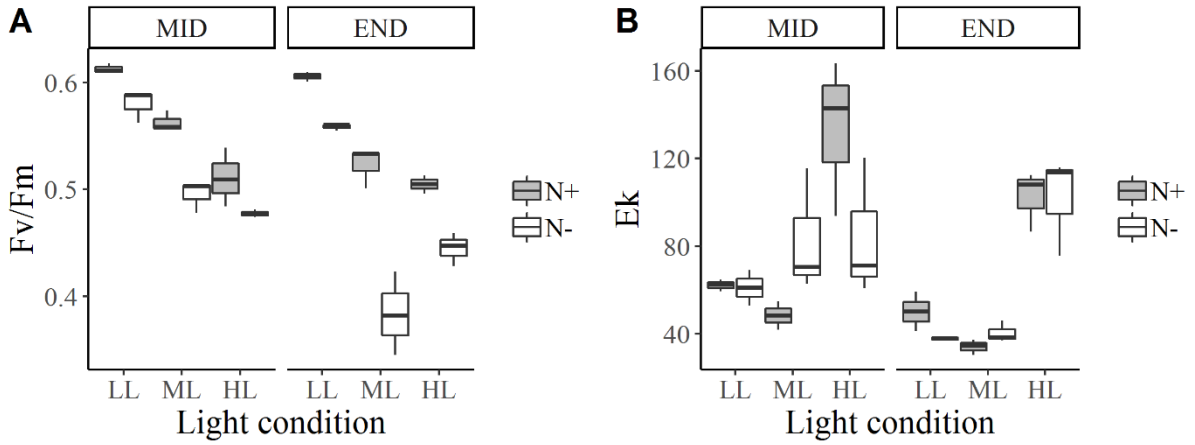

Figure V-4 Box and whisker plots for *Staurosira* sp. photosynthetic parameters: maximum PSII quantum efficiency, Fv/Fm (A) and maximum light saturation parameter, Ek (B) for each culture condition and for two growth stages: exponential growth phase (mid) and stationary phase (end).

2.4.4 Pigments

For *E. paludosa*, pigment concentrations, i.e Chl *a* and Car, were impacted by nitrogen ($p<0.001$) and light conditions ($p<0.001$) (Figure. V-5A). As expected, Chl *a* concentration in cells was higher under LL ($p<0.01$) due to the photoacclimation of cells. Chl *a* concentration was lower in N-, especially for ML and HL ($p<0.001$). Chl *a* content and Fv/Fm follow the same trend: Fv/Fm (Fig V-2A) decreasing could be linked to a lower production of Chl *a* by stressed cells. Car concentration was lower under N- conditions ($p<0.001$) and under HL ($p<0.01$) as for Chl *a*.

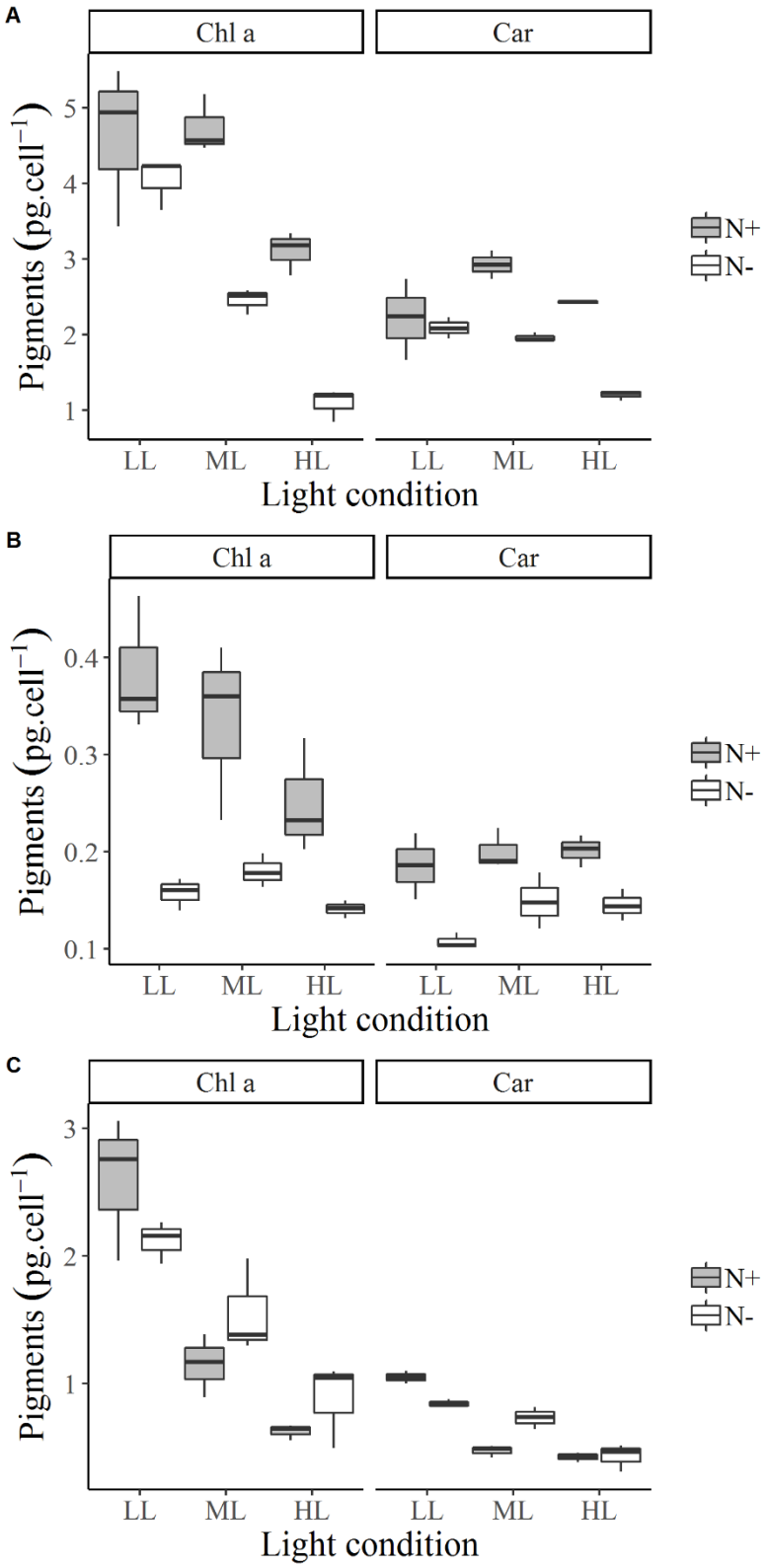

Figure V-5 Box and whisker plots for *E. paludosa* (A), *N. alexandrina* (B) *and Staurosira sp.* (C) of Chl *a* content (pg.cells^{-1}) and Carotenoids content (Car in pg.cells^{-1}) at the end of the growth for each culture condition.

For *N. alexandrina*, pigment concentrations were impacted by nitrogen ($p<0.001$) but not by light conditions ($p=0.073$) even if the expected decrease of Chl *a* with light can be observed (Figure V-5B). Chl *a* and Car concentrations were higher under N+ than N- whatever light conditions ($p<0.001$). As for *E. paludosa*, this tendency can be explained by nutrient limitation and on contrary of Fv/Fm results (which were similar between N+ and N- conditions), here we can see that nitrogen limitation induced a stop or a decrease of Chl *a* production. This could mean that the phosphate limitation observed for this strain (Table V-3) impacted the production of Chl *a* only when it occurred in synergy with a nitrogen limitation (N-).

For *Staurosira* sp. (Figure.V-5C), pigment concentrations were impacted by light ($p<0.001$) but not by nitrogen ($p=0.70$). As seen for *E. paludosa*, Chl *a* and Car concentrations were higher under LL ($p<0.001$) whatever nitrogen concentration. The absence of differences between N+ and N- for Chl *a* production can be explained by the low differences of nitrogen consumption between both conditions. Thereby, for this species, Chl *a* concentration was more impacted by light conditions.

2.4.5 Macromolecular content

Macromolecular content (lipids, proteins and carbohydrates) obtained with FTIR method showed that *E. paludosa*, *N. alexandrina* and *Staurosira* sp. showed different biochemical profiles (Figure V-6). Total lipid content decreased for *E. paludosa* growing under nitrogen limitation conditions ($p<0.05$), and was lower under LL ($p<0.05$) whereas it increased for *N. alexandrina* growing in the same nitrogen condition ($p<0.001$) but was also the lowest under LL ($p<0.05$). No impact of nitrogen ($p=0.06$) or light ($p=0.88$) on *Staurosira* sp. total lipid production was detected (Figure V-6A-C). Carbohydrate content increased for both strains, *E. paludosa* and *N. alexandrina* under nitrogen limitation medium ($p<0.001$) (Figure V-6D,E). However, carbohydrate concentration was not impacted by light for *E. paludosa* ($p=0.84$) but was higher under LL for *N. alexandrina* ($p<0.05$). Protein synthesis for these two species was

limited under N- conditions ($p<0.001$) (Figure V-6G,H). No impact of nitrogen concentration on carbohydrate and protein synthesis was found for *Staurosira* sp (Figure V-6F,I). The only production affected by light was for carbohydrates under LL ($p<0.001$). Results for this species could be explained by the small difference in nitrogen consumption between N+ and N- conditions illustrating no limitation of growth by nitrogen, confirmed by similar growth parameters (Table V-4). *E. paludosa* and *N. alexandrina* cultured in stressful conditions remobilize carbon to produce energy storage products (carbohydrates and/or lipids) for acclimation to the altered nutrient condition. For these two species, cells may produce less storage products (carbohydrates and proteins) when cultured under LL because they are less stressed, as demonstrated before by high Fv/Fm.

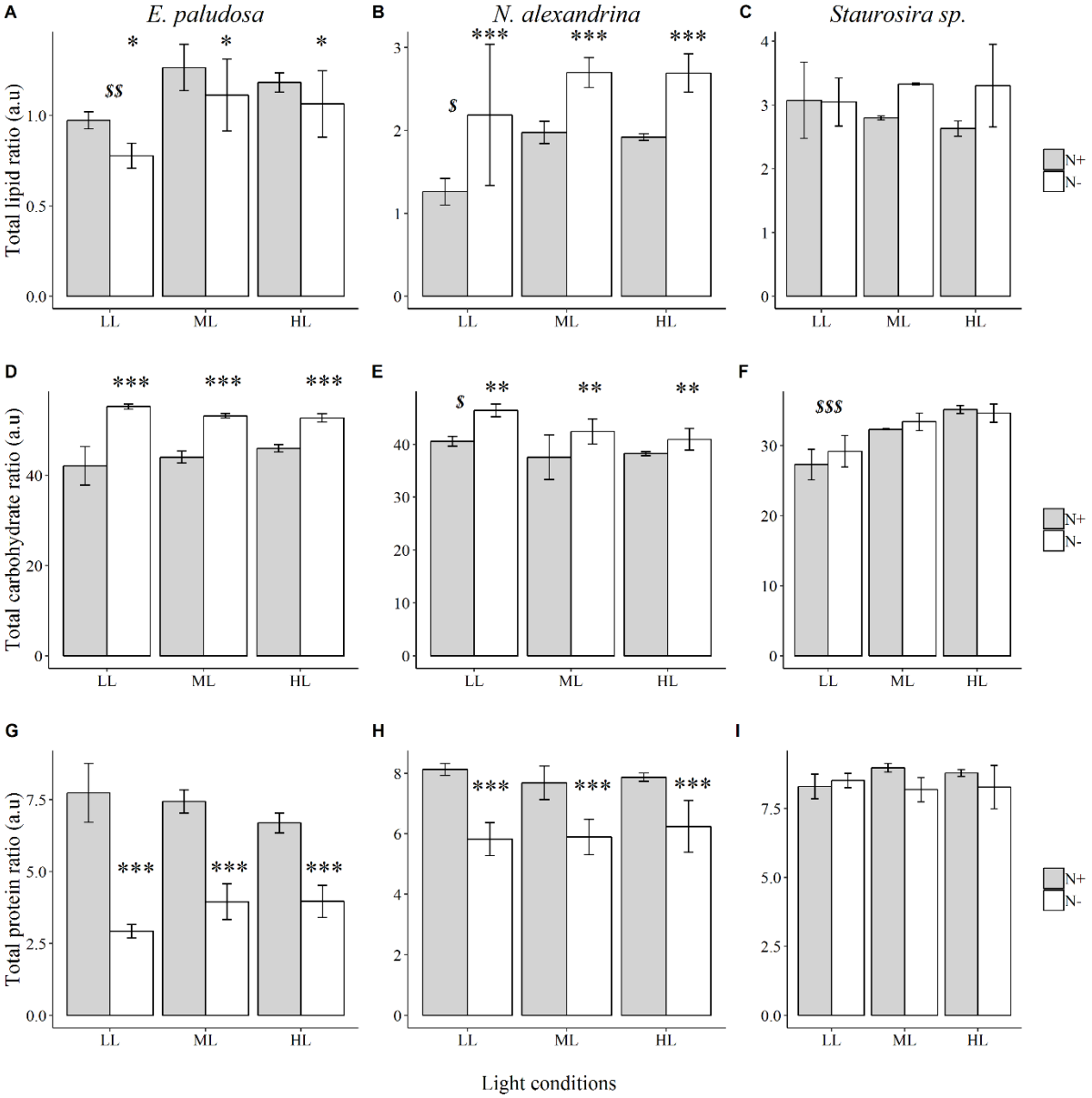

Figure V-6 Total lipid ratio (A,B,C), total carbohydrate ratio (D,E,F) and total protein ratio (G,H,I) of *E. paludosa*, *N. alexandrina* and *Staurosira* sp. for each condition.* $p<0.05$;** $p<0.01$;*** $p<0.001$ for nitrogen conditions and $^{\$}$ $p<0.05$;$^{\$\$}p<0.01$;$^{\$\$\$}p<0.001$ for light conditions.

2.4.6 Biomass and lipid content

The highest biomass for *E. paludosa* (57.77 ± 12.86 mg.L^{-1}), *N. alexandrina* (35.3 ± 3.9 mg.L^{-1}) and *Staurosira* sp (33.9 ± 0.28 mg.L^{-1}) was achieved under HL and N+ conditions (Figure V-7A,C). For *E. paludosa* and *N. alexandrina* biomass was higher in N+ conditions than N- (p<0.001) except for LL condition (p=0.88). For *Staurosira* sp. biomass was higher in N+ conditions (p<0.01) except for ML condition (p=0.55). These results were directly linked with growth parameters (Table V-4, Figure V-1).

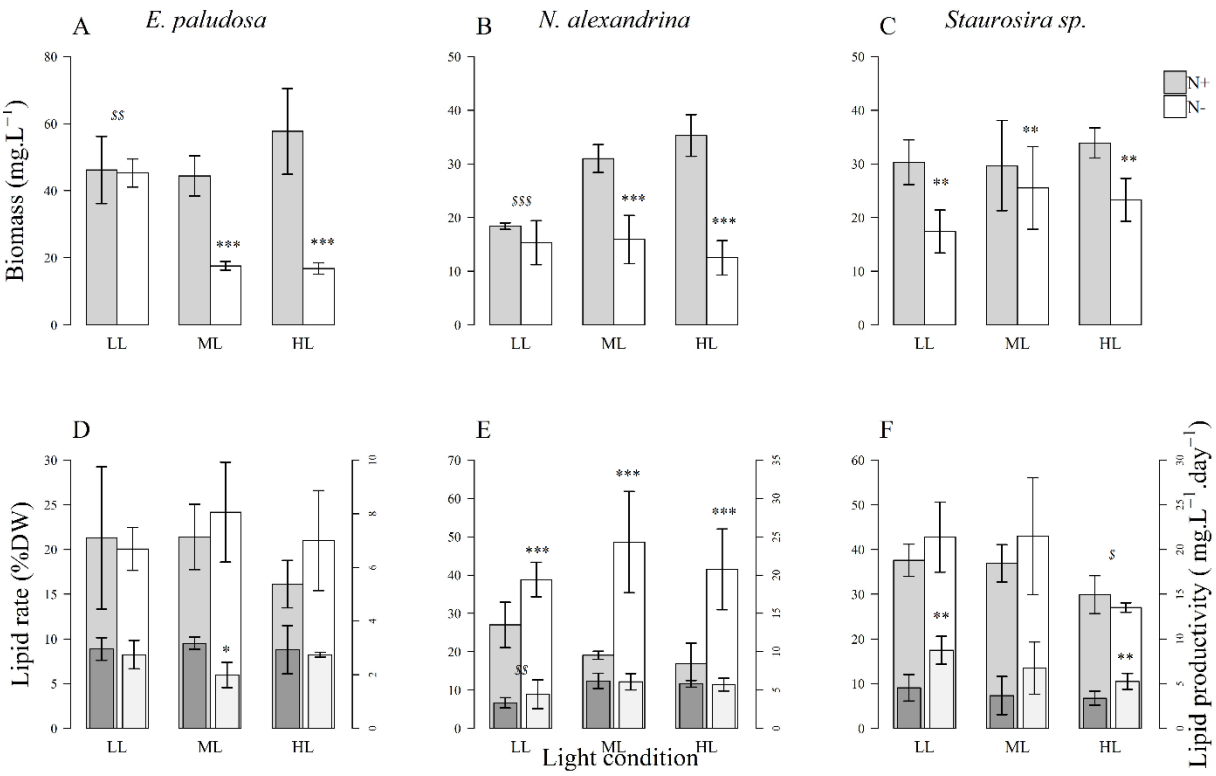

Figure V-7 Biomass (A, B, C), lipid rate and lipid production (D, E, F; high bar = lipid rate; low bar = lipid productivity) obtained at the end of the growth for *E. paludosa*, *N. alexandrina*, *Staurosira sp.* for each condition..* p<0.05;**p<0.01;***p<0.001 for nitrogen conditions and $^{\$}$ p<0.05;$^{\$\$}$$p$<0.01;$^{\$\$\$}$$p$<0.001 for light conditions.

Total lipid contents obtained with gravimetry where not impacted by light (p=0.30) or nitrogen concentration (p=0.79) for *E. paludosa* and corresponded to 20.68 ± 2.62%DW. However, lipid productivity was higher under N+ than N- conditions for ML (p<0.05). For *N. alexandrina*

total lipid content obtained by gravimetry was impacted by nitrogen concentration ($p<0.001$) but not by light ($p=0.63$). However, lipid productivity was the lowest under LL ($p<0.05$). This confirmed previous observations: *N. alexandrina* accumulated lipids under nitrogen limited conditions on the contrary to *E. paludosa*. Regarding photosynthetic parameters, *N. alexandrina* was less stressed under LL whatever nitrogen concentration, explaining a lower lipid production under LL, whereas highest lipid content for *N. alexandrina* was 42.99 ± 5.06% obtained under stressful N- conditions. For *Staurosira* sp. total lipid content obtained with gravimetry was lower under HL ($p<0.05$) but not impacted by nitrogen concentration ($p=0.41$). Lipid productivity was higher under N- conditions ($p<0.01$). Even though cells were stressed by nitrogen depletion (see Fv/Fm values Figure V-4A) this apparently did not induce the production of lipids and/or carbohydrates as seen for the others two species. *Staurosira* sp. was the species with the highest lipid rate under repleted nutrient conditions (36.21 ± 8.42%), whereas *N. alexandrina* was the only species who accumulated lipids under depleted nutrient conditions (42.99 ± 11.09%).

2.4.7 Fatty acid characteristics

The most abundant saturated fatty acid (SFA) was palmitic acid (C16:0), ranging from 18.1 ± 3.1% to 64.6 ± 6.0 % of total FA for all strains in all conditions. The most abundant unsaturated fatty acid (UFA) was oleic acid (C18:1) for *E. paludosa* and palmitoleic acid (C16:1) for *N. alexandrina* and *Staurosira* sp. (Table 5).

N. alexandrina was the only species that produced arachidonic acid (C20:4) and eicosapentaenoic acid (20:5). These fatty acids were mostly produced under N+ conditions and their concentration were higher under LL and ML compared to HL ($p<0.05$). For *N. alexandrina* and *Staurosira* sp., under a nitrogen limitation, UFA tends to decrease ($p<0.01$) and SFA increases ($p<0.001$). *E. paludosa* produced a significant amount of hydrocarbons (9.81 ± 3.18 – 18.12 ± 4.02%) which increased under N- conditions as for *Staurosira* sp. ($p<0.01$).

Table V-5 FAME composition of *E. paludosa*, *N. alexandrina* and *Staurosira* sp. for all cultured conditions. Cj: Conjugated, EPA: Eicosapentaenoic acid, ARA: Arachidonic acid, HC: hydrocarbons, UFA: unsaturated fatty acid, MUFA: Monounsaturated fatty acid, PUFA: Polyunsaturated fatty acid, SFA: Saturated fatty acid, ND: Not detected.

.

Fatty acid (% total fatty acid)	*E. paludosa*			*N. alexandrina*			*Staurosira* sp.		
	LLN+	MLN+	HLN+	LLN+	MLN+	HLN+	LLN+	MLN+	HLN+
C14 :0	10.0 ± 2.1	8.0 ± 5.4	10.1 ± 1.5	0.6 ± 1.1	1.5 ± 0.5	3.9 ± 1.9	1.9 ± 0.7	1.7 ± 0.8	1.3 ± 0.8
C15 :0				0.3 ± 0.4	0.5 ± 0.1	1.5 ± 1.1	0.5 ± 0.2	0.5 ± 0.2	ND
C16 :1	13.6 ± 4.1	11.8 ± 8.9	9.4 ± 2.6	12.7 ± 4.8	26.1 ± 2.9	22.6 ± 11.6	39.7 ± 14.0	35.1 ± 10.1	23.0 ± 4.6
C16 :0	31.7 ± 2.0	30.2 ± 1.3	36.5 ± 6.0	18.1 ± 3.1	23.6 ± 0.8	24.6 ± 6.4	37.7 ± 3.5	41.8 ± 2.4	47.4 ± 2.1
C16 :2 cj				ND	1.3 ± 0.5	2.9 ± 1.6	4.3 ± 5.2	4.6 ± 2.9	7.4 ± 3.8
C18 :2	1.0 ± 0.7	1.1 ± 1.0	0.3 ± 0.4						
C18 :1	19.2 ± 5.1	36.7 ± 23.2	8.9 ± 2.3	19.5 ± 15.1	9.4 ± 3.6	16.1 ± 14.6	5.5 ± 2.1	3.3 ± 0.4	2.8 ± 0.4
C18 :0	15.3 ± 5.0	5.2 ± 3.5	21.1 ± 4.7	11.1 ± 1.5	10.8 ± 4.4	7.7 ± 2.5	6.2 ± 3.0	9.0 ± 10.2	10.9 ± 6.7
C18 :02 cj				ND	ND	8.8 ± 10.3	0.8 ± 1.4	1.7 ± 2.7	3.8 ± 1.4
C20 :5 (EPA)				**1.5 ± 0.4**	**1.7 ± 0.2**	**0.3 ± 0.4**			
C20 :4 (ARA)				**10.8 ± 3.0**	**11.7 ± 3.1**	**2.3 ± 2.4**	1.1 ± 1.6	ND	ND
C20 :0				1.7 ± 0.5	0.9 ± 0.2	1.1 ± 0.5	0.5 ± 0.2	0.6 ± 0.2	0.8 ± 0.7
C22 :1				3.6 ± 1.2	3.7 ± 1.9	1.6 ± 1.8			
C22 :0				2.9 ± 1.4	0.8 ± 0.1	1.6 ± 1.2			
C24 :0				4.4 ± 1.8	1.7 ± 0.3	1.5 ± 0.2	0.5 ± 0.2	0.3 ± 0.3	1.0 ± 1.0
HC	9.3 ± 3.0	7.0 ± 6.6	13.7 ± 0.4	12.8 ± 5.7	7.8 ± 3.4	3.6 ± 2.9	2.1 ± 1.3	1.3 ± 1.0	0.5 ± 0.1
UFA	**33.6 ± 5.7**	**49.6 ± 15.2**	**18.6 ± 0.1**	**52.9 ± 4.9**	**52.6 ± 3.6**	**50.0 ± 8.7**	**51.4 ± 7.0**	**44.7 ± 14.0**	**37.0 ± 9.5**
MUFA	32.7 ± 4.8	48.5 ± 14.2	18.3 ± 0.3	40.8 ± 9.6	38.0 ± 2.0	39.5 ± 4.3	45.2 ± 11.9	38.4 ± 9.7	25.8 ± 4.4
PUFA	0.8 ± 0.9	1.1 ± 1.0	0.3 ± 0.4	12.2 ± 4.7	14.6 ± 2.8	10.5 ± 4.4	6.2 ± 5.7	6.3 ± 4.9	11.2 ± 5.1
SFA	**57.0 ± 2.6**	**43.4 ± 8.9**	**67.7 ± 0.3**	**37.4 ± 2.6**	**39.6 ± 4.8**	**45.0 ± 7.0**	**47.4 ± 6.8**	**53.8 ± 12.7**	**61.3 ± 7.6**
	LLN-	MLN-	HLN-	LLN-	MLN-	HLN-	LLN-	MLN-	HLN-
C14 :0	10.8 ± 2.7	9.9 ± 2.1	8.4 ± 2.4	4.6 ± 0.9	3.7 ± 1.0	3.0 ± 0.8	2.9 ± 1.2	3.7 ± 1.3	3..0 ± 1.1
C15 :0	0.9 ± 0.1	0.7 ± 0.1	1.1 ± 0.9	1.0 ± 0.2	1.0 ± 0.2	0.7 ± 0.1	0.3 ± 0.2	0.3 ± 0.3	0.7 ± 0.3
C16 :1	3.2 ± 0.2	4.0 ± 0.6	6.0 ± 2.1	25.2 ± 1.9	20.8 ± 3.6	25.2 ± 6.4	25.0 ± 9.0	6.9 ± 2.1	19.0 ± 7.0
C16 :0	36.6 ± 6.4	36.7 ± 6.9	33.3 ± 5.7	32.5 ± 4.3	39.2 ± 3.2	35.3 ± 1.2	50.9 ± 9.7	64.6 ± 6.0	58.0 ± 3.7
C16 :2 cj				5.5 ± 3.9	9.5 ± 2.0	5.8 ± 1.7	4.6 ± 3.8	9.5 ± 0.7	5.4 ± 2.3
C18 :2	1.4 ± 1.4	1.9 ± 1.8	0.9 ± 0.3						
C18 :1	11.3 ± 0.0	20.1 ± 3.2	12.8 ± 9.4	4.1 ± 0.6	5.7 ± 2.2	6.6 ± 2.8	4.6 ± 1.4	3.0 ± 2.0	3.9 ± 1.9
C18 :0	13.0 ± 4.0	13.5 ± 2.0	16.8 ± 4.2	8.9 ± 0.5	6.6 ± 0.9	13.0 ± 2.9	5.5 ± 0.9	4.6 ± 1.6	4.5 ± 0.5
C18 :02 cj				3.9 ± 1.9	4.7 ± 1.3	2.5 ± 0.7	ND	ND	0.3 ± 0.2
C20 :5 (EPA)				**1.0 ± 0.1**	**ND**	**ND**			
C20 :4 (ARA)				**3.9 ± 0.4**	**ND**	**ND**			
C20 :0	0.7 ± 0.3	1.2 ± 0.6	0.5 ± 0.5	0.8 ± 0.3	0.6 ± 0.2	0.8 ± 0.3	0.3 ± 0.2	0.2 ± 0.3	ND
C22 :1				1.7 ± 1.3	0.8 ± 0.3	1.3 ± 0.6			
C22 :0				0.7 ± 0.2	0.7 ± 0.1	0.7 ± 0.2			
C24 :0				0.9 ± 0.4	0.9 ± 0.1	1.0 ± 0.1			0.2 ± 0.2
HC	12.1 ± 1.9	18.1 ± 4.0	20.1 ± 8.8	3.3 ± 1.4	2.8 ± 0.9	5.0 ± 0.3	6.0 ± 1.0	7.2 ± 1.6	5.0 ± 1.0
UFA	**26.1 ± 13.8**	**26.1 ± 5.7**	**23.9 ± 6.2**	**43.9 ± 11.6**	**41.5 ± 1.2**	**40.5 ± 3.0**	**34.2 ± 9.3**	**19.4 ± 2.6**	**28.3 ± 6.4**
MUFA	25.2 ± 12.7	24.2 ± 3.8	23.2 ± 6.4	38.0 ± 8.4	27.4 ± 2.0	33.1 ± 3.9	29.6 ± 10.4	10.0 ± 1.9	23.0 ± 5.7
PUFA	0.9 ± 1.3	1.9 ± 1.8	0.7 ± 0.2	12.6 ± 4.2	14.1 ± 1.6	7.4 ± 3.2	4.6 ± 3.8	9.5 ± 0.7	5.4 ± 2.3
SFA	**61.7 ± 12.3**	**62.1 ±7.6**	**60.2 ± 4.9**	**46.7 ± 11.0**	**55.7 ± 2.0**	**54.5 ± 2.7**	**59.7 ± 8.4**	**73.4 ± 4.1**	**66.6 ± 5.5**

2.5 Discussion

2.5.1 Growth and photosynthetic performances

In comparison with our previous study (Cointet *et al*., 2019a,b), the three species studied in this current article show lower growth and biomass. However, this difference could be explained by their previously estimated growth under more favorable conditions: medium using enriched natural seawater and continuous light. Continuous light is known to be favorable because diatoms grow faster under longer photoperiods (Brand and Guillard, 1981). The use of artificial sea water made it possible to control nutrient concentrations more precisely than in enriched natural seawater but there can be shortages of essential elements in the basal salt mixture, omission of minor elements present in natural seawater or contamination of reagent grade salts (Allen, 1914; Berges *et al*., 2001; McLachlan, 1964) which can explain the achievement of a lower biomass in this study.

As expected growth rate and biomass increase under ML and HL especially under N+ (Guihéneuf *et al*., 2008; Shifrin and Chisholm, 1981). Latency phase is mostly impacted by light condition and is higher under LL as seen in the Guihéneuf *et al*, study (Guihéneuf *et al*., 2008) on *Skeletonema costatum*; where latency phase was 5 days longer than HL (340 µmol.photons.m^{-2}.s^{-1}) and ML (100 µmol.photons.m^{-2}.s^{-1}) under LL conditions (20 µmol.photons.m^{-2}.s^{-1}). However, species specific responses occur: growth rate is lower under N- conditions for *E. paludosa* while it is lower under LL for *N. alexandrina* and no difference was observed between all tested conditions for *Staurosira* sp. However, in the literature majority trends show that growth rate normally raises with light intensity to a certain extent where photoinhibition occurs (He *et al*., 2015; Norici *et al*., 2011; Rhee and Gotham, 1981; Solovchenko *et al*., 2008). In this study only *N. alexandrina* seems to follow this tendency while

E. paludosa and *Staurosira* sp. seem to have higher resistance to light conditions in terms of growth. Growth patterns of *E. paludosa* and *N. alexandrina* showed that under light-limited conditions and whatever nitrate concentration used, growth curves are similar. This similarity suggests that at low light intensity, light rather than nitrogen availability is growth limiting. Jauffrais *et al*, 2015 (Jauffrais *et al*., 2015) also found same the growth rate for *E. paludosa* when grown under N+ (1.15 ± 0.06 day^{-1}) and N- condition (1.13 ± 0.04 day^{-1}). However, growth rates found for this species in the present study are lower, this could be explained by artificial medium sea water composition that slightly differs. Artificial medium in Jauffrais *et al.* study contained more phosphate (72.4 µM) and H_3BO_3 (178 µM) and less Kbr (12.5 µM) and $SrCl_2$ (37.5 µM).

The photosynthetic efficiency, estimated by the Fv/Fm parameter, decreases for all species during growth, especially under N- conditions compared to N+ except for *N. alexandrina.* For this latter species, the photosynthetic efficiency decreases similarly under N+ and N-. The general decrease can be explained by the deprivation of nitrogen, known to be the most important element contributing to the dry weight of microalgae cells (Jiang *et al*., 2012; White *et al*., 2011). And the low photosynthetic parameter for *N. alexandrina* under N+ condition could also be the consequence of phosphate limitation (Napoléon *et al*., 2013). Regarding the Ek photoacclimation parameter, as expected, lower values were obtained for LL acclimated cells due to their light harvesting complex modification to optimize the capture of light (Anning *et al*., 2000; Wilhelm *et al*., 2014). The variations of both parameters, Fv/Fm and Ek, according to light for the three species studied are consistent with Cruz *et al* study (Cruz and Serôdio, 2008) in which the same trend for *Nitzschia palea* under HL (400 µmol.photons.m^{-2}.s^{-1}) and LL treatment (20 µmol.photons.m^{-2}.s^{-1}) was found. They obtained an Ek value of 162.4 under HL and 44.3 under LL. In the present study, similar Ek value were found for *Staurosira* sp. with an Ek value of 133.36 ± 35.8 under HL and 62.16 ± 2.65 under LL. Ek values under LL for *E.*

paludosa (43.06 ± 4.25) and *N. alexandrina* (48.6 ± 1.80) were similar with Cruz *et al* study. However Ek values for these two species under HL were lower than *Staurosira* sp. For *E. paludosa,* Ek value under HL was 65.68 ± 10.74 and 59 ± 3.6 for *N. alexandrina*. These results suggest that *N. palea* and *Staurosira* sp. have an adaptation capacity to the strongest light superior to *E. paludosa* and *N.alexandrina*. In Cruz *et al.* study, Fv/Fm value was higher under LL (0.63) than HL (0.55) which is in accordance with our study. On the same way, Jauffrais *et al*. (2016) concluded that on the parameter Fv/Fm reflects photochemical processes depending on chloroplast reactions that use ATP and reductants provided by photosynthesis. In our study lower Fv/Fm values obtained under HL were associated with a lesser production of Chl *a*. It is proven that the decline in pigments due to HL exposure (Behrenfeld *et al*., 2004; Cruz and Serôdio, 2008) or nutrient limitation (Beardall *et al*., 2001b; Turpin, 1991) affect photosynthetic activity and so impacted Fv/Fm value.

Under nitrogen (Alipanah *et al*., 2015; Berges *et al*., 1996; Converti *et al*., 2009; Jiang *et al*., 2012) and phosphorus limitation (Geider *et al*., 1993; Mamaeva *et al*., 2018), a decline in cells pigment content often appears and induces chlorosis. This phenomenon leads to a decrease in photosynthetic efficiency as demonstrated by previous studies (Beardall *et al*., 2001a; Turpin, 1991; Zulu *et al*., 2018). Namely, Zulu at al, 2018 (Zulu *et al*., 2018) studied the photosynthetic machinery of the *Phaeodactylum trinocornutum* diatom upon exposure to nitrogen limitation. Its machinery degradation is induced hence the cells become chlorotic, and the nitrogen pools shut down and the cellular proteins decrease. As a result, biomass production is negatively affected as in the current study. Even if cells are nitrogen limited they continue to consume phosphate. To continue their growth, they must use intracellular inorganic storages , as for exemple Rubisco (known to be N-rich), which stops pigment production (Alipanah *et al*., 2015).

Nutrient consumption is impacted by culture conditions. Under repleted conditions, nitrate and phosphate consumption are more important under HL and ML than under LL. This expected

result is due to a slower growth under LL which is low nutrient consuming. However, for *E. paludosa* nitrogen and phosphate consumption were mainly impacted by light conditions while for *N. alexandrina* and *Staurosira* sp. nutrient consumption was mainly impacted by nitrogen concentration whatever the light. These results suggest that for some species, increased irradiance results in higher nitrogen and phosphate consumption as seen in other studies (Davis, 1976; Goldman and Dennis Jr, 2003), while for other species, light conditions do not impact nutrient consumption which is not currently described in the literature.

For *N. alexandrina*, It is important to specify that all the phosphate available in the medium whatever the culture conditions in light and nitrate is consumed. This similar phosphate consumption could be explained by the fact that several diatom species are able to store phosphate in excess in intracellular pools to be used in case of limitation (Cade-Menun and Paytan, 2010). This evolutionary advantage allowing the cells to cope with the field phosphate which often is the first nutrient in depletion (Lai *et al*., 2011) can be shared with *N. alexandrina*.

In the objective to use strains in biotechnology, most studies applied light or nutrient stress without verifying the Fv/Fm physiological parameter (Chen, 2012; Dean *et al*., 2010; Giordano *et al*., 2001; Mortensen *et al*., 1988; Roessler, 1988; Roleda *et al*., 2013; Wichien Yongmanitchai and Ward, 1991). If strains do not support culture conditions their macromolecular content can change, and in our case lipid quantity can be positively impacted but not necessarily lipid quality. To obtain a stable production of valuable compound it is necessary to ensure photosynthetic machinery integrity. Ek parameter enable us to ensure good acclimation of the cells and Fv/Fm enable us to confirm physiological states. It is essential to find culture conditions that support good growth and good physiological states, in our study these conditions are respected under LL and N repleted conditions. Some studies did take into account physiological parameters (Gao *et al*., 2013; He *et al*., 2015; Huete-Ortega *et al*., 2018; Jiang *et al*., 2012) but they dis analyze the effect of different light intensity and nutrient

limitation simultaneously and diatoms strains used where different than ours (*Pheodactylum tricornutum*, *Chaetoceros muelleri*, *Chlorella sp. L1*, *Monoraphidum dybowskii*, *Nannochloropsis oceanica*, *Thalassiosira pseudonana*, *Dunaliella tertiolecta*).

2.5.2 Macromolecular content

Microalgae cultured in stressful conditions remobilized carbon to produce energy storage products (carbohydrates and/or lipids) for later consumption to cope with the altered culture condition and survive. Nonetheless, this accumulation mechanism is not well understood (Sayanova Olga *et al*., 2017; Yi *et al*., 2017). He *et al*, 2015 found a 30% decreased in lipid content for two species of microalgae *Chlorella sp. L1* and *Monoraphidium dybowskii* cultured under LL intensity (40 µmol.photons.m^{-2}.s^{-1}) compared to cultures grown under HL (400 µmol.photons.m^{-2}.s^{-1}) (He *et al*., 2015). The same tendency occurs in this study with the three strains analyzed, suggesting the same strategy for these diatom strains than the chlorophytes studied by He *et al*.: under light starvation condition (e.g, LL) limited energy is allocated to the growth and with the rising light intensity, more energy is provided to the synthesis of storage materials (i.e. carbohydrates and lipids). In this study, whereas *E. paludosa* and *N. alexandrina* accumulate lipids under highest light intensities, *Staurosira* sp. accumulates carbohydrates. However, these observations are not applicable to all diatom species: *N. alexandrina* shows a decrease in carbohydrates content with light intensity, as demonstrated previously for the *Skeletonema costatum* diatom by Vårum *et al* (Vårum and Myklestad, 1984).

Nitrogen limitation also reduces the ability of microalgae to use carbon fixed during photosynthesis process. This carbon is normally used for protein synthesis. However, the decline in protein synthesis does not prevent cells from storing energy, that's why a deficit in carbons linked with nitrogen limitation may result in the accumulation of carbohydrates and/or lipids depending on the species (Berges *et al*., 1996; Quigg and Beardall, 2003). Accumulation of carbohydrates under nitrogen limitation has already been reported for *E. paludosa* by

Jauffrais *et al*. (2015) (Jauffrais *et al*., 2015) with a carbohydrate content of 36% under nitrogen repleted conditions and 67% under nitrogen limited conditions was found for this species. To our knowledge, only one study exists for *Staurosira* sp. (Huntley *et al*., 2015), showing low lipid accumulation under nitrogen depleted conditions: 36% under high N fertilization and 45% under low N fertilization. These results are not consistent with our study, however, it could be explained by the low difference in nitrogen consumption between the two medium conditions: the *Staurosira* strain used in our does not seem to be stressed by nitrogen condition tested and exhibits the highest lipid content whatever the nitrogen and the light condition with more than 25% of its DW and able to exceed 40 %.

Fatty acid composition of *E. paludosa* and *Staurosira* sp. were studied here for the first time whereas few studies concern *Nitzschia* genera (Chen *et al*., 2007; Joseph *et al*., 2017; Kates and Volcani, 1966; Renaud *et al*., 1999) and several concern diatoms (Ackman *et al*., 1964; Dunstan *et al*., 1993; Gao *et al*., 2013; Griffiths *et al*., 2012; Guihéneuf *et al*., 2008; Jiang and Gao, 2004; Joseph *et al*., 2017; Kates and Volcani, 1966; Volkman *et al*., 1989, 1980). For exemple Renaud *et al*, 1999 studied the gross chemical and fatty acid composition of 18 species including *Nitzschia* sp. (Renaud *et al*., 1999). Lipid content and fatty acid composition found for this diatom species are in accordance with our results, with a production of EPA and ARA occuring under 80 $\mu mol.m^{-2}.s^{-1}$ with a 12h/12h photoperiod and using F/2 medium. Regarding nitrogen limitation, this parameter seems to be the most impacting parameter for the three analyzed strains. This limitation is especially efficient for lipid accumulation into *N. alexandrina* cultures. However several detrimental effects of nitrogen limitation on photosynthesis have been identified in our study in accordance with previous ones (Berges *et al*., 1996; Turpin, 1991) as a decrease in Chl *a* and a 10 to 40 fold protein content decrease, contributing to chlorosis (Plumley and Schmidt, 1989). A consequence of this lake of de novo protein synthesis is a decrease in acetyl CoA carboxylase activity, the first committed step in

fatty acid biosynthesis (Roessler, 1988; Yu *et al*., 2009). Nitrogen limitation is truly stressful for the cells and can imply a loss of the ability to synthetize and accumulate qualitative fatty acids of economic interest (Hildebrand *et al*., 2012). In our study, *N. alexandrina* lost the ability to produce ARA and EPA when cultured under nitrogen limitation and under ML or HL. This suggests that if photosynthetic machinery is affected, lipid quality is impacted. Moreover, in this study when cells are stressed they tend to produce more SFA but less UFA. This trend has been observed previously by Yongmanitchai *et al*, 1991 on *Phaeodactylum tricornutum* (Wichien Yongmanitchai and Ward, 1991). This species produces less EPA and tends to accumulate SFA (C16:0) but also some UFA (C16:1, C18:1) when it grows under nitrogen limitation. Xia *et al*, 2013 observed a similar trend on *Odontella aurita* with a decrease in EPA (5.6 vs 2.2%) and ARA (12.9 vs 9.0%) under nitrogen limitation and an increase in SFA (25.4 vs 39.0%) which is in accordance with our study (Xia *et al*., 2013a). This species has been reported to be interesting in aquaculture feed by the authors.

2.5.3 Biotechnologies application

Fatty acids like EPA and ARA are considered pharmacologically important for dietetics and therapeutics. They have been used for prophylactic and therapeutic treatment of chronic inflammations (e.g. rheumatism, skin diseases, and inflammation of the mucosa of the gastrointestinal tract) (Pulz and Gross, 2004). They are also believed to have a positive effect on cardio-circulatory diseases, coronary heart diseases, artherosclerosis, hypertension, cholesterol and cancer treatment (Shahidi and Barrow, 2007). Fatty acids like SFA and MUFA are associated with TAGs, which are preferred substrates for biodiesel storage production by transesterification (Rodolfi *et al*., 2009).

Diatoms are reported to have higher lipid content than other algal classes (Hildebrand *et al*., 2012) . A literature survey by Griffiths and Harrison of 55 microalgae species in various classes (Griffiths and Harrison, 2009) showed that diatoms, as a class, have an average lipid content of

30.6 %DW while they found an average lipid content of 8.6%DW for Cyanobacteria, 23.17% DW for Chlorophyta, 20.5% for Ochrophyta and 23.8% for other classes (Dinophyta, Prasinophyta, Euglenozoa, Haptophyta). To be considered as an efficient lipid producer in industrial terms, microalgae have to accumulate at least 20% of their dry biomass as lipids (Pessôa *et al*., 2019). Overpassing this threshold, the three strains presented in this study are good candidate for biotechnology applications: *E. paludosa* and *Staurosira* sp. could be used for biofuel production because of their high production of SFA et UFA. Fatty acids like EPA and ARA produced by *N. alexandrina* could be used in the cosmetic or nutraceutical industries. The main conclusion of this study is in accordance with previous ones (Gao *et al*., 2013; He *et al*., 2015; Huete-Ortega *et al*., 2018) : lipid quantity and quality depend fundamentally on culture conditions including light environment and medium composition. But processing to control conditions for lipid production at industrial scale has a cost (Hildebrand *et al*., 2012). To be economically sustainable, used strains have to be consistent lipid producers under varied environmental conditions rather than strains with higher productivity but under optimal conditions, even if it is for a shorter period of time (Hildebrand *et al*., 2012). Implementation of lipid production processes for microalgae strains have to take into account these economic constraints. Knowing physiological capacity of strains is a necessary requirement to optimize culture conditions. If strains do not resist to culture conditions, which can be only assessed with physiological analysis, production of lipids of interest can be lost as seen in this study under HL and N- conditions. If culture conditions are adapted to photosynthetic machinery, long term lipid production can be assessed. In this point of view, even if nitrogen limitation and HL can enhance lipid content, this strategy is not advised for the production of lipids at industrial scale. Regarding *E. paludosa*, nitrogen limitation is inefficient to raise lipid production especially under LL. Even if growth takes longer, biomass was the same when grown under HL or LL, and photosynthetic efficiency remains high. In terms of cost, the use of the LL condition is

very interesting especially since *E. paludosa* produces more UFA and SFA and also because the need for high power artificial light sources increases the operating cost of microalgae production (Amaro *et al*., 2011)

For large scale production, *N. alexandrina* should be grown under ML and N+ medium to have an interesting biomass and preserved ARA and EPA production. If grown under higher light and N- medium this strain will lose its ability to produce ARA and EPA and physiological states will be affected which is not desirable for a long term production of these compounds.

Staurosira sp produces high amounts of lipids under depleted and repleted nutrient conditions but UFA and in particularly MUFA were preferentially produced under repleted conditions while under depleted conditions SFA were mostly produced. This species can also be grown under LL as for *E. paludosa*. This species could be used for biodiesel production, which in agreement with Huntley *et al* study. This species should be grown under LL and nutrient repleted conditions to obtain equal proportion of MUFA and SFA compatible with biodiesel.

2.6 Conclusion

Effects of different nitrogen concentrations and light conditions on *Entomoneis paludosa*, *Nitzschia alexandrina* and *Staurosira* sp. has been explored by the evaluation of growth, photosynthetic performance including photosynthetic efficiency as well as pigment content, macromolecular content (lipids, carbohydrates, proteins) and fatty acid compositions. Nitrogen limitation stimulates the accumulation of carbohydrates for *Entomoneis paludosa* and the accumulation of lipids for *Nitzschia alexandrina*. An irradiance between 100 and 400 µmol.photons.m^{-2}.s^{-1} stimulates the accumulation of lipids for *Entomoneis paludosa* and *Nitzschia alexandrina* while for *Staurosira* sp. it stimulates the accumulation of carbohydrates. Under HL and nitrogen limited condition, the content of proteins and pigments decline, when photosynthetic efficiency decreases supporting our main conclusion to develop lipid production

process which must be a compromise between economical and ecophysiological contraints. The selection of strains which respond to both aspects is the best solution for sustainable production of lipid at an industrial scale. In fact, the increase in lipid level does not mean an increase in the production of lipids of interests, indeed, while PUFAs are economically valuable, under light or nitrogen stress SFAs increases and PUFAs decreased also the production of EPA and ARA was stopped. The three new strains studied here are good candidates for biotechnology applications due to their lipid quantity and quality production under simple culture conditions: LL and nitrogen enrichment. However to increase lipid content and quality, it would be interesting to test other culture conditions as nutrient limitation like phosphate for example known to increase lipids content in diatoms without damaging photosynthetic machinery like nitrogen limitation does (Geider *et al*., 1993; Sharma *et al*., 2012). Development of a specific photobioreactor (PBR)(Ozkan *et al*., 2012; Schultze *et al*., 2015; Silva-Aciares and Riquelme, 2008; Tian *et al*., 2010) supporting biofilm culturing could also be interesting because the three species are benthic and naturally form biofilms. The association of high lipid production and quality with low use of water and light for culturing these species could be the best solution for new development of sustainable economical activities.

Acknowledgments

This work was supported by the regional Atlantic Microalgae research program (AMI), funded by the Pays de la Loire region. We also express our sincere thanks to IFREMER (French Institute for the research and exploitation of the Sea) staff in particular Ewa Lukomska for support and advice for the determination of nutrients.

Conflict of interest

The authors declare that there is no conflict of interest. No conflicts, informed consent, human or animal rights are applicable to this work.

Author's contribution

Eva Cointet, Gaëtane Wielgosz-Collin, Vona Méléder and Olivier Gonçalves designed and supervised the research. Eva Cointet, Gaëtane Wielgosz-Collin, Vona Méléder and Olivier Gonçalves, Gaël Bougaran and Vony Rabesaotra conducted experiments. Eva Cointet, Gaëtane Wielgosz-Collin, Vona Méléder and Olivier Gonçalves analyzed and interpreted the data and drafted the manuscript. Eva Cointet, Gaëtane Wielgosz-Collin, Vona Méléder and Olivier Gonçalves critically reviewed the manuscript. All authors read and approved the final version of the manuscript.

3 Conclusion

L'impact de différentes conditions de cultures sur la production lipidique chez *E. paludosa*, *N. alexandrina* et *Staurosira* sp. a été exploré en évaluant la croissance, les performances photosynthétiques, y compris l'efficacité photosynthétique, ainsi que la teneur en pigment, le contenu macromoléculaire (lipides, glucides, protéines) et les compositions en acides gras. La limitation en azote stimule l'accumulation de glucides pour *E. paludosa* et l'accumulation de lipides pour *N. alexandrina*. Une luminosité comprise entre 100 et 400 µmol.photons.m^{-2}.s^{-1} stimule l'accumulation de lipides chez *E. paludosa* et *N. alexandrina*, tandis que pour *Staurosira* sp. elle stimule l'accumulation de glucides. Dans des conditions de forte intensité lumineuse et lorsque les cellules sont limitées en azote, la teneur en protéines et en pigments diminue ainsi que l'efficacité photosynthétique, ce qui conforte notre principale conclusion de développer un processus de production de lipides qui doit être un compromis entre contraintes économiques et contraintes écophysiologiques. La sélection de souches répondant à ces deux aspects constitue le meilleur moyen de produire durablement des lipides à l'échelle industrielle. En effet, l'augmentation du taux de lipides ne signifie pas une augmentation de la production de lipides d'intérêt. Alors que les AGPI ont une valeur économique, les SFA augmentent légèrement lorque la culture est soumise à un stress azoté, tandis que les AGPI diminuent et que la production d'EPA et d'ARA est arrêtée. Les trois souches étudiées dans cette étude sont des candidates potentielles pour des applications en biotechnologies en raison de leur production quantitative et qualitative de lipides dans des conditions de culture simples : faible lumière et enrichissement en azote. Cependant, pour augmenter la teneur et la qualité des lipides, il serait intéressant de tester d'autres limitations nutritives, en phosphate par exemple, connu pour augmenter la teneur en lipides des diatomées sans endommager la machinerie photosynthétique, contrairement à la limitation de l'azote. Le développement d'un

photobioréacteur (PBR) spécifique maintenant la culture sous forme de biofilms pourrait également être intéressant, car les trois espèces sont benthiques et forment naturellement des biofilms ce qui permettrait de simuler des conditions naturelles de croissance, adaptées à leurs fonctionnements physiologiques, et d'obtenir une production de lipides plus reproductible. L'association d'une production et d'une qualité lipidique élevée avec une faible utilisation d'eau et de lumière pour la culture de ces espèces pourrait constituer le meilleur moyen de développer de nouvelles activités économiques durables.

Conclusion générale et perspectives

L'objectif principal de ce travail de thèse était d'explorer le potentiel biotechnologique des diatomées marines benthiques. Cette thèse s'est principalement concentrée sur le potentiel lipidique des espèces et l'évaluation de la bioactivité des fractions TAG et glycolipidiques obtenues.

Ce travail s'est déroulé en plusieurs étapes et a consisté en un criblage sur plus de 100 espèces en prenant en compte différents critères, et plus particulièrement : la capacité de croissance et la teneur en lipides.

La première étape a consisté en une analyse bibliographique exhaustive des genres et espèces présentes dans la collection NCC et a permis de sélectionner 66 espèces. Cette revue de la littérature pourra faire l'objet d'une publication puisqu'elle recense les connaissances et utilisation actuelle disponible sur plus de 40 genres de diatomées marines benthique, ce qui n'a jamais été réalisé auparavant.

La deuxième étape a permis de mettre en place une technique rapide et efficace de sélection. La technique du PAM a été utilisée pour analyser les capacités de croissance et la technique FTIR-HTSXT a été utilisée pour identifier le potentiel lipidique des espèces criblées. Les 5 esp-ces possédant les plus forts taux de croissance et un fort potentiel oléagineux ont été sélectionnées : *Amphora* sp., *Nitzschia alexandrina*, *Nitzschia* sp., *Opephora* sp. et *Staurosira* sp. Une 6^{éme} espèce a été sélectionnée en tant que témoin : *E. paludosa*. L'approche originale développée dans ce travail ouvre la voie pour de futurs criblages rapide sur de grandes quantités de microalgues puisqu'elle est non invasive et peut être appliquée directement sur cellules entières.

La troisième étape a concerné les tests de production de ces 6 espèces en photobioreacteur airlift et en l'analyse fine de la composition lipidique de ces espèces. Cette étape a permis d'identifier trois espèces qui supportent la croissance en photobioréacteur et qui possèdent un profil lipidique intéressant à des fins industrielles : *Entomoneis paludosa*, *Nitzschia alexandrina* et *Staurosira* sp. Les résultats positifs obtenus pour l'espèce *E. paludosa* montre toutefois les limites du criblage puisque cette espèce, considéré comme témoin, à finalement supplantée les capacités de croissance et lipidique d'autres souches sélectionnées. Elle peut finalement atteindre une biomasse identique à *N. alexandrina* en PBR (1.16 $g.L^{-1}$) et elle est l'espèce qui produit le plus d'EPA (12.6 %). *Staurosira* sp. et *Nizschia* sp. restent cependant les espèces produisant le plus de lipides (40.9% et 20.8% respectivement) et *N. alexandrina* l'espèce avec la plus forte capacité de croissance, qu'elles soient cultivées en erlenmeyer ou en airlift. Ce qui démontre bien l'efficacité du criblage effectué avec des méthodes non-invasives.

La quatrième étape a permis d'évaluer le potentiel bioactif des fractions TAG et glycolipidiques obtenu sur ces trois espèces en les cultivant en ballon de 25 L. Des activités antibactériennes sur une bactérie à gram-positif (*B. subtilus*) ont été découvertes ainsi que des activités antiproliférives des fractions glycolipidiques sur des cellules appartenant à la lignée MCF-7 du cancer du sein et la lignée NSCLC-N6 du cancer du poumon. Les fractions TAG et pigments issues de l'espèce *Staurosira* sp. ont démontré une activité antibactérienne sur *B. subtilus*, ce qui suggére une utilisation direct de l'extrait lipidique de cette souche comme produit antibactérien. Les fractions glycolipidiques de *E. paludosa* (MGDG, DGDG and SQDG) et de *N. alexandrina* (DGDG) ont démontré une activité antiproliferative contre la lignée NSCLC-N6. L'activité potentielle découverte sur cette lignée est très intéressante puisqu'elle a été peu étudiée dans la littérature, exceptée dans l'étude de Kendel *et al*, 2015 ou des glycolipides issus de deux macroalgues (*Ulva armoricana* et *Soliera chordalis*) ont montrés une activité antiproliférative sur la lignée NSCLC-N6 avec une CI_{50} de 24 $\mu g.mL^{-1}$ pour la fraction DGDG

issues de *U. armoricana* et 23 µg.mL^{-1} pour la fraction MGDG issues de *S.chordalis*. Dans notre étude, des résultats supérieurs ont été obtenues sur la lignée NSCLC-N6 avec l'utilisation des fractions A4Ep (SQDG), A4Na (DGDG) et A5NA (DGDG) issues de *E. paludosa* et *N. alexandrina* puisque la CI_{50} est inférieure à 18 µg.mL^{-1}.

Nos travaux confirment le potentiel bioactif des glycolipides et notamment lorsqu'ils sont issus de diatomées marines benthiques. Ceci est encourageant dans la découverte de principes actifs valorisables en santé issus de ces diatomées.

Après avoir évalué le potentiel bioactif des souches étudiées, l'impact des conditions de cultures (lumière et nutriment) a été évalué pour optimiser la croissance et la production de lipides d'intérêt. Il en résulte que pour conserver la production d'acides gras valorisable et maintenir un bon fonctionnement photosynthétique des cellules, l'ensemble de ces espèces doivent être produites sous de faibles intensités lumineuses et dans un milieu non-limitant en azote. Ces résultats contredisent d'autres études qui suggèrent généralement de cultiver les souches sous un stress azoté et sous une très forte intensité lumineuse pour augmenter la capacité de production lipidique des souches (Chen, 2012; Dean *et al*., 2010; Giordano *et al*., 2001; Mortensen *et al*., 1988; Roleda *et al*., 2013). Cependant ces recommandations ne prennent pas en compte l'état photosynthétique des cellules et comme démontré dans notre étude, lorsque la machinerie photosynthétique est affectée, la quantité globale de lipides augmente, mais ce sont des classes lipidiques finalement peu intéressantes (comme les AGS) qui sont produites au détriments d'autres classes de lipides à hautes valeurs ajoutées (comme les AGPI). Afin de produire des microalgues avec l'objectif d'un usage en biotechnologie, la mesure des paramètres photosynthétiques devrait être systématique pour s'assurer du bon fonctionnement physiologique de la cellule et maintenir la production de composés valorisables.

Les résultats obtenus dans ce travail ouvrent de nombreuses perspectives. Les capacités de production obtenues en PBR airlift pourraient permettre un scalling-up en bassin sur l'ensemble

des trois espèces sélectionées. Cependant, des analyses complémentaires en photobioréacteur à petite échelle semblent encore nécessaires. En effet, les conditions de culture peuvent être encore optimisées pour mettre en place un milieu et des conditions de culture spécifiques pour chacune des espèces, ce qui permettrait de diminuer les coûts de production. La méthode de production en photobioréacteur airlift utilisée dans ce travail et impliquant un fed-batch quotidien n'est pas économiquement viable et difficilement applicable pour une production à grande échelle. Une formulation de milieu de culture adéquate par espèce est nécessaire en prenant en compte l'équation stoechiométrique de la biomasse telle qu'appliquée par Pruvost *et al*., 2009 (Pruvost *et al*., 2009). Il faudrait également tester la modification des conditions de culture directement en photobioréacteur afin de contrôler le plus de paramètres possible comme le pH par exemple, ce qui n'a pas pu être réalisé lors de l'étude de la capacité photosynthétique des espèces.

Il est cependant intéressant de préciser que lors du passage en culture en ballon de 25 L, la composition biochimique a finalement peu varié comparer aux résultats de l'étude physiologique. Cela permet d'envisager la production de composés chimiquement valorisables dans des conditions moins contrôlées ce qui pourrait faciliter le passage en production à grande échelle. Il faudrait cependant conserver une température entre 16 et 20°C et un flux lumineux de 127 µmol.photons.m^{-2}.s^{-1} en continu ce qui constitue un coût énergétique encore conséquent. Pour diminuer les coûts de production, il faudrait tester les capacités de croissance et de production lipidique des cultures en bassin soumis aux fluctuations naturelles de lumières et de températures.

Le stress en azote s'étant finalement révélé peu efficace, d'autres stress environnementaux devrait être testés sur les trois espèces sélectionnées : stress thermique, limitation en phosphate ou silice et également l'effet de l'apport en CO_2. Ces différents facteurs limitants pourraient permettre d'optimiser le profil lipidique de ces espèces. Il est par ailleurs conseillé de réaliser

ces tests en photobioréacteur pour dans un premier temps obtenir une biomasse suffisante pour les analyses et ensuite réaliser un stress. Les conditions de culture seront mieux contrôlées et l'impact de ces stress mieux évalués.

Les bioactivités obtenues sur les fractions glycolipidiques et TAG sont prometteuses, mais la structure des molécules bioactives est en cours d'identification. Des analyses complémentaires sont en cours sur ces fractions pour isoler et purifier le ou les composés specifiquement bioactifs.

En conclusion, la méthodologie de sélection mise en œuvre dans cette étude constitue un travail très original et transdisciplinaire puisqu'il couple des connaissances en génie des procédes, en chimie et en écophysiologie. Elle ouvre également la voie à l'utilisation d'outils non-invasifs pour établir un screening préalable sur une grande quantité de souches microalgales. L'ensemble de ces travaux ouvre la voie de l'utilisation des diatomées marines benthiques à des fins biotechnologiques et laisse apparaître de nombreuses perspectives au niveau expérimental.

Références bibliographique

Abedin, R.M., Taha, H.M., 2008. Antibacterial and antifungal activity of cyanobacteria and green microalgae. Evaluation of medium components by Plackett-Burman design for antimicrobial activity of *Spirulina platensis*. Global Journal of Biotechnology and Biochemistry 3, 22–31.

Ackman, R.G., Jangaard, P.M., Hoyle, R.J., Brockerhoff, H., 1964. Origin of marine fatty acids. I. Analyses of the fatty acids produced by the diatom *Skeletonema costatum*. Journal of the Fisheries Board of Canada, 21, 747–756.

Akoto, L., Pel, R., Irth, H., Udo, A.T., Vreuls, R.J., 2005. Automated GC–MS analysis of raw biological samples: Application to fatty acid profiling of aquatic micro-organisms. Journal of Analytical and Applied Pyrolysis 73, 69–75.

Al-Fadhli, A., Wahidulla, S., D'Souza, L., 2006. Glycolipids from the red alga *Chondria armata* (Kütz.) Okamura. Glycobiology 16, 902–915.

Alipanah, L., Rohloff, J., Winge, P., Bones, A.M., Brembu, T., 2015. Whole-cell response to nitrogen deprivation in the diatom *Phaeodactylum tricornutum*. Journal of experimental botany, 66, 6281–6296.

Allen, E.J., 1914. On the Culture of the Plankton Diatom *Thalassiosira grauida* cleve, in artificial sea-water. Journal of the Marine Biological Association of the United Kingdom 10, 417–439.

Alonso, D.L., Belarbi, E.-H., Fernández-Sevilla, J.M., Rodríguez-Ruiz, J., Grima, E.M., 2000. Acyl lipid composition variation related to culture age and nitrogen concentration in continuous culture of the microalga *Phaeodactylum tricornutum*. Phytochemistry 54, 461–471.

Amaro, H.M., Guedes, A.C., Malcata, F.X., 2011. Advances and perspectives in using microalgae to produce biodiesel. Applied Energy, Special Issue of Energy from algae: Current status and future trends 88, 3402–3410.

Amin, S.A., Hmelo, L.R., van Tol, H.M., Durham, B.P., Carlson, L.T., Heal, K.R., Morales, R.L., Berthiaume, C.T., Parker, M.S., Djunaedi, B., Ingalls, A.E., Parsek, M.R., Moran, M.A., Armbrust, E.V., 2015. Interaction and signalling between a cosmopolitan phytoplankton and associated bacteria. Nature 522, 98–101.

Aminot, A., Kérouel, R., 2004. Hydrologie des écosystèmes marins: paramètres et analyses. Editions Quae.

Anderson, R., Kates, M., Volcani, B., 1978. Identification of the sulfolipids in the non-photosynthetic diatom *Nitzschia alba*. Biochimica et Biophysica Acta (BBA)-Lipids and Lipid Metabolism 528, 89–106.

Anning, T., MacIntyre, H.L., Pratt, S.M., Sammes, P.J., Gibb, S., Geider, R.J., 2000. Photoacclimation in the marine diatom *Skeletonema costatum*. Limnology and Oceanography 45, 1807–1817.

Antia, N., Harrison, P., Oliveira, L., 1991. The role of dissolved organic nitrogen in phytoplankton nutrition, cell biology and ecology. Phycologia 30, 1–89.

Arao, T., Kawaguchi, A., Yamada, M., 1987. Positional distribution of fatty acids in lipids of the marine diatom *Phaeodactylum tricornutum*. Phytochemistry 26, 2573–2576.

Arao, T., Sakaki, T., Yamada, M., 1994. Biosynthesis of polyunsaturated lipids in the diatom, *Phaeodactylum tricornutum*. Phytochemistry, The International Journal of Plant Biochemistry 36, 629–635.

Armbrust, E.V., Berges, J.A., Bowler, C., Green, B.R., Martinez, D., Putnam, N.H., Zhou, S., Allen, A.E., Apt, K.E., Bechner, M., 2004. The genome of the diatom *Thalassiosira pseudonana*: ecology, evolution, and metabolism. Science 306, 79–86.

Artamonova, E., Svenning, J., Vasskog, T., Hansen, E., Eilertsen, H., 2017. Analysis of phospholipids and neutral lipids in three common northern cold water diatoms: *Coscinodiscus concinnus*, *Porosira glacialis*, and *Chaetoceros socialis*, by ultra-high performance liquid chromatography-mass spectrometry. Journal of Applied Phycology 29, 1241–1249.

Bajpai, P., Bajpai, P.K., 1993. Eicosapentaenoic acid (EPA) production from microorganisms: a review. Journal of biotechnology 30, 161–183.

Baker, N.R., 2008. Chlorophyll fluorescence: a probe of photosynthesis in vivo. Annual Review of Plant Biology. 59, 89–113.

Barnett, A., Méléder, V., Blommaert, L., Lepetit, B., Gaudin, P., Vyverman, W& Lavaud, J. (2015). Growth form defines physiological photoprotective capacity in intertidal benthic diatoms. The ISME journal, 9(1), 32.Barrett, S.M., Volkman, J.K., Dunstan, G.A., LeRoi, J., 1995. Sterols of 14 Species of marine diatoms (bacillariophyta) 1. Journal of Phycology 31, 360–369.

Bates, S., Bird, C.J., Freitas, A. de, Foxall, R., Gilgan, M., Hanic, L.A., Johnson, G.R., McCulloch, A., Odense, P., Pocklington, R., 1989. Pennate diatom *Nitzschia pungens* as the primary source of domoic acid, a toxin in shellfish from eastern Prince Edward Island, Canada. Canadian Journal of Fisheries and Aquatic Sciences 46, 1203–1215.

Beardall, J., Berman, T., Heraud, P., Kadiri, M.O., Light, B.R., Patterson, G., Roberts, S., Sulzberger, B., Sahan, E., Uehlinger, U., 2001a. A comparison of methods for detection of phosphate limitation in microalgae. Aquatic Sciences 63, 107–121.

Beardall, J., Young, E., Roberts, S., 2001b. Approaches for determining phytoplankton nutrient limitation. Aquatic sciences, 63, 44–69.

Becker, E.W., 1994. Microalgae: Biotechnology and Microbiology. Cambridge University Press.

Beer, S., Vilenkin, B., Weil, A., Veste, M., Susel, L., Eshel, A., 1998. Measuring photosynthetic rates in seagrasses by pulse amplitude modulated (PAM) fluorometry. Marine Ecology Progress Series 174, 293–300.

Behrenfeld, M.J., Prasil, O., Babin, M., Bruyant, F., 2004. In Search of a physiological basis for covariations in light-limited and light-saturated photosynthesis1. Journal of Phycology 40, 4–25.

Belarbi, E.H., Molina, E., Chisti, Y., 2000. A process for high yield and scaleable recovery of high purity eicosapentaenoic acid esters from microalgae and fish oil. Enzyme and Microbial Technology 26, 516–529.

Bellou, S., Baeshen, M.N., Elazzazy, A.M., Aggeli, D., Sayegh, F., Aggelis, G., 2014. Microalgal lipids biochemistry and biotechnological perspectives. Biotechnology Advances 32, 1476–1493.

Bergé, J., Bourgougnon, N., Carbonnelle, D., Le, V.B., Tomasoni, C., Durand, P., Roussakis, C., 1997. Antiproliferative effects of an organic extract from the marine diatom *Skeletonema costatum* (Grev.) Cleve. Against a non-small-cell bronchopulmonary carcinoma line (NSCLC-N6). Anticancer research 17, 2115–2120.

Bergé, J.-P., Barnathan, G., 2005. Fatty acids from lipids of marine organisms: molecular biodiversity, roles as biomarkers, biologically active compounds, and economical aspects, in: Marine Biotechnology I. Springer, pp. 49–125.

Bergé, J.-P., Bourgougnon, N., Alban, S., Pojer, F., Billaudel, S., Chermann, J.-C., Robert, J.M., Franz, G., 1999. Antiviral and anticoagulant activities of a water-soluble fraction of the marine diatom *Haslea ostrearia*. Planta Med 65, 604–609.

Berge, J.-P., Gouygou, J.-P., Dubacq, J.-P., Durand, P., 1995. Reassessment of lipid composition of the diatom, *Skeletonema costatum*. Phytochemistry 39, 1017–1021.

Berges, J.A., Charlebois, D.O., Mauzerall, D.C., Falkowski, P.G., 1996. Differential effects of nitrogen limitation on photosynthetic efficiency of photosystems I and II in microalgae. Plant Physiology 110, 689–696.

Berges, J.A., Falkowski, P.G., 1998. Physiological stress and cell death in marine phytoplankton: induction of proteases in response to nitrogen or light limitation. Limnology and Oceanography 43, 129–135.

Berges, J.A., Franklin, D.J., Harrison, P.J., 2001. Evolution of an artificial seawater medium: improvements in enriched seawater, artificial water over the last two decades. Journal of Phycology 37, 1138–1145.

Berthon, J.-Y., Nachat-Kappes, R., Bey, M., Cadoret, J.-P., Renimel, I., Filaire, E., 2017. Marine algae as attractive source to skin care. Free Radical Research 51, 555–567.

Bligh, E.G., Dyer, W.J., 1959. A rapid method of total lipid extraction and purification. Canadian Journal of Biochemistry and Physiology 37, 911–917.

Blunt, J.W., Copp, B.R., Munro, M.H., Northcote, P.T., Prinsep, M.R., 2015. Marine natural products. Natural product reports 28, 196–268.

Boelen, P., van Dijk, R., Damsté, J.S.S., Rijpstra, W.I.C., Buma, A.G., 2013. On the potential application of polar and temperate marine microalgae for EPA and DHA production. AMB Express 3, 26.

Bondioli, P., Della Bella, L., Rivolta, G., Zittelli, G.C., Bassi, N., Rodolfi, L., Casini, D., Prussi, M., Chiaramonti, D., Tredici, M.R., 2012. Oil production by the marine microalgae *Nannochloropsis* sp. F&M-M24 and *Tetraselmis suecica* F&M-M33. Bioresource technology 114, 567–572.

Borowitzka, M.A., 2013. High-value products from microalgae—their development and commercialisation. Journal of Applied Phycologie 25, 743–756.

Borowitzka, M.A., 1999. Commercial production of microalgae: ponds, tanks, and fermenters, in: Progress in Industrial Microbiology. Elsevier, pp. 313–321.

Borowitzka, M.A., Borowitzka, L.J., 1988. Micro-algal biotechnology. Cambridge University Press.

Bougaran, G., Bernard, O., Sciandra, A., 2010. Modeling continuous cultures of microalgae colimited by nitrogen and phosphorus. Journal of Theoretical Biology 265, 443–454.

Brand, L., Guillard, R., 1981. The effects of continuous light and light intensity on the reproduction rates of twenty-two species of marine phytoplankton. Journal of Experimental Marine Biology and Ecology 50, 119–132.

Brand, L.E., Guillard, R.R., Murphy, L.S., 1981. A method for the rapid and precise determination of acclimated phytoplankton reproduction rates. Journal of plankton research 3, 193–201.

Breil, C., Abert Vian, M., Zemb, T., Kunz, W., Chemat, F., 2017. “Bligh and Dyer” and Folch methods for solid–liquid–liquid extraction of lipids from microorganisms. comprehension of solvatation mechanisms and towards substitution with alternative solvents. International Journal of Molecular Sciences 18 (4), 708.

Breuer, G., Evers, W.A., de Vree, J.H., Kleinegris, D.M., Martens, D.E., Wijffels, R.H., Lamers, P.P., 2013a. Analysis of fatty acid content and composition in microalgae. Journal of visualized experiments: JoVE.

Breuer, G., Lamers, P.P., Martens, D.E., Draaisma, R.B., Wijffels, R.H., 2013b. Effect of light intensity, pH, and temperature on triacylglycerol (TAG) accumulation induced by nitrogen starvation in *Scenedesmus obliquus*. Bioresource technology 143, 1–9.

Breuer, G., Lamers, P.P., Martens, D.E., Draaisma, R.B., Wijffels, R.H., 2012. The impact of nitrogen starvation on the dynamics of triacylglycerol accumulation in nine microalgae strains. Bioresource Technology 124, 217–226.

Bromke, M.A., Sabir, J.S., Alfassi, F.A., Hajarah, N.H., Kabli, S.A., Al-Malki, A.L., Ashworth, M.P., Méret, M., Jansen, R.K., Willmitzer, L., 2015. Metabolomic profiling of 13 diatom cultures and their adaptation to nitrate-limited growth conditions. PLOS ONE 10, e0138965.

Brown, M.R., Dunstan, G.A., Norwood, S.J., Miller, K.A., 1996. Effects of harvest stage and light on the biochemical composition of the diatom *Thalassiosira pseudonana* 1. Journal of phycology 32, 64–73.

Cade-Menun, B.J., Paytan, A., 2010. Nutrient temperature and light stress alter phosphorus and carbon forms in culture-grown algae. Marine Chemistry 121, 27–36.

Chelf, P., 1990. Environmental control of lipid and biomass production in two diatom species. Journal of Applied Phycology 2, 121–129.

Chen, F., Jiang, Y., 2013. Algae and their Biotechnological Potential. Springer Science & Business Media.

Chen, G., Jiang, Y., Chen, F., 2007. Fatty acid and lipid class composition of the eicosapentaenoic acid-producing microalga, *Nitzschia laevis*. Food Chemistry 104, 1580–1585.

Chen, W., Zhang, C., Song, L., Sommerfeld, M., Hu, Q., 2009. A high throughput Nile red method for quantitative measurement of neutral lipids in microalgae. Journal of Microbiological Methods 77, 41–47.

Chen, X., Gao, K., 2004. Photosynthetic utilisation of inorganic carbon and its regulation in the marine diatom *Skeletonema costatum*. Functional Plant Biology 31, 1027–1033.

Chen, Y.-C., 2012. The biomass and total lipid content and composition of twelve species of marine diatoms cultured under various environments. Food Chemistry 131, 211–219.

Chen, Y.-C., 2007. Immobilization of twelve benthic diatom species for long-term storage and as feed for post-larval abalone *Haliotis diversicolor.* Aquaculture 263, 97–106.

Chesters, C.G., Stott, J., 1956. The production of antibiotic substances by seaweeds. Presented at the International Seaweed Symposium, pp. 49–53.

Chew, K.W., Yap, J.Y., Show, P.L., Suan, N.H., Juan, J.C., Ling, T.C., Lee, D.-J., Chang, J.-S., 2017a. Microalgae biorefinery: High value products perspectives. Bioresource Technology 229, 53–62.

Chisti, Y., 2007a. Biodiesel from microalgae. Biotechnology Advances 25, 294–306.

Chisti, Y., 2007b. Biodiesel from microalgae. Biotechnology Advances 25, 294–306.

Chtourou, H., Dahmen, I., Jebali, A., Karray, F., Hassairi, I., Abdelkafi, S., Ayadi, H., Sayadi, S., Dhouib, A., 2015. Characterization of *Amphora* sp., a newly isolated diatom wild strain, potentially usable for biodiesel production. Bioprocess and Biosystems Engineering 38, 1381–1392.

Chuecas, L., Riley, J.P., 1969. Component fatty acids of the total lipids of some marine phytoplankton. Journal of the Marine Biological Association of the United Kingdom 49, 97.

Coat, R., Montalescot, V., León, E.S., Kucma, D., Perrier, C., Jubeau, S., Thouand, G., Legrand, J., Pruvost, J., Gonçalves, O., 2014. Unravelling the matrix effect of fresh sampled cells

for in vivo unbiased FTIR determination of the absolute concentration of total lipid content of microalgae. Bioprocess and biosystems engineering 37, 2175–2187.

Cointet, E., Wielgosz-Collin, G., Méléder, V., Gonçalves, O., 2019. Lipids in benthic diatoms: A new suitable screening procedure. Algal Research 39, 101425.

Consalvey, M., Perkins, R.G., Paterson, D.M., Underwood, G.J.C., 2005. PAM fluorescence: a beginners guide for benthic diatomists. Diatom Research 20, 1–22.

Converti, A., Casazza, A.A., Ortiz, E.Y., Perego, P., Del Borghi, M., 2009. Effect of temperature and nitrogen concentration on the growth and lipid content of *Nannochloropsis oculata* and *Chlorella vulgaris* for biodiesel production. Chemical Engineering and Processing: Process Intensification 48, 1146–1151.

Cooksey, K.E., Guckert, J.B., Williams, S.A., Callis, P.R., 1987. Fluorometric determination of the neutral lipid content of microalgal cells using Nile Red. Journal of microbiological methods 6, 333–345.

Cooper, M.S., Hardin, W.R., Petersen, T.W., Cattolico, R.A., 2010. Visualizing “green oil” in live algal cells. Journal of Bioscience and Bioengineering 109, 198–201.

Croft, M.T., Lawrence, A.D., Raux-Deery, E., Warren, M.J., Smith, A.G., 2005. Algae acquire vitamin B 12 through a symbiotic relationship with bacteria. Nature 438, 90.

Cruz, S., Serôdio, J., 2008. Relationship of rapid light curves of variable fluorescence to photoacclimation and non-photochemical quenching in a benthic diatom. Aquatic Botany 88, 256–264.

Csögör, Z., Melgar, D., Schmidt, K., Posten, C., 1999. Production and particle characterization of the frustules of Cyclotella cryptica in comparison with siliceous earth. Journal of biotechnology 70, 71–75.

d’Ippolito, G., Sardo, A., Paris, D., Vella, F.M., Adelfi, M.G., Botte, P., Gallo, C., Fontana, A., 2015. Potential of lipid metabolism in marine diatoms for biofuel production. Biotechnology for biofuels 8, 28.

d’Ippolito, G., Tucci, S., Cutignano, A., Romano, G., Cimino, G., Miralto, A., Fontana, A., 2004. The role of complex lipids in the synthesis of bioactive aldehydes of the marine diatom *Skeletonema costatum*. Biochimica et Biophysica Acta (BBA) - Molecular and Cell Biology of Lipids 1686, 100–107.

Da Costa, E., Melo, T., Moreira, A., Bernardo, C., Helguero, L., Ferreira, I., Cruz, M., Rego, A., Domingues, P., Calado, R., 2017. Valorization of lipids from *Gracilaria* sp. through lipidomics and decoding of antiproliferative and anti-inflammatory activity. Marine drugs 15, 62.

Da Costa, E., Silva, J., Mendonça, S.H., Abreu, M.H., Domingues, M.R., 2016. Lipidomic approaches towards deciphering glycolipids from microalgae as a reservoir of bioactive lipids. Marine Drugs 14, 101.

Dalay, M.C., Gunes, S.S., others, 2014. Biodiesel from Microalgae: A Renewable Energy Source. Middle East Journal of Scientific Research 22, 350–355.

Davidovich, N., Davidovich, O., Podunai, Y.A., Shorenko, K., Kulikovskii, M., 2015. Reproductive properties of diatoms significant for their cultivation and biotechnology. Russian journal of plant physiology 62, 153–160.

Davis, C.O., 1976. Continuous culture of marine diatoms under silicate limitation. Ii. Effect of light intensity on growth and nutrient uptake of *Skeletonema costatum*1,2. Journal of Phycology 12, 291–300.

Davoodbasha, M., Edachery, B., Nooruddin, T., Lee, S.-Y., Kim, J.-W., 2018. An evidence of C16 fatty acid methyl esters extracted from microalga for effective antimicrobial and antioxidant property. Microbial Pathogenesis 115, 233–238.

De Castro Araújo, S., Garcia, V.M.T., 2005. Growth and biochemical composition of the diatom *Chaetoceros cf. wighamii brightwell* under different temperature, salinity and carbon dioxide levels. I. Protein, carbohydrates and lipids. Aquaculture 246, 405–412.

De Jesus Raposo, M.F., de Morais, R.M.S.C., de Morais, A.M.M.B., 2013. Health applications of bioactive compounds from marine microalgae. Life Sciences 93, 479–486.

De la Hoz Siegler, H., Ayidzoe, W., Ben-Zvi, A., Burrell, R., McCaffrey, W., 2012. Improving the reliability of fluorescence-based neutral lipid content measurements in microalgal cultures. Algal Research 1, 176–184.

De la Pena, M., 2007. Cell growth and nutritive value of the tropical benthic diatom, *Amphora* sp., at varying levels of nutrients and light intensity, and different culture locations. Journal of Applied Phycology 19, 647–655.

De Morais, M.G., Vaz, B. da S., de Morais, E.G., Costa, J.A.V., 2015. Biologically active metabolites synthesized by microalgae. BioMed research international 2015.

De Souza, M.P., Hoeltz, M., Gressler, P.D., Benitez, L.B., Schneider, R.C.S., 2018. Potential of microalgal bioproducts: General perspectives and main challenges. Waste and Biomass Valorization, 1-18.

Dean, A.P., Sigee, D.C., Estrada, B., Pittman, J.K., 2010. Using FTIR spectroscopy for rapid determination of lipid accumulation in response to nitrogen limitation in freshwater microalgae. Bioresource Technology 101, 4499–4507.

Delattre, C., Pierre, G., Laroche, C., Michaud, P., 2016. Production, extraction and characterization of microalgal and cyanobacterial exopolysaccharides. Biotechnology advances 34, 1159–1179.

Dempster, T.A., Sommerfeld, M.R., 1998. Effects of environmental conditions on growth and lipid accumulation in *Nitzschia communis* (Bacillariophyceae). Journal of Phycology 34, 712–721.

Derrien, A., Coiffard, L.J.M., Coiffard, C., De Roeck-Holtzhauer, Y., 1998. Free amino acid analysis of five microalgae. Journal of Applied Phycology 10, 131.

Desbois, A.P., Lebl, T., Yan, L., Smith, V.J., 2008. Isolation and structural characterisation of two antibacterial free fatty acids from the marine diatom, *Phaeodactylum tricornutum.* Appl Microbiol Biotechnol 81, 755–764.

Desbois, A.P., Mearns-Spragg, A., Smith, V.J., 2009. A fatty acid from the diatom *Phaeodactylum tricornutum* is antibacterial against diverse bacteria including multi-resistant *Staphylococcus aureus* (MRSA). Marine Biotechnology 11, 45–52.

Desbois, A.P., Smith, V.J., 2010. Antibacterial free fatty acids: activities, mechanisms of action and biotechnological potential. Applied Microbiology and Biotechnology 85, 1629–1642.

Doan, T.T.Y., Sivaloganathan, B., Obbard, J.P., 2011. Screening of marine microalgae for biodiesel feedstock. Biomass and Bioenergy 35, 2534–2544.

Dortch, Q., 1982. Effect of growth conditions on accumulation of internal nitrate, ammonium, amino acids, and protein in three marine diatoms. Journal of Experimental Marine Biology and Ecology 61, 243–264.

Dreissig, I., Machill, S., Salzer, R., Krafft, C., 2009. Quantification of brain lipids by FTIR spectroscopy and partial least squares regression. Spectrochimica Acta Part A: Molecular and Biomolecular Spectroscopy 71, 2069–2075.

Drum, R.W., Gordon, R., 2003. Star Trek replicators and diatom nanotechnology. Trends in Biotechnology 21, 325–328.

Dubinsky, Z., Rotem, J., 1974. Relations between algal populations and the pH of their media. Oecologia 16, 53–60.

Dufossé, L., Galaup, P., Yaron, A., Arad, S.M., Blanc, P., Murthy, K.N.C., Ravishankar, G.A., 2005. Microorganisms and microalgae as sources of pigments for food use: a scientific oddity or an industrial reality? Trends in Food Science & Technology 16, 389–406.

Dunstan, G.A., Volkman, J.K., Barrett, S.M., Leroi, J.-M., Jeffrey, S.W., 1993. Essential polyunsaturated fatty acids from 14 species of diatom (Bacillariophyceae). Phytochemistry, The international journal of plant biochemistry 35, 155–161.

Eilers, P., Peeters, J., 1988. A model for the relationship between light intensity and the rate of photosynthesis in phytoplankton. Ecological modelling 42, 199–215.

Eitsuka, T., Nakagawa, K., Igarashi, M., Miyazawa, T., 2004. Telomerase inhibition by sulfoquinovosyldiacylglycerol from edible purple laver (*Porphyra yezoensis*). Cancer Letters. 212, 15–20.

Elsey, D., Jameson, D., Raleigh, B., Cooney, M.J., 2007. Fluorescent measurement of microalgal neutral lipids. Journal of Microbiological Methods 68, 639–642.

Fajardo, A.R., Cerdán, L.E., Medina, A.R., Fernández, F.G.A., Moreno, P.A.G., Grima, E.M., 2007. Lipid extraction from the microalga *Phaeodactylum tricornutum*. European Journal of Lipid Science and Technology 109, 120–126.

Falkowski, P.G., Raven, J.A., 2013. Aquatic photosynthesis. Princeton University Press.

Fan, J., Cui, Y., Wan, M., Wang, W., Li, Y., 2014. Lipid accumulation and biosynthesis genes response of the oleaginous *Chlorella pyrenoidosa* under three nutrition stressors. Biotechnology for Biofuels 7, 17.

FAO, 2018. The State of World Fisheries and Aquaculture 2018: Meeting the sustainable development goals, The State of World Fisheries and Aquaculture. FAO, Rome, Italy.

Feng, G.-D., Zhang, F., Cheng, L.-H., Xu, X.-H., Zhang, L., Chen, H.-L., 2013. Evaluation of FT-IR and Nile Red methods for microalgal lipid characterization and biomass composition determination. Bioresource technology 128, 107–112.

Fernández, F.A., Perez, J.S., Sevilla, J.F., Camacho, F.G., Grima, E.M., 2000. Modeling of eicosapentaenoic acid (EPA) production from *Phaeodactylum tricornutum* cultures in tubular photobioreactors. Effects of dilution rate, tube diameter, and solar irradiance. Biotechnology and Bioengineering 68, 173–183.

Fields, F.J., Kociolek, J.P., 2015. An evolutionary perspective on selecting high-lipid-content diatoms (Bacillariophyta). Journal of Applied Phycology 27, 2209–2220.

Fischer, H., Gröning, C., Köster, C., 1977. Vertical migration rhythm in freshwater diatoms. Hydrobiologia 56, 259–263.

Flynn, K., Syrett, P., 1986. Utilization of L-lysine and L-arginine by the diatom *Phaeodactylum tricornutum*. Marine Biology 90, 159–163.

Flynn, K., Wright, C., 1986. The simultaneous assimilation of ammonium and L-arginine by the marine diatom *Phaeodactylum tricornutum* Bohlin. Journal of experimental marine biology and ecology 95, 257–269.

Fu, W., Wichuk, K., Brynjólfsson, S., 2015. Developing diatoms for value-added products: Challenges and opportunities. New biotechnology 32, 547–551.

Gao, Y., Yang, M., Wang, C., 2013. Nutrient deprivation enhances lipid content in marine microalgae. Bioresource Technology 147, 484–491.

Geider, R.J., La Roche, J., Greene, R.M., Olaizola, M., 1993. Response of the photosynthetic apparatus of *Phaeodactylum tricornutum* (bacillariophyceae) to nitrate, phosphate, or iron starvation 1. Journal of Phycology 29, 755–766.

Geng, H.-X., Yu, R.-C., Chen, Z.-F., Peng, Q.-C., Yan, T., Zhou, M.-J., 2017. Analysis of sterols in selected bloom-forming algae in China. Harmful algae 66, 29–39.

Gilstad, M., Sakshaug, E., 1990. Growth rates of ten diatom species from the Barents Sea at different irradiances and day lengths. Marine ecology progress series. Oldendorf 64, 169–173.

Giordano, M., Kansiz, M., Heraud, P., Beardall, J., Wood, B., McNaughton, D., 2001. Fourier transform infrared spectroscopy as a novel tool to investigate changes in intracellular macromolecular pools in the marine microalga *Chaetoceros muellerii* (Bacillariophyceae). Journal of Phycology 37, 271–279.

Gladu, P.K., Patterson, G.W., Wikfors, G.H., Chitwood, D.J., Lusby, W., 1991. Sterols of some diatoms. Phytochemistry 30, 2301–2303.

Göksan, T., Durmaz, Y., Gökpınar, Ş., 2003. Effects of light path lengths and initial culture density on the cultivation of *Chaetoceros muelleri* (Lemmermann, 1898). Aquaculture 217, 431–436.

Goldman, J.C., Dennis Jr, J.M., 2003. Effect of large marine diatoms growing at low light on episodic new production. Limnology and Oceanography 48, 1176–1182.

Gompertz, B., 1825. XXIV. On the nature of the function expressive of the law of human mortality, and on a new mode of determining the value of life contingencies. In a letter to Francis Baily, Esq. FRS &c. Philosophical transactions of the Royal Society of London 115, 513–583.

Gong, M., Bassi, A., 2016. Carotenoids from microalgae: a review of recent developments. Biotechnology Advances 34, 1396–1412.

Granum, E., Myklestad, S.M., 2002. A photobioreactor with pH control: demonstration by growth of the marine diatom *Skeletonema costatum*. Journal of Plankton Research 24, 557–563.

Griffiths, M.J., Harrison, S.T.L., 2009. Lipid productivity as a key characteristic for choosing algal species for biodiesel production. Journal of Applied Phycology 21, 493–507.

Griffiths, M.J., van Hille, R.P., Harrison, S.T.L., 2012. Lipid productivity, settling potential and fatty acid profile of 11 microalgal species grown under nitrogen replete and limited conditions. Journal of Applied Phycology 24, 989–1001.

Gross, M., 2012. The mysteries of the diatoms. Current Biology 22, R581–R585.

Grossi, V., Beker, B., Geenevasen, J.A., Schouten, S., Raphel, D., Fontaine, M.-F., Damsté, J.S.S., 2004. C25 highly branched isoprenoid alkenes from the marine benthic diatom *Pleurosigma strigosum*. Phytochemistry 65, 3049–3055.

Guedes, A.C., Amaro, H.M., Gião, M.S., Malcata, F.X., 2013. Optimization of ABTS radical cation assay specifically for determination of antioxidant capacity of intracellular extracts of microalgae and cyanobacteria. Food chemistry 138, 638–643.

Guerrini, F., Cangini, M., Boni, L., Trost, P., Pistocchi, R., 2000. Metabolic Responses of the Diatom *Achnanthes Brevipes* (bacillariophyceae) to Nutrient Limitation. Journal of Phycology 36, 882–890.

Guihéneuf, F., Mimouni, V., Ulmann, L., Tremblin, G., 2008. Environmental factors affecting growth and omega 3 fatty acid composition in *Skeletonema costatum*. The influences of irradiance and carbon source: Communication presented at the 25ème Congrès Annuel de l'Association des Diatomistes de Langue Francaise (ADLaF), Caen, 25-28 September 2006. Diatom Research 23, 93–103.

Guillard, R.R., 1975. Culture of phytoplankton for feeding marine invertebrates, in: Culture of Marine Invertebrate Animals. Springer, pp. 29–60.

Guillard, R.R., Ryther, J.H., 1962. Studies of marine planktonic diatoms: I. *Cyclotella nana hustedt*, and *Detonula Confervacea* (CLEVE) Gran. Canadian journal of microbiology 8, 229–239.

Guiry, M.D., 2012. How many species of algae are there? Journal of phycology 48, 1057–1063.

Guschina, I.A., Harwood, J.L., 2006. Lipids and lipid metabolism in eukaryotic algae. Progress in Lipid Research 45, 160–186.

Haimeur, A., Ulmann, L., Mimouni, V., Guéno, F., Pineau-Vincent, F., Meskini, N., Tremblin, G., 2012. The role of *Odontella aurita*, a marine diatom rich in EPA, as a dietary supplement in dyslipidemia, platelet function and oxidative stress in high-fat fed rats. Lipids in health and disease 11, 1.

Hallahan, B., Garland, M.R., 2005. Essential fatty acids and mental health. The British Journal of Psychiatry 186, 275–277.

Hamed, I., Özogul, F., Özogul, Y., Regenstein, J.M., 2015. Marine bioactive compounds and their health benefits: a review. Comprehensive reviews in food science and food safety 14, 446–465.

Hamm, C.E., Merkel, R., Springer, O., Jurkojc, P., Maier, C., Prechtel, K., Smetacek, V., 2003. Architecture and material properties of diatom shells provide effective mechanical protection. Nature 421, 841.

Hanashima, S., Mizushina, Y., Ohta, K., Yamazaki, T., Sugawara, F., Sakaguchi, K., 2000. Structure-activity relationship of a novel group of mammalian DNA polymerase inhibitors, synthetic sulfoquinovosylacylglycerols. Japanese Journal of Cancer Research 91, 1073–1083.

Hancke, K., Hancke, T.B., Olsen, L.M., Johnsen, G., Glud, R.N., 2008. Temperature effects on microalgal photosynthesis-light responses measured by O2 production, pulse-amplitude modulated fluorescence, and 14C assimilation 1. Journal of Phycology 44, 501–514.

Hansen, H.P., Koroleff, F., 1999. Determination of nutrients. Methods of seawater analysis 159–228.

Hansen, J.A., 1973. Antibiotic activity of the chrysophyte *Ochromonas malhamensis*. Physiologia Plantarum 29, 234–238.

Harwood, J.L., 1998. Membrane lipids in algae, in: Lipids in photosynthesis: Structure, function and genetics. Springer, pp. 53–64.

Harwood, J.L., Guschina, I.A., 2009. The versatility of algae and their lipid metabolism. Biochimie 91, 679–684.

He, Q., Yang, H., Wu, L., Hu, C., 2015. Effect of light intensity on physiological changes, carbon allocation and neutral lipid accumulation in oleaginous microalgae. Bioresource Technology 191, 219–228.

Hemaiswarya, S., Raja, R., Kumar, R.R., Ganesan, V., Anbazhagan, C., 2011. Microalgae: a sustainable feed source for aquaculture. World Journal of Microbiology and Biotechnology 27, 1737–1746.

Hildebrand, M., Davis, A.K., Smith, S.R., Traller, J.C., Abbriano, R., 2012. The place of diatoms in the biofuels industry. Biofuels 3, 221–240.

Honeywill, C., Paterson, D., Hagerthey, S., 2002. Determination of microphytobenthic biomass using pulse-amplitude modulated minimum fluorescence. European Journal of Phycology 37, 485–492.

Hornsey, I., Hide, D., 1974. The production of antimicrobial compounds by British marine algae I. Antibiotic-producing marine algae. British Phycological Journal 9, 353–361.

Hu, Q., Sommerfeld, M., Jarvis, E., Ghirardi, M., Posewitz, M., Seibert, M., Darzins, A., 2008. Microalgal triacylglycerols as feedstocks for biofuel production: perspectives and advances. The Plant Journal 54, 621–639.

Hubert, F., Poisson, L., Loiseau, C., Gauvry, L., Pencréac'h, G., Hérault, J., Ergan, F., 2017. Lipids and lipolytic enzymes of the microalga Isochrysis galbana.

Huete-Ortega, M., Okurowska, K., Kapoore, R.V., Johnson, M.P., Gilmour, D.J., Vaidyanathan, S., 2018. Effect of ammonium and high light intensity on the accumulation of lipids in *Nannochloropsis oceanica* (CCAP 849/10) and *Phaeodactylum tricornutum* (CCAP 1055/1). Biotechnology for biofuels 11, 60.

Hungerford, J.J., 1988. Diatoms: The Ignored Alga in High School Biology. The American Biology Teacher 50, 449–449.

Huntley, M.E., Johnson, Z.I., Brown, S.L., Sills, D.L., Gerber, L., Archibald, I., Machesky, S.C., Granados, J., Beal, C., Greene, C.H., 2015. Demonstrated large-scale production of marine microalgae for fuels and feed. Algal Research 10, 249–265.

Imada, T., Miyazaki, S., Nishida, M., Yamaguchi, K., Goto, S., 1992. In vitro and in vivo antibacterial activities of a new quinolone, OPC-17116. Antimicrobial agents and chemotherapy 36, 573–579.

Ingebrigtsen, R.A., Hansen, E., Andersen, J.H., Eilertsen, H.C., 2016. Light and temperature effects on bioactivity in diatoms. Journal of Applied Phycology 28, 939–950.

Islam, M., Magnusson, M., Brown, R., Ayoko, G., Nabi, M., Heimann, K., 2013. Microalgal species selection for biodiesel production based on fuel properties derived from fatty acid profiles. Energies 6, 5676–5702.

Iwamoto, H., Yonekawa, G., AsAI, T., Nagahashi, N., 1955. Fat Synthesis in Unicellular Algae: Part I. Culture conditions for fat accumulation in *Chlorella* cells Part II. Chemical composition of nitrogen-deficient *Chlorella* cells. Journal of the Agricultural Chemical Society of Japan 19, 240–252.

Jaeger, D., Pilger, C., Hachmeister, H., Oberländer, E., Wördenweber, R., Wichmann, J., Mussgnug, J.H., Huser, T., Kruse, O., 2016. Label-free in vivo analysis of intracellular lipid droplets in the oleaginous microalga *Monoraphidium neglectum* by coherent Raman scattering microscopy. Scientific reports 6, 35340.

Jaspars, M., De Pascale, D., Andersen, J.H., Reyes, F., Crawford, A.D., Ianora, A., 2016. The marine biodiscovery pipeline and ocean medicines of tomorrow. Journal of the Marine Biological Association of the United Kingdom 96, 151–158.

Jauffrais, T., Drouet, S., Turpin, V., Méléder, V., Jesus, B., Cognie, B., Raimbault, P., Cosson, R.P., Decottignies, P., Martin-Jézéquel, V., 2015. Growth and biochemical composition of a microphytobenthic diatom (*Entomoneis paludosa*) exposed to shorebird (*Calidris alpina*) droppings. Journal of experimental marine biology and ecology 469, 83–92.

Jauffrais, T., Jesus, B., Méléder, V., Turpin, V., Russo, A.D.P.G., Raimbault, P., Jézéquel, V.M., 2016. Physiological and photophysiological responses of the benthic diatom *Entomoneis paludosa* (Bacillariophyceae) to dissolved inorganic and organic nitrogen in culture. Marine Biology 163.

Jiang, H., Gao, K., 2004. Effects of lowering temperature during culture on the production of polyunsaturated fatty acids in the marine diatom *Phaeodactylum tricornutum* (bacillariophyceae)1. Journal of Phycology 40, 651–654.

Jiang, X., Han, Q., Gao, X., Gao, G., 2016. Conditions optimising on the yield of biomass, total lipid, and valuable fatty acids in two strains of *Skeletonema menzelii*. Food Chemistry 194, 723–732.

Jiang, Y., Yoshida, T., Quigg, A., 2012. Photosynthetic performance, lipid production and biomass composition in response to nitrogen limitation in marine microalgae. Plant Physiology and Biochemistry 54, 70–77.

Johansen, J., Lemke, P., Nagle, N., Chelf, P., Roessler, P., Galloway, R., Toon, S., 1987. Addendum to microalgae culture collection 1986-1987. National Renewable Energy Lab.(NREL), Golden, CO (United States).

Jørgensen, E.G., 1962. Antibiotic substances from cells and culture solutions of unicellular algae with special reference to some chlorophyll derivatives. Physiologia Plantarum 15, 530–545.

Joseph, M.M., Renjith, K.R., John, G., Nair, S.M., Chandramohanakumar, N., 2017. Biodiesel prospective of five diatom strains using growth parameters and fatty acid profiles. Biofuels 8, 81–89.

Juneau, P., Green, B.R., Harrison, P.J., 2005. Simulation of Pulse-Amplitude-Modulated (PAM) fluorescence: Limitations of some PAM-parameters in studying environmental stress effects. Photosynthetica 43, 75–83.

Kabara, J.J., Swieczkowski, D.M., Conley, A.J., Truant, J.P., 1972. Fatty acids and derivatives as antimicrobial agents. Antimicrobial agents and chemotherapy 2, 23–28.

Kates, M., Volcani, B.E., 1966. Lipid components of diatoms. Biochimica et Biophysica Acta (BBA) - Lipids and Lipid Metabolism 116, 264–278.

Kay, R.A., Barton, L.L., 1991. Microalgae as food and supplement. Critical reviews in food science and nutrition 30, 555–573.

Kellam, S.J., Walker, J.M., 1989. Antibacterial activity from marine microalgae in laboratory culture. British Phycological Journal 24, 191–194.

Kendel, M., Couzinet-Mossion, A., Viau, M., Fleurence, J., Barnathan, G., Wielgosz-Collin, G., 2013. Seasonal composition of lipids, fatty acids, and sterols in the edible red alga *Grateloupia turuturu*. Journal of Applied Phycology 25, 425–432.

Khan, M.I., Shin, J.H., Kim, J.D., 2018. The promising future of microalgae: current status, challenges, and optimization of a sustainable and renewable industry for biofuels, feed, and other products. Microbial Cell Factories 17.

Kim, S.M., Jung, Y.-J., Kwon, O.-N., Cha, K.H., Um, B.-H., Chung, D., Pan, C.-H., 2012. A Potential Commercial Source of Fucoxanthin Extracted from the Microalga *Phaeodactylum tricornutum.* Applied Biochemistry and Biotechnology 166, 1843–1855.

Kingston, M.B., 2009. Growth and motility of the diatom *Cylindrotheca closterium*: implications for commercial applications. Journal of the North Carolina Academy of Science 138–142.

Knuckey, R.M., Brown, M.R., Barrett, S.M., Hallegraeff, G.M., 2002. Isolation of new nanoplanktonic diatom strains and their evaluation as diets for juvenile Pacific oysters (*Crassostrea gigas*). Aquaculture 211, 253–274.

Koletzko, B., Decsi, T., Demmelmair, H., 1996. Arachidonic acid supply and metabolism in human infants born at full term. Lipids 31, 79–83.

Kooistra, W.H.C.F., Gersonde, R., Medlin, L.K., Mann, D.G., 2007. CHAPTER 11 - The origin and evolution of the diatoms: Their adaptation to a planktonic existence, in: Falkowski, P.G., Knoll, A.H. (Eds.), Evolution of Primary Producers in the Sea. Academic Press, Burlington, pp. 207–249.

Koreivienė, J., 2017. Microalgae Lipid Staining with Fluorescent BODIPY Dye.

Koroleff, F., 1970. Direct determination of ammonia in natural waters as indophenol blue. Information on techniques and methods for seawater analysis 19–22.

Kotaki, Y., Koike, K., Yoshida, M., Van Thuoc, C., Huyen, N.T.M., Hoi, N.C., Fukuyo, Y., Kodama, M., 2000. Domoic acid production in *Nitzschia* sp. (Bacillariophyceae) isolated from a shrimp-culture pond in Do Son, Vietnam. Journal of Phycology 36, 1057–1060.

Krichnavaruk, S., Loataweesup, W., Powtongsook, S., Pavasant, P., 2005. Optimal growth conditions and the cultivation of *Chaetoceros calcitrans* in airlift photobioreactor. Chemical Engineering Journal 105, 91–98.

Krichnavaruk, S., Powtongsook, S., Pavasant, P., 2007. Enhanced productivity of *Chaetoceros calcitrans* in airlift photobioreactors. Bioresource technology 98, 2123–2130.

Kröger, N., Bergsdorf, C., Sumper, M., 1994. A new calcium binding glycoprotein family constitutes a major diatom cell wall component. The EMBO journal 13, 4676–4683.

Kyriakopoulou, K., Papadaki, S., Krokida, M., 2015. Life cycle analysis of β-carotene extraction techniques. Journal of Food Engineering 167, 51–58.

Lafourcade, M., Larrieu, T., Mato, S., Duffaud, A., Sepers, M., Matias, I., De Smedt-Peyrusse, V., Labrousse, V.F., Bretillon, L., Matute, C., Rodríguez-Puertas, R., Layé, S., Manzoni, O.J., 2011. Nutritional omega-3 deficiency abolishes endocannabinoid-mediated neuronal functions. Nature Neuroscience 14, 345–350.

Lai, J., Yu, Z., Song, X., Cao, X., Han, X., 2011. Responses of the growth and biochemical composition of *Prorocentrum donghaiense* to different nitrogen and phosphorus concentrations. Journal of Experimental Marine Biology and Ecology 405, 6–17.

Larkum, A.W.D., Ross, I.L., Kruse, O., Hankamer, B., 2012. Selection, breeding and engineering of microalgae for bioenergy and biofuel production. Trends in Biotechnology 30, 198–205.

Laurens, L.M., Wolfrum, E.J., 2012. Rapid compositional analysis of microalgae by NIR spectroscopy. NIR news 23, 9–11.

Lauritano, C., Andersen, J.H., Hansen, E., Albrigtsen, M., Escalera, L., Esposito, F., Helland, K., Hanssen, K.Ø., Romano, G., Ianora, A., 2016. Bioactivity screening of microalgae for antioxidant, anti-inflammatory, anticancer, anti-diabetes, and antibacterial activities. Frontiers in Marine Science 3.

Le Gouic, B., 2013. Analyse et optimisation de l'apport de carbone en photobioréacteur.

Lebeau, T., Robert, J.-M., 2003. Diatom cultivation and biotechnologically relevant products. Part II: Current and putative products. Applied Microbiology and Biotechnology 60, 624–632.

León, E.S., Coat, R., Moutel, B., Pruvost, J., Legrand, J., Gonçalves, O., 2014. Influence of physical and chemical properties of HTSXT-FTIR samples on the quality of prediction models developed to determine absolute concentrations of total proteins, carbohydrates and triglycerides: a preliminary study on the determination of their absolute concentrations in fresh microalgal biomass. Bioprocess and biosystems engineering 37, 2371–2380.

Levitan, O., Dinamarca, J., Hochman, G., Falkowski, P.G., 2014. Diatoms: a fossil fuel of the future. Trends in Biotechnology 32, 117–124.

Li, Y., Naghdi, F.G., Garg, S., Adarme-Vega, T.C., Thurecht, K.J., Ghafor, W.A., Tannock, S., Schenk, P.M., 2014. A comparative study: the impact of different lipid extraction methods on current microalgal lipid research. Microbial cell factories 13, 14.

Liang, M.-H., Zhu, J., Jiang, J.-G., 2018. High-value bioproducts from microalgae: strategies and progress. Critical Reviews in Food Science and Nutrition 0, 01–53.

Liang, Y., Beardall, J., Heraud, P., 2006. Changes in growth, chlorophyll fluorescence and fatty acid composition with culture age in batch cultures of Phaeodactylum tricornutum and *Chaetoceros muelleri* (Bacillariophyceae). Botanica Marina 49, 165–173.

Lin, P.-Y., Tsai, C.-T., Chuang, W.-L., Chao, Y.-H., Pan, I.-H., Chen, Y.-K., Lin, C.-C., Wang, B.-Y., 2017. *Chlorella sorokiniana* induces mitochondrial-mediated apoptosis in human non-small cell lung cancer cells and inhibits xenograft tumor growth in vivo. BMC complementary and alternative medicine 17, 88.

Lincoln, R.A., Strupinski, K., Walker, J.M., 1990. Biologically active compounds from diatoms. Diatom research 5, 337–349.

Liu, Z.-Y., Wang, G.-C., Zhou, B.-C., 2008. Effect of iron on growth and lipid accumulation in *Chlorella vulgaris*. Bioresource Technology 99, 4717–4722.

Lomas, M., 2004. Nitrate reductase and urease enzyme activity in the marine diatom *Thalassiosira weissflogii* (Bacillariophyceae): interactions among nitrogen substrates. Marine biology 144, 37–44.

Lorenzen, C.J., 1966. A method for the continuous measurement of in vivo chlorophyll concentration, in: Deep Sea Research and Oceanographic Abstracts. Elsevier, pp. 223–227.

Mamaeva, A., Namsaraev, Z., Maltsev, Y., Gusev, E., Kulikovskiy, M., Petrushkina, M., Filimonova, A., Sorokin, B., Zotko, N., Vinokurov, V., 2018. Simultaneous increase in cellular content and volumetric concentration of lipids in *Bracteacoccus bullatus* cultivated at reduced nitrogen and phosphorus concentrations. Journal of Applied Phycology 30, 2237–2246.

Martínez Andrade, K., Lauritano, C., Romano, G., Ianora, A., 2018. Marine microalgae with anti-cancer properties. Marine drugs 16, 165.

Massé, G., Belt, S.T., Rowland, S.J., Rohmer, M., 2004. Isoprenoid biosynthesis in the diatoms *Rhizosolenia setigera* (Brightwell) and *Haslea ostrearia* (Simonsen). Proceedings of the National Academy of Sciences 101, 4413–4418.

Mata, T.M., Martins, A.A., Caetano, N.S., 2010. Microalgae for biodiesel production and other applications: A review. Renewable and Sustainable Energy Reviews 14, 217–232.

Mathieu, R., Bellier, J.-P., Granier, B., 2011. Manuel de Micropaléontologie. Association" Carnets de Géologie".

Matsubara, K., Matsumoto, H., Mizushina, Y., Mori, M., Nakajima, N., Fuchigami, M., Yoshida, H., Hada, T., 2005. Inhibitory effect of glycolipids from spinach on in vitro and ex vivo angiogenesis. Oncology Reports. 14, 157–160.

Matsufuji, M., Nagamatsu, Y., Yoshimoto, A., 2000. Protective effects of bacterial glyceroglycolipid M874B against cell death caused by exposure to heat and hydrogen peroxide. Journal of Bioscience and Bioengineering, 89, 345–349.

Matsumoto, M., Nojima, D., Nonoyama, T., Ikeda, K., Maeda, Y., Yoshino, T., Tanaka, T., 2017. Outdoor cultivation of marine diatoms for year-round production of biofuels. Marine drugs 15, 94.

Matsunaga, T., Takeyama, H., Miyashita, H., Yokouchi, H., 2005. Marine microalgae, in: Ulber, R., Le Gal, Y. (Eds.), Marine biotechnology I, advances in biochemical angineering/biotechnology. Springer Berlin Heidelberg, Berlin, Heidelberg, pp. 165–188.

McGinnis, K.M., Dempster, T.A., Sommerfeld, M.R., 1997. Characterization of the growth and lipid content of the diatom *Chaetoceros muelleri*. Journal of Applied Phycology 9, 19–24.

McLachlan, J., 1964. Some considerations of the growth of marine algae in artificial media. Canadian Journal of Microbiology 10, 769–782.

Medina, A.R., Grima, E.M., Giménez, A.G., González, M.I., 1998. Downstream processing of algal polyunsaturated fatty acids. Biotechnology advances 16, 517–580.

Méléder, V., Barillé, L., Launeau, P., Carrère, V., Rincé, Y., 2003. Spectrometric constraint in analysis of benthic diatom biomass using monospecific cultures. Remote Sensing of Environment 88, 386–400.

Mendiola, J.A., Torres, C.F., Toré, A., Martín-Álvarez, P.J., Santoyo, S., Arredondo, B.O., Señoráns, F.J., Cifuentes, A., Ibáñez, E., 2007. Use of supercritical CO2 to obtain extracts with antimicrobial activity from *Chaetoceros muelleri* microalga. A correlation with their lipidic content. European Food Research and Technology 224, 505–510.

Merz, C.R., Main, K.L., 2014. Microalgae (diatom) production—The aquaculture and biofuel nexus. Presented at the Oceans-St. John's, 2014, IEEE, pp. 1–10.

Metzger, P., Largeau, C., 2005. *Botryococcus braunii*: a rich source for hydrocarbons and related ether lipids. Applied Microbiology and Biotechnology 66, 486–496.

Mimouni, V., Ulmann, L., Pasquet, V., Mathieu, M., Picot, L., Bougaran, G., Cadoret, J.-P., Morant-Manceau, A., Schoefs, B., 2012. The potential of microalgae for the production of bioactive molecules of pharmaceutical interest. Current pharmaceutical biotechnology 13, 2733–2750.

Molina, E., Fernández, F.A., Camacho, F.G., Rubio, F.C., Chisti, Y., 2000. Scale-up of tubular photobioreactors. Journal of Applied Phycology 12, 355–368.

Monkonsit, S., Powtongsook, S., Pavasant, P., 2011. Comparison between airlift photobioreactor and bubble column for *Skeletonema costatum* cultivation. Engineering Journal 15, 53–64.

Morimoto, T., Murakami, N., Nagatsu, A., Sakakibara, J., 1993. Studies on glycolipids. VII. Isolation of two new sulfoquinovosyldiacylglycerols from the green alga *Chlorella vulgaris*. Chemical & pharmaceutical bulletin 41, 1545–1548.

Morimoto, T., Nagatsu, A., Murakami, N., Sakakibara, J., Tokuda, H., Nishino, H., Iwashima, A., 1995. Anti-tumour-promoting glyceroglycolipids from the green alga, *Chlorella vulgaris*. Phytochemistry 40, 1433–1437.

Mortensen, S.H., Børsheim, K.Y., Rainuzzo, J., Knutsen, G., 1988. Fatty acid and elemental composition of the marine diatom *Chaetoceros gracilis* Schütt. Effects of silicate deprivation, temperature and light intensity. Journal of Experimental Marine Biology and Ecology 122, 173–185.

Mosmann, T., 1983. Rapid colorimetric assay for cellular growth and survival: application to proliferation and cytotoxicity assays. Journal of immunological methods 65, 55–63.

Moura Junior, A.M., Bezerra Neto, E., Koening, M.L., Leça, E.E., 2007. Chemical compositon of three microalgae species for possible use in mariculture. Brazilian Archives of Biology and Technology 50, 461–467.

Mubarak, M., Shaija, A., Suchithra, T.V., 2015. A review on the extraction of lipid from microalgae for biodiesel production. Algal Research 7, 117–123.

Müller, P., Li, X.-P., Niyogi, K.K., 2001. Non-Photochemical Quenching. A Response to Excess Light Energy. Plant Physiology 125, 1558–1566. Muller-Feuga, A., 1997. Microalgues marines: les enjeux de la recherche.

Munn, C., 2011. Marine microbiology: Ecology & applications. Garland Science.

Murakami, C., Kumagai, T., Hada, T., Kanekazu, U., Nakazawa, S., Kamisuki, S., Maeda, N., Xu, X., Yoshida, H., Sugawara, F., 2003a. Effects of glycolipids from spinach on mammalian DNA polymerases. Biochemical pharmacology 65, 259–267.

Murakami, C., Kumagai, T., Hada, T., Kanekazu, U., Nakazawa, S., Kamisuki, S., Maeda, N., Xu, X., Yoshida, H., Sugawara, F., Sakaguchi, K., Mizushina, Y., 2003b. Effects of glycolipids from spinach on mammalian DNA polymerases. Biochemical Pharmacology 65, 259–267.

Murakami, C., Yamazaki, T., Hanashima, S., Takahashi, S., Ohta, K., Yoshida, H., Sugawara, F., Sakaguchi, K., Mizushina, Y., 2002. Structure–function relationship of synthetic sulfoquinovosyl-acylglycerols as mammalian DNA polymerase inhibitors. Archives of Biochemistry and Biophysics 403, 229–236.

Murdock, J.N., Wetzel, D.L., 2009. FT-IR Microspectroscopy enhances biological and ecological analysis of algae. Applied Spectroscopy Reviews 44, 335–361.

Murthy, K.N.C., Vanitha, A., Rajesha, J., Swamy, M.M., Sowmya, P.R., Ravishankar, G.A., 2005. In vivo antioxidant activity of carotenoids from *Dunaliella salina* — a green microalga. Life Sciences 76, 1381–1390.

Mus, F., Toussaint, J.-P., Cooksey, K.E., Fields, M.W., Gerlach, R., Peyton, B.M., Carlson, R.P., 2013. Physiological and molecular analysis of carbon source supplementation and pH stress-induced lipid accumulation in the marine diatom *Phaeodactylum tricornutum*. Applied Microbiology and Biotechnology 97, 3625–3642.

Mutanda, T., Ramesh, D., Karthikeyan, S., Kumari, S., Anandraj, A., Bux, F., 2011. Bioprospecting for hyper-lipid producing microalgal strains for sustainable biofuel production. Bioresource Technology 102, 57–70.

Nagao, K., Yanagita, T., 2005. Conjugated fatty acids in food and their health benefits. Journal of Bioscience and Bioengineering 100, 152–157.

Napoléon, C., Raimbault, V., Claquin, P., 2013. Influence of Nutrient Stress on the Relationships between PAM Measurements and Carbon Incorporation in Four Phytoplankton Species. PLOS ONE 8, e66423.

Nappo, M., Berkov, S., Codina, C., Avila, C., Messina, P., Zupo, V., Bastida, J., 2009. Metabolite profiling of the benthic diatom *Cocconeis scutellum* by GC-MS. Journal of applied phycology 21, 295.

Nappo, M., Berkov, S., Massucco, C., Di Maria, V., Bastida, J., Codina, C., Avila, C., Messina, P., Zupo, V., Zupo, S., 2012. Apoptotic activity of the marine diatom *Cocconeis scutellum* and eicosapentaenoic acid in BT20 cells. Pharmaceutical biology 50, 529–535.

Naviner, M., Bergé, J.-P., Durand, P., Le Bris, H., 1999. Antibacterial activity of the marine diatom *Skeletonema costatum* against aquacultural pathogens. Aquaculture 174, 15–24.

Nelson, D.M., Tréguer, P., Brzezinski, M.A., Leynaert, A., Quéguiner, B., 1995. Production and dissolution of biogenic silica in the ocean: revised global estimates, comparison with regional data and relationship to biogenic sedimentation. Global Biogeochemical Cycles 9, 359–372.

Nichols, D.S., Nichols, P.D., Sullivan, C.W., 1993. Fatty acid, sterol and hydrocarbon composition of Antarctic sea ice diatom communities during the spring bloom in McMurdo Sound. Antarctic Science 5, 271–278.

Nichols, P.D., Palmisano, A.C., Volkman, J.K., Smith, G.A., White, D.C., 1988. Occurrence of an isoprenoid C25 diunasaturated alkene and high neutral lipid content in antractic sea-ice diatom Communities1. Journal of Phycology 24, 90–96.

Nigjeh, S.E., Yusoff, F.M., Alitheen, N.B.M., Rasoli, M., Keong, Y.S., bin Omar, A.R., 2013. Research article cytotoxic effect of ethanol extract of microalga, *Chaetoceros calcitrans*, and its mechanisms in inducing apoptosis in human breast cancer cell line.

Niu, Y.-F., Zhang, M.-H., Li, D.-W., Yang, W.-D., Liu, J.-S., Bai, W.-B., Li, H.-Y., 2013. Improvement of neutral lipid and polyunsaturated fatty acid biosynthesis by overexpressing a type 2 diacylglycerol acyltransferase in marine diatom *Phaeodactylum tricornutum*. Marine Drugs 11, 4558–4569.

Norici, A., Bazzoni, A.M., Pugnetti, A., Raven, J.A., Giordano, M., 2011. Impact of irradiance on the C allocation in the coastal marine diatom *Skeletonema marinoi* Sarno and Zingone. Plant, Cell & Environment 34, 1666–1677.

Ohta, K., Hanashima, S., Mizushina, Y., Yamazaki, T., Saneyoshi, M., Sugawara, F., Sakaguchi, K., 2000. Studies on a novel DNA polymerase inhibitor group, synthetic sulfoquinovosylacylglycerols: inhibitory action on cell proliferation. Mutation Research/Genetic Toxicology and Environmental Mutagenesis 467, 139–152.

Ohta, K., Mizushina, Y., Hirata, N., Takemura, M., Sugawara, F., Matsukage, A., Yoshida, S., Sakaguchi, K., 1999. Action of a new mammalian DNA polymerase inhibitor, sulfoquinovosyldiacylglycerol. Biological Pharmaceutical Bulletin 22, 111–116.

Ohta, K., Mizushina, Y., Hirata, N., Takemura, M., Sugawara, F., Matsukage, A., Yoshida, S., Sakaguchi, K., 1998. Sulfoquinovosyldiacylglycerol, KM043, a new potent inhibitor of eukaryotic DNA polymerases and HIV-reverse transcriptase type 1 from a marine red alga, *Gigartina tenella*. Chem Pharm Bull (Tokyo) 46, 684–686.

Oswald, W.J., Golueke, C.G., 1960. Biological transformation of solar energy, in: Advances in Applied Microbiology. Elsevier, pp. 223–262.

Ozkan, A., Kinney, K., Katz, L., Berberoglu, H., 2012. Reduction of water and energy requirement of algae cultivation using an algae biofilm photobioreactor. Bioresource Technology 114, 542–548.

Paasche, E. é, Ostergren, I., 1980. The annual cycle of plankton diatom growth and silica production in the inner Oslofjord1. Limnology and Oceanography 25, 481–494.

Pan, Y., Subba Rao, D.V., Mann, K.H., 1996. Changes in domoic acid production and cellular chemical composition of the toxigenic diatom *Pseudo-Nitzschia multiseries* under phosphate limitation 1. Journal of Phycology 32, 371–381.

Parkhill, J., Maillet, G., Cullen, J.J., 2001. Fluorescence-based maximal quantum yield for PSII as a diagnostic of nutrient stress. Journal of Phycology 37, 517–529.

Parkinson, J., Gordon, R., 1999. Beyond micromachining: the potential of diatoms. Trends in biotechnology 17, 190–196.

Pasquet, V., Ulmann, L., Mimouni, V., Guihéneuf, F., Jacquette, B., Morant-Manceau, A., Tremblin, G., 2014. Fatty acids profile and temperature in the cultured marine diatom *Odontella aurita*. Journal of applied phycology 26, 2265–2271.

Peng, J., Yuan, J.-P., Wu, C.-F., Wang, J.-H., 2011. Fucoxanthin, a marine carotenoid present in brown seaweeds and diatoms: metabolism and bioactivities relevant to human health. Marine drugs 9, 1806–1828.

Pernet, F., Tremblay, R., Demers, E., Roussy, M., 2003. Variation of lipid class and fatty acid composition of *Chaetoceros muelleri* and *Isochrysis* sp. grown in a semicontinuous system. Aquaculture 221, 393–406.

Pesando, D., 1990. Antibacterial and antifungal activities of marine algae. Introduction to applied phycology 3–26.

Pessôa, M.G., Vespermann, K.A.C., Paulino, B.N., Barcelos, M.C.S., Pastore, G.M., Molina, G., 2019. Newly isolated microorganisms with potential application in biotechnology. Biotechnology Advances 37, 319–339.

Pham, Q.K., Durand-Chastel, H., 2003. Novel antiretroviral sulpholipids extracted from spirulinae, method for obtaining same, compositions containing same and use thereof as inhibitors of the hiv virus reverse transcriptase.

Pina-Pérez, M.C., Rivas, A., Martínez, A., Rodrigo, D., 2017. Antimicrobial potential of macro and microalgae against pathogenic and spoilage microorganisms in food. Food Chemistry 235, 34–44.

Plouguerné, E., da Gama, B.A., Pereira, R.C., Barreto-Bergter, E., 2014. Glycolipids from seaweeds and their potential biotechnological applications. Frontiers in cellular and infection microbiology 4, 174.

Plouguerné, E., de Souza, L., Sassaki, G., Cavalcanti, J., Villela Romanos, M., da Gama, B., Pereira, R., Barreto-Bergter, E., 2013. Antiviral sulfoquinovosyldiacylglycerols (SQDGs) from the Brazilian brown seaweed *Sargassum vulgare*. Marine drugs 11, 4628–4640.

Plumley, F.G., Schmidt, G.W., 1989. Nitrogen-dependent regulation of photosynthetic gene expression. Proceedings of the National Academy of Sciences 86, 2678–2682.

Ponomarenko, L., Stonik, I., Aizdaicher, N., Orlova, T.Y., Popovskaya, G., Pomazkina, G., Stonik, V., 2004. Sterols of marine microalgae *Pyramimonas cf. cordata* (Prasinophyta), *Attheya ussurensis* sp. nov.(Bacillariophyta) and a spring diatom bloom from Lake Baikal. Comparative Biochemistry and Physiology Part B: Biochemistry and Molecular Biology 138, 65–70.

Praveenkumar, R., Shameera, K., Mahalakshmi, G., Akbarsha, M.A., Thajuddin, N., 2012. Influence of nutrient deprivations on lipid accumulation in a dominant indigenous microalga *Chlorella* sp., BUM11008: Evaluation for biodiesel production. Biomass and Bioenergy 37, 60–66.

Pruvost, J., 2011. Cultivation of algae in photobioreactors for biodiesel production, in: Biofuels. Elsevier, pp. 439–464.

Pruvost, J., Van Vooren, G., Cogne, G., Legrand, J., 2009. Investigation of biomass and lipids production with *Neochloris oleoabundans* in photobioreactor. Bioresource technology 100, 5988–5995.

Pruvost, J., Van Vooren, G., Le Gouic, B., Couzinet-Mossion, A., Legrand, J., 2011. Systematic investigation of biomass and lipid productivity by microalgae in photobioreactors for biodiesel application. Bioresource Technology, Special Issue: Biofuels - II: Algal Biofuels and Microbial Fuel Cells 102, 150–158.

Pulz, O., 2001. Photobioreactors: production systems for phototrophic microorganisms. Applied Microbiology and Biotechnology 57, 287–293.

Pulz, O., Gross, W., 2004. Valuable products from biotechnology of microalgae. Applied Microbiology and Biotechnology 65, 635–648.

Quigg, A., Beardall, J., 2003. Protein turnover in relation to maintenance metabolism at low photon flux in two marine microalgae. Plant, Cell & Environment 26, 693–703.

Rajaram, M., Nagaraj, S., Manjunath, M., Boopathy, A., Kurinjimalar, C., Rengasamy, R., Jayakumar, T., Sheu, J.-R., Li, J.-Y., 2018. Biofuel and biochemical analysis of a*mphora coffeaeformis* RR03, a novel marine diatom, cultivated in an open raceway pond. Energies 11, 1341.

Ralph, P.J., Gademann, R., 2005. Rapid light curves: a powerful tool to assess photosynthetic activity. Aquatic botany 82, 222–237.

Ramachandra, T., Mahapatra, D.M., Gordon, R., 2009. Milking diatoms for sustainable energy: biochemical engineering versus gasoline-secreting diatom solar panels. Industrial & Engineering Chemistry Research 48, 8769–8788.

Rampen, S.W., Abbas, B.A., Schouten, S., Damsté, J.S.S., 2010. A comprehensive study of sterols in marine diatoms (Bacillariophyta): implications for their use as tracers for diatom productivity. Limnology and oceanography 55, 91.

Rampen, S.W., Schouten, S., Hopmans, E.C., Abbas, B., Noordeloos, A.A.M., Geenevasen, J.A.J., Moldowan, J.M., Denisevich, P., Sinninghe Damsté, J.S., 2009. Occurrence and biomarker potential of 23-methyl steroids in diatoms and sediments. Organic Geochemistry 40, 219–228.

Rao, D.S., Quilliam, M., Pocklington, R., 1988. Domoic acid—a neurotoxic amino acid produced by the marine diatom *Nitzschia pungens* in culture. Canadian journal of fisheries and aquatic sciences 45, 2076–2079.

Reichelt, J.L., Borowitzka, M.A., 1984. Antimicrobial activity from marine algae: results of a large-scale screening programme. Presented at the Eleventh International Seaweed Symposium, Springer, pp. 158–168.

Renaud, S.M., Thinh, L.-V., Parry, D.L., 1999. The gross chemical composition and fatty acid composition of 18 species of tropical Australian microalgae for possible use in mariculture. Aquaculture 170, 147–159.

Renaud, S.M., Zhou, H.C., Parry, D.L., Thinh, L.-V., Woo, K.C., 1995. Effect of temperature on the growth, total lipid content and fatty acid composition of recently isolated tropical microalgae *Isochrysis* sp., *Nitzschia closterium*, *Nitzschia paleacea*, and commercial species *Isochrysis* sp.(clone T. ISO). Journal of Applied phycology 7, 595–602.

Řezanka, T., Lukavský, J., Nedbalová, L., Kolouchová, I., Sigler, K., 2012. Effect of starvation on the distribution of positional isomers and enantiomers of triacylglycerol in the diatom *Phaeodactylum tricornutum*. Phytochemistry 80, 17–27.

Rhee, G.--ull, Gotham, I.J., 1981. The effect of environmental factors on phytoplankton growth: Light and the interactions of light with nitrate limitation1. Limnology and Oceanography 26, 649–659. Richmond, A., 2004. Handbook of microalgal culture: biotechnology and applied phycology. Wiley Online Library.

Ritchie, R.J., 2006. Consistent sets of spectrophotometric chlorophyll equations for acetone, methanol and ethanol solvents. Photosynthesis research 89, 27–41.

Robert, J.-M., 1983. Fertilité des eaux des claires ostréicoles et verdissement: utilisation de l'azote par les diatomées dominantes.

Robles Medina, A., Esteban Cerdán, L., Giménez Giménez, A., Camacho Páez, B., Ibáñez González, M.J., Molina Grima, E., 1999. Lipase-catalyzed esterification of glycerol and polyunsaturated fatty acids from fish and microalgae oils. Journal of Biotechnology, Biotechnological Aspects of Marine Sponges 70, 379–391.

Rodolfi, L., Chini Zittelli, G., Bassi, N., Padovani, G., Biondi, N., Bonini, G., Tredici, M.R., 2009. Microalgae for oil: Strain selection, induction of lipid synthesis and outdoor mass cultivation in a low-cost photobioreactor. Biotechnology and Bioengineering 102, 100–112.

Roessler, P.G., 1990. Envionmental control of glycerolipid metabolism in microalgae: commercial implication and future research directions. Journal of Phycology 26, 393–399.

Roessler, P.G., 1988. Effects of silicon deficiency on lipid composition and metabolism in the diatom *Cyclotella cryptica* 1. Journal of phycology 24, 394–400.

Roleda, M.Y., Slocombe, S.P., Leakey, R.J.G., Day, J.G., Bell, E.M., Stanley, M.S., 2013. Effects of temperature and nutrient regimes on biomass and lipid production by six oleaginous microalgae in batch culture employing a two-phase cultivation strategy. Bioresource Technology 129, 439–449.

Round, F., Eaton, J., 1966. Persistent, vertical-migration rhythms in benthic microflora: III. The rhythm of epipelic algae in a freshwater pond. The Journal of Ecology 609–615.

Round, F., Palmer, J., 1966. Persistent, vertical-migration rhythms in benthic microflora.: II. Field and laboratory studies on diatoms from the banks of the River Avon. Journal of the Marine Biological Association of the United Kingdom 46, 191–214.

Roussakis, C., Robillard, N., Riou, D., Biard, J., Pradal, G., Piloquet, P., Debitus, C., Verbist, J., 1991. Effects of bistramide A on a non-small-cell bronchial carcinoma line. Cancer chemotherapy and pharmacology 28, 283–292.

Rowland, S.J., Belt, S.T., Wraige, E.J., Massé, G., Roussakis, C., Robert, J.-M., 2001. Effects of temperature on polyunsaturation in cytostatic lipids of *Haslea ostrearia*. Phytochemistry 56, 597–602.

Ruangsomboon, S., 2012. Effect of light, nutrient, cultivation time and salinity on lipid production of newly isolated strain of the green microalga, *Botryococcus braunii* KMITL 2. Bioresource Technology, Special Issue: Innovative Researches on Algal Biomass 109, 261–265.

Ruxton, C., Reed, S.C., Simpson, M., Millington, K., 2004. The health benefits of omega-3 polyunsaturated fatty acids: a review of the evidence. Journal of Human Nutrition and Dietetics 17, 449–459.

Ryckebosch, E., Bruneel, C., Termote-Verhalle, R., Goiris, K., Muylaert, K., Foubert, I., 2014. Nutritional evaluation of microalgae oils rich in omega-3 long chain polyunsaturated fatty acids as an alternative for fish oil. Food Chemistry 160, 393–400.

Sabia, A., Clavero, E., Pancaldi, S., Rovira, J.S., 2018. Effect of different CO 2 concentrations on biomass, pigment content, and lipid production of the marine diatom *Thalassiosira pseudonana*. Applied microbiology and biotechnology 102, 1945–1954.

Samarakoon, K.W., Ko, J.-Y., Shah, M., Mahfuzur, R., Lee, J.-H., Kang, M.-C., Kwon, O.-N., Lee, J.-B., Jeon, Y.-J., 2013. In vitro studies of anti-inflammatory and anticancer activities of organic solvent extracts from cultured marine microalgae. Algae 28, 111–119.

Sánchez Mirón, A., Cerón García, M.-C., García Camacho, F., Molina Grima, E., Chisti, Y., 2002. Growth and biochemical characterization of microalgal biomass produced in bubble column and airlift photobioreactors: studies in fed-batch culture. Enzyme and Microbial Technology 31, 1015–1023.

Sánchez Mirón, A., Contreras Gómez, A., García Camacho, F., Molina Grima, E., Chisti, Y., 1999. Comparative evaluation of compact photobioreactors for large-scale monoculture of microalgae. Journal of Biotechnology, Biotechnological Aspects of Marine Sponges 70, 249–270.

SanGiovanni, J.P., Chew, E.Y., 2005. The role of omega-3 long-chain polyunsaturated fatty acids in health and disease of the retina. Progress in retinal and eye research 24, 87–138.

Sansone, C., Braca, A., Ercolesi, E., Romano, G., Palumbo, A., Casotti, R., Francone, M., Ianora, A., 2014. Diatom-derived polyunsaturated aldehydes activate cell death in Human cancer cell lines but not normal cells. PLOS ONE 9, e101220.

Sarthou, G., Timmermans, K.R., Blain, S., Tréguer, P., 2005. Growth physiology and fate of diatoms in the ocean: a review. Journal of Sea Research 53, 25–42.

Sasso, S., Pohnert, G., Lohr, M., Mittag, M., Hertweck, C., 2012. Microalgae in the postgenomic era: a blooming reservoir for new natural products. FEMS microbiology reviews 36, 761–785.

Sastry, P.S., 1985. Lipids of nervous tissue: composition and metabolism. Progress in lipid research 24, 69–176.

Sayanova Olga, Mimouni Virginie, Ulmann Lionel, Morant-Manceau Annick, Pasquet Virginie, Schoefs Benoît, Napier Johnathan A., 2017. Modulation of lipid biosynthesis by stress in diatoms. Philosophical Transactions of the Royal Society B: Biological Sciences 372, 20160407.

Schaub, I., Wagner, H., Graeve, M., Karsten, U., 2017. Effects of prolonged darkness and temperature on the lipid metabolism in the benthic diatom *Navicula perminuta* from the Arctic Adventfjorden, Svalbard. Polar Biology 1–15.

Schnurr, P.J., Allen, D.G., 2015. Factors affecting algae biofilm growth and lipid production: A review. Renewable and Sustainable Energy Reviews 52, 418–429.

Scholz, B., Liebezeit, G., 2013. Biochemical characterisation and fatty acid profiles of 25 benthic marine diatoms isolated from the Solthörn tidal flat (southern North Sea). Journal of Applied Phycology 25, 453–465.

Schultze, L.K., Simon, M.-V., Li, T., Langenbach, D., Podola, B., Melkonian, M., 2015. High light and carbon dioxide optimize surface productivity in a Twin-Layer biofilm photobioreactor. Algal research 8, 37–44.

Shahidi, F., Barrow, C., 2007. Marine nutraceuticals and functional foods. CRC Press.

Sharma, K.K., Schuhmann, H., Schenk, P.M., 2012. High lipid induction in microalgae for biodiesel production. Energies 5, 1532–1553. Sheehan, J., Dunahay, T., Benemann, J., Roessler, P., 1998. Look Back at the U.S. Department of Energy's Aquatic Species Program: Biodiesel from Algae; Close-Out Report (No. NREL/TP-580-24190). National Renewable Energy Lab., Golden, CO. (US).

Shifrin, N.S., Chisholm, S.W., 1981. Phytoplankton lipids: interspecific differences and effects of nitrate, silicate and light-dark cycles 1. Journal of phycology 17, 374–384.

Shuba, E.S., Kifle, D., 2018. Microalgae to biofuels: 'Promising' alternative and renewable energy, review. Renewable and Sustainable Energy Reviews 81, 743–755.

Siegenthaler, P.-A., Murata, N., 2006. Lipids in photosynthesis: structure, function and genetics. Springer Science & Business Media.

Silva-Aciares, F.R., Riquelme, C.E., 2008. Comparisons of the growth of six diatom species between two configurations of photobioreactors. Aquacultural Engineering 38, 26–35.

Simopoulos, A.P., 2008. The importance of the omega-6/omega-3 fatty acid ratio in cardiovascular disease and other chronic diseases. Experimental biology and medicine 233, 674–688.

Sinninghe Damsté, J.S., Rijpstra, W.I.C., Schouten, S., Peletier, H., van der Maarel, M.J.E.C., Gieskes, W.W.C., 1999. A C25 highly branched isoprenoid alkene and C25 and C27n-polyenes in the marine diatom *Rhizosolenia setigera*. Organic Geochemistry 30, 95–100.

Siron, R., Giusti, G., Berland, B., 1989. Changes in the fatty acid composition of *Phaeodactylum tricornutum* and *Dunaliella tertiolecta* during growth and under phosphorus deficiency. Marine Ecology Progress Series 55, 95–100.

Slocombe, S.P., Zhang, Q., Ross, M., Anderson, A., Thomas, N.J., Lapresa, Á., Rad-Menéndez, C., Campbell, C.N., Black, K.D., Stanley, M.S., 2015. Unlocking nature's treasure-chest: screening for oleaginous algae. Scientific reports 5, 9844.

Smith, V.J., Desbois, A.P., Dyrynda, E.A., 2010. Conventional and unconventional antimicrobials from fish, marine invertebrates and micro-algae. Marine drugs 8, 1213–1262.

Soares, A.T., Silva, B.F., Fialho, L.L., Pequeno, M.A.G., Vieira, A.A.H., Souza, A.G., Antoniosi Filho, N.R., 2013. Chromatographic characterization of triacylglycerides and fatty acid methyl esters in microalgae oils for biodiesel production. Journal of Renewable and Sustainable Energy 5, 053111.

Solovchenko, A.E., Khozin-Goldberg, I., Didi-Cohen, S., Cohen, Z., Merzlyak, M.N., 2008. Effects of light intensity and nitrogen starvation on growth, total fatty acids and arachidonic acid in the green microalga *Parietochloris incisa*. Journal of Applied Phycology 20, 245–251.

Sourial, N., Wolfson, C., Zhu, B., Quail, J., Fletcher, J., Karunananthan, S., Bandeen-Roche, K., Béland, F., Bergman, H., 2010. Correspondence analysis is a useful tool to uncover the relationships among categorical variables. Journal of Clinical Epidemiology 63, 638–646.

Spoehr, H.A., Milner, H.W., 1949. The chemical composition of *Chlorella*; effect of environmental conditions. Plant Physiol 24, 120–149.

Spolaore, P., Joannis-Cassan, C., Duran, E., Isambert, A., 2006. Commercial applications of microalgae. Journal of Bioscience and Bioengineering 101, 87–96.

Sriharan, S., Sriharan, T., 1990. Effects of nutrients and temperature on lipid and fatty acid production in the diatomHantzshia DI-60. Applied Biochemistry and Biotechnology 24, 309.

Stehfest, K., Toepel, J., Wilhelm, C., 2005. The application of micro-FTIR spectroscopy to analyze nutrient stress-related changes in biomass composition of phytoplankton algae. Plant Physiology and Biochemistry 43, 717–726.

Steinman, A.D., Lamberti, G.A., Leavitt, P.R., Uzarski, D.G., 2017. Biomass and pigments of benthic algae, in: methods in stream ecology, Volume 1. Elsevier, pp. 223–241.

Stonik, V., Stonik, I., 2015. Low-molecular-weight metabolites from diatoms: structures, biological roles and biosynthesis. Marine drugs 13, 3672–3709.

Subhash, G.V., Rajvanshi, M., Kumar, B.N., Govindachary, S., Prasad, V., Dasgupta, S., 2017. Carbon streaming in microalgae: extraction and analysis methods for high value compounds. Bioresource technology 244, 1304–1316.

Suh, I.S., Joo, H.-N., Lee, C.-G., 2006. A novel double-layered photobioreactor for simultaneous Haematococcus pluvialis cell growth and astaxanthin accumulation. Journal of Biotechnology 125, 540–546.

Suman, K., Kiran, T., Devi, U.K., Sarma, N.S., 2012. Culture medium optimization and lipid profiling of *Cylindrotheca*, a lipid-and polyunsaturated fatty acid-rich pennate diatom and potential source of eicosapentaenoic acid. Botanica marina 55, 289–299.

Sumich, J.L., Morrissey, J.F., 2004. Introduction to the Biology of Marine Life. Jones & Bartlett Learning.

Sunda, W.G., Huntsman, S.A., 2004. Relationships among photoperiod, carbon fixation, growth, chlorophyll a, and cellular iron and zinc in a coastal diatom. Limnology and Oceanography 49, 1742–1753.

Swanson, D., Block, R., Mousa, S.A., 2012. Omega-3 fatty acids EPA and DHA: health benefits throughout life. Advances in nutrition 3, 1–7.

Syrett, P., Flynn, K., Molloy, C., Dixon, G., Peplinska, A., Cresswell, R., 1986. Effects of nitrogen deprivation on rates of uptake of nitrogenous compounds by the diatom, *Phaeodactylum tricornutum* Bohlin. New Phytologist 102, 39–44.

Tadros, M.G., Johansen, J.R., 1988. Physiological characterization of six lipid-producting diatoms from the southeastern United States 1. Journal of phycology 24, 445–452.

Taguchi, S., Hirata, J.A., Laws, E.A., 1987. Silicate defiency and lipid synthesis of marine diatoms 1, 2. Journal of Phycology 23, 260–267.

Talero, E., García-Mauriño, S., Ávila-Román, J., Rodríguez-Luna, A., Alcaide, A., Motilva, V., 2015. Bioactive compounds isolated from microalgae in chronic inflammation and cancer. Marine drugs 13, 6152–6209.

Tanaka, T., Yabuuchi, T., Maeda, Y., Nojima, D., Matsumoto, M., Yoshino, T., 2017. Production of eicosapentaenoic acid by high cell density cultivation of the marine oleaginous diatom *Fistulifera solaris*. Bioresource technology 245, 567–572.

Taraldsvik, M., MYKLESTAD, S.M., 2000. The effect of pH on growth rate, biochemical composition and extracellular carbohydrate production of the marine diatom *Skeletonema costatum*. European Journal of Phycology 35, 189–194.

Thompson Jr, G.A., 1996. Lipids and membrane function in green algae. Biochimica et Biophysica Acta (BBA)-Lipids and Lipid Metabolism 1302, 17–45.

Tian, X., Liao, Q., Zhu, X., Wang, Y., Zhang, P., Li, J., Wang, H., 2010. Characteristics of a biofilm photobioreactor as applied to photo-hydrogen production. Bioresource technology 101, 977–983.

Tonon, T., Harvey, D., Larson, T.R., Graham, I.A., 2002. Long chain polyunsaturated fatty acid production and partitioning to triacylglycerols in four microalgae. Phytochemistry 61, 15–24.

Tredici, M.R., 2004. Mass production of microalgae: photobioreactors. Handbook of microalgal culture: Biotechnology and applied phycology 1, 178–214.

Trentacoste, E.M., Shrestha, R.P., Smith, S.R., Gle, C., Hartmann, A.C., Hildebrand, M., Gerwick, W.H., 2013. Metabolic engineering of lipid catabolism increases microalgal lipid accumulation without compromising growth. Proceedings of the National Academy of Sciences 110, 19748–19753.

Trites, M., Kaczmarska, I., Ehrman, J.M., Hicklin, P., Ollerhead, J., 2005. Diatoms from two macro-tidal mudflats in Chignecto Bay, upper Bay of Fundy, New Brunswick, Canada. Hydrobiologia 544, 299–319.

Tsai, Cheng-Jung, Sun Pan, B., 2012. Identification of sulfoglycolipid bioactivities and characteristic fatty acids of marine macroalgae. Journal of agricultural and food chemistry 60, 8404–8410.

Tsai, C.-J., Sun Pan, B., 2012. Identification of sulfoglycolipid bioactivities and characteristic fatty acids of marine macroalgae. Journal of Agricultural and Food Chemistry 60, 8404–8410.

Turpin, D.H., 1991. Effects of inorganic N availability on algal photosynthesis and carbon metabolism. Journal of Phycology 27, 14–20.

Ulmann, L., Blanckaert, V., Mimouni, V., X Andersson, M., Schoefs, B., Chenais, B., 2017. Microalgal fatty acids and their implication in health and disease. Mini reviews in medicinal chemistry 17, 1112–1123.

Valenzuela, J., Mazurie, A., Carlson, R.P., Gerlach, R., Cooksey, K.E., Peyton, B.M., Fields, M.W., 2012. Potential role of multiple carbon fixation pathways during lipid accumulation in *Phaeodactylum tricornutum*. Biotechnology for Biofuels 5, 40.

Van Vooren, G., Le Grand, F., Legrand, J., Cuiné, S., Peltier, G., Pruvost, J., 2012. Investigation of fatty acids accumulation in *Nannochloropsis oculata* for biodiesel application. Bioresource Technology 124, 421–432.

Vardi, A., 2008. Cell signaling in marine diatoms. Communicative & integrative biology 1, 134–136.

Varela, J.C., Pereira, H., Vila, M., León, R., 2015. Production of carotenoids by microalgae: achievements and challenges. Photosynthesis research 125, 423–436.

Vårum, K.M., Myklestad, S., 1984. Effects of light, salinity and nutrient limitation on the production of β-1,3-d-glucan and exo-d-glucanase activity in *Skeletonema costatum* (Grev.) Cleve. Journal of Experimental Marine Biology and Ecology 83, 13–25.

Vassiliev, I.R., Prasil, O., Wyman, K.D., Kolber, Z., Hanson, A.K., Prentice, J.E., Falkowski, P.G., 1994. Inhibition of PS II photochemistry by PAR and UV radiation in natural phytoplankton communities. Photosynthesis Research 42, 51–64.

Veloso, V., Reis, A., Gouveia, L., Fernandes, H.L., Empis, J.A., Novais, J.M., 1991. Lipid production by *Phaeodactylum tricornutum*. Bioresource Technology, Algal biotechnology 38, 115–119.

Viegelmann, C., Parker, J., Ooi, T., Clements, C., Abbott, G., Young, L., Kennedy, J., Dobson, A.D., Edrada-Ebel, R., 2014. Isolation and identification of antitrypanosomal and antimycobacterial active steroids from the sponge *Haliclona simulans*. Marine drugs 12, 2937–2952.

Vílchez, C., Forján, E., Cuaresma, M., Bédmar, F., Garbayo, I., Vega, J.M., 2011. Marine carotenoids: biological functions and commercial applications. Marine drugs 9, 319–333.

Vinayak, V., Manoylov, K.M., Gateau, H., Blanckaert, V., Hérault, J., Pencréac'h, G., Marchand, J., Gordon, R., Schoefs, B., 2015. Diatom Milking: A Review and New Approaches. Marine Drugs 13, 2629–2665.

Vincent, W.F., 1992. The daily pattern of nitrogen uptake by phytoplankton in dynamic mixed layer environments, in: The daily growth cycle of phytoplankton. Springer, pp. 37–52.

Viriyayingsiri, T., Sittplangkoon, P., Powtongsook, S., Nootong, K., 2016. Continuous production of diatom Entomoneis sp. in mechanically stirred tank and flat-panel airlift photobioreactors. Preparative Biochemistry and Biotechnology 46, 740–746.

Viron, C., Saunois, A., Andre, P., Perly, B., Lafosse, M., 2000. Isolation and identification of unsaturated fatty acid methyl esters from marine micro-algae. Analytica Chimica Acta 409, 257–266.

Viso, A., Pesando, D., Baby, C., 1987. Antibacterial and antifungal properties of some marine diatoms in culture. Botanica Marina 30, 41–46.

Viso, A.-C., Marty, J.-C., 1993. Fatty acids from 28 marine microalgae. Phytochemistry 34, 1521–1533.

Volcani, B.E., 1978. Role of silicon in diatom metabolism and silicification. Presented at the Biochemistry of silicon and related problems, Springer, pp. 177–204.

Volkman, J.K., Barrett, S.M., Dunstan, G.A., 1994. C25 and C30 highly branched isoprenoid alkenes in laboratory cultures of two marine diatoms. Organic Geochemistry 21, 407–414.

Volkman, J.K., Eglinton, G., Corner, E.D.S., 1980. Sterols and fatty acids of the marine diatom *biddulphia sinensis*. Phytochemistry 19, 1809–1813.

Volkman, J.K., Hallegraeff, G.M., 1988. Lipids in marine diatoms of the genus *Thalassiosira*: Predominance of 24-methylenecholesterol. Phytochemistry 27, 1389–1394.

Volkman, J.K., Jeffrey, S.W., Nichols, P.D., Rogers, G.I., Garland, C.D., 1989. Fatty acid and lipid composition of 10 species of microalgae used in mariculture. Journal of Experimental Marine Biology and Ecology 128, 219–240.

Vos, P.C., De Wolf, H., 1993. Diatoms as a tool for reconstructing sedimentary environments in coastal wetlands; methodological aspects. Hydrobiologia 269, 285–296.

Vyhnalek, V., Fišar, Z., Fišarová, A., Komarkova, J., 1993. In vivo fluorescence of chlorophyll a: Estimation of phytoplankton biomass and activity in Římov Reservoir (Czech Republic). Water Science and Technology 28, 29–33.

Wagner, H., Dunker, S., Liu, Z., Wilhelm, C., 2013. Subcommunity FTIR-spectroscopy to determine physiological cell states. Current Opinion in Biotechnology 24, 88–94.

Wahidin, S., Idris, A., Shaleh, S.R.M., 2013. The influence of light intensity and photoperiod on the growth and lipid content of microalgae *Nannochloropsis* sp. Bioresource technology 129, 7–11.

Wang, P., Shen, H., Xie, P., 2012. Can hydrodynamics change phosphorus strategies of diatoms?—nutrient levels and diatom blooms in lotic and lentic ecosystems. Microbial ecology 63, 369–382.

Wang, X.-W., Liang, J.-R., Luo, C.-S., Chen, C.-P., Gao, Y.-H., 2014. Biomass, total lipid production, and fatty acid composition of the marine diatom *Chaetoceros muelleri* in response to different CO2 levels. Bioresource Technology 161, 124–130.

Waser, N., Harrison, P., Nielsen, B., Calvert, S., Turpin, D., 1998. Nitrogen isotope fractionation during the uptake and assimilation of nitrate, nitrite, ammonium, and urea by a marine diatom. Limnology and Oceanography 43, 215–224.

Wen, Z.-Y., Chen, F., 2000. Production potential of eicosapentaenoic acid by the diatom Nitzschia laevis. Biotechnology Letters 22, 727–733.

Werner, D., 1978. Regulation of metabolism by silicate in diatoms. Presented at the Biochemistry of silicon and related problems, Springer, pp. 149–176.

White, S., Anandraj, A., Bux, F., 2011. PAM fluorometry as a tool to assess microalgal nutrient stress and monitor cellular neutral lipids. Bioresource technology 102, 1675–1682.

Wilhelm, C., Jungandreas, A., Jakob, T., Goss, R., 2014. Light acclimation in diatoms: From phenomenology to mechanisms. Marine Genomics, Marine Diatoms 16, 5–15.

Williams, D.H., Fleming, I., 1980. Spectroscopic methods in organic chemistry. McGraw-Hill.

Williams, P.J. le B., Laurens, L.M., 2010. Microalgae as biodiesel & biomass feedstocks: review & analysis of the biochemistry, energetics & economics. Energy & Environmental Science 3, 554–590.

Wraige, E.J., Johns, L., Belt, S.T., Massé, G., Robert, J.-M., Rowland, S., 1999. Highly branched C25 isoprenoids in axenic cultures of *Haslea ostrearia*. Phytochemistry 51, 69–73.

Xia, S., Wan, L., Li, A., Sang, M., Zhang, C., 2013a. Effects of nutrients and light intensity on the growth and biochemical composition of a marine microalga *Odontella aurita*. Chin. Journal of Oceanology and Limnology 31, 1163–1173.

Xia, S., Wang, K., Wan, L., Li, A., Hu, Q., Zhang, C., 2013b. Production, characterization, and antioxidant activity of fucoxanthin from the marine diatom *Odontella aurita*. Marine Drugs 11, 2667–2681.

Xiao, X., Si, X., Yuan, Z., Xu, X., Li, G., 2012. Isolation of fucoxanthin from edible brown algae by microwave-assisted extraction coupled with high-speed countercurrent chromatography. Journal of separation science 35, 2313–2317.

Xu, D., Gao, Z., Li, F., Fan, X., Zhang, X., Ye, N., Mou, S., Liang, C., Li, D., 2013. Detection and quantitation of lipid in the microalga *Tetraselmis subcordiformis* (Wille) Butcher with BODIPY 505/515 staining. Bioresource Technology 127, 386–390.

Xue, J., Niu, Y.-F., Huang, T., Yang, W.-D., Liu, J.-S., Li, H.-Y., 2015. Genetic improvement of the microalga *Phaeodactylum tricornutum* for boosting neutral lipid accumulation. Metabolic Engineering 27, 1–9.

Yang, Z.-K., Niu, Y.-F., Ma, Y.-H., Xue, J., Zhang, M.-H., Yang, W.-D., Liu, J.-S., Lu, S.-H., Guan, Y., Li, H.-Y., 2013. Molecular and cellular mechanisms of neutral lipid accumulation in diatom following nitrogen deprivation. Biotechnology for biofuels 6, 67.

Yao, L., Gerde, J.A., Lee, S.-L., Wang, T., Harrata, K.A., 2015. Microalgae lipid characterization. Journal of agricultural and food chemistry 63, 1773–1787.

Yao, Y., Lu, Y., Peng, K.-T., Huang, T., Niu, Y.-F., Xie, W.-H., Yang, W.-D., Liu, J.-S., Li, H.-Y., 2014. Glycerol and neutral lipid production in the oleaginous marine diatom *Phaeodactylum tricornutum* promoted by overexpression of glycerol-3-phosphate dehydrogenase. Biotechnology for biofuels 7, 110.

Yashodhara, B., Umakanth, S., Pappachan, J., Bhat, S., Kamath, R., Choo, B., 2009. Omega-3 fatty acids: a comprehensive review of their role in health and disease. Postgraduate medical journal 85, 84–90.

Yeh, K.-L., Chang, J.-S., 2011. Nitrogen starvation strategies and photobioreactor design for enhancing lipid content and lipid production of a newly isolated microalga *Chlorella vulgaris* ESP-31: Implications for biofuels. Biotechnology Journal 6, 1358–1366.

Yi, Z., Xu, M., Di, X., Brynjolfsson, S., Fu, W., 2017. Exploring valuable lipids in diatoms. Frontiers in Marine Science 4.

Ying, L., Kang-sen, M., Shi-chun, S., 2002. Effects of harvest stage on the total lipid and fatty acid composition of four *Cylindrotheca* strains. Chinese Journal of Oceanology and Limnology 20, 157–161.

Yongmanitchai, W., Ward, O.P., 1991. Growth of and omega-3 fatty acid production by *Phaeodactylum tricornutum* under different culture conditions. Applied and Environmental Microbiology 57, 419–425.

Yu, E.T., Zendejas, F.J., Lane, P.D., Gaucher, S., Simmons, B.A., Lane, T.W., 2009. Triacylglycerol accumulation and profiling in the model diatoms *Thalassiosira pseudonana* and *Phaeodactylum tricornutum* (Baccilariophyceae) during starvation. J Appl Phycol 21, 669.

Zapata, M., Rodríguez, F., Fraga, S., Barra, L., Ruggiero, M.V., 2011. Chlorophyll c pigment patterns in 18 species (51 strains) of the genus p*seudo-nitzschia* (bacillariophyceae) 1. Journal of phycology 47, 1274–1280.

Zeroual, W., Choisy, C., Doglia, S.M., Bobichon, H., Angiboust, J.-F., Manfait, M., 1994. Monitoring of bacterial growth and structural analysis as probed by FT-IR spectroscopy. Biochimica et Biophysica Acta (BBA) - Molecular Cell Research 1222, 171–178.

Zhao, F., Liang, J., Gao, Y., Luo, Q., Yu, Y., Chen, C., Sun, L., 2016. Variations in the total lipid content and biological characteristics of diatom species for potential biodiesel production. Journal of fundamentals of Renewable Energy and Applications 6, 22–26.

Zulu, N.N., Zienkiewicz, K., Vollheyde, K., Feussner, I., 2018. Current trends to comprehend lipid metabolism in diatoms. Progress in lipid research.

Zupo, V., 2000. Effect of microalgal food on the sex reversal of *Hippolyte inermis* (Crustacea: Decapoda). Marine Ecology Progress Series 201, 251–259.

Zupo, V., 1994. Strategies of sexual inversion in *Hippolyte inermis* Leach (Crustacea, Decapoda) from a Mediterranean seagrass meadow. Journal of Experimental Marine Biology and Ecology 178, 131–145.

Zupo, V., Messina, P., Buttino, I., Sagi, A., Avila, C., Nappo, M., Bastida, J., Codina, C., Zupo, S., 2007. Do benthic and planktonic diatoms produce equivalent effects in crustaceans? Marine and Freshwater Behaviour and Physiology 40, 169–181.

ANNEXES I

Table S1. Supplementary data. Strains who did not grown.

Species	NCC strain identification	Sampling location
Amphora sp. B2	NCC261	*France,NW Atlantic coast*
Amphora sp. AC16	NCC410	*France,NW Atlantic coast*
Amphora sp. AE8	NCC413	*France,NW Atlantic coast*
Berkeleya rutilans	NCC210.2	*France,NW Atlantic coast*
Berkeleya rutilans	NCC309	*France, Mediterranean sea*
Brockmaniella brockmanii 2	NCC403	*France,NW Atlantic coast*
Caloneis sp. 1	NCC180	*France,NW Atlantic coast*
Catacombas sp. 1	NCC337	*France, Mediterranean sea*
Cocconeis scutellum 1	NCC209.1	*France, NW Atlantic coast*
Cocconeis scutellum 2	NCC209.2	*France, NW Atlantic coast*
Cocconeis scutellum 2	NCC209.3	*France, NW Atlantic coast*
Craspedostauros sp. 3	NCC57	*France, NW Atlantic coast*
Craspedostauros sp. 4	NCC58	*France, NW Atlantic coast*
Craspedostauros sp. 5	NCC204	*France, NW Atlantic coast*
Entomoneis alata 1	NCC16	*France, NW Atlantic coast*
Entomoneis alata 2	NCC448	*Portugal, NW Atlantic coast*
Entomoneis sp. BAB2	NCC415	*France, NW Atlantic coast*
Gyrosigma sp. 1	NCC411	*France, NW Atlantic coast*
Gyrosigma sp. 2	NCC412	*France, NW Atlantic coast*
Gyrosigma tenuissimum	NCC258	*France, NW Atlantic coast*
Halamphora coffeaformis	UTCC58	*Canada, NW Atlantic coast*
Helicotheca tamesis 1	NCC59	*, France, Mediterranean sea*
Helicotheca tamesis 2	NCC60	*France,NW Atlantic coast*
Lampriscus sp.	NCC347	*France, Mediterranean sea*
Leptocylindrus danicus 1	NCC205	*France,NW Atlantic coast*
Leptocylindrus danicus 2	NCC206	*France,NW Atlantic coast*
Melosira nummuloîdes 1	NCC25	*France,NW Atlantic coast*
Melosira nummuloîdes 2	NCC25.1	*France,NW Atlantic coast*
Navicula sp. Z4	NCC224	*France,NW Atlantic coast*
Navicula sp. e1	NCC269	*France, NW Atlantic coast*
Navicula cf ramosissima	NCC449	*France, NW Atlantic coast*
Nitzschia laevis	NCC39	*France, NW Atlantic coast*
Nitzschia salinicola	NCC41	*France, NW Atlantic coast*
Nitzschia sp. B4	NCC114	*France, NW Atlantic coast*
Opehora sp. 2	NCC365	*France, NW Atlantic coast*
Paralia sulcata	NCC177	*France, NW Atlantic coast*
Pleurosigma sp. K	NCC339	*Ukraine, Black sea*
Pleurosigma sp. LM	NCC404	*France, NW Atlantic coast*
Pleurosigma sp. BC1	NCC423	*France, NW Atlantic coast*
Pleurosigma sp. BC7	NCC425	*France, NW Atlantic coast*
Pleurosigma sp. BC15	NCC428	*France, NW Atlantic coast*
Rhizosolenia setigera	NCC127	*France, NW Atlantic coast*
Tabularia tabulata	NCC338	*France, NW Atlantic coast*

Table S2: Lipid quantification evaluated by FTIR and ATR method for all the species.

Species	code	FTIR					ATR	
		Carb/si	Prot/si	Eb/si	CH2/si	CH3/si	eb	CH2 + CH3
Amphora acutiuscula	NCC216	53.6 ± 8.2	45.8 ± 5.7	22.1 ± 4.9	65.7 ± 8.0	53.5 ± 7.8	6.2 ± 0.9	24.3 ± 2.4
Amphora sp. 1	NCC260	63.6 ± 2.9	40.0 ± 2.0	12.2 ± 2.3	57.3 ± 3.3	39.2 ± 0.6	4.5 ± 0.7	18.1 ± 3.1
Amphora sp. 2	NCC169	58.1 ± 4.3	42.4 ± 1.1	17.2 ± 3.4	59.7 ± 3.4	49.7 ± 3.0	7.1 ± 0.7	42.1 ± 11.0
Brockmaniella brockmanii	NCC161	51.2 ± 5.5	25.2 ± 6.4	12.8 ± 4.0	57.7 ± 5.5	41.8 ± 5.5	4.1 ± 1.6	21.1 ± 5.6
Conticriba weissflogii	NCC133	47.4 ± 0.5	40.2 ± 0.8	5.03 ± 1.5	48.4 ± 2.6	41.7 ± 1.9	4.7 ± 0.3	20.0 ± 0.7
Conticriba weissflogii	CCMP1336	48.3 ± 2.8	43.5 ± 3.3	9.8 ± 1.8	48.7 ± 3.0	40.9 ± 2.7	5.0 ± 0.7	16.9 ± 2.2
Craspedostauros britannicus	NCC195	60.7 ± 2.4	69.8 ± 11	23.2 ± 3.3	80.7 ± 8.0	66.0 ± 6.9	4.8 ± 0.4	19.2 ± 1.8
Craspedostauros britannicus	NCC199	55.1 ± 3.4	47.5 ± 5.7	26.9 ± 3.4	62.2 ± 2.7	44.2 ± 3.3	5.4 ± 0.6	20.5 ± 1.9
Craspedostauros sp. 1	NCC228	44.3 ± 0.1	37.8 ± 4.3	6.2 ± 0.4	46.3 ± 6.4	37.8 ± 6.0	3.9 ± 0.8	15.2 ± 3.4
Craspedostauros sp. 2	NCC218	54.6 ± 2.6	49.4 ± 3.5	7.5 ± 0.3	46.0 ± 3.8	39.0 ± 4.0	4.7 ± 0.3	17.9 ± 2.5
Cymatosira belgica	NCC208	41.6 ± 4.8	25.4 ± 3.3	6.7 ± 1.1	55.4 ± 5.1	41.5 ± 3.7	5.9 ± 0.7	22.7 ± 3.2
Entomoneis paludosa	NCC18.1.1	39.6 ± 0.3	26.0 ± 2.7	2.9 ± 0.1	27.3 ± 2.4	19.4 ± 1.8	3.9 ± 0.7	23.1 ± 1.8
Entomoneis paludosa	NCC18.2.1	45.7 ± 0.6	40.9 ± 1.4	6.1 ± 0.1	34.5 ± 0.9	22.5 ± 0.6	3.1 ± 0.4	21.6 ± 1.1
Entomoneis sp. 1	NCC350	39.9 ± 0.1	30.4 ± 0.8	5.5 ± 1.5	28.6 ± 0.9	21.2 ± 1.7	2.7 ±0.1	30.6 ± 4.3
Entomoneis sp. 2	NCC20	42.5 ± 0.5	32.5 ± 0.3	9.5 ±0 .3	40.0 ± 0.4	26.0 ± 0.6	4.7 ± 0.3	18..6 ± 0.4
Entomoneis sp. 3	NCC351	45.5 ± 2.9	41.4 ± 4.2	14.4 ± 3.4	37.2 ± 0.8	28.3 ± 0.6	3.9 ± 1.7	15.8 ± 5.6
Entomoneis sp. 4	NCC301	62.5 ± 4.8	56.7 ± 6.4	12.5 ± 2.5	64.0 ± 7.9	46.7 ± 5.6	2.9 ± 0.1	17.0 ± 0.8
Entomoneis sp. 5	NCC302	37.6 ± 0.7	36.8 ± 0.8	3.43 ± 0.1	33.9 ± 0.7	23.9 ± 0.5	3.3 ± 0.3	19.6 ± 1.5
Entomoneis sp. 6	NCC335	50.5 ± 0.6	35.3 ± 2.7	6.6 ± 0.7	29.9 ± 1.9	19.0 ± 1.1	3.1 ± 0.2	13.4 ± 3.0
Entomoneis sp. 7	NCC445	40.6 ± 0.9	27.0 ± 2.7	8.5 ± 0.2	37.7 ± 0.4	29.2 ± 0.3	4.1 ± 0.9	17.5 ± 4.3
Extubocellulus cf cribriger	NCC229	49.8 ± 3.7	38.1 ± 2.6	10.1 ± 1.2	48.0 ± 1.9	38.0 ± 1.1	4.9 ± 0.3	34.2 ± 1.7
Fallacia sp. 1	NCC303	64.7 ± 1.8	74.4 ± 7.0	14.2 ± 2.5	64.5 ± 4.1	55.5 ± 5.4	6.9 ± 0.3	26.4 ± 2.9
Fallacia sp. 2	NCC304	46.0 ± 6.2	45.7 ± 3.2	31.3 ± 4.0	72.8 ± 2.7	53.3 ± 2.1	5.1 ± 1.0	18.9 ± 3.4
Licmophora sp. 1	NCC253	53.1 ± 2.7	65 ± 10	4.4 ± 1.1	57.9 ± 5.4	50.3 ± 5.2	3.6 ± 0.3	22.6 ± 0.6
Lithodesmium sp	NCC353	34.2 ± 2.0	25.8 ± 0.8	2.4 ± 0.3	31.1 ± 1.1	23.1 ± 0.4	2.1 ± 0.3	28.0 ± 3.2
Navicula sp. 1	NCC113	63.3 ± 4.7	43.8 ± 8.9	33.4 ± 4.7	68.2 ± 9.6	52.4 ± 5.6	3.4 ± 0.4	28.8 ± 1.2
Navicula sp. 2	NCC226	54.2 ± 4.3	27.0 ± 3.0	5.2 ± 0.9	53.1 ± 3.8	39.5 ± 2.8	4.2 ± 0.7	22.4 ± 0.7
Nitzschia sp. 5	NCC109	62.0 ± 2.8	42.4 ± 6.7	22.0 ± 2.3	72.7 ± 4.6	61.3 ± 4.8	6.9 ± 0.4	45.1 ± 28.9
Nitzschia alexandrina	NCC33	58.2 ± 7.2	44.0 ± 4.6	20.7 ± 3.3	56.1 ± 4.0	45.8 ± 0.7	5.7 ± 0.3	21.3 ± 2.3
Opephora sp. 1	NCC366	58 ± 12	40.1 ± 8.8	31.6 ± 6.1	50.6 ± 4.5	42.0 ± 2.5	6.9 ± 1.1	26.3 ± 4.4
Pseudonitzschia americana	PNA06 KER	56.6 ± 1.4	60.6 ± 3.9	3.9 ± 1.0	44.0 ± 2.8	39.1 ± 3.2	4.0 ± 0.3	38 ± 28
Staurosira sp.	NCC182	47.7 ± 6.6	30.7 ± 4.1	30.9 ± 5.4	61.6 ± 4.0	49.0 ± 2.3	7.3 ± 0.1	31.6 ± 0.6
Surirella sp. 1	NCC270	58.5 ± 2.4	54.4 ± 8.4	22.0 ± 4.6	56.1 ± 5.3	51.3 ± 5.4	7.1 ± 0.4	27.1 ± 0.6

ANNEXES II

S3. Lipid class distribution for the six species

Species	% lipid classes (% CLE)									
	NL	TAG/HC	FFA	Sterols	Pigments	**GL**	Pigments +MGDG	DGDG	SQDG	**PL**
Amphora sp.	**22.6**	/	11	9	1	**51.0**	31	7	13	**26.5**
E. paludosa	**46.7**	12	17	16	2	**38.5**	17	16	6	**14.9**
N. alexandrina	**39.2**	14	10	11	4	**45.1**	17	24	4	**15.7**
Nitzschia sp.	**59.1**	19	20	18	2	**30.8**	17	6	8	**10.1**
Opephora sp.	**29.0**	22	4	3		**58.5**	32	20	7	**12.5**
Staurosira sp.	**76.4**	71	/	6		**17.6**	8	3	7	**6.0**

S4. Unsaponifiable composition of the 6 species

Compounds	% (% unsaponifiable fraction)					
	Amphora sp.	*E. paludosa*	*N. alexandrina*	*Nitzschia* sp.	*Opephora* sp.	*Staurosira* sp.
Phytol	18.9	4.3	9.1	26.6	40.4	15.0
Hydrocarbons	16.1	1.1	4.7	3.5	18.2	
With squalene	tr	tr	1.9	tr		
Sterols						
Cholesta-5-en-3β-ol **(1a)**	tr		23.6			
Cholesta-5,22-dien-3β-ol **(1b)**			30.8			45.8
24-Methylcholest-5-en-3β-ol **(1c)**		2.2	3.9	10.7	2.2	
24-Methylcholesta-5,22*E*-dien-3β-ol **(1d)**	tr	tr	12.5			34.6
24-Methylcholesta-5,24(28)-dien-3β-ol **(1e)**			15.4			
24-Ethylcholest-5-en-3β-ol **(1f)**		61.1		59.2		
24-Ethylcholesta-5,22*E*-dien-3β-ol **(1g)**	62.2	28.7			7.1	4.6
24-Ethylcholest-7,22*E*-en-3β-ol **(2g)**					16.3	
24-Ethylcholesta-5,22-dien-3-one **(3g)**					13.6	
24-Ethylcholesta-3,5-dien-7-one **(4f)**		2.3				
Σ sterols	62.2	94.3	86.2	69.9	39.2	85.0

S5. Total FA composition (%FA) of the six species

Fatty acid	% FA (% total FA)					
	Amphora sp.	*E. paludosa*	*N. alexandrina*	*Nitzschia* sp.	*Opephora* sp.	*Staurosira* sp.
Saturated FA						
14:0	**12.4**	**18.9**	3.7	3.0	1.9	3.7
15:0	2.4	0.7	2.1	0.8	Tr	Tr
16:0	**24.9**	**22.4**	**19.4**	**32.2**	**23.5**	**29.4**
18:0	0.9	0.5	0.8	0.6	0.9	0.6
Σ SFA	40.6	42.5	26.0	36.6	26.3	33.7
Monounsaturated FA						
9-16:1	**36.3**	**28.3**	**43.5**	**45.3**	**50.2**	**51.8**
9-18:1	1.2	1.1	0.9	3.5	0.7	1.0
11-18:1	1.9	1.3	1.9	2.3	3.1	1.4
24:1	-	1.1	-	-	-	-
Σ MUFA	39.4	31.8	46.3	51.1	54.0	54.2
Polyunsaturated FA						
6,9-16:2	-	2.9	6.4	-	1.5	-
6,9,12-16:3	4.5	-	-	1.3	-	0.6
6,9,12-18:3	0.5	0.8	1.8	1.8	Tr	0.9
5,9,12-18:3	1.2	2.4	-	-	1.5	0.5
9,12-18:2	1.2	1.8	Tr	1.8	0.7	Tr
5,8,11,14-20:4	1.0	Tr	4.7	0.6	2.7	0.9
5,8,11,14,17-20:5	**8.0**	**12.6**	**5.4**	**2.8**	**7.1**	**5.5**
Σ PUFA	16.4	20.5	18.3	8.3	13.5	8.4

Tr : traces < 0.5% ; - : Not detected

ANNEXE III

Annexe S6 : Table de clé de détermination des AGs par CPG-SM

Esters méthyliques

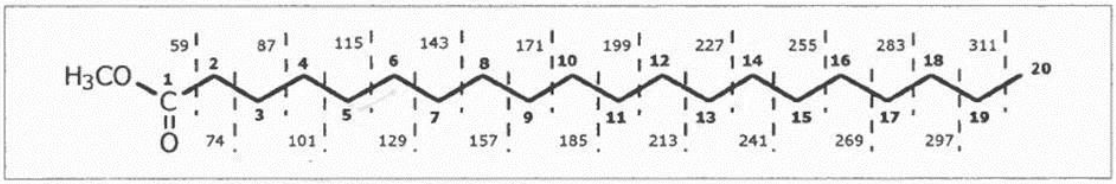

- Pics importants des esters méthyliques saturés :
  m/z **74**, Mac Lafferty (pic de base)
  m/z 87, M^+, $(M-29)^+$, $(M-31)^+$, $(M-43)^+$
- Tous les fragments homologues ne sont pas présents.

N-acyl pyrrolidides

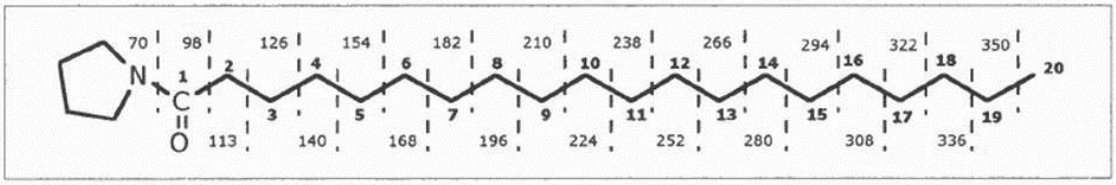

- Pics importants des pyrrolidides saturés :
  m/z **113**, Mac Lafferty (pic de base)
  m/z 55, 70, 98, 126.
- Il est possible d'observer presque tous les fragments homologues à partir de 126 (avec agrandissement).

Nombre de carbones	14	15	16	17	18	19	20	21	22	23	24	25	26	27	28	29	30
Méthyl ester	242	256	270	284	298	312	326	340	354	368	382	396	410	424	438	452	466
Méthyl ester α-hydroxylé	258	272	286	300	314	328	342	356	370	384	398	412	426	440	454	468	482
Méthyl ester α-méthoxylé	272	286	300	314	328	342	352	370	384	398	412	426	440	454	468	482	496
Pyrrolidide	281	295	309	323	337	351	365	379	393	407	421	435	449	463	477	491	505
Pyrrolidide α-hydroxylé	297	311	325	339	353	367	381	395	409	423	437	451	465	479	493	507	521
Pyrrolidide α-méthoxylé	311	325	339	353	367	381	395	409	423	437	451	465	479	493	507	521	535

Annexe S7 : Table de clé de détermination des spectres de masse des stérols libres (A) et des sterols acétylés (B)

A

nb C / nb d.l.	21	22	23	24	25	26	27	28	29	30	31
0	304	318	332	346	360	374	388	402	416	430	444
1	302	316	330	344	358	372	386	400	414	428	442
2	300	314	328	342	356	370	384	398	412	426	440
3	298	312	326	340	354	368	382	396	410	424	438
4	296	310	324	338	352	366	380	394	408	422	436

nb C : nombre de carbones ;nb d.l : nombre de doubles liaisons

B

Ion $[M\text{-}AcOH]^+$ ($\Delta 5$)

nb C / nb d.l.	21	22	23	24	25	26	27	28	29	30	31
0	286	300	314	328	342	356	370	384	398	412	426
1	284	298	312	326	340	354	368	382	396	410	424
2	282	296	310	324	338	352	366	380	394	408	422
3	280	294	308	322	336	350	364	378	392	406	420
4	278	292	306	320	334	348	362	376	390	404	418

nb C : nombre de carbones
nb d.l. : nombre de doubles liaisons

Ions M+ de l'acétate ($\Delta 0$, $\Delta 7$)

nb C / nb d.l.	21	22	23	24	25	26	27	28	29	30	31
0	346	360	374	388	402	416	430	444	458	472	486
1	344	358	372	386	400	414	428	442	456	470	484
2	342	356	370	384	398	412	426	440	454	468	482
3	340	354	368	382	396	410	424	438	452	466	480
4	338	352	366	380	394	408	422	436	450	464	478

UNIVERSITE BRETAGNE LOIRE / SCIENCES DE LA MER ET DU LITTORAL

UNIVERSITÉ DE NANTES

Titre : Diatomées marines benthiques : une ressource originale de souches "oléagineuses" pour une application en santé et nutrition

Mots clés : Diatomées marines benthiques, lipides, EPA, CG-SM, FTIR, airlift

Résumé : Les diatomées marines benthiques représentent à ce jour un vivier sous-exploité et constituent donc une ressource potentielle pour la valorisation de lipides d'intérêt en santé et nutrition. Dans ce cadre, après un criblage réalisé sur plus d'une centaine de souches de la collection régionale NCC, six espèces : *Amphora* sp. NCC169., *Entomoneis paludosa* NCC18.2, *Nitzschia* sp. NCC109, *Nitzschia alexandrina* NCC33, *Opephora* sp. NCC366 et *Staurosira* sp. NCC182 ont été retenues sur la base de leurs productions lipidiques et de leur capacité de croissance. Ces six espèces ont ensuite été produites en photobioréacteur airlift pour établir leur capacité de croissance et de production lipidique. Une étude lipidique approfondie a également été menée à la fois sur les lipides neutres (TAG, stérols) et les lipides polaires (glycolipides, phospholipides) afin d'évaluer leur potentiel en matière de diversité lipidique et de production de lipides d'intérêt. Trois espèces ont été séléctionnées (*E. paludosa*, *N. Alexandrina* et *Staurosira* sp.) pour évaluer le potentiel bioactif des fractions lipidiques extraites. Il a été démontré que les fractions glycolipidiques possèdent une activité antiproliférative sur les lignées cancéreuse MC-F7 (sein) et NSCLC-N6 (poumon) ainsi qu'une activité antibactérienne sur les souches de bactéries à gram-positif (*B. subtillus*). Enfin l'étude de l'impact des conditions de cultures (lumière et azote) sur la qualité des acides gras produits a démontré que pour optimiser la production de lipides d'intérêt un milieu non-limitant et une faible intensité lumineuse devraient être utilisés pour une production à grande échelle.

Title : Marine benthic diatoms : an original ressource of « oleaginous » strains for health and nutrition

Keywords : Marine benthic diatoms, lipids, EPA, GC-MS, FTIR, airlift

Abstract : Marine benthic diatoms represent an under-exploited pool and therefore constitue a potential resource for the valorization of lipids of interest in heath and nutrition. In this framework, after a screening of more than one hundred strains from the NCC regional collection, six species : *Amphora* sp. NCC169., *Entomoneis paludosa* NCC18.2, *Nitzschia* sp. NCC109, *Nitzschia alexandrina* NCC33, *Opephora* sp. NCC366 et *Staurosira* sp. NCC182 have been selected on the basis of their lipid production and growth capacity. These six species were then produced in airlift photobioreactor to establish their capacity for growth and lipid production. A thorough lipid study was also conducted on both neutral lipids (TAG, sterols) and polar lipids (glycolipids, phospholipids) to evaluate their potential for lipid diversity and lipid production of interest. Three species (*E. paludosa*, *N. Alexandrina* et *Staurosira* sp.) have been selected to evaluate the bioactive potential of extracted lipid fractions. The glycolipids fractions shown antiproliferative activity on the MCF-7 (breast) and NSCLC-N6 (lung) cancer cell lines as an antibacterial activity on gram-positive bacterial strains (*B. subtillus*). Finally, this study demonstrated the impact of culture conditions (light and nitrogen) on the fatty acids quality. To optimize the production of lipids of interest a non-limiting medium and low light intensity should be used for large scale production.

UNIVERSITE BRETAGNE LOIRE / SCIENCES DE LA MER ET DU LITTORAL

UNIVERSITÉ DE NANTES